SYNTHESIS AND BIOLOGICAL EVALUATION OF GLYCOSYLPHOSPHATIDYLINOSITOLS FROM *TRYPANOSOMA BRUCEI*

Inaugural-Dissertation
to obtain the academic degree
Doctor rerum naturalium (Dr. rer. nat.)

submitted to the Department of Biology, Chemistry and Pharmacy
of Freie Universität Berlin

by

Maurice Grube

from Torgau

2016

The work in this PhD thesis was performed between July 2012 and July 2016 in the Department of Biomolecular Systems and the GPI Group, Max Planck Institute of Colloids and Interfaces and Institute of Chemistry and Biochemistry, Freie Universität Berlin under the guidance of Dr. Daniel Varón Silva.

1st Reviewer: Dr. Daniel Varón Silva
2nd Reviewer: Prof. Dr. Christoph A. Schalley

Date of oral defense:

CONTENTS

SUMMARY

Glycosylphosphatidylinositol (GPI) anchors are among the most complex class of natural products as they combine lipids, carbohydrates and phosphate groups. The structure comprises a conserved core presented throughout all eukaryotic cells. It consists of three mannose residues, a glucosamine, and *myo*-inositol connected to a phospholipid ($H_2N(CH_2)_2OPO_3H$-6Manα1→2Manα1→6Manα1→4GlcNα1→6*myo*-Ino1-OPO_3H-Lipid) (Figure 1). Depending on tissue, organism and cell-type, typical appendages to this core structure include addition of monosaccharide units such as galactose and mannose to Man III, or Man I, additional phosphorylations and lipidations. The main and primary function of GPIs is anchoring of proteins to the cell membrane. However, participation in microdomain formation and protein sorting has been described as well. Furthermore, GPIs of pathogenic parasites have been linked to regulation of a host immune response.

The extracellular parasite *Trypanosoma brucei* is transmitted by the tsetse fly and causes Nagana in animals and human African trypanosomiasis (HAT) in humans. Due to unspecific symptoms in early stage infection the disease is difficult to diagnose and expensive in treatment. The parasite uses GPIs to attach an impenetrable coat of Variant Surface Glycoproteins (VSGs) to the outer leaflet of the biomembrane. VSG-GPI conjugates and parts thereof enhance immune evasion by intensive antigen switching and activate the immune system to release chemo- and cytokines. Notably, only the N-terminal domain of the conjugate varies heavily over time, rendering the little varied C-terminus with the attached GPI a more conserved structural feature.

Due to the lack of defined homogeneous GPI structures from natural sources, it is difficult to annotate exact functions to certain protein and GPI epitopes. Therefore, chemical synthesis of C-terminal VSG and GPI fragments is by all means the best method to accumulate the quantities of defined material required to investigate these specific functions.

A general convergent strategy for the synthesis of GPI has recently been established in the group. This strategy relies on an orthogonal set of protecting groups for introduction of late stage modifications and a set of target specific fragments. This strategy poses limitations towards introduction of specific structures present by *T. brucei* GPIs (Figure 1).

Therefore, the goal of this thesis was to show the feasibility of this method in generating the *T. brucei* VSG 221 GPI anchor **a**. Due to the design of new building blocks and fragments, expansion of the number of orthogonal protecting groups was required.

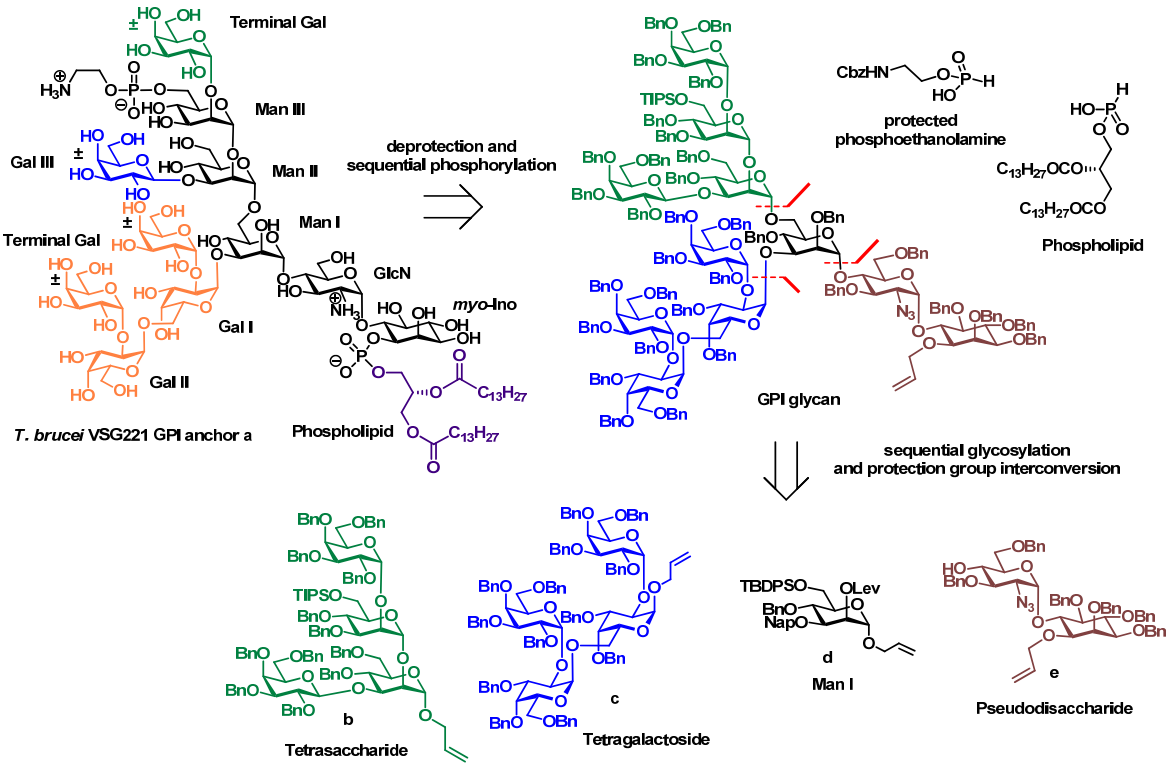

Figure 1: Synthetic analysis of the GPI-anchor structure of *T. brucei* VSG 221 with indicated variations and unique modifications

Moreover, during synthesis of larger fragments **b** and **c** for assembling this complex GPI structure two sets of *T. brucei* related carbohydrate libraries comprising the unique structural moieties of **a** were generated. One set of GPIs and GPI fragments was investigated in their potential of activating macrophages to release chemo- and cytokines, evaluating the influence of particular structural features. The second set of synthesized structures was used in glycan microarray to investigate recognition of distinct structural features by anti-GPI antibodies.

In the first part of this thesis, assembly of novel *T. brucei* GPI fragments **b** and **c** was investigated by synthesizing a set of new building blocks (chapter 4). Stepwise glycosylation and subsequent modification of Gal III, Man II, a Man III building block and terminal Gal including a synthetically challenging α-galactosylation gave **b** in high yields of all reactions involved. A second approach to isolate the first tetrasaccharide was evaluated using terminal Gal instead of Gal III. Due to the lack of a neighboring participating group, the first step gave lower β-selectivity, however, assembling of **b** along this sequence was successfully achieved in fewer steps and high yields.

Afterwards, synthesis of tetragalactoside **c** was investigated in a [2+2]-glycosylation strategy. Therefore, an orthogonally protected Gal I/II building block was generated. Removal of the PMB ether, gave an acceptor which was glycosylated with terminal Gal in a challenging α-galactosylation. The isolated corresponding disaccharide was used to synthesize

acceptor and donor for consecutive [2+2]-glycosylation in a divergent approach. However, formation of tetragalactoside **c** in a glycosylation of these compounds was not possible by the used protocols. In the following, an analogue of **c**, was used to glycosylate Man I **e**. Unfortunately, a combination of successfully assembled fragments **c** and **e** to consecutively assemble the full glycan of the target GPI was not feasible by the method used in this thesis.

Nevertheless, assembled large fragments **b** and **c** comprised the important structural features of the *T. brucei* VSG 221 GPI. Accordingly, a set of structures containing these fragments was generated by modification with a thiol linker, enabling fabrication of glycan microarray (Figure 2). Here, the structures were investigated in their recognition by antibodies from sera obtained from a murine *T. brucei* infection model and HAT infections from sub-Saharan Africa (chapter 5).

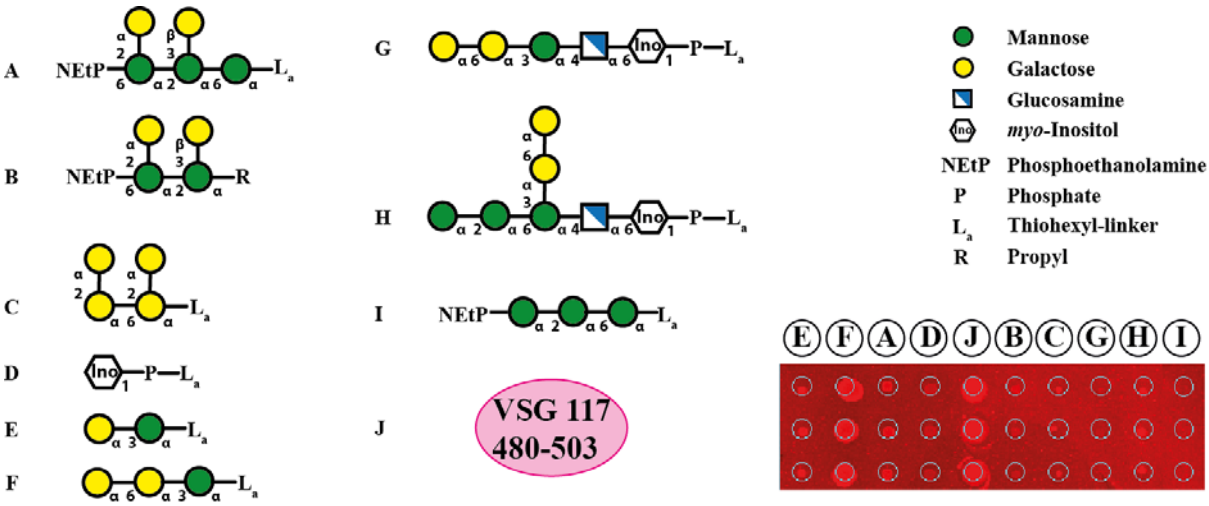

Figure 2: Synthesized structures used in glycan microarray fabrication and a representative scan of fluorescence pattern indicating recognition by anti-GPI IgM from sera of a *T. brucei gambiense* stage 1 infection. With exception of **I** and **J**, substances were obtained in this thesis by combination or minor modification of introduced building blocks and fragments.

Analysis of generated glycan microarrays confirmed significant recognition of *T. brucei* VSG-GPI structures. More specifically α-galactose modified compounds **A**, **C**, **G** and **H** were recognized by IgM of infection positive sera involved in the study. Additionally, C-terminal VSG peptide **J** was significantly recognized by IgM. High significance of binding was confirmed as well by excluding cross-reactivity with mammalian GPI structures. Additionally, screening of anti-GPI-antibodies from sera of toxoplasmosis patients against *T. brucei* GPI structures showed no cross-reactivity, highlighting the significance of the conducted experiments. Further investigations have to show the applicability of synthetic GPI structure as potential diagnostic antigens for *T. brucei* related infections.

In the second part of this thesis, building blocks and larger fragments were used to generate an additional set of *T. brucei* VSG-GPI structures with a phospholipid attached at

myo-inositol (chapter 6). Analogously, an alkyl chain was attached at the reducing end when *myo*-inositol was absent (Figure 3).

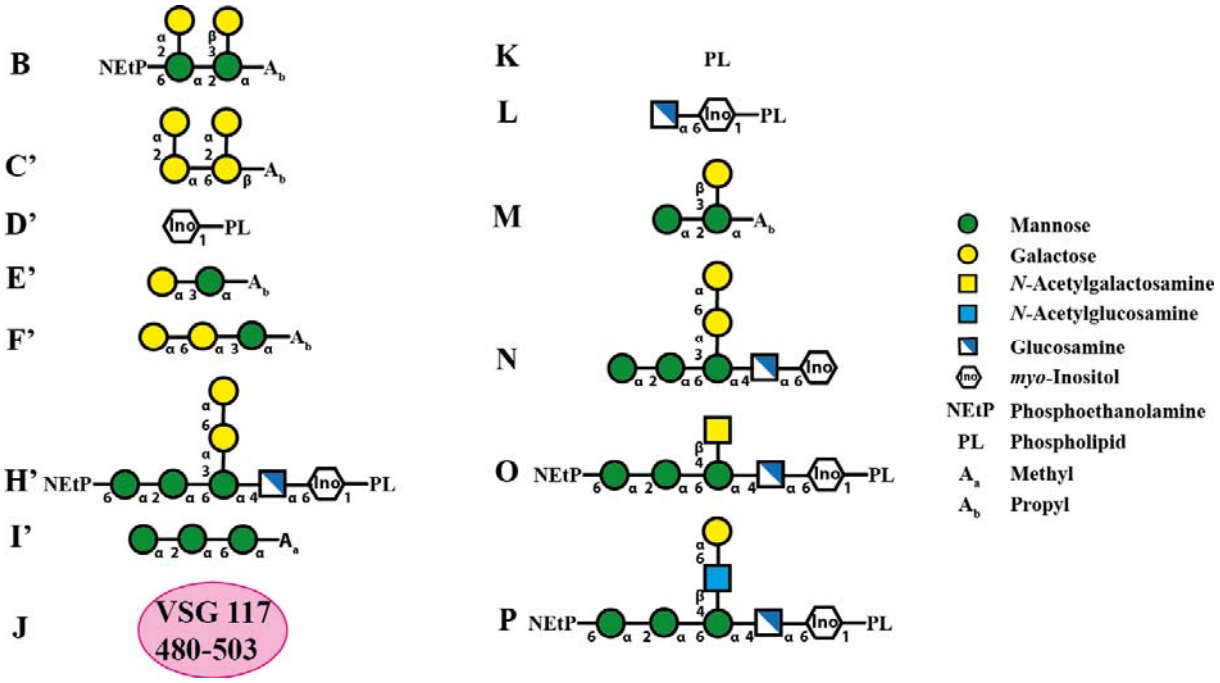

Figure 3: Synthetic structures used for investigation in an *in vitro* murine macrophage activation assay. With exception of **H'-J** and **O-P**, substances were obtained in this thesis by combination or minor modification of introduced building blocks and fragments

The structures were used in an *in vitro* assay to investigate activation of murine macrophages (in collaboration with Dr. Benoit Stijlemans, chapter 7). In this study, release of TNF-α by macrophages was induced by GPI phosphoglycans **B**, **H'**, **L**, **O** and **P**, complete *T. brucei* VSG117 GPI glycan **N** and C-terminal VSG peptide **J** (Figure 4**)**. Moreover, by stimulating the same cell line with IFN-γ prior to incubation, production of TNF-α was induced by all *T. brucei* derived structures. These studies indicate a structure-activity relationship for C-terminal VSG-GPI compounds. Experiments in human cell lines as well as spleen and liver derived cells will be performed and will give further insights in the role of these structures during activation of the immune system.

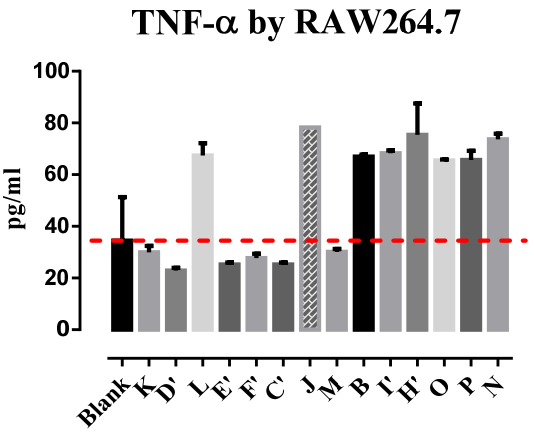

Figure 4: Murine macrophages are triggered by synthetic *T. brucei* GPI structures to release TNF-α.

In the third part, a ligation method of *T. brucei* GPI fragments to peptide thioester from the C-terminal region of VSG 117 was investigated (chapter 8). Three strategies to obtain a CKD-Man III intermediate were evaluated in their feasibility. The strategy involving the combination of a GPI fragment and the CKD tripeptide by fragment condensation was applied to synthesize a CKD-GPI conjugate using **B**. The conjugate will be investigated in a chemoselective ligation with VSG117 480-500.

In this thesis the synthesis of *T. brucei* VSG 221 GPI anchor by a convergent strategy was investigated. Although, the strategy proofed to be not feasible for this complex structure, it was possible to assemble the important structural fragments of this GPI. Nevertheless, generation of two sets of carbohydrate structures to investigate glycan-antibody interactions and biological activity was possible and highlighted the suitability of evaluating fragments rather than complex GPI structures. The synthesized fragments comprising important epitopes were recognized by anti-GPI antibodies of sera from *T. brucei* infections and activated murine macrophages to release TNF-α without requiring IFN-γ.

ZUSAMMENFASSUNG

Glykosylphosphatidylinositol (GPI) Anker gehören zu einer der komplexesten Klassen an Naturstoffen. Sie vereinen Fette, Kohlenhydrate und Phosphatgruppen und verfügen über eine konservierte Kernstruktur, die in allen eukaryotischen Zellen vorkommt. Diese Kernstruktur ($H_2N(CH_2)_2OPO_3H$-6Manα1→2Manα1→6Manα1→4GlcNα1→6*myo*-Ino1-OPO_3H-Lipid) besteht aus drei Mannosen, einem Glukosamin und einem *myo*-Inositol welches an ein Phospholipid gebunden ist (Abbildung 1). Abhängig von Gewebe, Organismus oder Zelltyp kann die Kernstruktur über verschiedenste Ergänzungen verfügen. So gehören zusätzliche Monosaccharide wie Galaktose und Mannose an Mannose I oder Mannose III genauso zu möglichen Erweiterungen wie weitere Phosphate und Fettsäuren. Die Hauptfunktion von GPIs ist das Verankern von Proteinen in der Zellmembran. Weiterhin wurden die mögliche Beteiligung an der Proteinsortierung und der Formierung von Mikrodomänen beschrieben. Besonders GPIs von pathogenen Parasiten werden mit der Regulierung des Immunsystems des Wirtes in Verbindung gebracht.

Der extrazelluläre Parasit *Trypanosoma brucei* wird durch den Stich einer Tsetsefliege übertragen und verursacht Nagana in Wirtstieren und die afrikanische Schlafkrankheit im Menschen. Durch die unspezifischen Symptome im frühen Infektionsstadium ist die Krankheit schwer zu diagnostizieren und somit kostenintensiv in der späteren Behandlung. Der Parasit nutzt GPI um eine undurchdringliche Schicht von variablen Oberflächenproteinen (VSG) an der Biomembran zu verankern. Das somit vorliegende VSG-GPI Konjugat, sowie Teile davon, erleichtern die Vermeidung des Immunsystems durch intensives Austauschen der Primärstruktur. Kommt es in Kontakt mit diesen Strukturen, wird das Immunsystem aktiviert und schüttet Chemo- und Zytokine aus. Bemerkenswerterweise verändert der Parasit dabei nur den N-terminalen Teil der Primästruktur, während der C-terminale Teil mit dem GPI weitestgehend unverändert bleibt.

Durch den Mangel an homogenen GPI Strukturen aus natürlichen Quellen ist es schwierig die genaue Funktion von Protein und GPI Epitopen in der Erkrankung zu bestimmen. Die chemische Synthese von C-terminalen VSG und GPI Strukturen ist daher der einzige Weg genügend homogenes Material zur Untersuchung dieser Funktionen zu generieren.

Eine generelle und konvergente Synthese von GPIs wurde jüngst durch unsere Gruppe vorgestellt. Diese Strategie basiert auf einer Gruppe orthogonaler Schutzgruppen für die späte Einführung von Modifikationen sowie auf Zielmolekül spezifischen größeren Fragmenten.

Allerdings, verfügt die Strategie über Limitierungen hinsichtlich der Einführung von Fragmenten der GPIs von *T. brucei*.

Das Ziel dieser Dissertation war daher die Anwendbarkeit der generellen Strategie auf die Synthese des VSG221 GPI Ankers von *T. brucei* zu zeigen. Durch den Entwurf neuer Monosaccharid Bausteine und größerer Fragmente war die Erweiterung der Zahl benutzter orthogonaler Schutzgruppen unumgänglich.

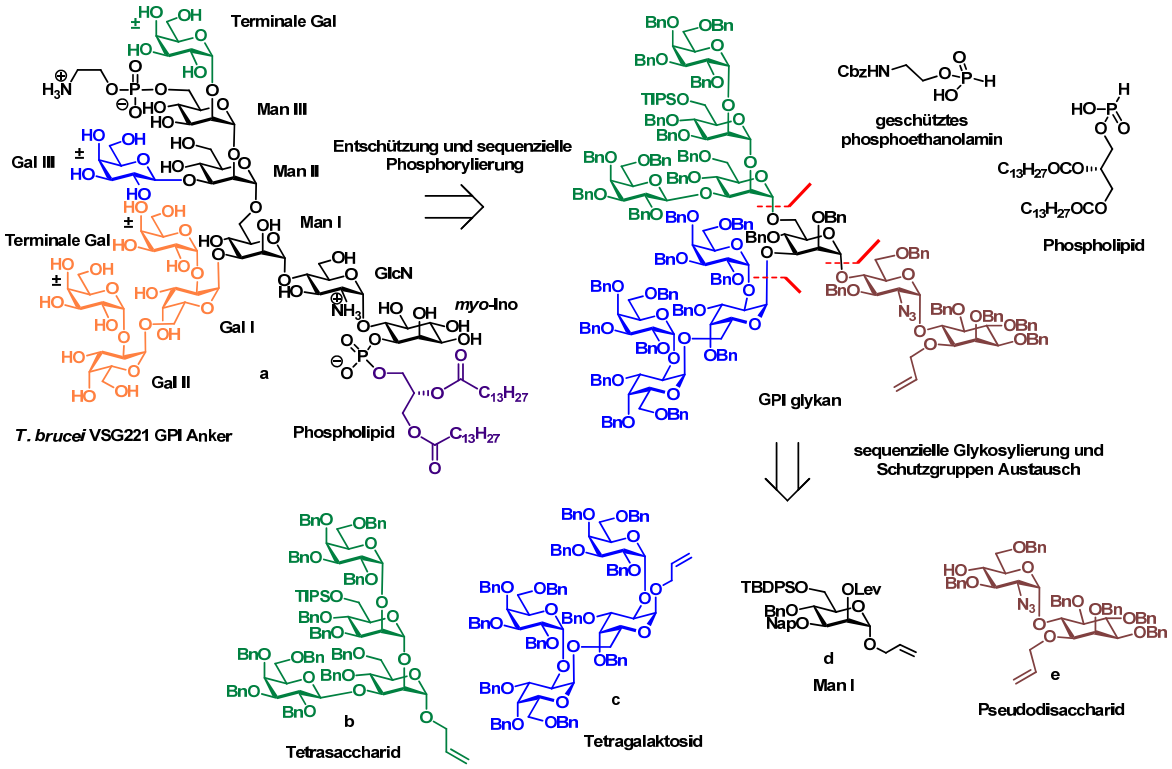

Abbildung 1: Die Retrosynthese des VSG221 GPI Ankers von *T. brucei*. Mögliche Variationen und einzigartige Modifikationen sind entsprechend markiert

Weiterhin sollten durch die Synthese der großen Fragmente **b** und **c**, sowie der Kombination mit weiteren strukturellen Motiven des komplexen GPI Ankers, zwei Molekülbibliotheken generiert werden. Diese, die wichtigen Modifikationen widerspiegelnden, Substanzen wurden in ihrem Potential untersucht, die Ausschüttung von Chemo- und Zytokinen durch Makrophagen zu bewirken. Ein weiterer Satz der Substanzen wurde zur Untersuchung der Erkennung von spezifischen Strukturen durch anti-GPI Antikörper in Glykan-Microarrays benutzt.

Im ersten Teil der Arbeit, wurde die Synthese der einzigartigen GPI Fragmente **b** und **c** aus neuartigen Monosaccharid-Bausteinen untersucht (Kapitel 4). Die Synthese von Fragment **b** wurde durch die Nutzung drei neuer sowie eines etablierten Bausteins auf zwei verschiedenen Wegen in hohen Ausbeuten und unter Optimierung einer herausfordernden α-Glykosylierung gezeigt.

Im Anschluß daran sollte die Synthese von Fragment **c** durch eine [2+2]-Glykosylierungsstrategie gezeigt werden. Hierzu wurde ein orthogonal geschützter Baustein Gal I/II unter Nutzung der PMB-Schutzgruppe entworfen und in einer weiteren α-Glykosylierung mit dem terminalen Galaktose Baustein umgesetzt. Das isolierte Disaccharid wurde im Anschluss in einer divergenten Synthese für die Darstellung des Glykosyldonors und des Glykosylakzeptors für die geplante [2+2]-Glykosylierung verwandt. Unglücklicherweise war die Synthese des Fragmentes **b** durch diese Methode nicht durchführbar. Im Anschluss wurde ein Analog von **c** in einer Reaktion mit Mannose I **d** genutzt. Leider zeigte sich auch hier, dass die Anwendung der generellen Synthesestrategie für GPI auf den VSG 221 GPI Anker von *T. brucei* nicht von Erfolg gekrönt war.

Nichtsdestotrotz wurden die Fragmente **b** und **c**, sowie die entworfenen Monosaccharid Bausteine genutzt um einen Satz Thiollinker modifizierter Substanzen zu synthetisieren. Die Strukturen wurden zur Herstellung von Glykan-Microarrays verwendet und auf die Erkennung durch anti-VSG-GPI Antikörper in Seren von mit *T. brucei* infizierten Menschen sowie von einem *T. brucei* Infektionsmodell in Mäusen hin untersucht (Abbildung 2, Kapitel 5).

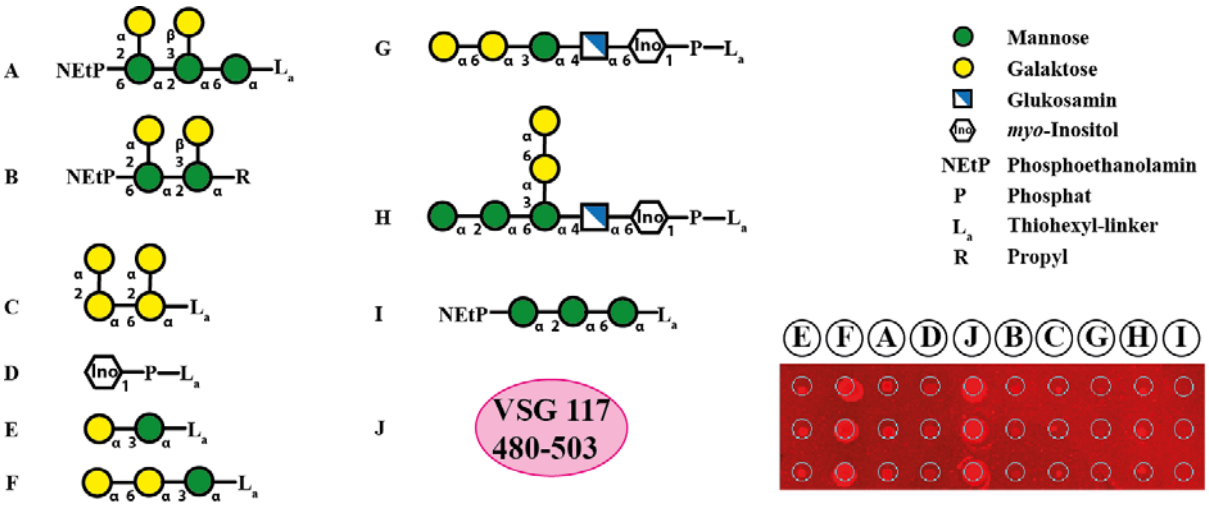

Abbildung 2: Synthetisierte Strukturen die zur Herstellung von Glykan-Microarrays verwandt wurden, sowie ein repräsentativer Scan der Fluoreszenzverteilung resultierend aus der Erkennung der Strukturen durch IgM im Serum einer humanen *T. brucei gambiense* Infektion im ersten Stadium. Mit Ausnahme der Verbindungen **I** und **J**, wurden alle Verbindungen im Laufe dieser Arbeit durch Verwendung der vorgestellten Bausteine und Fragmente oder in Variationen davon synthetisiert.

Die Analyse der generierten Glykan-Mikroarrays ergab die signifikante Erkennung von *T. brucei* VSG-GPI Strukturen. Besonders die α-Galaktose modifizierte Strukturen **A**, **C**, **G** und **H** wurden von IgM in infektionspositiven Seren gebunden. Die Auswertung ergab weiterhin, dass das C-terminale Peptid des VSG117 **J** signifikante Interaktionen mit IgM einging. Die Signifikanz der Erkennung von *T. brucei* VGS-GPI Strukturen zeigte sich auch in der Tatsache, dass ein synthetisches GPI von Säugetieren nicht von anwesenden

X

Antikörpern gebunden wurde. Abschließend wurde gezeigt, dass Antikörper in Seren von Toxoplasmosepatienten keine signifikante Interaktionen mit den synthetisierten Strukturen eingehen. Beide Untersuchungen zeigten somit keinen Hinweis auf existierende Kreuzreaktivität von Antikörpern hinsichtlich GPI Strukturen unterschiedlicher Herkunft. Weitere Evaluierungen sind nötig, um zu zeigen, ob GPI Strukturen als möglicher diagnostischer Marker für eine *T. brucei* Infektion dienen können.

Im zweiten Teil der vorliegenden Arbeit, wurden die vorgestellten Monosaccharid Bausteine und Fragmente genutzt, um einen weiteren Satz an *T. brucei* GPI Strukturen zu synthetisieren (Kapitel 6). Entweder wurde ein Phospholipid am *myo*-Inositol eingeführt, oder bei dessen Abwesenheit eine kurze Alkylkette in der anomeren Position installiert (Abbildung 3).

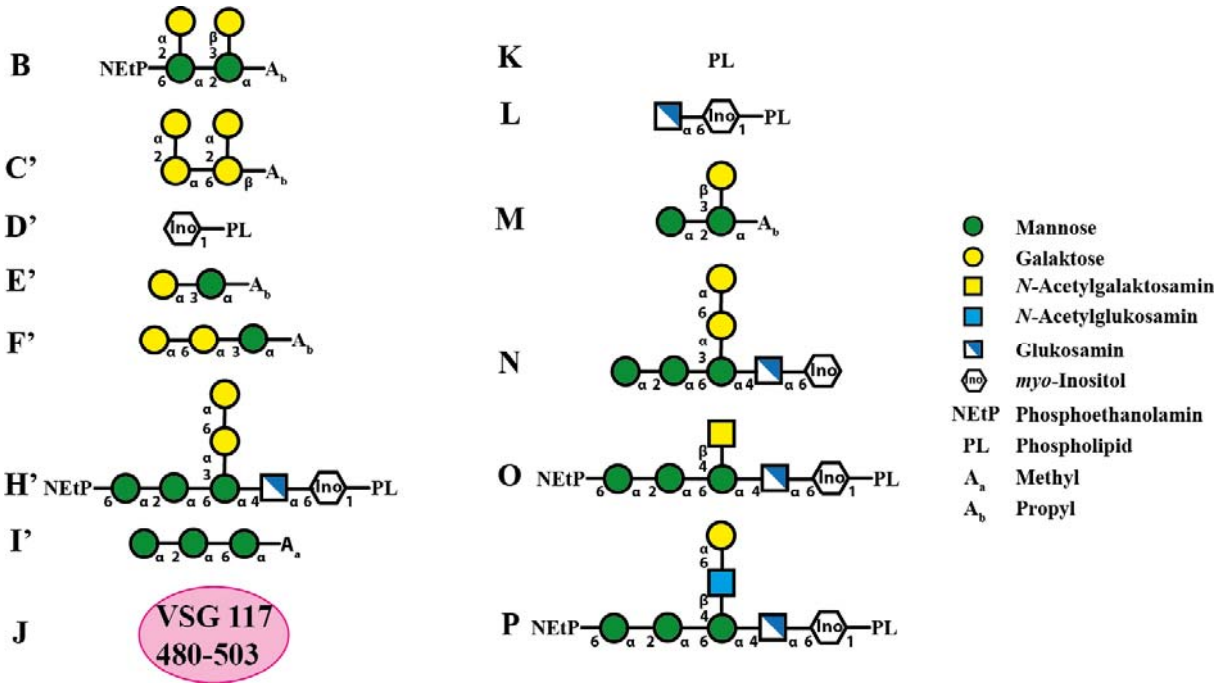

Abbildung 3: Synthetisierte Strukturen die zur Untersuchung in einem in vitro Assay zur Aktivierung von Makrophagen verwendet wurden. Mit Ausnahme von **H'-J** und **O**–**P** wurden alle Substanzen im Laufe der Arbeit durch Verwendung der eingeführten Bausteine und Fragmente oder Variationen davon synthetisiert.

Die so hergestellten Verbindungen wurden in einem *in vitro* Assay hinsichtlich der Aktivierung von Makrophagen untersucht (in Kollaboration mit Dr. Benoit Stijlemans, Kapitel 7). Die Produktion von TNF-α durch Makrophagen wurde durch die GPI phosphoglykane **B**, **H'**, **L**, **O** und **P** induziert. Weiterhin rief das VSG117 GPI Glykan **N** und das C-terminale VSG Peptid **J** die Ausschüttung des Zytokins hervor (Abbildung 4). In einer weiteren Untersuchung wurden die Makrophagen vor der Inkubation mit den synthetisierten Substanzen mit Hilfe von IFN-γ stimuliert. In diesem Fall wurde die Produktion von TNF-α durch alle beteiligten *T. brucei* VSG-GPI Strukturen hervorgerufen. Diese Studien lassen eine

Struktur-Aktivitäts-Beziehung für C-terminale VSG-GPI Verbindungen vermuten. Weitere Untersuchungen in humanen Zelllinien als auch in Zellen von Leber und Milz sind nötig, um weitere Einblicke in die exakte Rolle der Verbindungen zu gewähren.

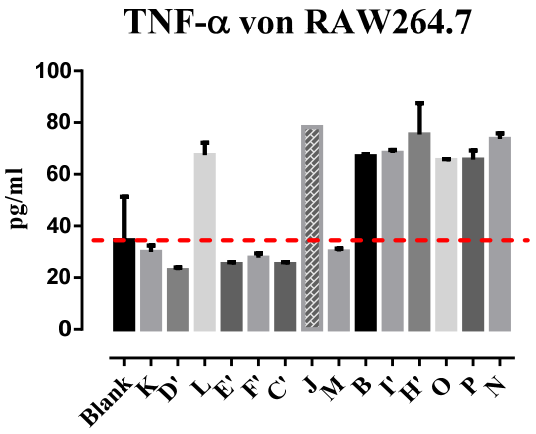

Abbildung 4: Makrophagen der Maus schütten TNF-α nach Kontakt mit synthetischen *T. brucei* GPI aus.

Im dritten Teil der Arbeit wurde eine Ligationsmethode von *T. brucei* GPI Fragmenten und Peptidthioestern C-terminaler VSG117 Sequenzen untersucht (Kapitel 8). Hierzu wurden drei Strategien der Synthese einen CKD-Man III Intermediates auf ihre Durchführbarkeit hin ausgewertet. Die Strategie, welche die Kombination eines GPI Fragments und des CKD Tripeptids durch Fragmentkondensation vorsieht, wurde auf die Darstellung eines CKD-GPI Konjugates unter der Verwendung von **B** angewandt. Dieses Konjugat ist Gegenstand gegenwärtiger Untersuchungen zur Nutzung in chemoselektiven Ligationen mit VSG117 480-500.

In dieser Arbeit wurde die Synthese des *T. brucei* VSG221 GPI Ankers durch eine konvergente Synthese untersucht. Obwohl, die Strategie sich als nicht durchführbar erwies, war es möglich die wichtigen strukturellen Komponenten zu synthetisieren. Dadurch war die die Darstellung zweier Sätze an Kohlenhydratstrukturen möglich, welche zur Untersuchung von Glykan-Antikörper Wechselwirkungen und ihrer biologischen Aktivität verwendet wurden. Die synthetisierten Fragmente stellten wichtige Epitope in der Erkennung durch anti-GPI Antikörper aus Seren von *T. brucei* Infektionen dar. Weiterhin wurde gezeigt, dass Maus Makrophagen durch synthetische GPI dahingehend aktiviert werden, TNF-α auch ohne Stimulation durch IFN-γ zu produzieren. Die Ergebnisse und Durchführbarkeit der hier gezeigten Experimente unterstreicht die mögliche Anwendung von kleineren Fragmenten gegenüber komplexen Strukturen.

ABBREVIATIONS

$[\alpha]_D^{20}$	specific rotation
°C	degree celsius
µm	micro meter
µmol	micro mole
^{13}C-NMR	carbon-13 nuclear magnetic resonance
^{1}H-^{13}C-HSQC	proton - carbon-13-heteronuclear single quantum coherence spectroscopy
^{1}H-NMR	proton nuclear magentic resonance
2C11/12	mouse *macrophage* hybridoma cells
^{31}P-NMR	phosphorous-31 nuclear magnetic resonance
AAG	acylalkylglycerole
Ac	acetyl
Ac_2O	acetic anhydride
AcCl	acetyl chloride
AChE	acetylcholinersterase
ACN	acetonitrile
AcOH	acetic acid
AEP	aminoethylphosphate
AnTat1.1E	*Trypanosoma brucei* strain
Ar	aromatic
BF_3-Et_2O	boron trifluoride diethyletherate
Bn	benzyl
BnBr	benzyl bromide
brsm	by reisolated starting material
Bu_2SnO	dibutyltinoxide
Bz	benzoyl
BzCl	benzoyl chloride
c	concentration
calcd	calculated
CAM	Ceric Ammonium Molybdate
Cbz	carboxybenzyl
CCl_3CN	trichloracetonitrile
CD	cluster of differentiation
CDC	Center for disease control and prevention
$CDCl_3$	deuterated chloroform
$CHCl_3$	chloroform
CKD	tripeptide cysteine-lysine-aspartic acid
cm^{-1}	wavenumber
CNS	central nervous system
CoA	coenzyme A
COD	1,5-cylcooctadiene
COSY	correlation spectroscopy
CSA	camphorsulfonic acid
d	dublett
D_2O	deuterium oxide, heavy water
DAG	diacylglycerol
DBU	1,8-diazabicycloundec-7-ene
DCC	N,N'-dicyclohexylcarbodiimide
DCM	dichlormethane
dd	dublets of dublets
DDQ	2,3-dichloro-5,6-dicyano-1,4-benzoquinone
DIPEA	N,N'-diisopropylethylamine
DMAP	4-dimethylaminopyridine
DMF	dimethylformamide
DNA	deoxyribonucleic acid
Dol	dolichol
dt	dublet of triplets
e.g.	exempli gratia
EA	ethyl acetate
ELISA	enzyme-linked immunosorbent assay
ER	endoplasmatic reticulum
ESI-MS	electrospray inoization mass spetrometry
et al.	et alii
$Et(OEt)_3$	triethylorthoformate
Et_2O	diethylether
Et_3SiH	triethylsilane
EtOAc	ethyl acetate
EtOH	ethanol

EtSH	ethanethiol
FTIR	fourier transform infrared spectroscopy
g	gram
G-15	gel type: fractionation range ≤1500
G-25	gel type: fractionation range ≤1000-5000
Gal	galactose
Glc	glucose
GlcN	glucoseamine
GlcNAc	*N*-acetylglucoseamine
gp	glycoprotein
GPI	glycosylphosphatidylinositol
H^+	proton
H_2	hydrogen
H_2O	water
HAT	human african trypanosomiasis
HCl	hydrochloric acid
Hex	hexane
HexNAc	*N*-acetyl-hexose
HF	hydrogen flouride
HFIP	hexafluoro-2-propanol
$HgCl_2$	mercury (I) chloride
HgO	mercury (II) oxide
HMBC	heteronuclear multiple-bond correlation spectroscopy
HPLC	high-performance liquid chromatography
HVE cells	human vascular endothelial cells
Hz	hertz
i.e.	id est
I_2	iodine
IFN-γ	interferon-gamma
IgG	immunoglobulin G
IgM	immunoglobulin M
IHC	immunohistochemistry
IL-12	interleukin 12
Imid	imidazole
Ino	inositol
Ir	iridium
J	indirect dipole-dipole coupling
K_2CO_3	potassium carbonate
kDa	kilo dalton
KOH	potassium hydroxide
L	litre
l	liquid
Lev	levulinoyl
LG	leaving group
LH20	cross-linked dextran, hydroxypropylated
Lutidine	2,6-dimethylpyridine
m	meter
M	molar mass
m/z	mass-to-charge ratio
MALDI	Matrix-assisted laser desorption/ionization
Man	mannose
MeOD	deuterated methanol
MeOH	methanol
mg	milli gram
MHz	mega hertz
mmol	milli mole
n.d.	not determined
n.s.	not separated
Na	sodium
NaH	sodium hydride
NANA	*N*-acetylneuraminic acid
NaOAc	sodium acetate
NaOME	sodium methoxide
Nap	2-mehtyl-naphthyl group
NCAM	neural cell adhesion molecule
NCL	native chemical ligation
NEt_3	triethylamine
NF-κB	nuclear factor kappa-light-chain enhancer of activated B cells
NH3	ammonia
NIS	*N*-iodosuccinimide
NKT cells	natural killer T cells
NO	nitric oxide
NOESY	nuclear Overhauser effect spectroscopy
P	phosphate
P. falciparum	plasmodium falciparum
p.i.	post injection
PARP	procyclic acidic repetitive

	protein
PB-A	protein blocking agent
PB-T	protein blocking agent
Pd/C	palladium on carbon
PEtN	phosphoethanolamine
PF_6	hexaflourophosphat
PG	protection group
PhSH	thiophenol
PI	phosphinositol
PI-PLC	phosphatidylinositol-specific phospholipase
PivCl	pivaloylchloride
PMB	*para*-methoxy-benzyl
PMBCl	*para*-methoxy-benzyl chloride
$PMePh_2$	methyl diphenyl phosphine
ppm	parts per million
PrP	prion protein
PyBOP	benzotriazol-1-yl-oxytripyrrolidinophosphonium hexafluorophosphate
pyr	pyridine
R	rest
R_f	retention factor
rISG64-1	*T. brucei* cell lysate protein
ROESY	rotating frame nuclear Overhauser effect spectroscopy
rPrP	recombinant prion protein
s	second
$Sc(OTf)_3$	scandium (III) triflate
SEM	scanning electron microscope
SFC	supercritical fluid chromatography
SGC	segmental gene conversion
SPPS	solid phase peptide synthesis
t	time
T. brucei	*Trypanosoma brucei*
T. cruzi	*Trypanosoma cruzi*
T. gondii	*Toxoplasma gondii*
TBAB	tetra-n-butylammonium bromide
TBAF	tetra-n-butylammonium fluoride
TBAI	tetra-n-butylammonium iodide
Tbb	*Trypanosoma brucei brucei*
TBDPS	*tert*-Butyldiphenylsilyl
Tbg	*Trypanosoma brucei gambiense*
Tbr	*Trypanosoma brucei rhodesiense*
TBS	*tert*-Butyldimethylsilyl
TBSOTf	*tert*-Butyldimethylsilyl triflate
TCEP	*tris*(2-carboxyethyl)phosphine
TFA	trifluoroacetic acid
TfOH	triflic acid
THF	tetrahydrofuran
Thy-1	thymocyte differentiation antigen 1
TIPS	triisopropylsilyl, triisopropylsilane
TIPSCl	triisopropylsilyl chloride
TLC	thin layer chromatography
TLF-1	human trypanolytic factor 1
TLF-2	human trypanolytic factor 2
TLR	Toll-like-receptor
TMS	trimethylsilyl
TMSOTF	trimethylsilyl triflate
TNF-α	tumor necrosis factor alpha
TOCSY	total correlation spectroscopy
UDP	uridine diphosphate
VIB	Vlaams Instituut voor Biotechnolgie
VSG	variant surface glycoprotein
WHO	World Health Organization
δ	chemical shift

1. INTRODUCTION

1.1 PROTOZOAN PARASITES

Protozoan parasites are eukaryotic single cell organisms that engage in a heterotrophic life style. They are often classified as animals due to their mobility and medicine refers to them as protists.[1] Human and animal infections usually occur by an insect's bite or by ingestion of contaminated food, but the parasites can also be transmitted by sexual contact. Examples for parasites transmitted by contaminated food are *Entamoeba histolytica*, *Giardia Lamblia*, *Baltandium coli* and *Toxoplasma gondii* that represents the biggest burden, concerning infection rates in developed countries.[2] Parasites that are transmitted by contaminated food are not restricted to a certain part of the world. However, parasites transmitted by an insect bite are mainly limited to developing countries in tropic and sub-Saharan regions since they are mostly transmitted by the tsetse fly. *Plasmodium falciparum* causing malaria, *Leishmania* being responsible for leishmaniasis, *Trypanosoma cruzi* inducing the chagas disease and *Trypanosoma brucei* causing the sleeping sickness in Africa are responsible for millions of deaths each year and are a significant reason for the underdevelopment of the affected countries.[3]

AFRICAN TRYPANOSOMES – *TRYPANOSOMA BRUCEI*

Trypanosoma are single cell parasites belonging to the genus of kinetoplastids and include diverse species such as *Trypanosoma brucei* and *Trypanosoma cruzi*. The distribution is one important distinction that can be observed and used for their designation. Therefore, these two species are also referred to as African (*T. brucei*) or American (*T. cruzi*) trypanosoma. African Trypanosoma are distinguished in three species: *Trypanosoma brucei*, *Trypanosoma evansi,* and *Trypanosoma congolense*, wherby *Trypanosoma brucei* has three subspecies: *Trypanosoma brucei brucei (Tbb)*, *Trypanosoma brucei gambiense (Tbg)* and *Trypanosoma brucei rhodesiense (Tbr)*. As it can be seen in Figure 5, *Tbg* infects humans only and is distributed in central and western Africa. *Tbr* infects mainly animals and lifestock, but is also infectious to humans in southern and eastern Africa. *Tbg* and *Tbr* parasites cause human African trypanosomiasis (HAT), which is also referred as sleeping sickness. *Tbb* is only infectious to animals and lifestock, causing animal African trypanosomiasis, also referred to as Nagana.[4]

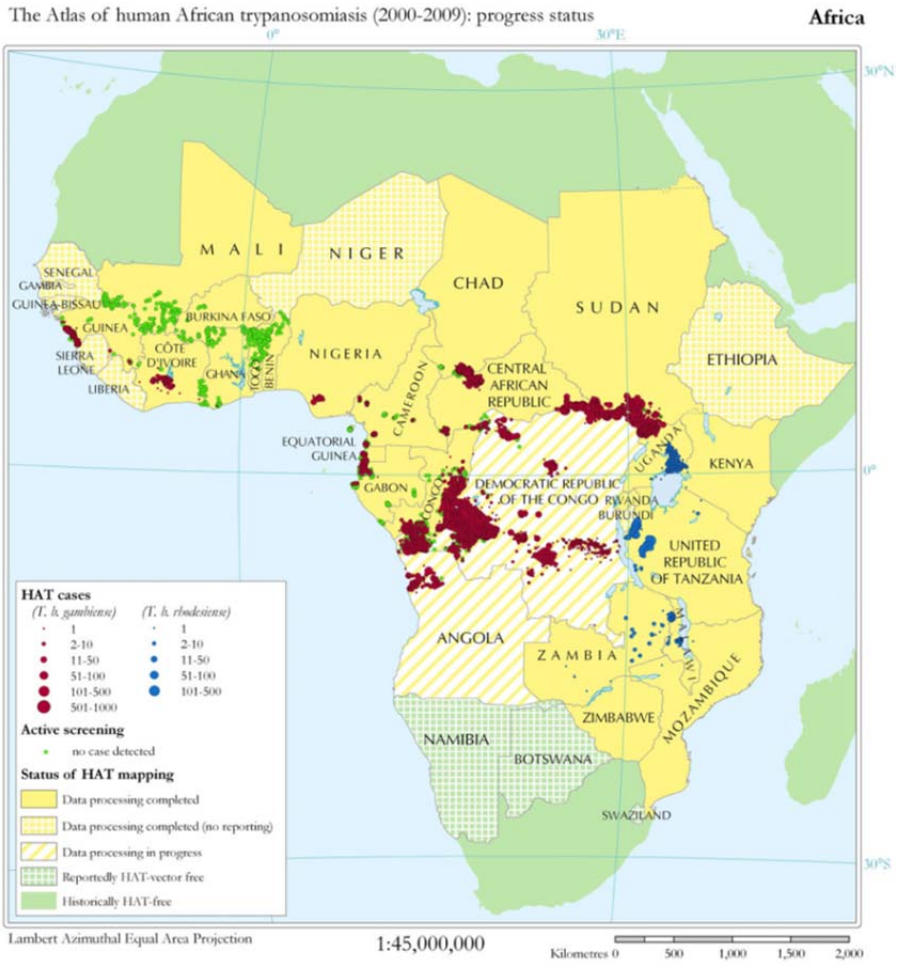

Figure 5: Atlas of human African Trypanosomiasis, a map which precisely determines distribution of the disease[5]

The reason of infection of humans and animals by *Tbr* and *Tbg* is a special protein belonging to the class of Variant Surface Glycoproteins (VSG). This protein is assumed to have its origin in a population of *Tbb*, where the corresponding gene mutated and distributed through Africa by recombination with other *Tb* subspecies. The mutation resulted in auto immunity against the human trypanolytic factors (TLF-1 and TLF-2).[6] Experiments showed that transfer of this gene to *Tbb* parasites reinstalled the ability to infect human cells. These experiments and the fact that *Tbb* is not infectious to humans, makes the parasite the model organism of choice when investigating african trypanosoma.

CHARACTERISTICS OF *TRYPANOSOMA BRUCEI*

T. brucei, like all other African trypanosomes, is an extracellular parasite of 8-50 µm length with a single flagellum arising from the basal body, as depicted in Figure 6. It exhibits a kinetoplast, which contains the whole of mitochondrial DNA and functions as a single mitochondrion.

The parasite is mainly transmitted by the tsetse fly *Glossina*, however a mother to child and sexual transmission might also be possible.[7] In transmission of Nagana, it is assumed that other flies such as *Tabanidae* and *Muscidae* are engaged in a seasonal way.[8]

Figure 6: *Trypanosoma brucei*. A SEM image of the procyclic form from the tsetse fly midgut[9]

The life cycle is a common characteristic of trypanosomes. This is shown exemplarily for human infection in Figure 7.[10] The cycle starts with injection of metacyclic trypomastigotes into the skin of a host by the fly vector (**1**). After passing into the bloodstream, parasites transform into bloodstream trypomastigotes (**2**). Afterwards, trypomastigotes migrate throughout the body, infecting every blood supported vessel and combine in binary fusion (**3**). This stage is called diagnostic stage (**d**), during which parasites are circulating in the blood and can be detected by microscope and immunodiagnostic methods. Furthermore, at this stage (**4**, **5**) a fly can take up trypomastigotes during a blood meal. In the gut of the fly binary fission takes place, releasing two procyclic trypomastigotes out of one (**6**). Transforming into epimastigotes, they leave the gut (**7**). In the final step epimastigotes move to the fly's glands, still engaging in binary fission (**8**). With this, the infectious stage is reached and the fly can transmit the parasites to a new host.

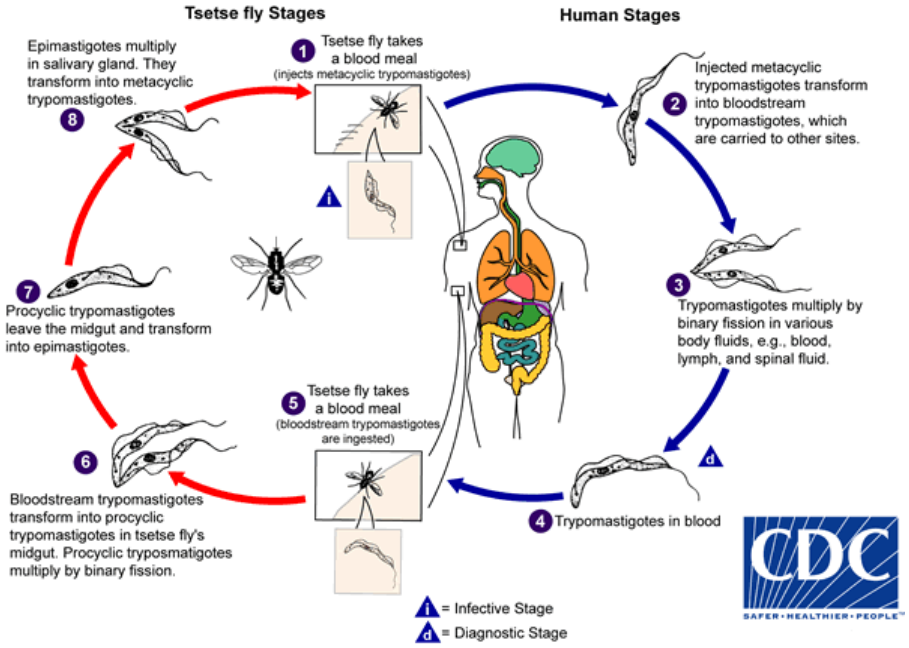

Figure 7: The general life cycle of *Trypanosoma*[11]

PREVENTION, SYMPTOMS, DIAGNOSIS AND TREATMENT OF HAT

Due to the lack of vaccines or prophylactic substances, prevention of infection by trypanosomes is carried out by other measures. Best results can be reached by minimization of contact with tsetse flies, *e.g.* using the right clothing, safety measures in traffic and housing and the use of insect repellent at all times. Habitants of endemic areas often are aware of heavily infected regions and are a good source of information on this matter.[11]

After infection, the parasites proliferate in the bloodstream and increase their number without crossing the blood-brain-barrier, *i.e.* the haemolymphatic phase.[12] During this phase, headaches and bouts of fever go in hand with fatigue. In the neurologic phase, or phase two, parasites cross the blood-brain-barrier inducing serious sleep cycle disruptions, paralysis, progressive mental deterioration and ultimately death.

Due to the unspecific nature of the symptoms during the haemolymphatic phase, the infection generally goes undiagnosed, thereby enhancing transition into the second disease stage. Definite confirmation of infection by trypanosomes can be accomplished by examining a drop of blood under the microscope.[11] However, this method gives only information about infection by an extracellular parasite. The specific type has to be investigated by serological test, such as ELISA or IHC. Additionally, to distinguish between blood phase and haemolymphatic phase a lumbar puncture is needed to examine the cerebrospinal fluid. For the detection of *Tbg* a card agglutination test has been developed.[11] This card is generally used to confirm already suspected infections.

Low reliability and the difficulty of available tests highlight the necessity of better diagnostic tools. In this regard, recently a promising test has been developed by Ferguson *et al.*[12] The protein rISG64-1, contained in the lysate of trypanosomes, was combined with the isolated surface protein VSG 117 in a dual lateral flow test. Screening studies of a sera pool of infected persons delivered 99.3% specificity for an infection by *Tbg* and 83.9% specificity for an infection by *Tbr*. However, the main drawback of this method is the cultivation of the parasites for the isolation of the proteins.

Depending on the results of diagnosis, a standardized medication plan is developed.[11] The first line drugs for both stages are still highly effective and only single cases showed resistance of parasites against the compounds.[13] Suramin, Pentamidine, Eflornithine, Nifurtimox, Melarsoprol and Prednisolone are established on the market as anti-parasitic drugs, posing activity against tumors and other microorganism as well. Site effects are often severe and contradictory to pregnancy, during lactation and childhood. These cost intensive drugs are administrated in long and complicated dosing schedules often together with chemotherapy and require handling in clinical environment. All these implications of late stage diagnosis and treatment highlights the need for facile and cost effective early stage diagnosis.

1.2 HOST IMMUNE SYSTEM AND PARASITE INTERACTION

During infection with African trypanosomiasis, the parasite and the host undergo an interaction of their respective armory. Over the time of a myriad of infection cycles within the same type of hosts, the parasite developed a strategy to survive. This strategy is a cooperation of several mechanisms to evade, suppress or weaken the host immune system. It relies on the production of virulence factors and the pathogenesis of the trypanosome.[14]

VIRULENCE FACTORS IN TRYPANOSOMES

Both, living and dead parasites, contribute to the control of the host immune system. Membrane bound substances and biomolecules in the lysate of a parasite cell can come in contact with the cells of the host. A major role is played by variant surface glycoproteins (VSG) that densely cover the parasite with several million copies and are part of the evasion strategy of the parasite. These glycoproteins are bound to the cell membrane by a glycosylphosphatidylinositol (GPI) anchor. Beside VSGs, trypanosomes produce a number of enzymes to enhance the control of the host immune system.

Sialidases have been found in several trypanosome subspecies.[14] These GPI-anchored enzymes hydrolyze the sialic acids from thrombocytes resulting in serious phagocytosis of the affected platelets.[15] Furthermore, the treatment of red blood cells and macrophages with a sialidase leads to subsequent phagocytosis and loss of binding capacity respectively.[16]

Proteases, such as cysteine proteases and serine oligopeptidases, trigger upon specific immune responses, which are vital for the survival of trypanosomes. Cysteine proteases control the transendothelial migration of parasites through the blood-brain-barrier.[17] Additionally, they are active in causing anemia and are responsible for the degradation of a number of protein substrates.[18] Oligopeptidases are accountable for the degradation of peptide hormones such as the atrial natriuretic factor.[18a, 19] This process leads to hypervolemia[20] and cardiomyopathy,[21] and is a direct consequence of the beginning phagocytosis of the parasites.[18a]

Autolysed trypanosomes set free phospholipases that generate free fatty acids in the host.[22] These released acids can destabilize membranes[23] and act as hemolytic and cytotoxic detergents.[24] Observed results of these processes are erythrocyte degradation, damage to vascular endothelial cells and hemolysis. Finally, the trypanosomes generate substances which are classified as trypanokines. These B-cell mitogens[25] and T lymphocyte triggering factors[26] are believed to influence the immune cascade of the host to enhance survival and proliferation.

PATHOGENICITY OF TRYPANOSOMES

Evasion is a major mechanism in the survival of the trypanosomes under the influence of the immune system. Antigenic variation, excessive activation of the complement system, down regulation of nitric oxide production, marked immunosuppression and polyclonal B-lymphocyte activation are the driving forces of the evasion mechanism.[27]

Anemia, the most typical symptom of the disease, is generally caused by detergent activity of released fatty acids and the mechanical injury through the flagella of the parasites.[28] Platelet aggregation, undulating pyrexia, tumor necrosis factor (TNF) and nitric oxide (NO), toxins and metabolites of trypanosomes, lipid peroxidation and malnutrition contribute to the lack of red blood cells, blood cells in general and the body's capability to regenerate.[22, 28-29]

The infection by the parasite leads to the discharge of trypanosome-released triggering factor. This factor stimulates the production of interferon-gamma (IFN-γ), which usually goes in hand with a protective response in virus and protozoa infections. However, trypanosomes

are using IFN-γ as a parasite growth factor, reversing the intended effect of the natural inflammation markers.[26]

The use of immune mechanisms for the benefit of the parasite is also true for nitric oxide (NO), a common immune defense radical, and tumor necrosis factor alpha (TNF-α), a major representative of the cytokines. Beside its anti-trypanosomial effects, TNF-α is involved in mechanisms that can destroy host tissues and favor parasite growth by inducing fever, asthenia, inflammation, cachexia and hypertriglyceridemia.[30]

Immunosuppression is often achieved by polyclonal B-cell activation to hamper a specific response against the infectious organism.[31] Trypanosomes generate suppressor T cells and suppressor macrophages by using the factors mentioned above.[32]

The synthesis and release of NO in the host competes with the needs of the parasite for L-Arginine for DNA synthesis and L-Ornithine biosynthesis. While, a depletion of plasma L-Arginine hampers trypanosomial proliferation, it abrogates the release of NO in the host.[30, 33]

ROLE OF VSGS AND GPI GLYCOLIPIDS IN AFRICAN TRYPANOSOMIASIS

VSGs are the major surface proteins of *Tb* and are connected to the cell membrane via attachment to a GPI anchor (Figure 9). Beside dense packing of up to 10^6-10^7 copies of dimers of the glycoprotein, resulting in the construction of a diffusion barrier, the main function is antigenic variation.[34] New copies of VSGs are released upon stress from the immune system, switching to a random number of different amino acid sequences. Dead parasite cells release their VSG coat in the blood stream inducing an immune response. This mechanism raises antigenic variation, and leaves the immune system overwhelmed by the presented antigens.[35]

Invariant surface proteins of *T. brucei* are protected by the present of VSGs, which shield them from binding and complement processes.[36] If the immune system produces antibodies against a VSG, marked copies are transported to the flagellar pocket by the parasites mobility drag. Reaching this position, the copies are internalized, degraded and recycled.[37]

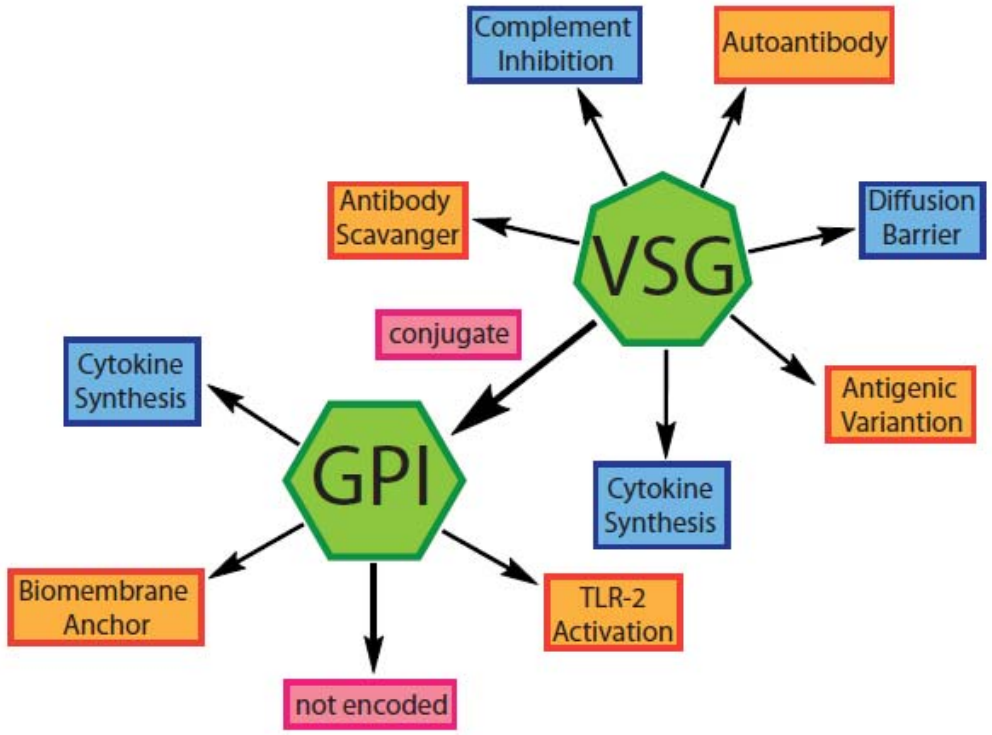

Figure 8: Representation of the interaction of VSG and GPI and their respective roles played in the infection process

The GPI anchor is bound to the C-terminus of VSG and is released with the protein from the membrane by phospholytic cleavage of the anchoring lipids. Thus, VSG and GPI are often initiating an immune response together, complicating distinction of respective functions. Isolated GPIs, however, show the ability to induce inflammatory effects by activation of Toll-like-receptor 2.[38] Interacting with GPIs, macrophages release IL-12, TNF-α, reactive oxygen species and nitric oxides.[39] Especially the release of TNF-α has been associated to distinct GPI structural features.[40] The unique α-galactosides in the side branch of *Tb* GPI are essential for the induction of TNF-α. However, it has been shown, that the pseudodisaccharide together with the diacylgylcerol suppresses the protein tyrosine kinase signal maximizing the TNF-α gene expression.[40]

Glycosylation mechanisms and glycan biosynthesis are controlled by the enzyme machinery of the cell and the available monosaccharides substrates. Thus, the variation on the GPI is not directly encoded in the gene apparatus of *Tb* and underlies less variation than the VSG itself.

HOST RESPONSES TO INFECTION BY TRYPANOSOMES

Susceptibility of the host is a requirement for an infection by African trypanosomes. When the host is not protected from infection by a camouflage coat color, trypanodestructive antibodies are required to prevent of a severe infection. Reduced levels of parasites and elevated serum concentrations of red blood cells are key to survival.

In endemic areas, a certain trypanotolerance is known to be present in domestic livestock. This tolerance is connected to a higher endurance in severe anemia and to a higher capacity of parasitemia control.[41] The control of anemia starts in the bone marrow, where more red blood cells are produced. In addition, new red blood cells expose more sialic acids that are added through upregulation of the corresponding sialyltransferases.[42] Furthermore higher complement levels and a superior humoral response enhance the control of the parasite number.[43]

1.3 VARIANT SURFACE GLYCOPROTEIN (VSG)

VSGs are a master piece of evolutionary progress. Its early described electron-dense coat[28b, 44] on the surface of the trypanosome parasite plays three major roles in host immune evasion. First, with up to 90% VSGs are the overwhelming amount of proteins, dwarfing any number of other important proteins. The pure number of VSG copies shields these other proteins from being recognized by the immune system. The second role is antigenic variation. The constant release of immunological distinct VSGs keeps the immune system occupied, enhancing the infections progress and the host immune evasion. A third role is the activity of VSGs as an antibody scavenger. Attached antibodies are easily removed from the cell surface by internalization and degradation of corresponding VSGs.

To understand the role of the VSGs during the infection process and the life cycle of the trypanosomes, their structure, biosynthesis and antigenic variation have to be considered. As part of this it was shown, that rapid modification of the GPI by the VSG,[45] transport of the conjugate to the cell surface in extraordinary speed,[46] fast endocytosis and recycling pathways[47] and realization of the vast amount of VSG copies,[48] are arguments for a metabolism fully focused on maintaining the VSG barrier.

STRUCTURE

VSGs are a family of proteins that vary in amino acid sequence and glycosylation site and state. These glycoproteins have a molecular weight of around 58 kDa, are attached to the membrane by GPI anchors and have a dimerized α-helical structure as shown in Figure 9. While the C-terminal, modified with the GPI, is deeply buried within the complex, the N-terminus is exposed, highly variable and monoallelically expressed from a repertoire of a few hundred genes.[49]

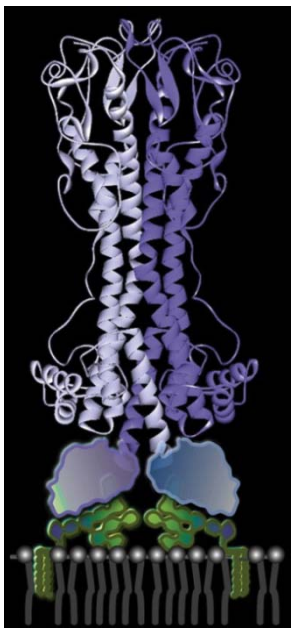

Figure 9: Structure of VSG; heavily glycosylated α-helices are protecting the surface from being in contact with foreign substances; VSGs are anchored to the outer leaflet of the biomembrane by a GPI[50]

The N-terminal sequence of VSGs consists of 350-400 amino acids, the C-terminal region is build up from 50-100 amino acids.[51] Several attempts to unify VSGs in classes have been made. A common approach to classify proteins of the same origin or to determine a relation to a protein of another organism is to compare the cysteine residues within the amino acid sequence. Cysteine residues often form disulfide bridges, limiting the chemical and structural space resulting from the fixed secondary and tertiary structure in their direct environment. By this approach, VSGs were divided into three different types (A, B, C) concerning their N-terminal region, and four different types (1, 2, 3, 4) determined by their C-terminal region.[52] In both cases the amount of conserved cysteine residues is increasing towards the latter types. This classification makes any combination of N- and C-terminal regions possible.

In the VSG biosynthesis, the N-glycosylation with glucose residues at the non-reducing end[53] and the pathways of mannose-glycosyltransferases for triantennary structures are abrogated. These processes result in paucimannoses as the major glycosylation type.[54]

BIOSYNTHESIS

The high number of VSGs being expressed within an eight hour cell cycle underlines the dependence of trypanosomes on the synthesis of VSGs to protect themselves from the host's immune system (Figure 10).[47a] Approximately 20 000 mature, correctly processed and targeted VSGs are produced per minute.[55] Together with the assumption that VSG synthesis and processing is far from perfect, the real number may approach six digits.[56] This significant burden on the parasite results in adaption of the biosynthesis to support the demand of VSGs.[57]

The expressed polypeptide of the nascent VSG bears an N-terminal signal sequence that directs the complex to the ER using a non-elucidated transport mechanism.[58] Reaching the ER, the maturation of the protein complex begins with the cleavage of the signal peptide by an unknown protein.[58e, 58f] After that, post translational modification at a glycosylation site is conducted by an oligosaccharyltransferase complex. Its homologue has been identified in *T. brucei*.[53, 59] This complex, in comparison to the eight subunits of higher eukaryotes, consists of only three proteins, mirroring a level of biosynthetic minimization. Only paucimannose type glycans are transferred. It is believed, that the spared resources of not having high-mannose structures with glucose residues at the non-reducing end, support the stressed biosynthesis of the required GPIs.[54]

The C-terminal region bears a GPI signal sequence that is cleaved off in the ER and replaced with a GPI by the GPI *trans*-amidase complex.[58f, 60] Only GPI modified VSGs are subjected to proper folding and transfer mechanisms. This is ensured by a number of homologues of quality control, such as folding and oligosaccharide processing, proteins found in *T. brucei*.[60-61]

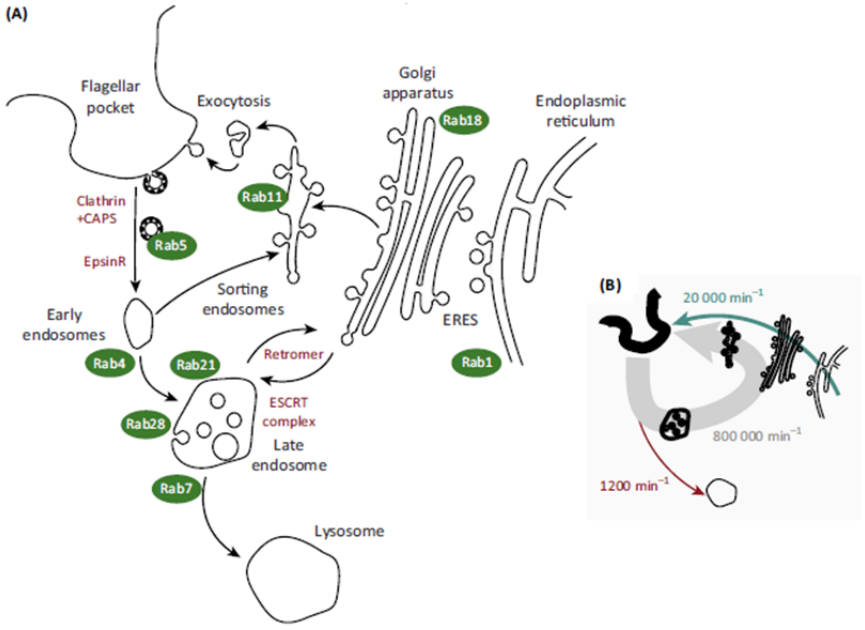

Figure 10: A) intracellular compartments responsible for VSG biosynthesis and trafficking; Rab-protein family members mark points where eukaryotic homologues are known; arrows indicate the known transport routes; B) smaller version of the biosynthetis-endocytosis-recycling pathways indicating the concentration gradient of the VSGs[62]

The release of the glycosylated and dimerized VSGs from the ER to the Golgi apparatus takes place at ER specific exit sites. In the case of *T. brucei,* they are unusual close to the Golgi apparatus and could represent another adaptation for streamlining the VSG production.[63] Within the Golgi, the α-galactoside side chain of the GPI is extended. At least one galactose is already transferred in the ER.[64] In addition, modification of the *N*-glycans takes place, which is again defined by the lack of mannosyltransferases.[65]

The transport of the mature VSG-GPI-conjugate to the cell surface has been less investigated. This is in part due to the high amount of recycled VSGs that is internalized from the cell surface and dwarfs the amount of newly biosynthesized VSG. However, it is suggested, that sufficient amounts of new protein are accumulated in microdomains, controlled by lipid interactions.[48b, 66]

New VSGs reach the cell surface within 7 to 8 minutes.[46] The transport to the surface is fast and efficient at multiple levels and it is supported by vesicles which transport new VSGs in a density comparable to the surface of 30 000 dimers per µm². This mechanism is supported by the low concentration of VSGs along the ER and the Golgi compared to the dramatically increased number of VSGs at the exit site of the Golgi.[47b, 48b, 55]

ENDOCYTOSIS AND RECYCLING

All endocytosis processes are upregulated by a factor of ten in the mammalian phases of the parasite compared to its insect form, enabling the parasite to internalize its entire plasma surface within 12 minutes.[47b, 67] Some reports suggest that this speed of internalization is achieved by the knock-out of concentration dependent transporter proteins, which are abundant in other eukaryotes. This results in a prioritization of the removal of VSG molecules over other surface molecules. A mechanism, that likely supports the integrity of the diffusion barrier build by the VSG.[68]

The speed of internalization requires a specific recycling system and the knowledge of this process is far from advanced.[69] However, it was shown that the recycling cascade of trypanosomes distinguishes surface proteins with a transmembrane domain from GPI anchored proteins by sorting transmembrane domains out. This results in a process, which rather considers non-VSG type proteins for degradation, leading to a more efficient control system and faster turnover of VSGs.[36c, 70]

ANTIGENIC VARIATION AND MOSAICISM

Trypanosoma brucei possesses several thousand genes in subtelomeric sites that can undergo expression to result in a new distinct VSG sequence.[71] When the parasite interacts with the host immune system, this spontaneous gene switching occurs in a range of 0.1% to 1% per parasite and generation.[72]

Beside other pathogens[73] *T. brucei* undergoes a process called segmental gene conversion (SGC).[74] Here, a conversion occurs in the open reading frame, where segments of an expressed gene are replaced by other genes, resulting in a totally new variant. Usually this progress occurs only in smaller regions of the genes, resulting in related but distinct new sequences. *T. brucei* makes use of these regions, as they are the immunodominant region of the N-terminal domain.[75] In considerably fewer cases the interconversed regions are part of the C-Terminus, an exception where SGC is called mosaicism.[76]

Interestingly, the process of heavy SGC and mosaicism accumulates towards later, chronic stages of an infection with the parasite.[77] Constantly new waves with high numbers of distinct variants are released simultaneously in an infection process as shown in Figure 11A.[77b] This is explained by the fact that upon engagement of a particular VSG by the immune system, only those parasites will survive, which are undergoing antigenic variation during proliferation. In later phases, simple gene switching might not by sufficient, although

B-cell activation is considerably reduced in heavy parasitemia. SGC and Mosaicism will be more efficient in these phases. The new variants are more likely to pose little or no cross-reactivity towards their predecessor.[77a] When the immune system begins to break down, reduced SGC and mosaicism are observed and the waves are flattened as illustrated Figure 11B.[77b]

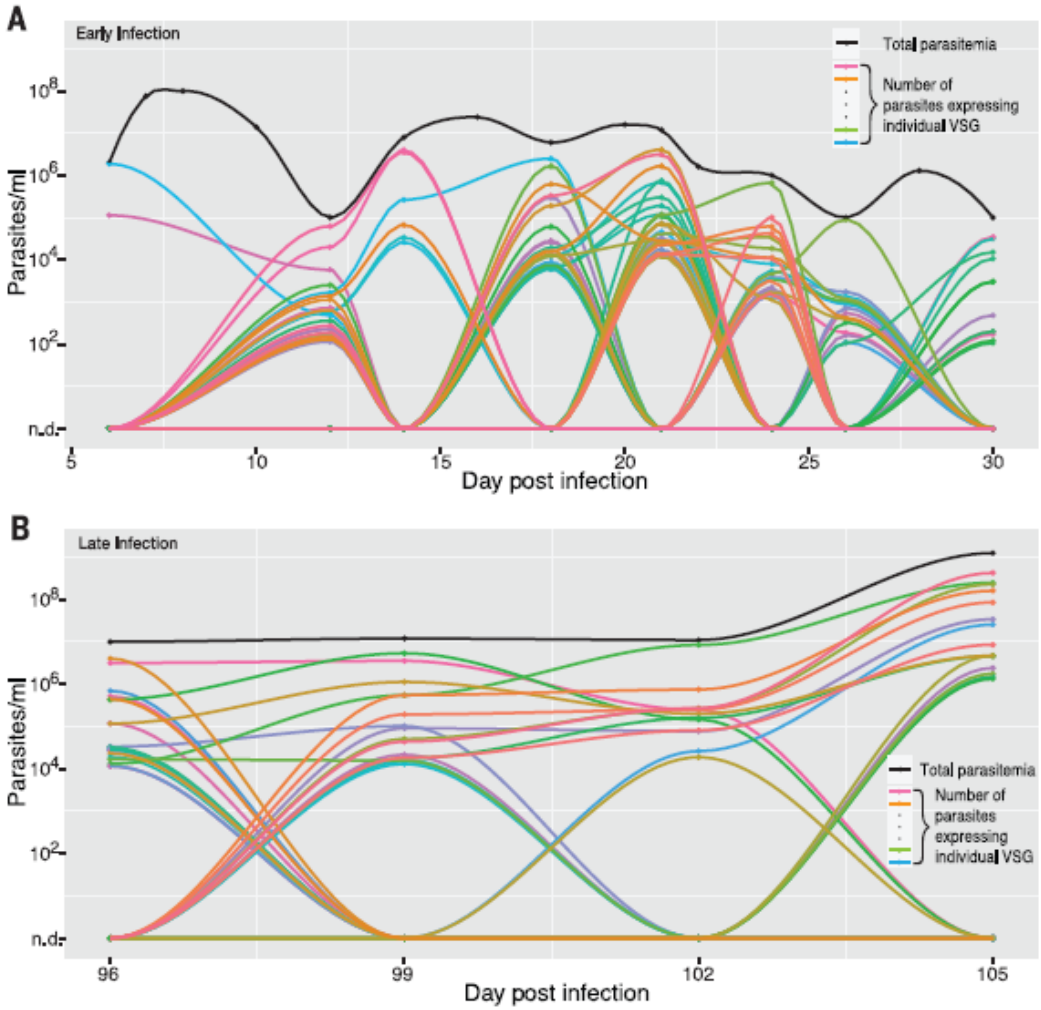

Figure 11: Diagram visualizing distinct VSG released at any given time point during infection of a mouse. A) During early and advanced infection phase, number of new variants is increasing and waves of single variants are short and step; B) During late phases, approaching the breakdown of the immune system, waves are longer and more flattened due to the lack of immune response; Note: Same colors do not indicate the same variant, once a variant disappears due to assay sensitivity it was not observed again[77b]

1.4 GLYCOSYLPHOSPHATIDYLINOSITOL (GPI)

CHEMICAL STRUCTURE OF GLYCOSYLPHOSPHATIDYLINOSITOLS

GPIs have a conserved core structure presented throughout all eukaryotic cells, that consists of three mannose residues, a glucosamine, and myo-inositol connected to a phospholipid ($H_2N(CH_2)_2OPO_3H$-6Manα1→2Manα1→6Manα1→4GlcNα1→6*myo*-Ino1-OPO_3H-Lipid)[78]. Depending on tissue, organism and cell-type, appendages to this core structure include: addition of monosaccharide units such as galactose and mannose to the Man III, branching at either the C3 or C4 position of the Man I, and additional phosphorylations and lipidations (Figure 12 and Table 1).

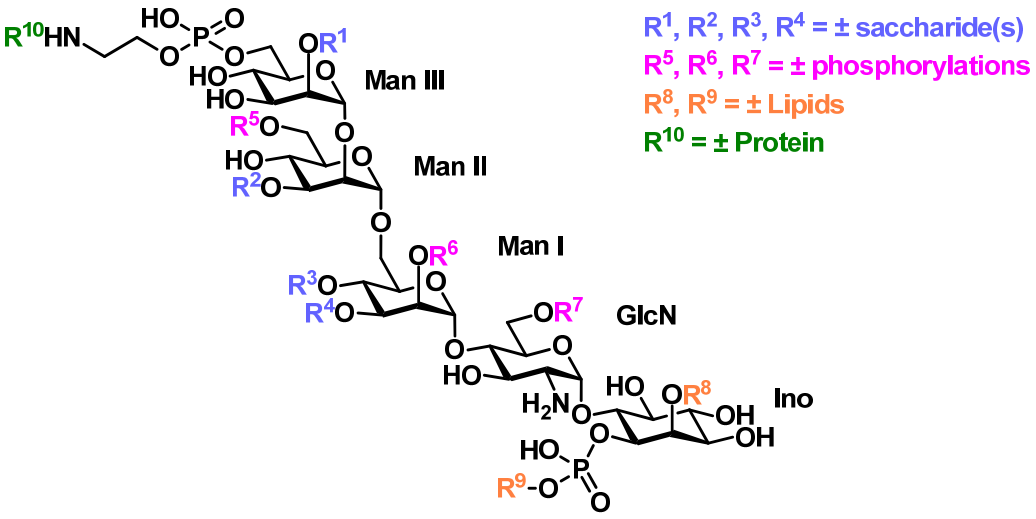

Figure 12: General structure of GPIs. The black core can bear different appendages depending on the species, tissue and cell-type origin (see Table 1).

Protozoan parasites (entry 1 to 12, Table 1) often bear highly specific and unique saccharide units which endow the activity of the structures in inflammation. The GPI of *Plasmodium falciparum* (entry 1) has been assigned to be the toxin of the disease.[79] The GPI of *Toxoplasma gondii* (entry 2) is the low molecular weight antigen and thus useful for the diagnostic of the corresponding infection.[80] Similar roles are assumed to be played by the galactose residue in trypanosomes. *Trypanosoma cruzi*'s GPIs, with known origin, usually do not exhibit galactose residues (entry 9 to 11). However, a GPI anchor with its source from the parasite bears the same α-tetra-galactoside as *Trypanosoma brucei* (entry 5 to 7) making it a specific structure of highly virulent trypanosomes.[81] Mammalian GPIs present a specific additional phosphorylation at the Man I (entry 13 to 22).[82] In addition to that, a β-linked GalNAc structure is commonly attached at C4 of the Man I.

Entry	Species	R^1	R^2	R^3	R^4	R^5	R^6	R^7	R^8	R^9	R^{10}
1	*Plasmodium falciparum*	±Manα	H	H	H	H	H	H	acyl	DAG	±Protein
2	*Toxoplasma gondii*	H	H	GalNAcβ	H	H	H	H	H	DAG	Protein
3	*Toxoplasma gondii*	H	H	Glcα-GalNAcβ	H	H	H	H	H	DAG	H
4	*Trypanosoma congolense*	H	H	Galα-GlcNAcβ	H	H	H	H	H	DAG	±Protein
5	*Trypanosoma brucei VSG117*	H	H	H	$Gal_{2\text{-}4}α$	H	H	H	H	DAG	Protein
6	*Trypanosoma brucei VSG121*	H	Galβ	H	$Gal_{2\text{-}4}α$	H	H	H	H	DAG	Protein
7	*Trypanosoma brucei VSG221*	±Galα	±Galβ	H	$Gal_{2\text{-}4}α$	H	H	H	H	DAG	Protein
8	*Trypanosoma brucei PARP*	H	H	Sialylated	H	H	H	H	acyl	AG	Protein
9	*Trypanosoma cruzi epimastigote*	Manα	H	H	H	H	H	H	acyl	AAG	Protein
10	*Trypanosoma cruzi NETNES*	Manα	H	H	H	H	H	AEP	H	AAG	Protein
11	*Trypanosoma cruzi 1G7*	Manα	H	H	H	H	H	±AEP	H	AAG	Protein
12	*Leishmania major PSP*	H	H	H	H	H	H	H	H	AAG	Protein
13	*Human kidney membrane dipeptidase*	±Manα	H	(±Galβ1−3)GalNAcβ	H	nd	PEtN	H	H	nd	Protein
14	*Human erythrocyte AChE*	H	H	H	H	±PEtN	PEtN	H	acyl	AAG	Protein
15	*Human urine CD59*	±Manα	H	±GalNAcβ	H	H	PEtN	H	acyl	nd	Protein
16	*Human placental Apase*	H	H	H	H	±PEtN	PEtN	H	H	AAG	Protein
17	*Human CD52*	±Manα	H	H	H	±PEtN	PEtN	H	acyl	DAG	Protein
18	*Rat brain Thy-1*	±Manα	H	±GalNAcβ	H	H	PEtN	H	H	AAG	Protein
19	*Mouse skeletal muscle NCAM*	±Manα	H	±GalNAcβ	H	H	PEtN	H	H	nd	Protein
20	*Hamster brain scrapie prion protein*	±Manα	H	±NANA)- (±Gal)-GalNAcβ	H	H	PEtN	H	H	nd	Protein
21	*Pig kidney membrane dipeptidase*	H	H	±Galβ1−3)GalNAcβ or (±NANA) - GalNAcβ	H	H	PEtN	H	H	DAG	Protein
22	*Bovine liver 5'-nucleotidase*	±Manα	H	±HexNAc or	±HexNAc	±PEtN	PEtN	H	H	nd	Protein
23	*Aspergillus fumigatus PhoAp*	Manα1−3Manα	H	H	H	H	H	H	H	ceramide	Protein
24	*Saccharomyces Cerevisiae gp125*	±Manα1−2Manα or Manα1−3Manα	H	H	H	H	H	H	H	DAG	Protein
25	*Pholiota communis arabinogalactan proteins*	H	H	GalNAcβ	H	H	H	H	H	ceramide	Protein
26	*Dictyostelium discoideum PsA*	±Manα	H	H	H	nd	nd	H	H	ceramide	Protein

Table 1: Representation of the structurally elucidated GPI Anchors; nd = not determined, AAG = acylalkylglycerol, DAG = diacylglycerol, NANA = sialic acid, PEtN = phosphoethanolamine, AEP = aminoethylphosphonat

The role of the state of the lipidation and its saturation is heavily discussed in literature.[83] Additional acylation at the 2-O position of inositol is required in GPI biosynthesis, since this modification prevents the phosphatidylinositol-specific phospholipase C (PI-PLC) enzyme from cleaving the glycan part from the membrane in intact GPIs. The exact composition of the fatty acids present in a GPI strongly influences its interaction within regions of elevated cholesterol and sphingolipid content. These so called lipid rafts are rich in GPI-bound Proteins.[84] Finally, unsaturated lipids (entry 1 and 9 to 11) are believed to have an influence on the role of the GPI played in the immune response in infected individuals.[14, 85]

BIOLOGICAL FUNCTION OF GPIS

Beside the primary role of the GPI as an anchor for cell surface proteins to the outer leaflet of the biomembrane, other roles are difficult to prove and investigate. One can assume, that GPIs, considering their conserved structural properties in all eukaryotic cells and simpler ways of anchoring proteins, are responsible for a number of mechanisms in and between cells. Special functions such as protein sorting, microdomain formation, immunomodulatory, diagnostic antigens and cross reacting antigen, have been proven only for certain GPIs and thus, are not to be generalized.

PROTEIN SORTING

The change of the anchoring mechanism, from a GPI to a transmembrane domain, can lead to a dislocation of the corresponding process in polarized cells. While GPI anchored Thy-1 proteins are sorted in the apical domain in epithelial cells, this location changes to a basolateral sorting when the GPI is abstinent.[86] The GPI thereby seems to function as an inducer of an apical targeting signal for these cell types.[87] Similar to this, GPIs are often found along the axons of polarized neurons.[88]

MICRODOMAIN FORMATION

GPIs may be organized in microdomains for the delivery of a cellular response. However, until today it is theorized, that these microdomains organize upon a not yet fully understood mechanism[89] by the accumulation of smaller domains of up to 15 GPI anchored proteins. Small and microdomains both were observed in experiments.[90]

IMMUNOMODULATOR

GPIs are ligands of Natural killer T cells and macrophages, where they can trigger an immune response.[91] While the carbohydrate moiety of the GPI is sufficient to induce the

TNF-α production in macrophages, the activation of the CD1 complex in NKT cells requires a lipid moiety.[92]

Human Vascular endothelial (HVE) cells and macrophages incubated with only the isolated GPI structures of *Plasmodium falciparum* and *Trypanosoma brucei* differ in the release of cytokines. Macrophages produced TNF-α and IL-1, while HVE cells released nitric oxide synthase, intercellular adhesion molecules and vascular cell adhesion molecules.[93] These experiments suggest that a certain structural component of the GPI is responsible for the release of the chemokines.

In the case of Malaria it was shown, that the GPI of *Plasmodium falciparum* plays the role of a toxin. Schofield and coworkers showed that the injection of isolated GPI to mice induced processes similar to an acute malaria infection, including pyrexia, hypoglycemia and death.[94] Similarly, isolated and synthetic GPIs of *Toxoplasma gondii* induce macrophages to release TNF-α when the structure is not lipidated.[95] The activation takes place through toll-like receptors and the transcription of factor NF-κB.

Taking these observations into account, it is clear that GPIs play an important role as immunomodulators. However, a common feature is yet to be indentified.

GPI IN CROSS REACTION WITH ANTI-GPI ANTIBODIES

Although the GPI glycan structure bears specific modifications depending on species, tissue and cell-type, the core structure and two phosphorylation sites are conserved. It is this core structure which defines a cross-reacting determinant.[96] Antibodies raised against isolated structures or from patient and animal sera, recognize specific motifs of the corresponding GPI.[96-97] However, recognition of structures lacking these epitopes was observed. This second binding is much weaker, making a distinction of certain GPIs only possible by measuring the binding intensity.

At the same time, glycobiology of GPI is difficult to investigate, when pure homogeneous material is missing. Low amounts, impurities and heterogeneity hamper assays and might lead to false positives or artifacts. Total synthesis of defined GPI structures and their deletion sequences facilitates the field of cross-reactivity research. Specific structures can be tested for their binding to patient sera, deciphering the smallest and specific binding epitope, thus enabling the development of vaccines and diagnostics. At the same time, the cross-reacting determinant and other applications of the specific GPIs can be further investigated.

One of the most powerful tools to investigate carbohydrate protein interactions are glycan microarrays. Here, isolated structures from natural sources,[98] libraries generated from natural glycans[99] and fully synthetic glycans[100] are typically investigated in their recognition by proteins, antibodies, viruses, bacteria and mammalian cells. Immobilization of these compounds is performed on microtiter plates, functionalized glass slides, nitrocellulose coated slides, gold slides and others.[101] Depending on the structures used and the target being investigated, a different mechanism of immobilization is applied. Beside affinity adsorption which predominantly uses electrostatic interactions[102] and non-covalent immobilization, employing a self-assembled alkylthiolate monolayer to immobilize lipidated structures,[103] covalent immobilization is widely used. Site-specific covalent immobilization methods are mostly based on the reaction between thiol or amine functionalized structures and malemide or epoxy groups on the slide.[101d, 102c, 103a, 104] Other non-specific methods to covalently attach glycans to the surface are condensation, amide coupling, Diels-Alder reactions, carbenes and radical coupling.[103a, 105] Once the compounds are bound to the slide, the interaction partner, *e.g.* sera, proteins, cells, is left for incubation. The most common type for detection methods of carbohydrate arrays relies on fluorescence. This is typically achieved by employing a protein equipped with a fluorescence tag directly or indirectly as a secondary antibody. Evaluation of binding is executed using a fluorescent microarray scanner. Albeit recent improvements such as live-cell imaging, autofocusing, faster image analysis and coupling with mass spectrometry, fluorescence read out is still predominantly used to examine glycan microarray.[106]

PLASMODIUM FALCIPARUM GPI – AN ANTI-GPI ANTIBODY TARGET

During the effort in developing an anti-toxic vaccine against malaria, the group of Seeberger, synthesized the GPI of *Plasmodium falciparum* and ligated it to the Keyhole limpet hemocyanin protein for the injection into mice.[79a] The recipients were protected against consecutive malarial acidosis, pulmonary oedema, cerebral syndrome and fatality after infection with the parasite. Beside these results, one main finding of the investigation was that isolated anti-glycan IgG are binding to infected erythrocytes (Figure 13).

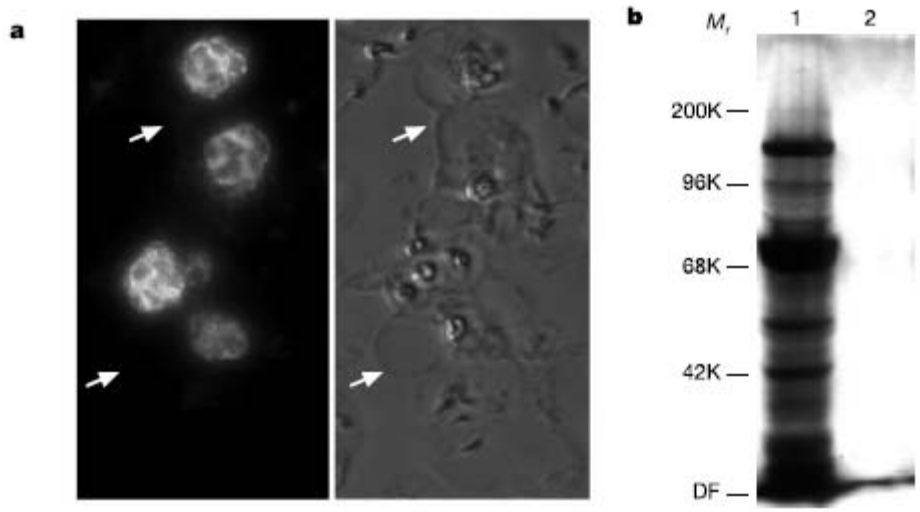

Figure 13: a) immunofluoescence assay of infected (bright) and uninfected (arrow) erythrocytes, b) western blot of anti-glycan IgG against parasite infected (lane 1) and unifected erythrocytes (lane 2)[107]

Interestingly, the isolated antibodies showed no binding to uninfected erythrocytes, neither in an immunofluorescence assay, nor in a western blot. Erythrocytes and *Plasmodium falciparum* are bearing structurally closely related GPIs. Differences are an additional phosphorylation site on Man I for the erythrocytes and an additional mannose residue on Man III (Table 1) for *Plasmodium falciparum*. This result indicates, that there is no cross reactivity between GPIs from *Plasmodium falciparum* and those of mammal erythrocytes, highlighting the specificity of these anti-glycan antibodies.[107a]

In a later study the group designed a set of fully synthetic molecules, which were structurally related to the GPI of *Plasmodium falciparum* (see Figure 14).[108] These compounds were investigated in a glycan microarray[109] towards their binding to antibodies from sera of infected and uninfected persons.[107a]

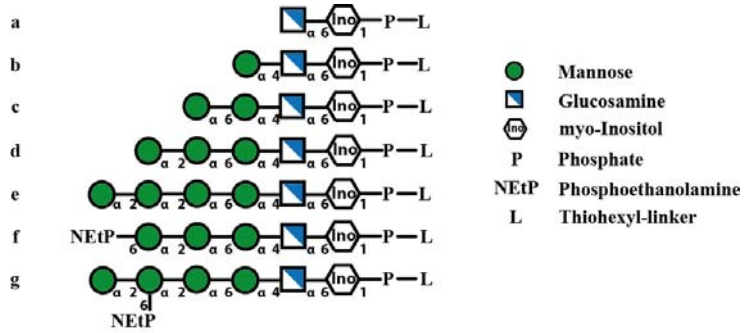

Figure 14: synthetic GPI structures of *P. falciparum* used in the glycan microarray

Persons exposed to parasite endemic areas have high IgG titers against the corresponding presented antigens. Thus, it was not surprising to find intensive binding of malaria-exposed adult Africans sera to the full structures of *Plasmodium falciparum* GPI, and

to smaller fragments with the core of Man_3-$GlcNH_2$-Ino (Figure 14, compounds **d** – **g**) respectively. The sera of European adults with no contact to malaria were binding the higher mannose structures Man_4-$GlcNH_2$-Ino (compounds **f** and **g**), but showed no activity against the shorter sequences (compounds **a** – **e**). These results suggest that mono-phosphorylated Man_3-$GlcNH_2$-Ino structures might present the epitope of an anti-Malaria-GPI response. To solve this question the sera of European volunteers, involved in a sporozoite challenge vaccine trial, were investigated with the compounds. Interestingly, the sera showed the development of a robust anti Man_3-$GlcNH_2$-Ino response.

With this investigation it was shown, that GPI structures, differing from the mammalian version by the lack of the phosphorylation at Man I, are not cross reactive with other body own structures.

TOXOPLASMA GONDII GPI – A DIAGNOSTIC ANTIGEN FOR TOXOPLASMOSIS

Glycan-microarray screening of *Toxoplasma gondii*'s GPI and its deletion sequences was initially performed in our group to evaluate a potential diagnostic epitope for the corresponding disease, toxoplasmosis.[80] The results of this particular experiment revealed the applicability of a *Toxoplasma gondii* GPI as a diagnostic antigen for the distinction of acute and chronic state of the disease and not infected specimen (Figure 15).

However, it also demonstrated the specificity of the structure, as GPI structures from *Plasmodium falciparum* and *Chryptosporidium parvum* showed no binding of antibodies.[80] High-mannan structures from pathogenic yeast, employed as a positive control, showed interaction with the sera.

More importantly, the pseudodisaccharide, a conserved motif of all GPIs, showed no interaction with the tested sera, while smaller fragments of the *Toxoplasma gondii* GPI, containing the specific branch, showed weaker binding. These results suggest that the immune system of an infected specimen can distinguish foreign from body's own structures by the phosphoethanolamine moiety on Man I, thereby posing no cross-reactivity of the produced antibodies.

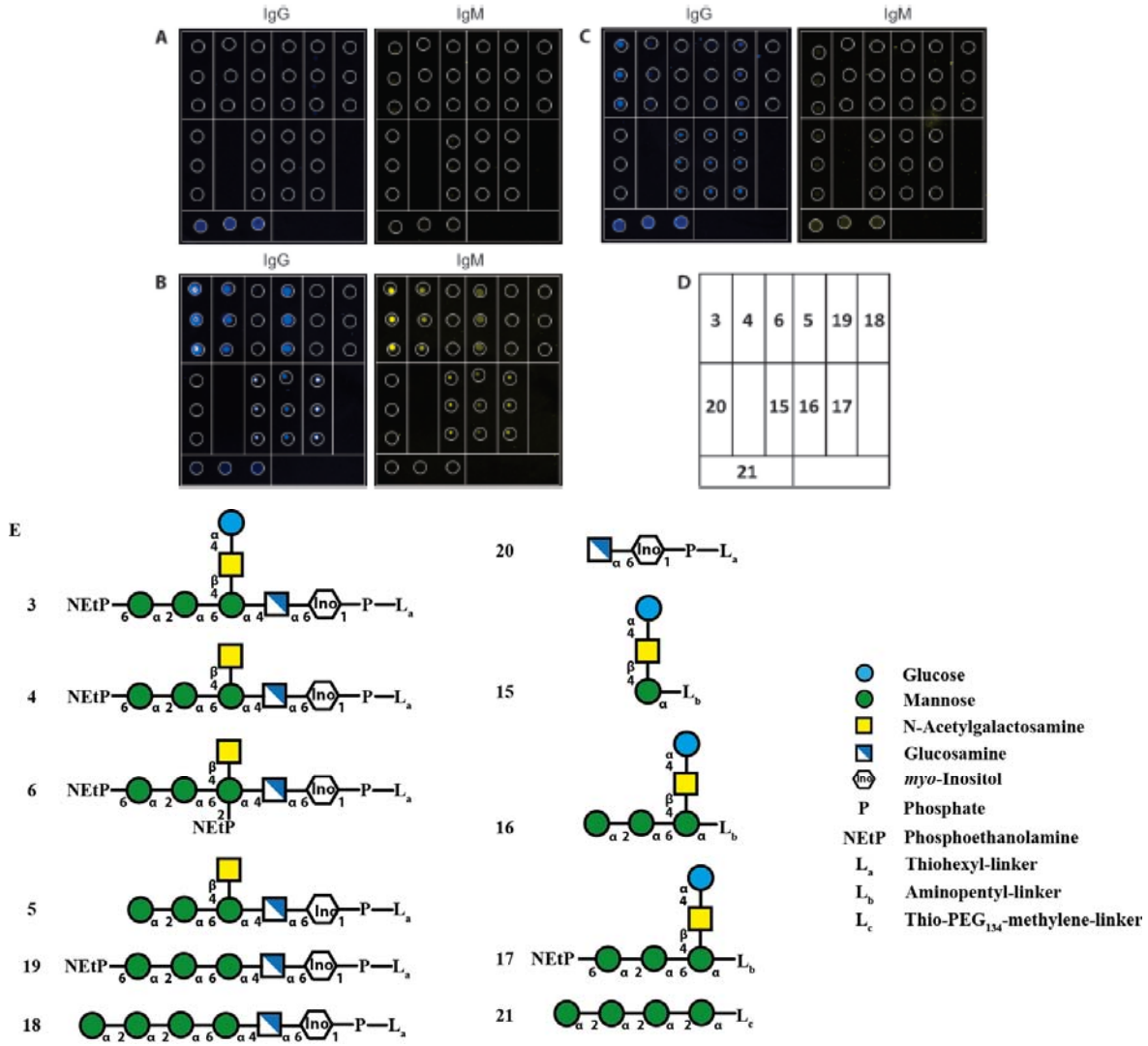

Figure 15: glycan microarray of synthetic carbohydrate structures; A) not infected, B) acute infection, C) chronic infection, D) position of compounds on the array E) printed synthetic structures: GPI of *Toxoplasma gondii* (3-5), minimal structure of mammalian GPI (6), *Plasmodium falciparum* GPI (18) and *Cryptosporidium parvum*'s GPI (19), deletion sequences of *Toxoplasma gondii* GPI (15-17, 20) and control compound, a high-mannose of pathogenic yeast (21)[80]

BIOSYNTHESIS

The biosynthesis machinery of GPIs has been studied and is well understood (Figure 16).[61c, 110] Most eukaryotic cells follow the same central pathway, but small differences occur in the parasitic species *Plasmodium falciparum*, *Toxoplasma gondii* and *Trypanosoma brucei*. Abrogation of the GPI synthesis concludes in malfunction and lack of important proteins and carriers.[111] Thus, the differences in enzyme and pathway of mammalian and parasitic cells account for perfect targets for the development of antiparasitic drugs.[112] In the following part the mammalian pathway (Figure 16A) is described and the main differences with the parasitic process are mentioned afterwards.

The first step of the GPI biosynthesis in mammalian cells is the transfer of *N*-acetylglucosamine (GlcNAc) to a phosphatidylinositol by the use of an UDP-GlcNAc

donor (**a**). This step takes place at the cytosplasmic site of the ER and conducted by a protein complex consisting of PIG-A, PIG-C, PIG-H, and hGPI1.[113] Deacetylation, a crucial and unique step in the biosynthesis, is catalyzed in the cytosol by a deacetylase, presumably the PIG-L protein[114] (**b**). The following step is the acylation of the C2-position of the GlcN-PI[115] complex by palmitoyl-CoA[116] (**c**). At this point, it is believed that the lipid chains undergo variation from a diacyl-moiety towards a more heterogeneous acyl-alkyl-moiety.[117] After the molecule has flipped to the luminal site of the ER, Mannoses are transferred by a not yet identified protein complex[113a] (**d**). The substrate source of Mannose is always dolicholphosphatemannose (Dol-P-Man).[118] After the second Mannose has been transferred, phosphoethanolamine is added subsequently (**e**). The third mannosylation is a complex which may be formed from PIG-B.[119] After this step, subsequent phosphorylation of all remaining mannose residues takes place by phosphoethanolamine. Finally, the protein is transferred to the Man III phosphoethanolamine by cleaving of the GPI signal peptide (**f**). After the attachment of the protein, palmitate (**g**) and the Man II phosphoethanolamine (**h**) are cleaved off the compound to initiate the transport to the Golgi apparatus. Arriving in the Golgi,[120] additional monosaccharides can be transferred to the GPI.

Trypanosoma brucei shows some major differences in the GPI biosynthesis.[113a, 121] Transfer of palmitate occurs after Man I has been added to the GlcN-PI and no phosphorylation at Man I and Man II are part of the biosynthesis. In addition, the transfer of the several galactose residues is believed to happen after the VSG is conjugated to the GPI, since no galalactose bearing intermediates have been isolated during the GPI biosynthesis.[122]

Toxoplasma gondii is showing several differences to the mammalian pathway. Homologues of the GlcNAc transferases for PI are not to be found in the genome.[123] After Man III is transferred, palmitate is removed and the compound is modified with a GalNAc monosaccharide (**i**).[112] After this step, subsequent phosphorylation and protein transfer occur.

Plasmodium falciparum lacks the second and third phosphorylation and is transferring a forth Mannose residue to the backbone of the molecule. In subsets of isolated GPIs the palmitate is still present.[124]

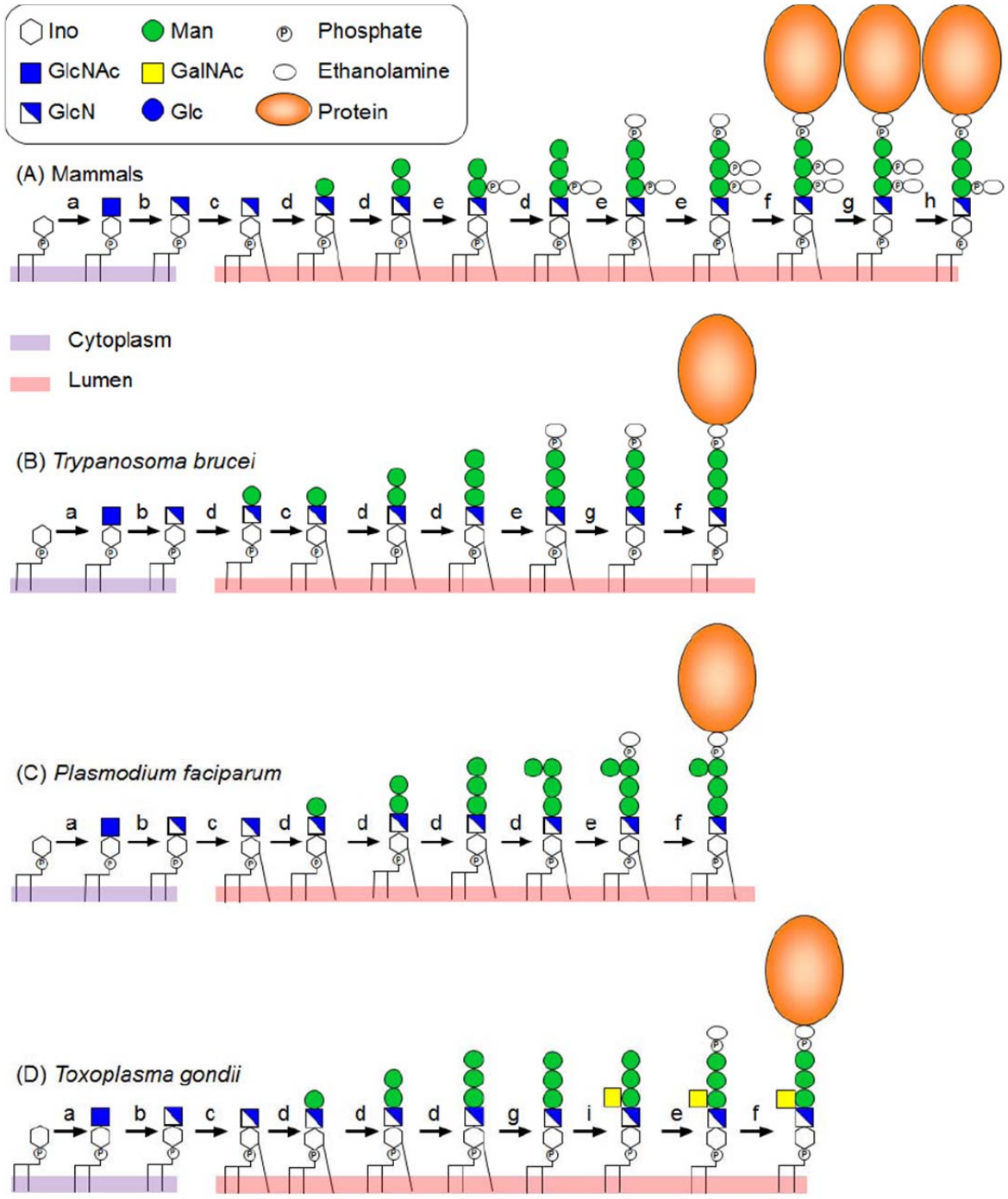

Figure 16: Comparison of the biosynthesis pathways of GPI for Mammalian cells (A), *T. brucei* (B), *P. falciparum* (C) and *Toxoplasma gondii* (D). (a) transfer of GlcNAc; (b) De-*N*-acetylation, followed by flipping of GlcN-PI into the luminal side of ER; (c) acylation of Ino; (d) mannosylation using dolichol-phosphate-mannose; (e) addition of PEtN; (f) attachment of GPI to protein by GPI transamidase; (g) Inositol deacylation; (h) removal of the second PEtN; (i) addition of GalNAc.

1.5 CARBOHYDRATE CHEMISTRY

PROTECTING GROUPS

Depending on the role played, a protecting group is either defined as temporary or permanent. Temporary protecting groups are masking a position for future modification. During building block synthesis, this might be due to concurring reactivity or selectivity of the protected hydroxyl group. In later synthesis steps however, temporary protecting groups are employed to mask positions which are planned to participate in glycosylations, phosphorylations, sulfatizations and others. In this case, multiple present protecting groups are often orthogonal, which describes the possibility to selectively remove one over another.

Typical temporary protecting groups in building block synthesis are bulky, such as TBDPS or Trityl, or used to mask multiple hydroxyl groups at once, such as *O*-isopropylidenes or *O*-benzylidenes. Temporary anomeric protecting groups are chosen to either protect this position until the glycosylation takes place, *e.g.* allyl, or to be the activated group, *i.e.* leaving group, *e.g.* thioalkyl. Often used orthogonal protecting groups are TIPS ether, allyl ether, levulinic ester, 2-methylene-naphthyl ether, fluorenylmethyloxycarbonyl and others.

Permanent protecting groups mask hydroxyl groups during glycosylations and are only removed during final deprotection. The benzyl ether is most frequently used along with 2-methyl-naphthyl ether, acetals and silyl ethers.

STEREOSELECTIVE GLYCOSYLATION

The process of glycosylation describes a chemical reaction, wherein the anomeric leaving group of a glycosyl donor is nucleophilic displaced by a hydroxyl group of a glycosyl acceptor. To activate the leaving group, like imidates, thioalkyl chains, sulfoxides or phosphonates, a specific promotor, depending on the species of leaving group, is applied. Promoters are lewis acids, often triflates with a specific counterpart, such as silver, different substituted silyl groups (TMS, TBS) or alkyl groups (Methyl). Activated glycosyl donors bear a flat oxocarbenium ion, which is attacked by nucleophiles from either top or bottom site. The α- and the β-anomer are almost equally formed. Possible influences of selectivity are reaction temperature, solvent, steric hindrance, promotor, nature of the anomeric leaving group and protecting groups in both, glycosyl donor and acceptor. Along these factors the neighboring group participation is of outstanding importance. An ester, amide or carbonate function at the C-2 position of the glycosyl donor participates in the glycosylation via formation of a cyclic

acyloxonium ion. This ion is blocking the *cis*-face of the donor and though 1,2-*trans*-products are formed dominantly.[125]

1,2-*cis*-Oligosaccharides are much more challenging in their synthesis.[126] Nevertheless, some strategies to increase selectivity, such as intramolecular delivery,[127] fluorides,[128] bromides,[129] and remote group participation[130] have been developed over the years and ensure synthesis of more complex saccharides.

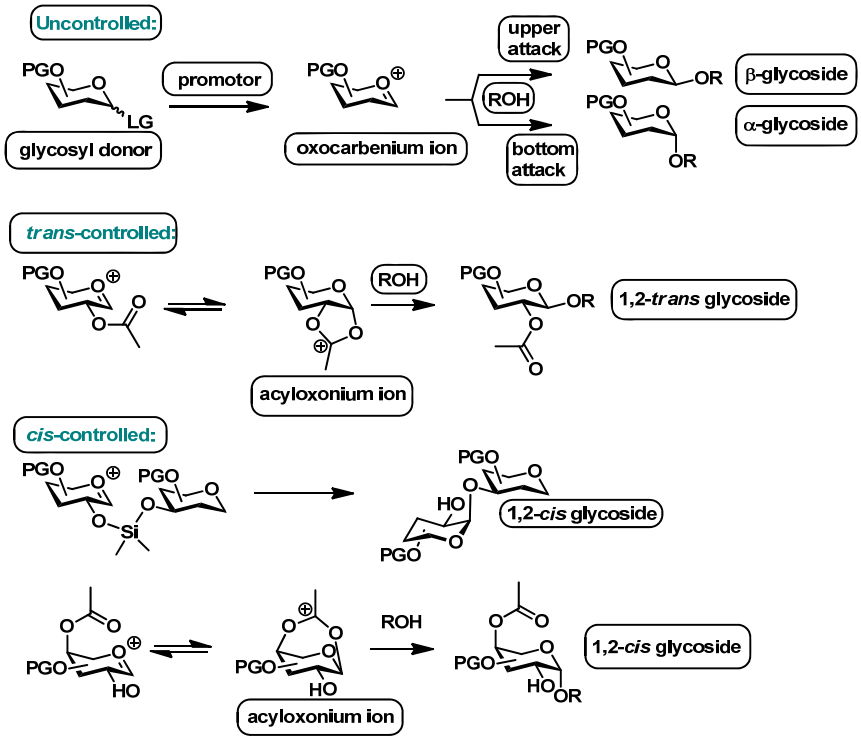

Scheme 1: Possibilities of controlling selectivity in glycosylation reactions

1.6 Chemical Synthesis of GPI

GPIs are among the most complex natural structures to synthezise combining phosphate, carbohydrate, inositol, and lipid chemistry. The combination of these different chemical systems requires well trained synthetic specialists and sophisticated methods, considering convergent approaches, orthogonal protection groups and stability issues. Since the description of the GPI structure by Ferguson *et al*,[81a] diverse synthetic approaches have been described to obtain these complex glycolipids.

Linear Synthesis of *Trypanosoma brucei* GPI by Ogawa

Ogawa and his group reported the first total synthesis of a GPI from *Trypanosoma brucei* in 1991.[128, 131] The synthesis of the GPI was target oriented and approached by first assembling the glycan structure, followed by the consecutive phosphorylation steps as depicted in Scheme 1.This concept of the initial assembly of the glycan part of GPIs and the

following consecutive phosphorylation remains the standard approach until today. However, the use of acetyl groups as temporary protection groups and glycosyl halides as donor, established the order of the glycosylation and a manipulation was only possible in one position at a time.[132]

The synthesis of the GPI glycan started by assembling a pseudotrisaccharide building block. Glycosylation (**I**) of a Man I building block **a** and a glucosylazide acceptor **b** gave a disaccharide, which was further manipulated to give a disaccharide donor. This donor was reacted (**II**) with a *myo*-inositol unit **c** to furnish the first key fragment. In the next step, a digalactoside was generated (**III**) from thiodonor **d** and galactosylacceptor **e** to build up the side branch of the GPI. After preparation of the corresponding fluoride donor, the digalactoside was used in a [3+2]-glycosylation reaction (**IV**) with the transformed trisaccharide acceptor. Removal of the acetyl group of the resulting pseudopentasaccharide gave rise to the acceptor for the glycosylation (**V**) with the Man II residue **f**. To furnish the full glycan structure of the envisaged GPI, the last glycosylation (**VI**) was performed with mannoside **g** after the removal of the acetyl group from the non-reducing end. In a first phosphorylation step (**VII**), a phosphoramidite building block **h** was used to install the phosphoethanolamine moiety. The second phosphorylation (**VIII**) installed the diacylglycerol **i** to afford the protected GPI. Finally, oxidation of the phosphonate to the corresponding phosphodiesters and global deprotection (**IX**) gave the full structure **j**.

This linear approach, although first of its kind, bears several disadvantages for the synthesis of a bigger range of GPI targets. The pseudodisaccharide is an important structural motif of GPIs. Nonetheless, it is directly used to glycosylate the Man I residue. This limits the use of this building block for other GPI structures, differing in the linkage and modification of Man I. Furthermore, the use of glycosylhalides as donors, dictates the sequence of the different glycosylations. They pose specific reactivities, which are difficult to be directed by a corresponding activator in a glycosylation reaction. Taken together, this approach is target oriented and not applicable to other structures with a distinguished modification and connection pattern.

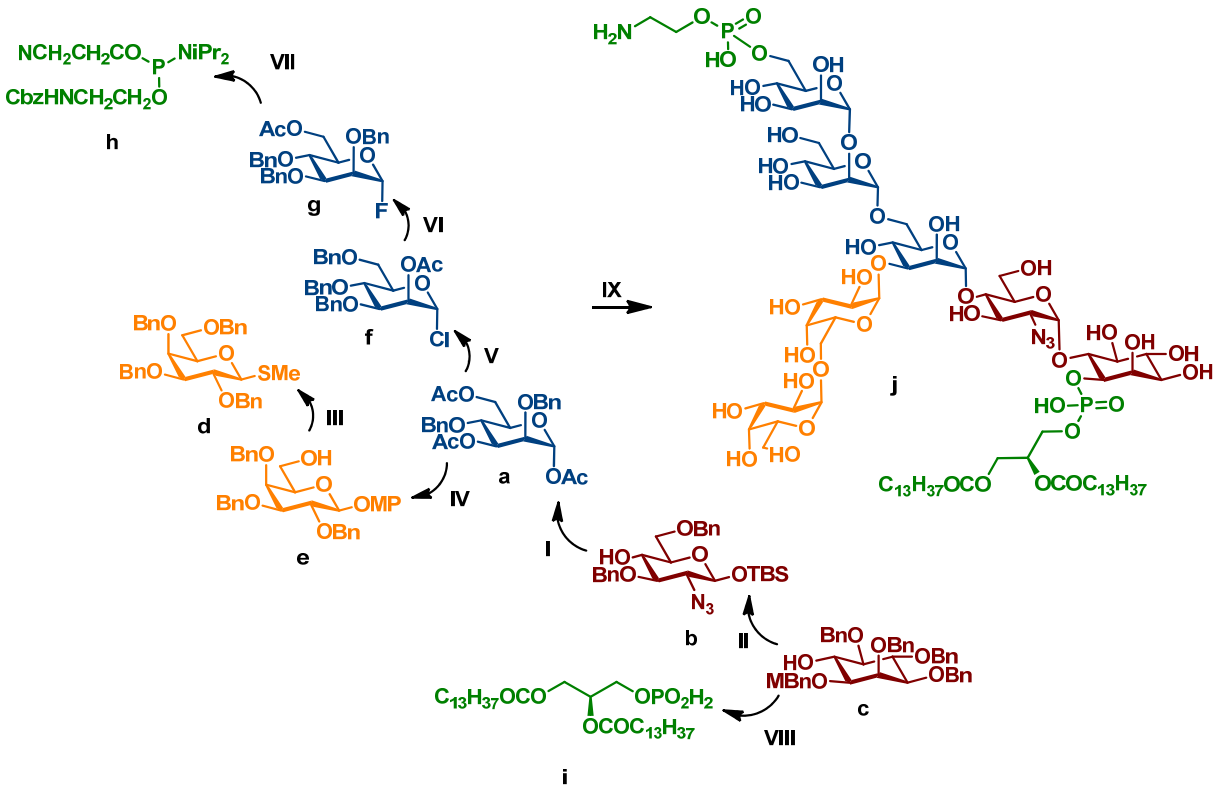

Scheme 2: Ogawa's synthesis of a GPI from *Trypanosoma brucei* in 1991 was target oriented

CONVERGENT SYNTHESIS OF *TRYPANOSOMA BRUCEI* GPI BY LEY

A new approach, the introduction of different temporary, often orthogonal protection groups and a bigger set of leaving groups for reactivity control was developed by Ley and coworkers. [133] The same GPI Anchor as Ogawa was synthesized, but in a sequence with fewer steps. As can be seen in Scheme 3, this was achieved by fewer requirements concerning functional group interconversion, more convergent characteristics and a higher flexibility. Additionally, a central role is played by the pseudodisaccaride in GPI synthesis. This structure seldom bears any modification and is identical for almost all GPI structures known. Therefore, it was synthesized as a standardized separate building block. Furthermore, by using diacetals in addition to benzyl groups as permanent protection groups, the authors were able to optimize the reactivity of the used building blocks. This resulted in a reduction of interconversion steps for the installation of leaving groups.

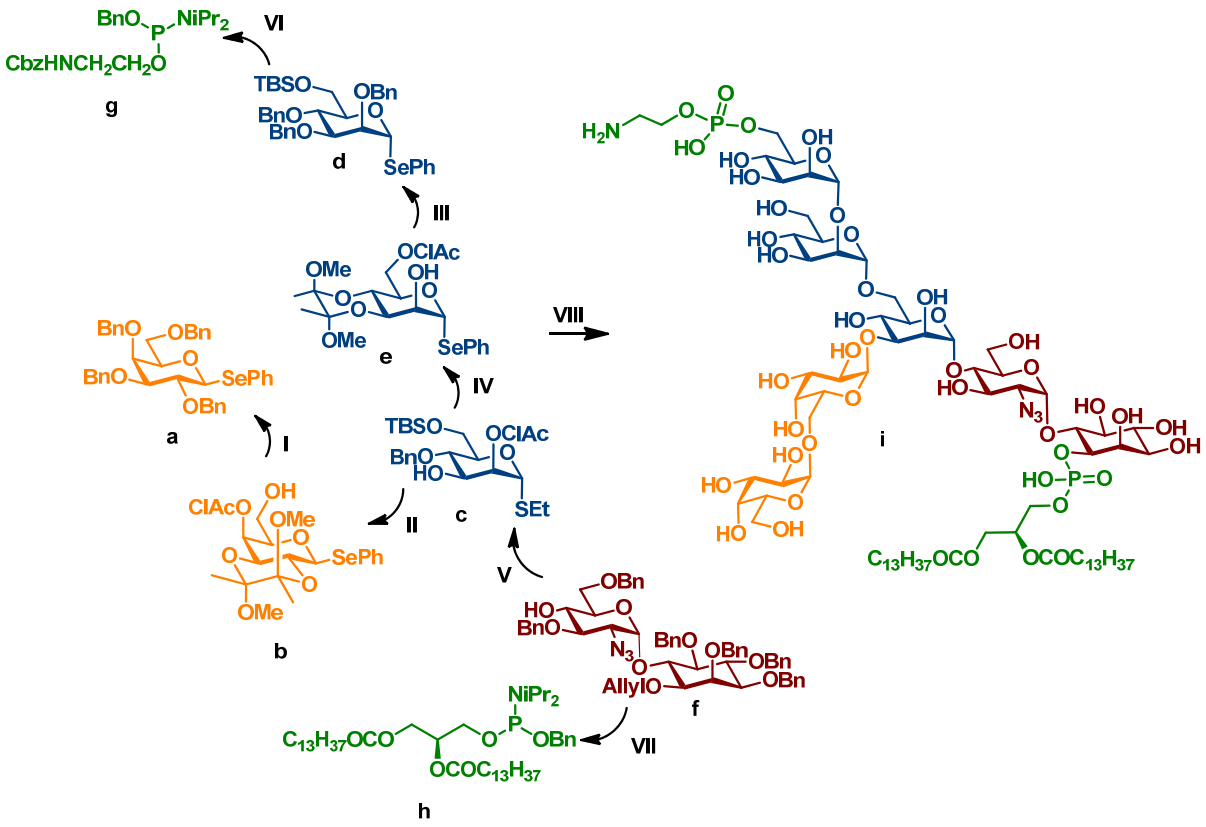

Scheme 3: *Trypanosoma brucei* GPI by Ley – selectivity in reactions were controlled by reactivity of building blocks

The branch of the GPI, consisting of a digalactoside, was synthesized by activating the perbenzylated selenoside **a** (**I**), while leaving the other galactoside donor **b** intact. The following glycosylation (**II**) with the Man I residue **c** resulted in the formation of the expected trisaccharide. Before undergoing a [3+2]-glycosylation, the required dimannoside was synthesized (**III**). Selectivity was achieved by employing an armed mannoside species **d** in a glycosylation with a disarmed species **e**. The subsequent glycosylation (**IV**) was selective for the selenoside over the thiodonor. To furnish the glycan structure of the GPI, the pseudodisaccharide **f** was reacted (**V**) with the resulting glycosyldonor. The following phosphorylations were conducted by using a phosphoramidite for both, the envisaged phosphoethanolamine **g** (**VI**) and the phosphodiacylglycerol **h** (**VII**). Final deprotection by hydrogenolysis (**VIII**) released the full GPI **i** structure.

Albeit the convergent strategy of this approach, the synthesis of the GPI-anchor from *Trypanosoma brucei* remains target oriented. This is mainly due to the free hydroxyl groups of all the building blocks and the corresponding leaving groups, which settle the order of the glycosylation.

A CONVERGENT GENERAL METHOD FOR GPI SYNTHESIS: *TRYPANOSOMA BRUCEI* GPI

Finally, a general strategy to obtain pure samples of any given GPI structure was recently developed by our group.[134] As illustrated in Scheme 4, the strategy relies on Benzyl ethers as permanent protecting groups and considers different monosaccharides, fatty acids and phosphorylation sites by the introduction of an orthogonal set of protecting groups. These groups are the TIPS-ether, the allyl-ether, the levulinic ester and the naphtylmethyl-ether. While the TIPS-ether, the ally-ether and the levulinic ester are mostly the protecting groups for late stage phosphorylations, they can be employed in the protection of the used monosaccharides as well. One of the central building blocks, Man I is additionally protected with a naphtylmethyl-ether protection group to mask either the C3 or the C4 position for the introduction of branched structures. Bigger fragments are chosen in a way, that they mirror similarities of different GPIs. In this way, protected full glycans, building blocks and different key fragments used for their assembling, show high feasibility for a number of manipulations and targets.

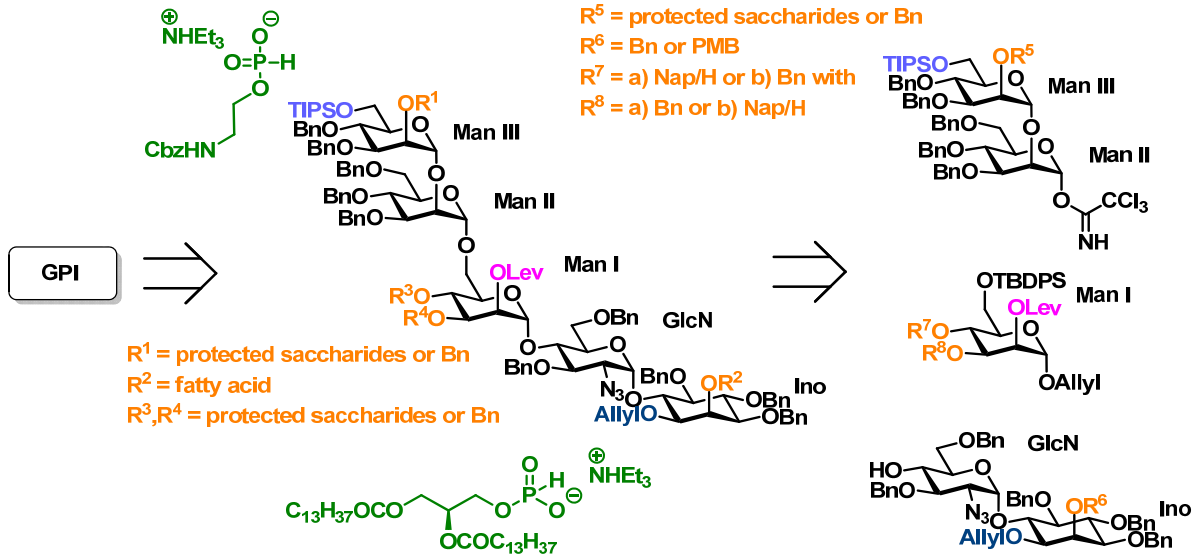

Scheme 4: TIPS, Allyl and Lev were introduced as a full set of orthogonal protection groups. Naphtylmethylgroups are employed during the assembling to ensure further orthogonality.

While initially developed by synthesizing a GPI of *Toxoplasma gondii*, also referred to as low molecular weight antigen,[135] the strategy was used to show its practicability on a number of different GPI targets. As depicted in Scheme 5, the GPI of *Trypanosoma brucei* was chosen as an example with modifications at the C-3 position of Man I **a**. Since the corresponding full structure of the GPI bears no third phosphorylation site, Man I **a** was equipped with an acetyl group instead of a levulinic group. Thereby, protection group interconversion is enhanced, still ensuring stereoselectivity in glycosylation reactions. After

removing the naphthylmethyl group, the first glycosylation (**I**) was approached by combining the Man I building block with the branching digalactoside **b**. The anticipated glycosylation (**II**) with the pseudodisaccharide **c** required functional group interconversion in the anomeric position from an allyl to an imidate group. Installation of the imidate donor was followed by its glycosylation with **c**. Functional group interconversion yielded a pseudopentasaccharide as acceptor for the final glycosylation (**III**) with the dimannoside-donor **d**. Subsequent phosphorylations (**IV** and **V**) with the corresponding H-phosphonates, **e** and **f**, gave the protected GPI anchor. Global deprotection by hydrogenolysis (**VI**) gave GPI **g** in this highly convergent approach.

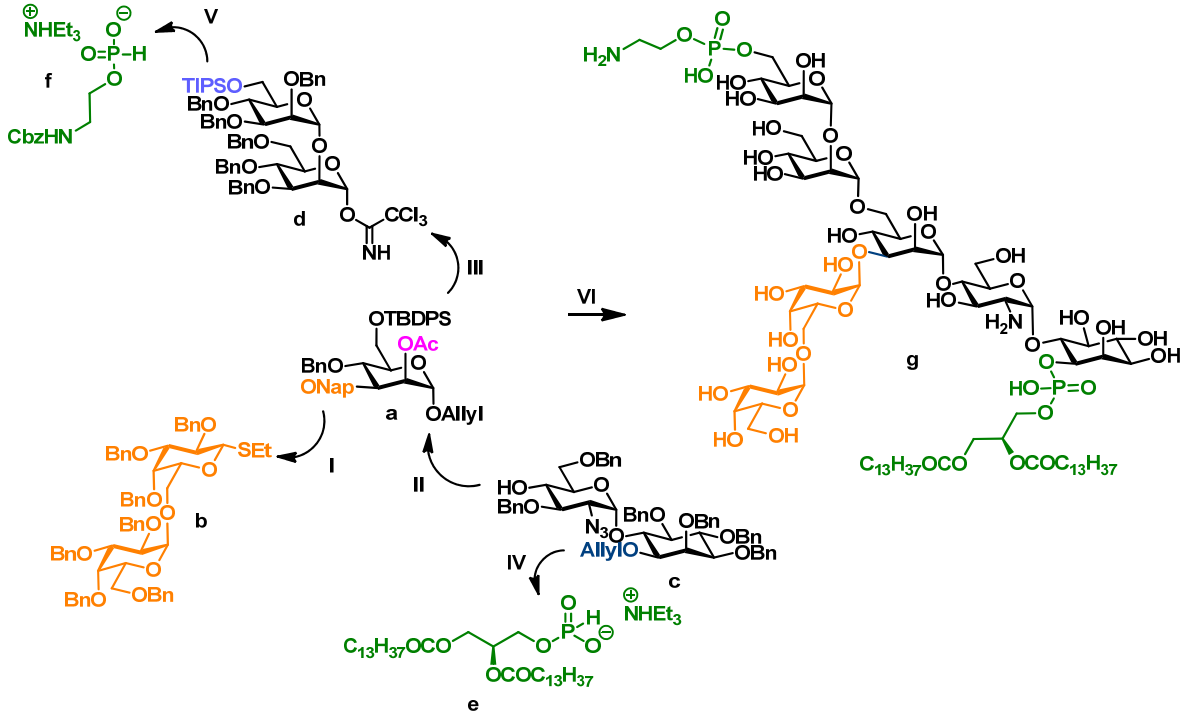

Scheme 5: The general convergent strategy to obtain GPI: certain key structural elements are chosen, depending on the target, while others can be used for every GPI.

While this convergent approach solves the problem of the reaction sequence and is able to give access to a number of different GPI structures, a few limitations are still prevalent.

First, more complex GPIs, with highly branched structures, such as *T. brucei* and *T. cruzi* (Table 1, entry 5-11) with more than two galactosides at Man I, require their own set of building blocks specifically designed for this kind of galactosylations. Especially, highly α-selective conditions in systems which require a 1,2-*cis* linkage are rare and challenging.

Secondly, the current building blocks do not allow a branching at Man II, which is required for the synthesis of GPI fragments of the GPI Anchors of *T. brucei* VSG 221 and 121 (Table 1, entry 7, 8). To obtain pure samples of structures with these modifications,

adaptations of the strategy is required. More specific building blocks with bigger scope and fragments with unique connection pattern are still desirable.

Until recently, a third limitation was the introduction of unsaturated lipids to the GPI structures. Usually, hydrogenation is the last step in the synthesis of GPIs. Double bonds are reduced under these conditions, thus other methods, which have to be non-nucleophile as well, are desirable. Beside others,[136] 2-methylnaphtylene groups are ideal candidates to solve this problem.[137] They can be removed via hydrogenation, but are also labile under slightly acidic conditions, using TFA or DDQ. When replacing benzyl groups with 2-methylnaphtylene groups, modification of the synthesis strategy of the corresponding building blocks is not required. When Man I is protected with a 2-methylnaphtylene group, the substitute protection group is *p*-methoxybenzyl. These advantages in comparison to other protection groups, illustrate the beauty of the use of the 2-methylnaphtylene group.

1.7 SYNTHESIS OF GPI-CONJUGATES

Most known GPIs anchor a protein to the cell membrane (Table 1). This anchoring and localization of the complex is thought to be the most important function of the GPIs. However, little is known about the interplay or the biological functions of GPI and attached protein. This is mainly due to the lack of pure homogeneous GPI-anchored proteins for investigation and difficulties in their production. Thus, soon after general and reliable methods for GPI synthesis existed, the design of peptide and protein conjugates was approached.

For the synthesis of these conjugates two methods proved to be reliable. In chemical synthesis of proteins native chemical ligation (NCL) is a powerful tool. Often it is applied in a sequential manner for proteins which are not accessible in an expression vector or bear post-translational modifications. NCL requires a C-terminal thioester that is reacted with an N-terminal cysteine. For the application in the synthesis of GPI-anchored proteins the process requires the introduction of an artificial cysteine at the phosphoethanolamine moiety at Man III of the GPI. A second approach uses the amine function of phosphoethanolamine at the GPI as a coupling partner with the C-terminal carboxylic acid of the peptide. This approach enables the synthesis of natural homogeneous probes, but is limited to shorter peptide sequences.

SEMISYNTHETIC GPI-ANCHORED PRION PROTEIN

The Prion Protein, a GPI-anchored protein, causes transmissible spongiform encephalopathies in its pathogenic isoform (PrP^{Sc}).[138] For the investigation of the pathogenicity of the conjugate, Seeberger and coworkers synthesized the GPI-glycan core and ligated it to a recombinant Prion Protein (rPrP) (Scheme 6).[139] In this semisynthetic approach, the GPI was equipped with a cysteine at phosphoethanolamine of Man III. After deprotection of the assembled structure (**I**), glypidation[140] by native chemical ligation[141] followed (**II**). The GPI-anchored rPrP, the first ever synthesized GPI-anchored protein, was afterwards tested for its capability to dislocate in lipid membranes and its role in the infection process.

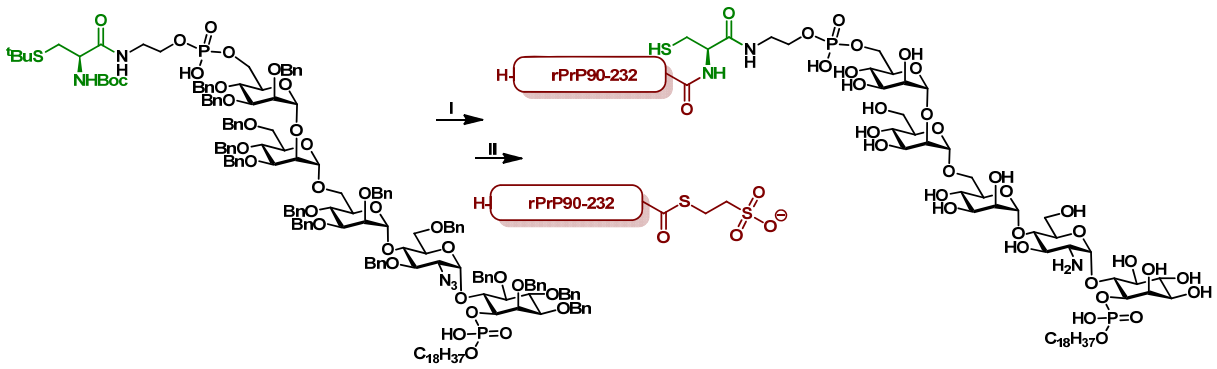

Scheme 6: Semisynthesis of a GPI-anchored Prion Protein: a synthetic GPI equipped with an additional cysteine is combined with a recombinant expressed protein by native chemical ligation

SYNTHESIS OF A SPERM CD52 GPI-ANCHORED GLYCOPEPTIDE

CD52, a 12 amino acid containing glycopeptide, is present at human lymphocytes and sperms.[142] Being GPI-anchored, it plays a major role in reproduction and immune system mechanisms.[143] The investigation of these mechanisms demand pure and homogeneous probes of the compound. Guo and coworkers synthesized[144] a glycopeptide by solid phase peptide synthesis (SPPS), using a 2-Chloro-Trityl-resin. After releasing the fully protected glycopeptide from the resin, it was coupled to the fully protected GPI-anchor. After global deprotection the GPI-anchored glycopeptide was obtained.

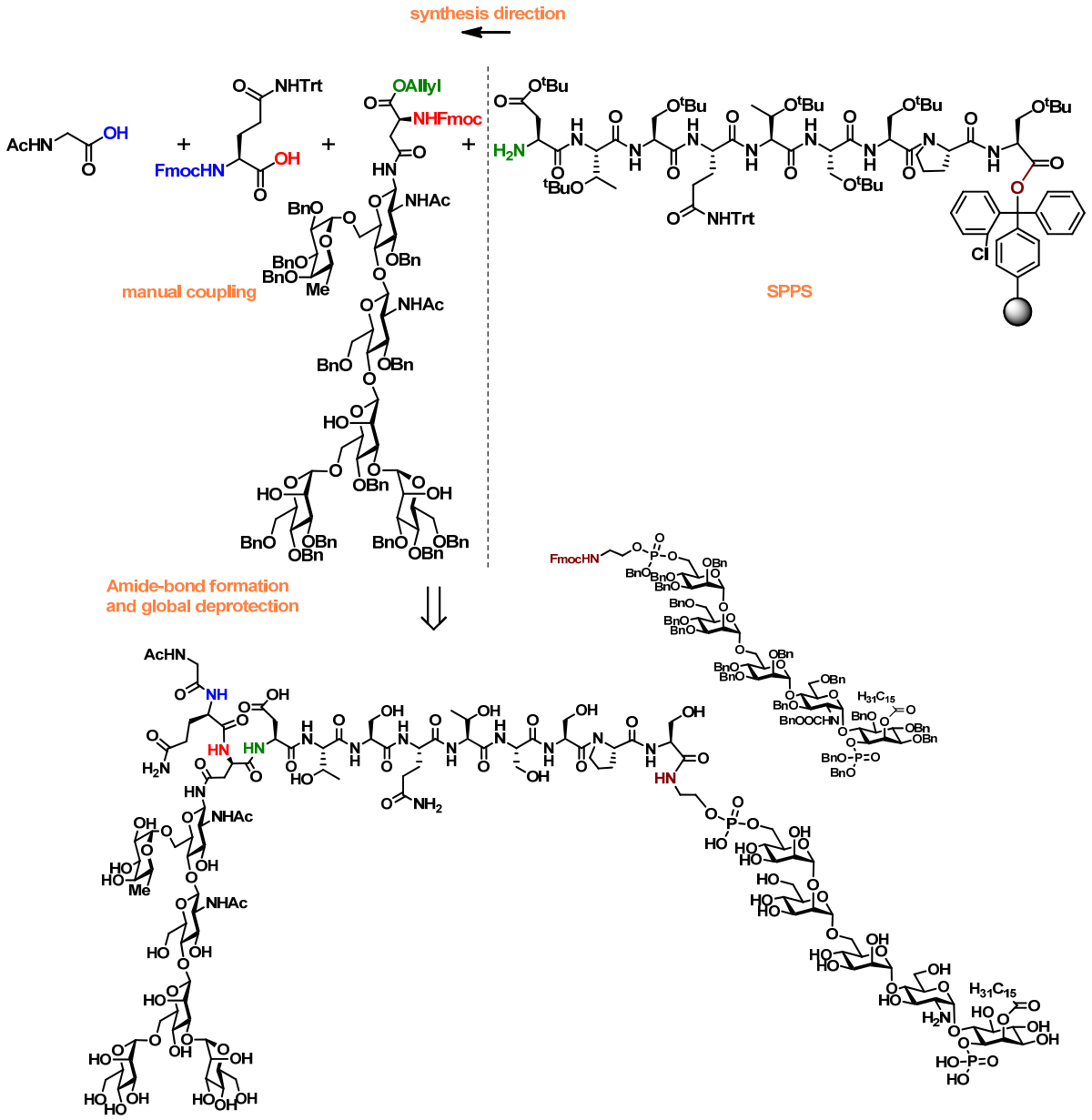

Scheme 7: First synthesis of a GPI-Anchored glycopeptide – the C-Terminus of the glycopeptide was directly coupled with the phosphoethanolamine of the GPI-Anchor

2. AIM OF THE THESIS

African trypanosomiasis is a parasitic infection in humans and animals caused by *Trypanosomoa brucei brucei*, *Trypanosomoa brucei gambiense* and *Trypanosomoa brucei rhodesiense*. After transmission of the parasite by the tsetse fly symptoms are fevers, headaches, itchiness and joint pains. Due to these unspecific indicators, the disease is often untreated and the parasite can reach the central nervous system (CNS). Current diagnosis methods require detection of the parasite in a blood sample or fluid of a lymph node. However, to distinguish between blood and CNS-stage a lumbar puncture is needed.[145] Taking this into account, better understanding of the pathogenesis as well as development of a cheap diagnostic tool is essential to fight the disease in sub-Saharan Africa.

The GPI anchored Variant Surface Glyoprotein plays a crucial role in many processes essential in the parasite pathogenesis. Compared to constant antigenic variation in the N-terminal domain,[75] the C-terminal VSG-GPI-conjugate shows little variance.[76] These properties extend from the VSG to conserved moieties in the carbohydrate side chain and the lipid of the GPI. It was shown, that these domains of the GPI play important roles in activating the immune system.[38-40] However, since results are obtained from heterogeneous isolated structures of GPIs and VSGs it is difficult to assign specific functions to each of these functionalities. Therefore, defined fully synthetic structures will help to address questions raised from the role played by VSG and GPI.

Recently, our group has developed a general strategy to synthesize GPIs.[134] However, this strategy poses limitations with regard to complex *T. brucei* GPI structures. The glycan structure of the *T. brucei* VSG 221 GPI bears unique modifications and unusual complexity thereof. Both limitations require new synthetic strategies applied on a novel set of building blocks. Additionally, it has been shown by our group that synthetic GPI used in glycan microarray are recognized by anti-GPI antibodies.[80, 107a] The information gained in these experiments was used to determine distinct structure-activity relationships of epitopes found in GPI, enabling the use of synthetic GPI structures as diagnostic marker.

Therefore, the aim of this thesis is the synthesis of the *T. brucei* VSG221 GPI. This process comprises introduction of novel building blocks and synthesis of GPI fragments for the assembling of a set of unique *T. brucei* GPI structures. Additionally, a method for ligation of *T. brucei* GPI derivatives to a C-terminal VSG peptide is investigated. Synthesized compounds are used in immunological experiments to investigate their role in the activation of macrophages and in glycan microarray to evaluate particular interaction with anti-GPI

antibodies. Immobilized GPI structures are used to examine the potential use in diagnosis of African trypanosomiasis and in experiments analyzing the cross-reactivity of anti-GPI-antibodies with synthetic GPI of different origin.

3. SYNTHETIC ANALYSIS

3.1 CONJUGATION OF GLYCANS TO VSG FRAGMENTS

The linkage between GPI glycolipids and attached proteins involves a phosphoethanolamine moiety between the C-6 position of Man III and the C-terminal amino acid of the protein. Synthesis of this linkage has been approached by two strategies.[139, 146] The first strategy comprises synthesis of the GPI and solid phase peptide synthesis (SPPS) of the fully protected peptide followed by a coupling reaction of the two compounds and removal of the protecting groups from the GPI-anchored peptide. This strategy allows generation of natural homogeneous GPI-anchored peptides, but is limited to short peptides fragments. The second strategy uses GPI anchor equipped with a cysteine residue at the phosphoethanolamine residue and a chemoselective ligation reaction to synthetic peptide thioesters or protein thioesters. Thereby, generation of GPI-anchored peptides, glycopeptides and proteins is possible, allowing potential evaluation of the role of GPI-anchors.

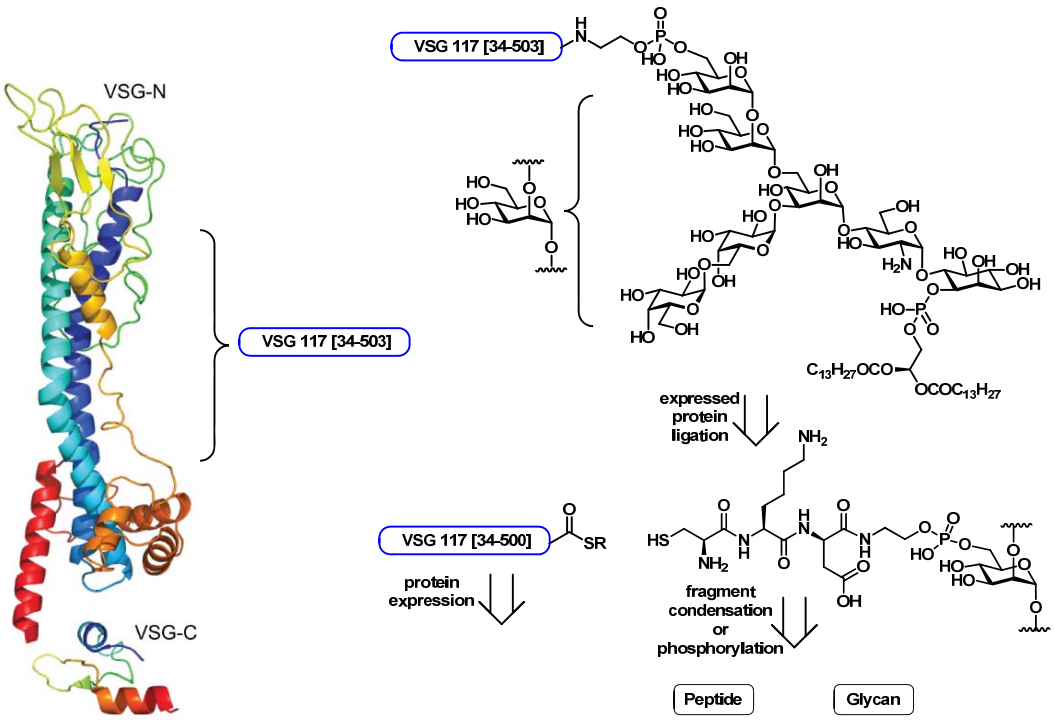

Figure 17: Synthesis of homogeneous GPI-anchored VSG

Here, a combination of the two approaches is explored to generate a homogeneous GPI anchored VSG peptide in its natural form without additional cysteine in the C-terminus of the peptide sequence. Therefore, the earliest cysteine residue in the C-terminus of VSG117 will be used generating a small, fully protected peptide VSG117[501-503] (CKD) by SPPS on a Trityl ChemMatrix™. This protected tripeptide is combined with a synthetic GPI.

Additionally, the VSG117[34-500] protein can be expressed in cell lines (Figure 17). However, to explore the strategy a smaller VSG117 fragment is synthesized as peptide thioester.

3.2 GPI GLYCAN SYNTHESIS

The synthetic analysis of the most complex and largest *T. brucei* GPI, *i.e.* VSG221 GPI, is discussed to illustrate the generation of GPI molecules from required building blocks and fragments. Accordingly smaller fragments and deletion sequences can be synthesized from intermediates with minor modifications of this GPI synthesis. As depicted in Figure 18, the GPI Anchor of VSG221 **a** shows unique modifications and requires new synthetic methods and protocols for the assembly. As outlined in chapter 1.6, late stage phosphorylation and global deprotection are the final steps in GPI synthesis. Here, the H-phosphonates of Cbz protected phosphoethanolamine **b** and dimyristoyl glycerol **c** serve as phosphorylation agents prior to hydrogenolysis.

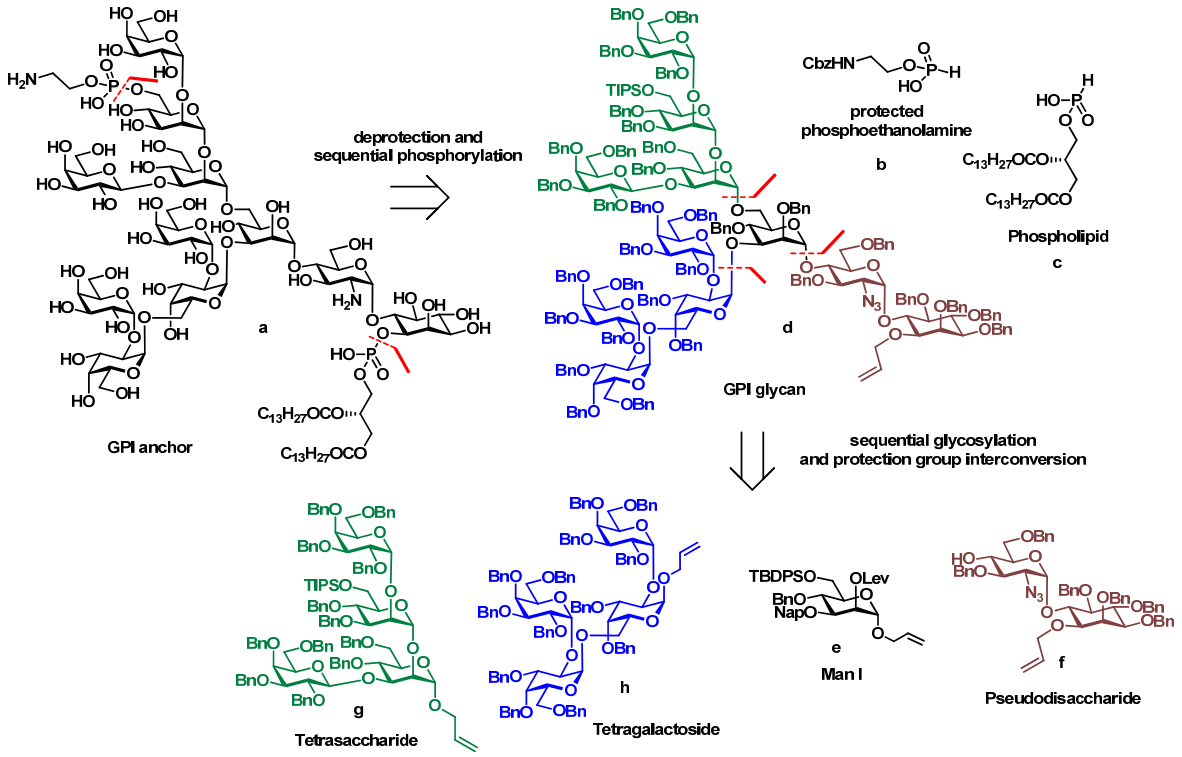

Figure 18: Synthetic analysis of the GPI Anchor from VSG 221

Following the general strategy introduced earlier, synthetic analysis of glycan **d** at the central branching point result in four carbohydrate fragments, consisting of two tetrasaccharides **g** and **h**, central Man I building block **e** and conserved pseudodisaccharide **f**.

Orthogonal protected Man I building block **e** is congruent with building blocks used in earlier GPI synthesis projects.[134a] To ensure formation of 1,2-*trans* linkages during glycosylation a neighboring participating ester function is installed in the C-2 position. The C-6 position of Man I is masked with a silyl ether. The TBDPS group can be selectively removed for elongation of the backbone. Additionally, the C-3 position is protected with a naphthylmethyl group, giving the possibility to install tetragalactoside **h**.

Pseudodisaccharide **f** can be synthesized from a GlcN building block and a *myo*-inositol building block. Before glycosylation GlcN is protected by a cyclic acetal in the C-4 and C-6 position. This moiety can be opened selectively towards the C-6 position, revealing the alcohol function of the acceptor on the C-4 position. Furthermore, the amine is masked as an azide until late stage reduction and deprotection. The *myo*-inositol building block is synthesized by de-novo synthesis from glucose. The alcohol group for glycosylation is in the C-6 position and the C-1 position is protected by allyl for orthogonal protection of a phosphorylation site.

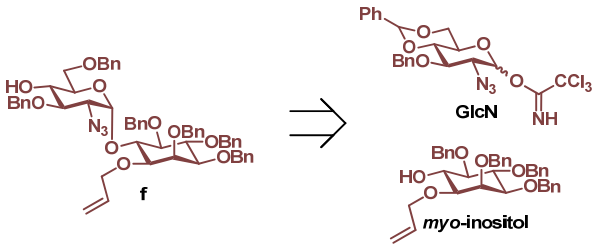

Figure 19: Synthetic analysis of conserved pseudodisaccharide **f**

Tetrasaccharide **g** comprises Man II and Man III from the conserved GPI backbone with two Gal residues as unique attachments. The desired product is generated in sequential glycosylation steps starting with the synthesis of a disaccharide consisting Gal III and Man II.

By using two different Gal III thioglycoside building blocks, two strategies can be applied for this reaction. The first building block having a benzoyl ester function in the C-2 position, to ensure formation of 1,2-*trans* linkages requires modification steps at the target compound after glycosylation. The second Gal III building block is perbenzylated, thereby having no neighboring participating group. Yet, no further modifications are required after glycosylation, enhancing synthesis of tetrasaccharide **g**.

Man II is a second branching point in the GPI and therefor requires orthogonal acetyl protection at the C-2 position and masking of the anomeric position with an allyl ether. For glycosylation to Gal III building blocks the C-3 position remains unprotected. After generating the desired disaccharide, acetyl is removed for reaction with Man III. The allyl ether in the anomeric position will remain until the complete assembly of tetrasaccharide **g**.

Man III building blocks equipped with orthogonal protecting groups in the C-6 and C-2 positions are known.[134b] For late stage phosphorylation the C-6 position is protected by a TIPS ether. α-Selectivity in glycosylations is achieved by an acetyl group masking the C-2 position, which, after glycosylation to Man II, is removed for the installation of an α-galactoside. The building block is equipped with an imidate or a phosphate leaving group.

Finally, for the installation of terminal Gal at the Man III residue perbenzylated thioglycoside Gal III is used requiring α-selective reaction conditions.

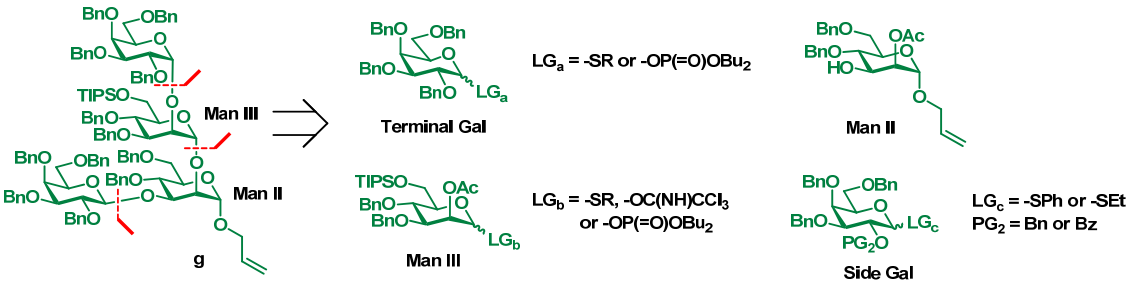

Figure 20: Retrosynthesis of tetrasaccharide **g**

Tetragalactoside **h** of the side branch of *T. brucei* GPIs, shown in Figure 21, contains four α-galactose residues, making it a synthetic challenging target. Due to repetitive connection pattern of the non-reducing end galactose, *i.e.* α1→2-linkages, possible strategies for assembling are either a [2+2]-glycosylation approach, or a stepwise glycosylation strategy.

A [2+2]-approach makes use of a divergent synthesis of acceptor and donor from a precursor digalactoside. The synthesis of this digalactoside requires a central orthogonal protected Gal I/II building block. The C-6 position is protected with TBDPS and the anomeric position is masked with an allyl ether. Additionally, to allow higher α-selectivity[130] in later glycosylation reactions, an ester function is installed in the C-4 position. The C-2 position is masked as a PMB ether and will be deprotected before use in glycosylation reaction with perbenzylated thiodonor terminal Gal. Afterwards, the digalactoside is converted into an acceptor by removal of the TBDPS group. To gain access to the doner for the [2+2] reaction, the TBDPS group is removed and a benzyl protection group is installed at the C-6 position. Removal of allyl and conversion of the hemiacteal into an imidate donor gives the desired donor for the [2+2] strategy.

The stepwise strategy uses the aforementioned digalactoside acceptor, which is reacted with Gal II thiodonor to give the desired trisaccharide. The orthogonal PMB protecting group at the C-2 position of the Gal II building is removed after glycosylation. Subsequently, the free hydroxyl group is reacted with the perbenzylated terminal Gal thiodonor to generate tetragalactoside **h**.

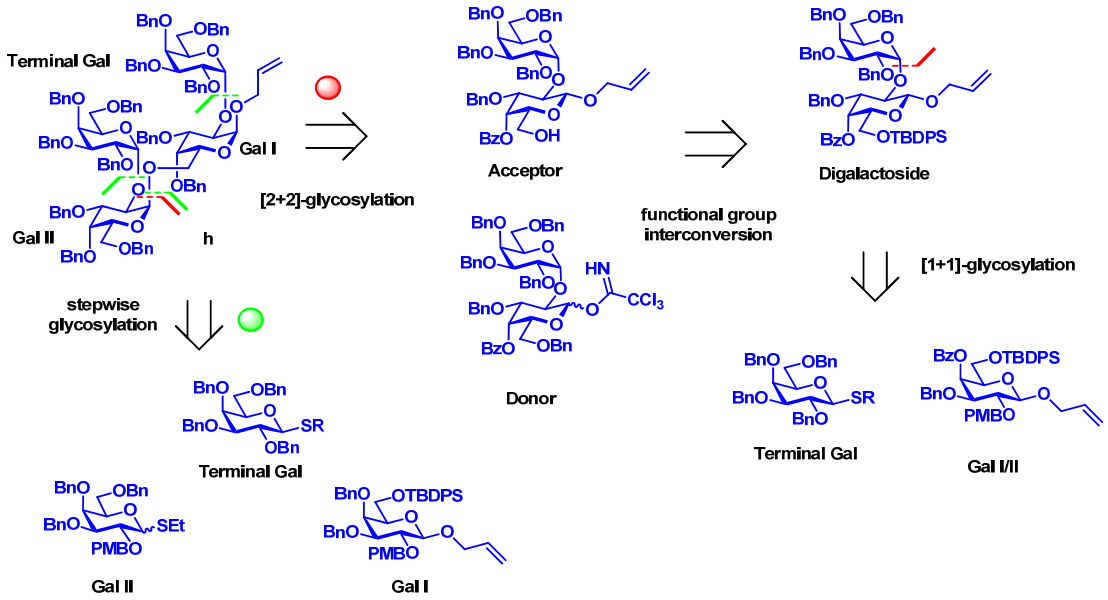

Figure 21: Retrosynthesis of novel tetragalactoside **h**: two general methods can be applied

The synthetic analysis shown for *T. brucei* VSG221 GPI anchor highlights building blocks and fragments, which can be used to generate a library of smaller compounds comprising the structural features of the full structure. Therefore, introduction of a linker moiety instead of a phospholipid for compounds planned to use in the investigation in glycan microarray is required. Accordingly, fragments without a *myo*-inositol unit are modified at their respective anomeric position. Analogously, to investigate activation of macrophages the compounds are equipped with a short alkyl chain, when not phosphorylated. Depending on the synthetic target, modified building blocks are used for the synthesis.

4. RESULTS AND DISCUSSION: SYNTHESIS OF GPIS FOR GLYCAN MICROARRAY

Glycan microarrays are a powerful tool to investigate multiple protein-glycan interactions at once by simple fluorescence read out. Recently recognition of GPIs from parasitic protozoa by antibodies in sera of patients has been shown for different diseases.[80, 107a, 147] In contrast to these studies involving the easily accessible GPIs from *Plasmodium falciparum* and *Toxoplasma gondii*, GPIs of *T. brucei* are deeply covered by a dense coat of proteins,[148] shielding the surface from access by foreign substances. Chronic infections with *T. brucei* lead to B cell apoptosis and depletion of the B-cell repertoire. However, single VSG and GPI are released during phagocytosis and may induce an immune response.[149]

As shown in the retrosynthesis chapter, large fragments are required for the assembling of *T. brucei* VSG 221 GPI anchor. By synthesizing these fragments, comprising the isolated structural features of the VSG 221 GPI a library of compounds having a thiol linker is assembled. Together with the full GPI structure, the different compounds can be immobilized on activated glass slides and investigated in their recognition by antibodies from sera of individuals having a *T. brucei* infection. Here, the assembling process towards the VSG 221 GPI and all required fragments and building blocks is explained stepwise and methods are introduced where and when necessary.

4.1 TETRASACCHARIDE g

Synthesis of tetrasaccharide **g** required availability of a number of new building blocks and the optimization of their assembling.

BUILDING BLOCK 5 FOR β-SIDE GALACTOSYLATION

Synthesis of tetrasaccharide **g** started with the generation of galactose building block **5a** and **5b** with a neighboring participating group in the C-2 position.

Peracetylated galactose was formed by treating D-galactose **1** with acetic anhydride in pyridine or sodium acetate in acetic anhydride. Both procedures resulted in quantitative formation of the product. In the following, formation of galactosyl orthoester **2** was investigated using a two stepped protocol. In the first step, peracetylated galactose was treated with iodine and triethylsilane to form an anomeric iodide, which consecutively was substituted by the neighboring acetyl group. Noteworthy, better yields were observed when

methanol instead of toluene was used to remove water formed during reaction. In the second step, conditions mediated by TBAB and lutidine stabilized an acyloxonium ion, which was trapped by ethanol to form orthoester **2** in 62% yield. Subsequent reactions showed significant hydrolysis of the orthoester functionality under even slightly acidic conditions, *e.g.* silica gel.

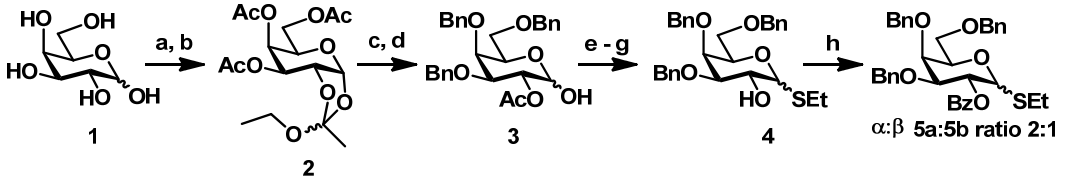

Scheme 8: Synthesis of galactose building blocks **5** equipped with a neighboring participating group: a) Ac_2O, pyr or NaOAc, Ac_2O, quant.; b) i) I_2, Et_3SiH, MeOH, ii) TBAB, lutidine, EtOH, 62%; c) KOH, BnBr, toluene, reflux, 82%; d) CSA, DCM, H_2O, 83%; e) DBU, CCl_3CN, DCM, 0°C, 76%; f) EtSH, TMSOTf, DCM, 0°C; g) NaOMe, MeOH/DCM, 50°C, 76% over two steps; h) BzCl, pyr, quant.

Therefore, instead of a stepwise protocol a one pot deacetylation benzylation with potassium hydroxide and benzyl bromide in refluxing toluene was attempted. Successfully the desired product was formed in 82% yield. Attempts of opening the orthoester using CSA and ethanethiol as nucleophile to directly generate the ethylthio galactoside resulted in formation of various side products. Therefore, the orthoester was hydrolyzed employing water and CSA in 83% yield. Using trichloroacetonitril and DBU, obtained hemiacetal **3** was converted into an imidate donor in 76%. After forming the thioglycoside in a glycosylation with ethanethiol, the acetyl group was removed using sodium methoxide in a mixture of DCM and methanol at 50°C. Desired product **4** was generated in 72% over two steps. Alcohol **4**, a mixture of α- and β-anomer, was benzoylated with benzoyl chloride in pyridine giving building blocks **5a/b** in quantitative yield. Consecutively, separation of α-anomer **5a** and β-anomer **5b** by silica column chromatography gave the products in a 2:1 ratio.

GALACTOSE BUILDING BLOCK 8 AND 10 WITHOUT PARTICIPATING GROUP

Perbenzylated galactose building blocks were synthesized having a phosphate[1], an ethylthio and a phenylthio group as leaving groups. D-galactose **1** was peracetylated with acetic anhydride in pyridine in quantitative yield. Peracetylated galactose was reacted with excess of ethanethiol in a BF_3-Et_2O catalyzed reaction at room temperature to yield corresponding α-galactoside **6** within three hours in quantitative yield. Removal of remaining acetyl groups with sodium methoxide gave ethylthiogalactoside **7**, which was directly benzylated using Williamson etherification[150] in 20% yield. The low yield in this reaction was

[1] Synthesized by Dr. Ivan Vilotijević

attributed to contamination of the compound due to Amberlite H^+ resin used for neutralization of sodium methoxide in the previous step.

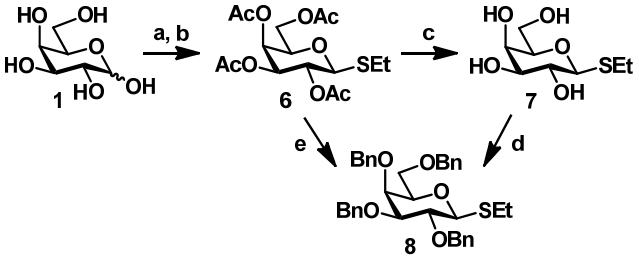

Scheme 9: Synthesis of galactose building block **8**, suitable for α- and β-galactosides: a) Ac_2O, pyr; b) EtSH, BF_3-Et_2O, DCM, quant. over two steps; c) NaOMe, MeOH/DCM, quant.; d) NaH, BnBr, DMF, 74% e) KOH, BnBr, toluene, reflux, 80%

This problem was solved by introducing a silica column chromatography purification step after deacetylation, improving the yield of **8** to 74%. Alternatively, an approach involving a one pot deacetylation benzylation with potassium hydroxide and benzyl bromide in refluxing toluene gave **8** in 80% yield.

Corresponding phenylthiogalactoside **10** was synthesized in similar manner. A quantitative peracetylation step with acetic anhydride in pyridine was followed by introduction of a thiophenyl group in a BF_3-Et_2O catalyzed reaction. Glycosylation with thiophenol resulted in incomplete conversion. Therefore, acetyl groups were removed using sodium methoxide. Phenylthiogalactoside **9** was observed in 54% yield over two steps. In the following, perbenzylation with benzyl bromide and sodium hydride delivered galactose building block **10** as a mixture of anomers in 85% yield.

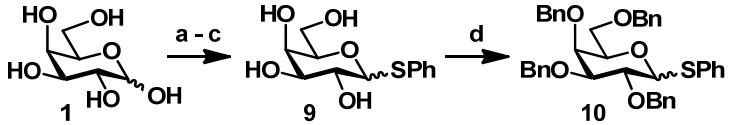

Scheme 10: Synthesis of galactose building block **10**, suitable for α- and β-galactosides: a) Ac_2O, pyr, quant.; b) PhSH, BF_3-Et_2O, DCM; c) NaOMe, MeOH/DCM, 54% over two steps; d) NaH, BnBr, DMF, 85%

MAN II BUILDING BLOCK 14 WITH ALLYL PROTECTION

The synthesis of mannose building blocks having an allyl protection at the anomeric center started by refluxing D-mannose **11** in allyl alcohol in presence of BF_3-Et_2O to obtain the α-allyl mannoside. After neutralization with NEt_3 and evaporation of the solvent, the allyl mannoside was protected at the C-6 position with TBDPS using TBDPS chloride and imidazole in DMF at 50°C to deliver the mannosyl triol in 76% yield over two steps. The synthesis of compound **12** was completed by formation of a 2,3-*iso*-propylidene acetal in 92% yield by stirring the triol in dimethoxypropane in presence of catalytic amounts CSA.

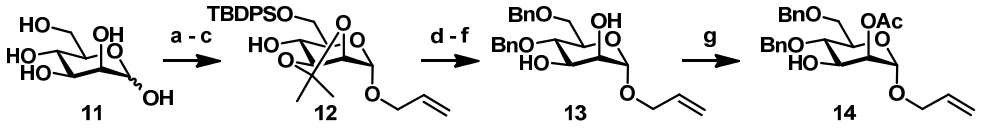

Scheme 11: Synthesis of mannose building block precursor **12** and a Man II building block **14**: a) AllylOH, BF_3-Et_2O; b) imidazole, TBDPSCl, 50°C, 76% over two steps; c) CSA, acetone, dimethoxypropane, 92%; d) TBAF, THF; e) NaH, BnBr, DMF; f) 80% AcOH, 72% over three steps; g) i) $Et(OEt)_3$, CSA; ii) 80% AcOH, 69%

Removal of the TBDPS group by treatment with TBAF in THF delivered a diol which was benzylated using benzyl bromide and sodium hydride. Subsequently, the 2,3-*iso*-propylidene acetal was hydrolyzed with 80% acetic acid to give diol **13** in 72% yield over three steps. Finally, *in situ* formation of the 2,3-orthoester with triethylorthoformate and CSA and hydrolysis in 80% acetic acid gave desired building block **14** in 69%.

MAN II BUILDING BLOCK 18 WITH THIOPHENYL PROTECTION

Additionally, mannose building block 18 was prepared, having a 2-methyl-5-*tert*-butyl-thiophenyl leaving group. This bulky group is stable towards other glycosylation methods, including more reactive thioglycoside donor. Therefore, the mannose building block is suitable for modification and glycosylation without functional group interconversion.

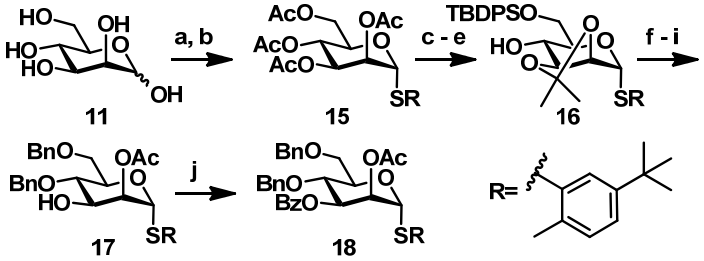

Scheme 12: Synthesis of mannose building block precursor **16** and Man II building block **18**: a) Ac_2O, pyr, quant.; b) 2-Methyl-5-*tert*-butyl-thiophenol, BF_3-Et_2O, DCM, 81%; c) NaOMe, MeOH/DCM, quant.; d) TBDPSCl, imidazole, DCM; e) CSA, acetone, 20% over two steps; f) TBAF, THF; g) NaH, BnBr, DMF; h) 80% AcOH; i) i) $Et(OEt)_3$, CSA; ii) 80% AcOH, 97% over four steps; j) BzCl, pyr, 92%

The process started with peracetylation of D-mannose **11** with acetic anhydride in pyridine. Quantitative peracetylation was followed by introduction of a thiophenyl group in a BF_3-Et_2O catalyzed reaction at the anomeric position. Thiomannoside **15** was obtained in 81% yield. The acetyl groups were removed with sodium methoxide in methanol. The formed tetra-ol was protected with TBDPS in C-6 position with TBDPS chloride and imidazole. 2,3-*iso*-propylidene acetal at C-2/C-3 positions was formed using CSA and acetone. During the reaction cleavage of TBDPS was observed, delivering alcohol **16** in 20% yield over two steps. Fortunately, the following step involved removal of TBDPS with TBAF to deliver a mannosyl diol, and the side product was used in this synthesis of mannose building block **18** as well. The mannosyl diol was benzylated using benzyl bromide and sodium hydride in DMF. Thereafter, *iso*-propylidene acetal was hydrolyzed in 80% acetic acid and the 2,3-orthoester

was formed with triethylorthoformate and CSA. Subsequent hydrolysis in 80% acetic acid delivered desired ester **17** in 97% yield over four steps without purification by column chromatography. Finally, esterification with benzoyl chloride in pyridine lead to building block **18** in 92% yield.

MAN III BUILDING BLOCK 21 WITH THIOPHENYL PROTECTION

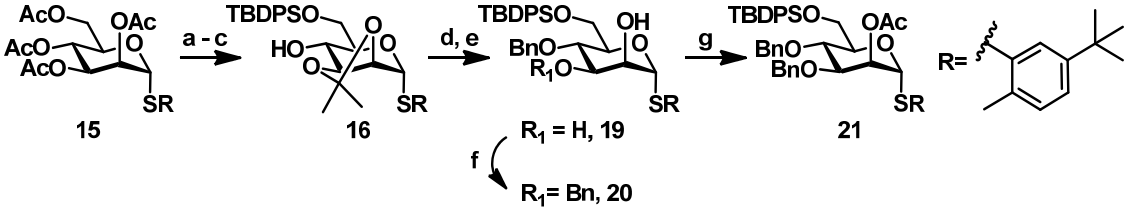

Scheme 13: Synthesis of mannose building block precursor **16** and Man III building block **21**: a) NaOMe, MeOH/DCM, quant.; b) TBDPSCl, imidazole, DCM; c) CSA, acetone, 20% over two steps; d) NaH, BnBr, DMF; e) 80% AcOH, 88% over two steps; f) Bu_2SnO, TBAI, BnBr, 43%; g) AcCl, pyr, quant.

The synthesis started with benzylation of the hydroxyl group at C-4 position of **16** using benzyl bromide and sodium hydride in DMF. Ketal hydrolysis in 80% acetic acid gave corresponding diol **19** in 88% yield over two steps. Regioselective installation of a second benzyl group by reaction of benzyl bromide with an *in situ* formed 2,3-tin-acetal delivered **20** in 43% yield. Acetylation of the C-2 hydroxyl group with acetylchloride in pyridine gave **21** in quantitative yield.

STEREOCONTROLLED SYNTHESIS OF TETRASACCHARIDE *g*

The stereocontrolled synthesis of tetrasaccharide g started with the glycosylation of mannose acceptor **14** with galactose donors **5a** and **5b** to give the disaccharide **22** in quantitative yield. The galactosides were activated using NIS and TMSOTf at 0°C. In the following, removal of acetyl in presence of benzoyl by using basic cleavage conditions resulted in undesired side reactions. Potassium carbonate cleaved both esters and the use of sodium methoxide resulted in a mixture of desired product **22** and the diol. Variation of sodium methoxide concentration and reaction time failed to selectively remove acetyl on this disaccharide. In contrast, an acidic deacetylation using anhydrous hydrochloric acid, generated in situ by addition of acetylchloride to a solution of the compound in DCM and methanol, gave desired alcohol **23** in 67 % yield with 80% conversion. Long reaction times ranging from two days to one week failed to improve conversion. With increased reaction temperature, full conversion was observed, but the benzoyl ester was removed as well.

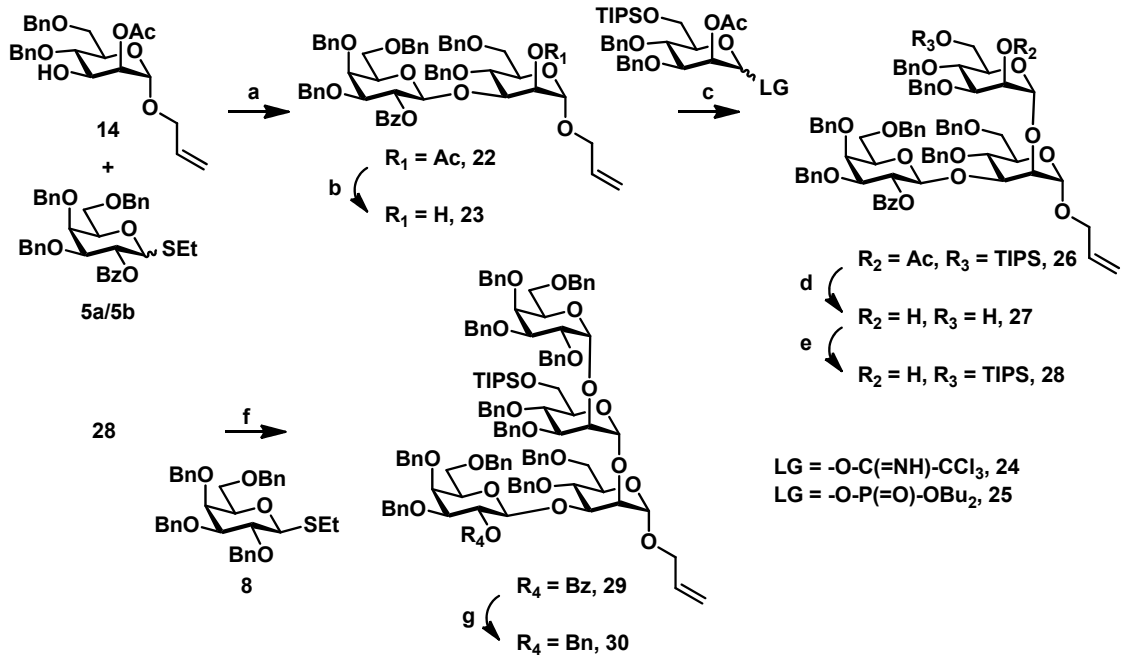

Scheme 14: Synthesis of tetrasaccharide **30** by stereocontrol of the first glycosylation: a) NIS, TMSOTf, 0°C, DCM, quant.; b) AcCl, MeOH/DCM, 67%, c) 5 eq **24**, TMSOTf, 0°C, DCM, 95%; d) AcCl, MeOH/DCM, 88%; e) TIPSCl, Imidazole, DMAP, 80°C, 96%; f) **28**, **8**, NIS, TMSOTf, Et_2O, -11°C, 88%, α,β-not separated; g) i) NaOMe, MeOH/DCM, 40°C; ii) NaH, BnBr, DMF and $CCl_3C(=NH)$-OBn, TMSOTf, DMF, 50% over two steps

The following [2+1] glycosylation reaction of **23** with imidate donor **24**[2] delivered trisaccharide **26** in 78% yield. Disaccharide **23** was a poor acceptor and was isolated together with hydrolyzed donor. Similar results were observed in reactions with phosphate donor **25**[3]. Even after eight hours reaction time no full conversion was observed.

The poor results obtained in this reaction with imidate **24** and phosphate **25** demonstrated the properties of acceptor **23** hamper efficient formation of product **26**. The low reactivity was attributed to the galactose residue since this effect was already observed during the removal of the acetyl group. Additionally, the theory is supported by previous and recent results of the group showing that [1+1]-glycosylation of Man II and Man III is readily achieved in high yields.

The best strategy to furnish trisaccharide **26** was a prolonged reaction time of eight hours and consecutive addition of new donor. A reaction using 5 eq imidate donor **24** delivered α-product **26** in 95% yield. The acceptor for the following [3+1]-glycosylation was synthesized by removing the acetyl group in the C-2 position of Man III under the optimized conditions applied for disaccharide **22**. However, as expected, the TIPS ether was removed during acid mediated deacetylation giving diol **27** in 88% yield. Reinstallation of TIPS using

[2] Synthesized by Dr. Ivan Vilotijević

[3] Synthesized by Dr. Ivan Vilotijević

Imidazole, DMAP and TIPSCl in DMF at 80°C delivered acceptor **28** in 96% yield. For stereocontrolled synthesis of α-galactosyl **29** glycosylation of thioethyl donor **8** was not efficient alone. Therefore, ether as solvent and TMSOTf/NIS as activator system were screened at different temperatures to optimize the glycosylation outcome. The results are summarized in *Table* 2 below. High yields of 72% to 88% were obtained at temperatures between 0°C and -18°C. By evaluating the ^{1}H-NMR spectra higher α-selectivity was observed towards lower temperatures of -11°C and -18°C. The screened temperatures below -40°C failed to show high conversion.

Temperature	Yield	α:β-Ratio	Conversion
0°C	77%	5.25:1	<90%
-4°C	72%	7:1	<90%
-11°C	88%	10:1	<90%
-18°C	81%	10:1	<90%
-40°C	66%	-*	<70%
-78°C	37%	-*	<40%

Table 2: Overview of the screening for α-selective galactosylations; * - not separated; yields are brsm

Taking the optimized conditions into account, glycosylation was performed at -11°C resulting in 88% yield of tetrasaccharide **29**. Additionally, glycosylation with thiophenyl donor **10** and the corresponding phosphate donor were evaluated using these optimized conditions, giving similar results as obtained with **8**. To identify the configuration of the anomers a coupled ^{1}H-^{13}C-HSQC NMR experiment was performed (Figure 22). The C-H coupling constants determined for the α-mannoses were 170.92 Hz and 172.56 Hz. 173.55 Hz and 161.71 Hz were found for the α-galactose and β-galactose respectively. These values suit well in the expected range of the desired anomers and thereby confirm the successful synthesis of tetrasaccharide **29**.[151]

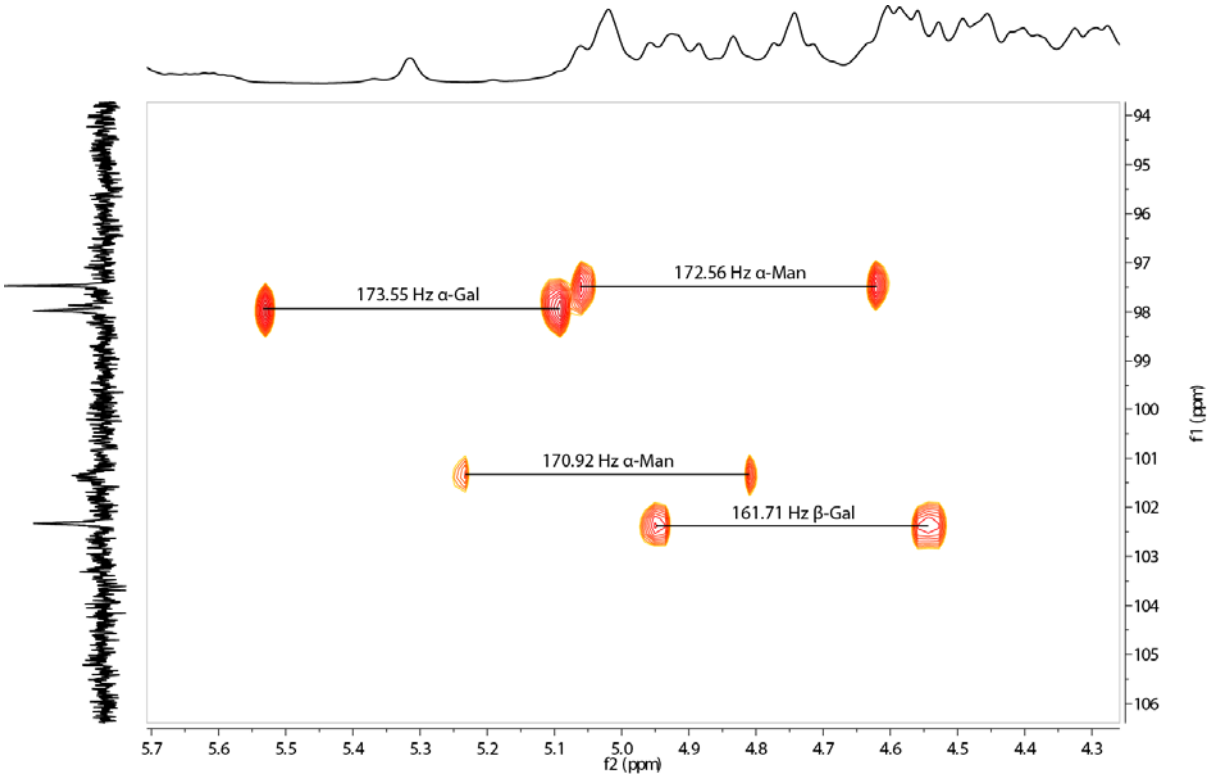

Figure 22: Coupled ^{1}H-^{13}C-HSQC of tetrasaccharide **29**, coupling constants are shown for each anomeric position

To complete the synthesis of the tetrasaccharide fragment **30**, the remaining benzoyl ester was replaced with a benzyl ether. Since deacetylation with sodium methoxide at 40°C was not complete after long reaction times, several repetitions of the reaction were necessary to complete removal of the protecting group. Moreover, the purification of the compound was hampered, due to the similar R_f of starting compound and product. The following benzylation also presented difficulties and failed to go to completion, even when using a reactive imidate of benzylalcohol. Again, multiple repetitions of the step were necessary to completely consume the starting material. The overall yield of the two reaction sequence to obtain **30** was 50%. Tetrasaccharide **30** was used for the synthesis of larger GPI fragments.

NON-STEREOCONTROLLED SYNTHESIS OF TETRASACCHARIDE g

To obtain **30** a second approach was evaluated. The process started with the glycosylation of mannose **14** and galactose **8**. Due to the lack of a participating neighboring group, the control of the reaction was exerted by temperature and solvent. The reaction at 0°C in DCM gave the desired β-disaccharide **31** in 66% yield, with quantitative conversion. The anomers were separated by silica column chromatography. When using the less reactive thiophenyl donor **10** similar results were obtained. Although, thiophenyl donor **10** tends to form the thermodynamically more stable product, the α-compound, the addition of acetonitrile as solvent shifted the equilibrium towards the β-compound **31**. The following deacetylation

with sodium methoxide in a mixture of methanol and DCM at 40°C gave acceptor **32** in 71% yield. Additionally, traces of undesired α-compound were removed.

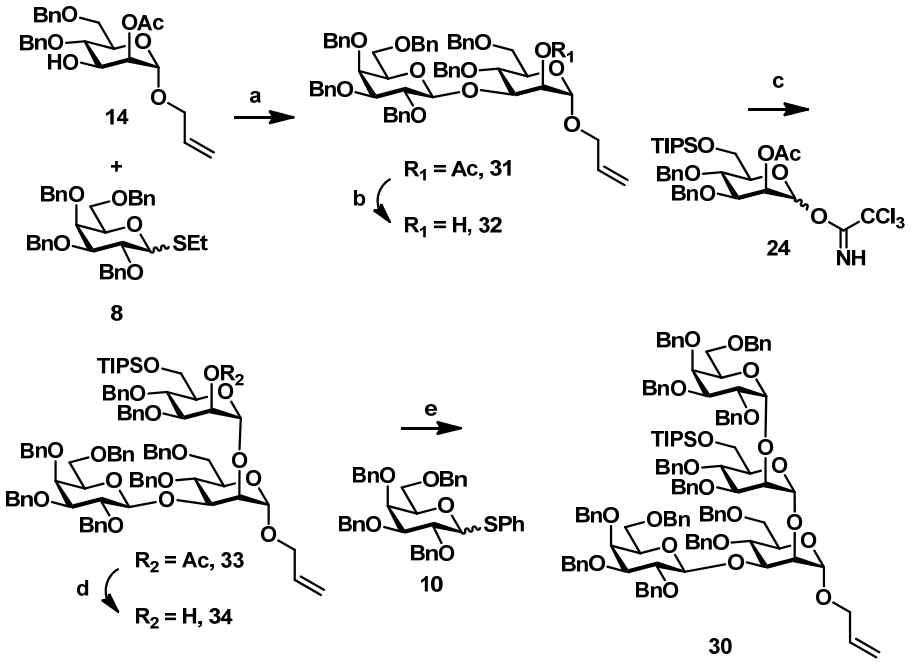

Scheme 15: Synthesis of tetrasaccharide **30** without stereocontrol of the first glycosylation: a) NIS, TMSOTf, DCM, 0°C, 66%; b) NaOMe, MeOH/DCM, 40°C, 71%; c) 3 eq **24**, TMSOTf, DCM 0°C; d) two cycles: NaOMe, MeOH/DCM, 82%; e) **10**, NIS, TfOH, Et2O, -11°C, 51%

The following step was the glycosylation of **32** with imidate **24** using multiple additions of donor to the reaction mixture. The poor reactivity of acceptor disaccharide **32** was comparable to the results observed for the stereo controlled strategy. Three equivalents of donor were required to give trisaccharide **33**. The corresponding glycosylation with thioglycoside donor **21** was not successful. Deacetylation of **33** was performed with sodium methoxide at room temperature. Due to incomplete conversion, **33** was resubmitted to a second deacetylation yielding **34** in 82% over two deprotection steps.

With the trisaccharide **34** in hand, the next glycosylation was approached. Due to its lower reactivity, thiophenyl donor **10** was used for the envisaged α-selective reaction with NIS and TfOH at -11°C in a 3.5:1 mixture of Et_2O and DCM. The desired α-product **30** was isolated in 51% yield and was separated from the β-compound by silica column chromatography. A coupled ^{1}H-^{13}C-HSQC NMR showed four anomeric signals with coupling constants of 170.79 Hz and 169.94 Hz for the two α-mannosides, 169.28 Hz for the α-galactoside and 158.51 Hz for the β-galactoside. With the compound **30** in hand, the synthesis of larger fragments of the *T. brucei* GPI was approached.

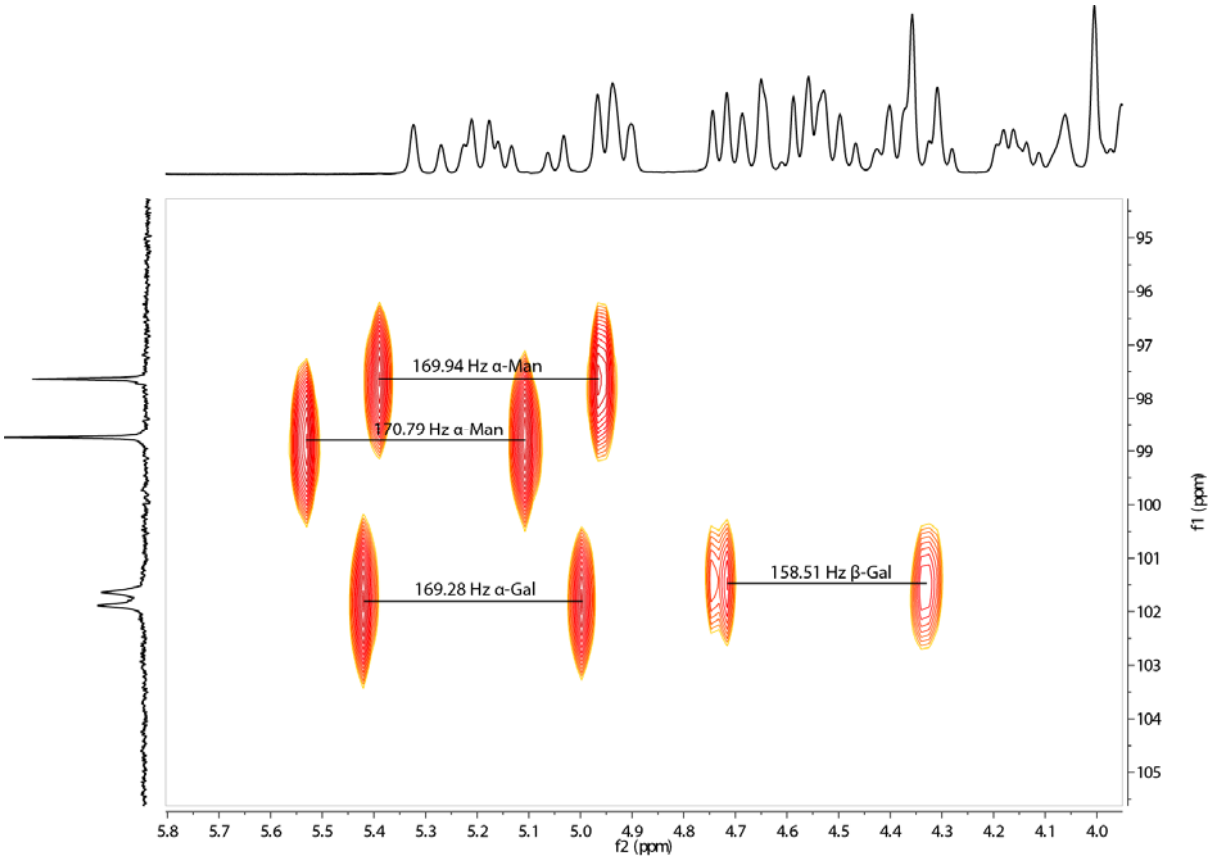

Figure 23: Coupled ^{1}H-^{13}C-HSQC of synthesized tetrasaccharide **30**, J_{CH} is shown for each anomeric position.

4.2 PENTASACCHARIDE WITH THIOLINKER 45

The assembling of a pentasaccharide involved the synthesis of Man I building block **38** equipped with a thiolinker.

Accordingly, thiolinker **35**[4] was glycosylated with mannose **25** using TMSOTF in DCM at 0°C. After deacetylation with sodium methoxide in a mixture of DCM and methanol product **36** was observed in 41% yield over two steps. Next, the C-2 position was benzylated in quantitative yield and the TIPS ether was removed using scandium triflate to give **38** in 71% yield.

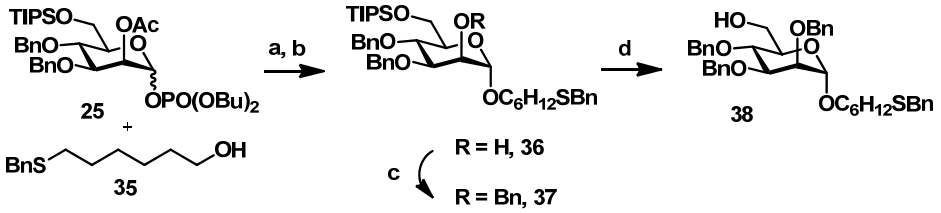

Scheme 16: Equipment of Man I building block **25** with thiolinker 35: a) 35, TMSOTf, DCM, 0°C; b) NaOMe, DCM/MeOH, 41% over two steps; c) NaH, BnBr, DMF, quant.; d) $Sc(OTf)_3$, H_2O, ACN/DCM, reflux, 71%

[4] Synthesized by Monika Garg

With the acceptor **38** in hand, **30** was used to synthesize corresponding imidate donor **40**. First, the allyl moiety was isomerized by an iridium catalyst and hydrolyzed by using an acidic mercury salt solution.

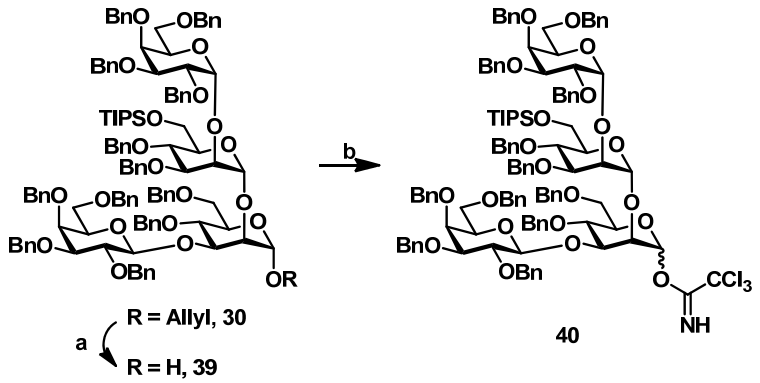

Scheme 17: Tetrasaccharide **30** was transferred into corresponding imidate donor 40: a) i) H_2, $[Ir(COD)(PMePh_2)_2]PF_6$, THF; ii) HgO, $HgCl_2$, acetone, water, 5:1, 61%; b) CCl_3CN, DBU, DCM, 95%

Under these conditions lactol **39** was formed in 61% yield with the corresponding enol ether isolated as a side product. The installation of the imidate leaving group using trichloroacetonitril and DBU in DCM at 0°C delivered **40** in 95% yield.

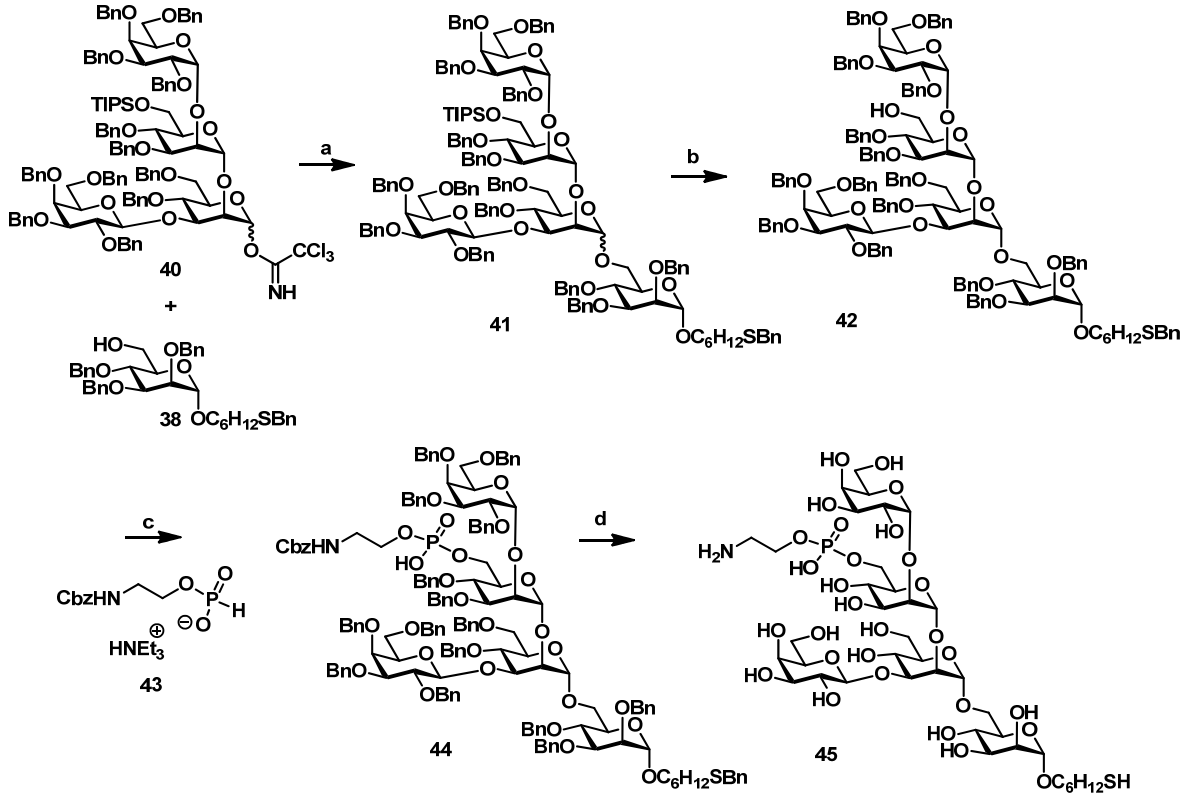

Scheme 18: Synthesis of pentasaccharide **45** applying a [4+1]-approach: a) TMSOTf, DCM, 0°C, 47%; b) $Sc(OTf)_3$, H_2O, ACN/DCM, reflux, 24%; c) i) **43**, PivCl, pyr; ii) I_2, H_2O, pyr, 0°C, 97%; d) $NH_{3(l)}$, Na, MeOH, -78°C, 10%

Tetrasaccharide donor **40** and mannose acceptor **38** were reacted in a [4+1]-glycosylation to give pentasaccharide **41** in 47% yield using TMSOTf in DCM at 0°C. In the next step, the TIPS ether was removed with scandium triflate and refluxing with water

in DCM. Separation of α- and β-product of pentasaccharide **41** was performed by preparative TLC giving **42** in 24% yield.

H-phosphonate **43**[5] was used for phosphorylation of alcohol **42** by activation with pivaloyl chloride in pyridine. Direct oxidation of the phosphonate diester with iodine and water in pyridine at 0°C gave compound **44** in 97% yield. Deprotection of thiolinker equipped compounds is possible under standard hydrogenolysis conditions. However, methods applied require additives to prevent Pd/C from deactivation by sulfur. Therefore, reductive conditions introduced by Birch[152] were selected as the best method to remove all protecting groups. Additionally to benzyl and napthylmethylethers, thioethers, esters, azides and small silyl groups are cleaved or reduced by sodium dissolved in liquid ammonia. Treatment of **44** under Birch conditions gave crude compound **45**, which was purified by G15 size exclusion in 5% ethanol in water and RP-HPLC (hypercarb column 150×10mm, ThermoFisher, 5 μ, acetonitrile in water 0-100% in 60 min). Product **45** was observed in 10% yield.

4.3 Assembly of a Pseudoheptasaccharide with thiolinker

The synthesis of a pseudoheptasaccharide lacking the tetragalactoside side branch of the VSG221 GPI required the synthesis of pseudotrisaccharide acceptor **51,** consecutive glycosylation using tetrasaccharide donor **40** and introduction of a linker.

To synthesize acceptor **51**, Man I building block **46** was used to glycosylate pseudodisaccharide **47** in 89% yield using NIS and TfOH in DCM at 0°C. Trisaccharide **48** was subjected to removal of the levulinic ester using sodium methoxide in a mixture of DCM and methanol and **49** was observed in 93% yield. Thereafter, **49** was benzylated using sodium hydride and benzyl bromide in DMF to give **50** in 93% yield. The TBDPS ether was removed using two different protocols, either TBAF or HF-pyridine in THF, in 83% and 68% yield respectively. Resulting acceptor **51** was used to glycosylate tetrasaccharide donor **40** using TMSOTf in THF at 0°C. Unfortunately, independent of the activation method used product **52** was formed only in traces. These results were in agreement with previous observations showing that modifications at Man II of tetrasaccharide fragment **40** are influenced by the β-galactose residue, significantly reducing reactivity.

[5] Synthesized by Ankita Malik

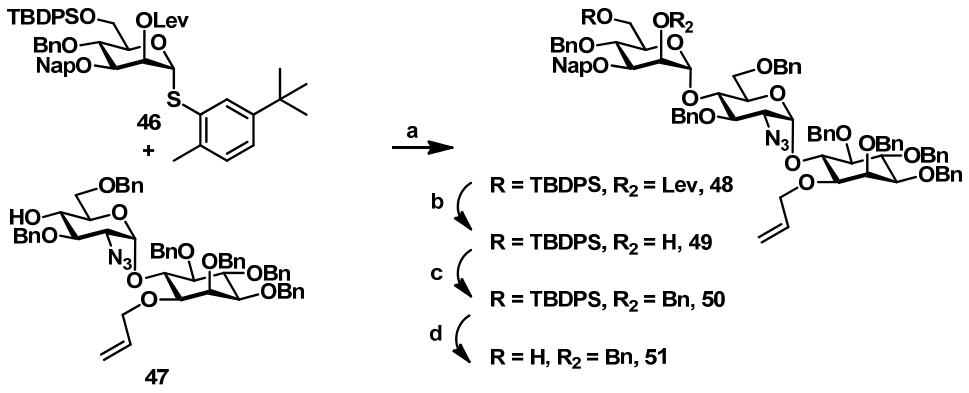

Scheme 19: Synthesis of pseudotrisaccharide acceptor **51** from thiodonor **46** and pseudodisaccharide **47**: a) NIS, TfOH, DCM, 0°C; b) NaOMe, MeOH/DCM, 93% over two steps; c) NaH, BnBr, DMF, 93%; d) TBAF, THF, 83% or HF-Pyridine, THF, 68%

To synthesize acceptor **51**, Man I building block **46** was used to glycosylate pseudodisaccharide **47** in 89% yield using NIS and TfOH in DCM at 0°C. Trisaccharide **48** was subjected to removal of the levulinic ester using sodium methoxide in a mixture of DCM and methanol and **49** was observed in 93% yield. Thereafter, **49** was benzylated using sodium hydride and benzyl bromide in DMF to give **50** in 93% yield. The TBDPS ether was removed using two different protocols, either TBAF or HF-pyridine in THF, in 83% and 68% yield respectively. Resulting acceptor **51** was used to glycosylate tetrasaccharide donor **40** using TMSOTf in THF at 0°C. Unfortunately, independent of the activation method used product **52** was formed only in traces. These results were in agreement with previous observations showing that modifications at Man II of tetrasaccharide fragment **40** are influenced by the β-galactose residue, significantly reducing reactivity.

Therefore, to obtain desired pseudoheptasaccharide **52** an alternative approach using Man II building block **18** in a glycosylation with pseudotrisaccharide **51** was followed. This [3+1]-reaction using NIS and TfOH in DCM at 0°C was successful and delivered tetrasaccharide **53** in 93%. The intermediate can be elongated along two sequences at Man II. The first sequence involves selective protection of the C-3 position and reaction of a Man III donor with the C-2 position. The second sequence requires a protection of the C-2 position, a single glycosylation at the C-3 position with a galactose donor and chain extension along the C-2 position. Evoking knowledge from the synthesis of donor **40**, it was decided to follow the second approach.

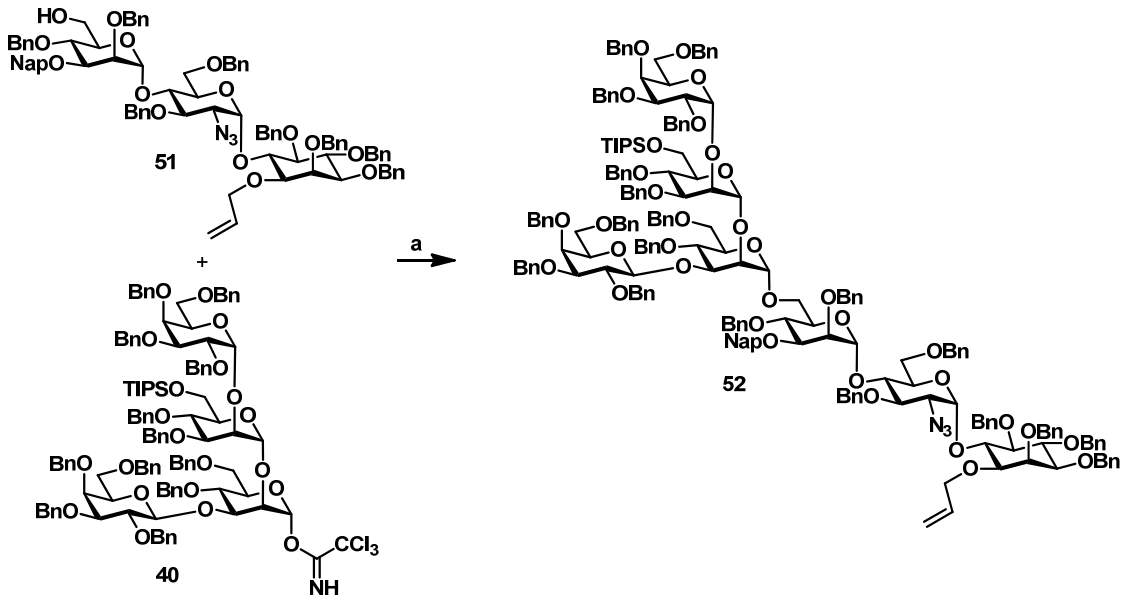

Scheme 20: Synthesis of pseudoheptasaccharide **52**: a) TMSOTf, THF, 0°C, traces

Therefore, to obtain desired pseudoheptasaccharide **52** an alternative approach using Man II building block **18** in a glycosylation with pseudotrisaccharide **51** was followed. This [3+1]-reaction using NIS and TfOH in DCM at 0°C was successful and delivered tetrasaccharide **53** in 93%. The intermediate can be elongated along two sequences at Man II. The first sequence involves selective protection of the C-3 position and reaction of a Man III donor with the C-2 position. The second sequence requires a protection of the C-2 position, a single glycosylation at the C-3 position with a galactose donor and chain extension along the C-2 position. Evoking knowledge from the synthesis of donor **40**, it was decided to follow the second approach.

Consequently, diester **53** was subjected to removal of the esters by potassium carbonate in a mixture of DCM and methanol giving diol **54** in 95% yield. Afterwards, acetyl was reinstalled in the C-2 position via an orthoester formation using triethylorthoformate and CSA. Subsequent hydrolysis by 80% acetic acid gave **55** in 70% yield over two steps. Tetrasaccharide **55** was glycosylated using donor **10** with the established protocol for β-selective galactosylations using NIS and TfOH in a 5:2 mixture of acetonitrile and DCM. Pentasaccharide **56** was synthesized in 63% yield. With **56** in hand the next reaction involves glycosylation to Man III. However, further elongation towards pseudoheptasaccharide **52** remains to be investigated.

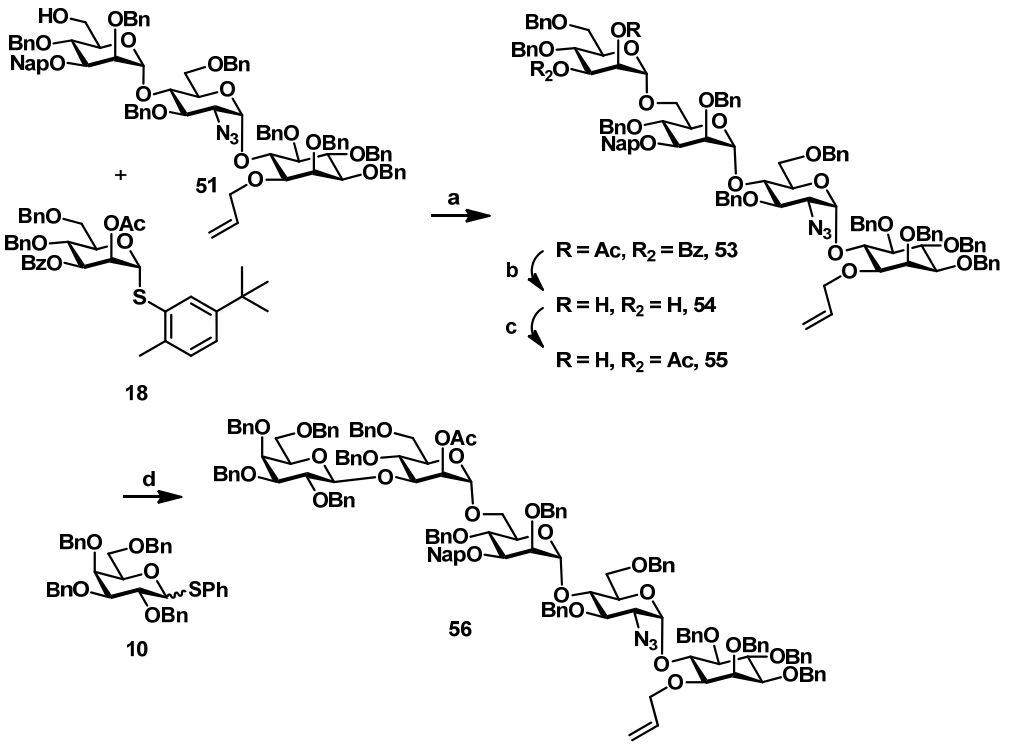

Scheme 21: Summary of synthetic efforts of an alternative route to **52**: a) **18**, NIS, TfOH, DCM, 0°C, 93%, b) K_2CO_3, DCM, 95%; c) i) $CH_3C(OEt)_3$, CSA, ACN; ii) 80% AcOH, 70% over two steps; d) **10**, NIS, TfOH, ACN/DCM, 0°C, 63%

4.4 ASSEMBLY OF TETRAGALACTOSIDE h

The synthesis of tetragalactoside **h** of the *T. brucei* side branch via a [2+2]-glycosylation approach required synthesis of new galactose building blocks and introduction of new methods for their assembling.

SIDE BRANCH GALACTOSE BUILDING BLOCK 60

To assemble tetragalactoside h, synthesis of three galactose building blocks was required. Depending on the strategy introduced in chapter 3.2 and their respective conditions, different orthogonal protecting groups are required. All building blocks were synthesized starting from the same precursor compound **60** shown in Scheme 22.

Starting from peracetylated galactose **57**, a stable allyl protecting group was introduced at the anomeric position using BF_3-Et_2O and allyl alcohol. Although, stereoselective outcome of allylation was determined by the 2-*O*-acetyl group, a mixture of α- and β-product resulted. The β-product was isolated in 65% yield. Removal of the acetyl groups with potassium carbonate in methanol gave allyl galactoside **58** in 92%. The next step, installation of the TBDPS group in the C-6 position using TBPDS chloride and imidazole in DCM, delivered the desired triol in 64% yield. Next, 3,4-*cis*-isopropylidene **58** was formed using CSA and dimethoxypropane in a yield of 96%. To yield building block **60**, PMB was

installed at the C-2-position using sodium hydride and PMB chloride in DMF. Long reaction time of one week, addition of TBAI and heating to 50°C was necessary to isolate product **60** in 71% yield. However, removal of TBDPS was observed during the reaction.

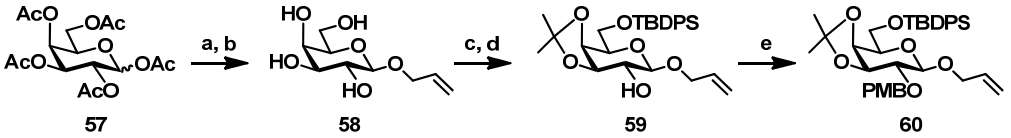

Scheme 22: Synthesis of galactose building block precursor **60**: a) AllylOH, BF_3-Et_2O, DCM, 65%; b) K_2CO_3, MeOH/DCM, 92%; c) TBDPSCl, imidazole, DCM, 64%; d) CSA, dimethoxypropane, 96%; e) NaH, PMBCl, TBAI, DMF, 50°C, 71%

GAL I/II BUILDING BLOCK 64 FOR [2+2]-GLYCOSYLATION

A building block synthesized from **60** was equipped with a benzoyl group in the C-4 position. According to literature[130], esters in this position can increase α-selectivity in galactosylations by remote participation. Ketal **60** was hydrolyzed using CSA in methanol to deliver diol **61** in 56% yield. To circumvent removal of the TBDPS group prolonged reaction times over one hour were avoided. According to TLC TBDPS cleavage started at this time. However, side products without TBDPS on the one hand and the ketal still intact on the other hand, are useful precursors for synthesis of other galactose building blocks, such as **69**. Regioselective benzylation by stannylation using Bu_2SnO for *in situ* formation of a tin acetal in the first step and TBAI and benzyl bromide in DMF for the second step delivered product **62** in 71 % yield. In contrast to reported procedures in literature,[153] refluxing in methanol instead of toluene gave better results. The following benzoylation of the C-4 position with benzoyl chloride in pyridine was conducted at 50°C. This procedure gave fully protected galactose **63** in 86% yield. For the required deprotection of the C-2 position, a 10:1 mixture of DCM and TFA was applied at 0°C for a maximum of 15 minutes and delivered product **64** in 90% yield.

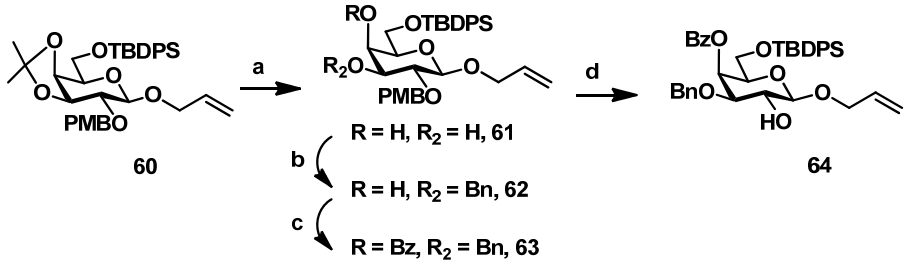

Scheme 23: Synthesis of galactose building block **64** from precursor **60**: a) CSA, MeOH, 56%; b) i) Bu_2SnO,MeOH; ii) BnBr, TBAI, DMF, 71%; c) BzCl, Pyr, 50°C, 86%; d) TFA, DCM, 0°C, 15 min, 90%

GAL I BUILDING BLOCK 65 WITH ALLYL PROTECTION

To complete synthesis of a building block containing orthogonal protecting groups at the C-2, C-6 and the anomeric position, ketal **60** was hydrolyzed in 80% AcOH leading to

diol **61** in 41% yield. The low yield was caused by TBDPS removal under the used conditions and isolated side product was used for synthesis of galactose building block **69**. The next reaction, a benzylation step using sodium hydride and benzyl bromide in DMF delivered **65** in 60% yield.

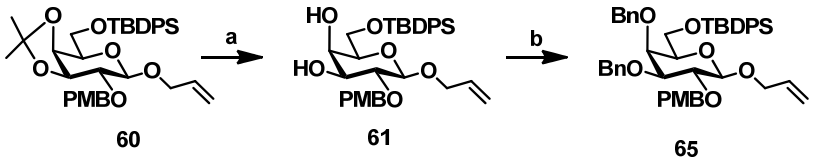

Scheme 24: Synthesis of orthogonal protected galactose building block **65**: a) 80% AcOH, 41%; b) NaH, BnBr, DMF, 60%

GAL II BUILDING BLOCK WITH THIOETHYL PROTECTION

A third building block **69** for synthesis of the galactose branch, was prepared as a thioglycoside. The TBDPS group of **60** was cleaved with TBAF in THF and the resulting alcohol was submitted to the removal of the ketal function using 80% acetic acid. Triol **66** was obtained in a yield of 48% over two steps. In the following, the three free hydroxyl groups of **66** were benzylated using sodium hydride and benzyl bromide in DMF to obtain **67** in 98% yield. The allyl group of galactose **67** was isomerized to the corresponding enol ether using an iridium catalyst and hydrogen and hydrolyzed using acidic mercury salt solution in aqueous acetone. To obtain the desired donor the intermediate hemiacetal was converted into imidate building block **68** in 29% over three steps. Higher selectivity towards activation conditions and higher stability in storage was achieved by converting imidate **68** in thioglycoside **69** in 77% yield (Scheme 25).

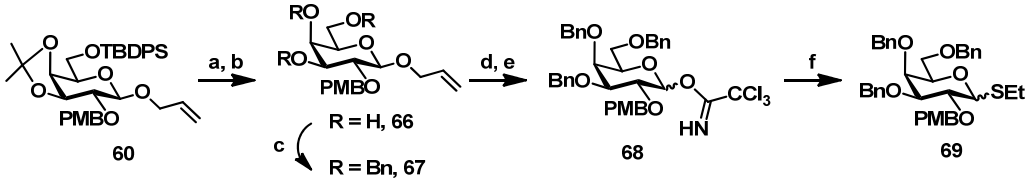

Scheme 25: Synthesis of thioglycoside **69** from precursor **60**: a) TBAF, THF; b) 80% AcOH, 50°C, 48% over two steps; c) NaH, BnBr, DMF, 98%; d) i) H_2, $[Ir(COD)(PMePh_2)_2]PF_6$, THF; ii) HgO, $HgCl_2$, acetone, water; c) DBU, CCl_3CN, DCM, 29% over three steps; f) EtSH, TMSOTf, DCM, 0°C, 77%

SYNTHESIS OF TETRAGALACTOSIDE h

With building blocks **8** and **64** in hand, synthesis of tetra-α-galactoside **h** was investigated according to the introduced [2+2]-glycosylation approach in chapter 3.2. For this synthesis, it was crucial to use optimized conditions for the initial [1+1]-α-selective glycosylation. According to the previous studies with **8**, optimized reaction temperatures for armed thioglycoside donor are between 0°C and -20°C. To investigate transferability of these

findings, glycosylation with thiodonor **8** was evaluated using NIS and TMSOTf as activating agent and ether as solvent at five different temperatures (Table 3).

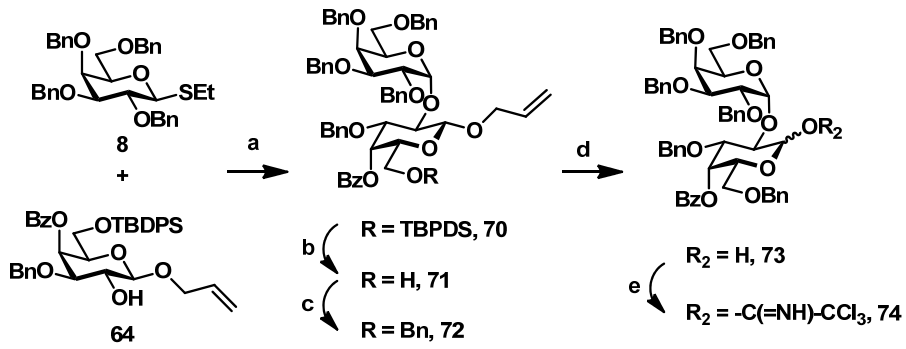

Scheme 26: Summary of synthetic efforts to synthesize acceptor **71** and donor **74**: a) NIS, TMSOTf, Et_2O, 59%; b) HF-Pyridine, THF, 69%; c) NaH, BnBr, DMF, 54%; d) i) H_2, $[Ir(COD)(PMePh_2)_2]PF_6$, THF; ii) HgO, $HgCl_2$, acetone, water, 5:1, 95%; e) CCl_3CN, DBU, DCM, 0°C, traces

However, reactions at 0°C and -18°C showed significant TMS coupling in the anomeric position. Therefore, TMSOTf was replaced by triflic acid as a promotor. In comparison, following reactions showed higher yields of product **70** and lower conversion rates towards lower temperatures. **70** was synthesized using triflic acid at -11°C in 59% yield as a mixture of anomers. The desired α-disaccharide was obtained after purification by silica column chromatography.

Temperature	Activator	Yield	α:β-Ratio	Conversion
0°C	TMSOTf	43%	2,5:1	-
0°C	TfOH	33%	2:1	<70%
-11°C	TfOH	59%	1,6:1	<70%
-18°C	TMSOTf	49%	1:1,4	-
-18°C	TfOH	45%	3:1	<70%
-40°C	TfOH	56%	-*	<60%
-78°C	TfOH	-		-

Table 3: Overview of screening α-galactosylation of **8** and **64**

With α-disaccharide **70** in hand, synthesis of building blocks **71** and **74** required for a [2+2]-glycosylation strategy to obtain tetrasaccharide **75** was explored. For both building blocks the TBDPS group in the C-6 position was removed in 69% yield by employing HF-pyridine in THF. Product **71** was kept as acceptor. In the following, benzylation of the C-6 position was completed to deliver **72** in 54% yield using sodium hydride and benzyl bromide in DMF. Afterwards, allyl was removed using an iridium catalyst and hydrogen for isomerization and acidic mercury salt solution in aqueous acetone for hydrolysis giving hemiacetal **73** in 95% yield. Synthesis of envisaged imidate **74** using trichloracetonitrile and DBU in DCM at 0°C gave only traces of the product and rearranged amide as the main

product. Investigation to obtain tetrasaccharide **75** using [2+2]-glycosylation with TMSOTf in DCM at 0°C showed no formation of the product.

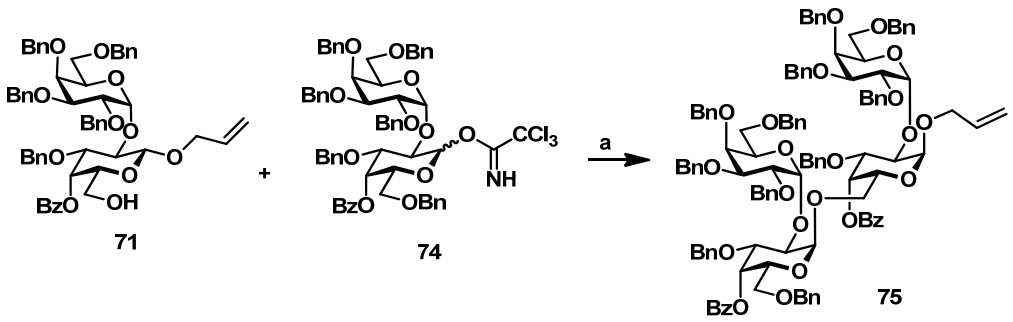

Scheme 27: Optimal [2+2]-glycosylation conditions for synthesis of 75 require further investigation: a) TMSOTf, DCM, 0°C, traces

Therefore, optimal conditions for a [2+2] strategy for assembling the side branch α-tetra-galactoside require further investigation. Taking into account, that formation of imidate **74** already resulted in low conversion, it is indicated that **74** has a low reactivity mediated by steric hindrance of the anomeric position.

4.5 TETRAGALACTOSE-MAN I WITH THIOLINKER

Synthesis of a pentasaccharide required glycosylation of a Man I building block and the corresponding donor of tetraglactoside **76**[6].

ORTHOGONAL PROTECTED MAN I BUILDING BLOCK 79

Synthesis of Man I building blocks started from precursor building block **12.** After benzylation with sodium hydride and benzyl bromide in DMF in 71% yield, hydrolysis of the ketal was performed using 80% acetic acid at 40°C. These conditions gave desired product **77** in 84% yield. Selective protection of the C-3 hydroxy group was accomplished by *in situ* formation of a tin acetal with Bu_2SnO in methanol and consecutive regioselective methyl naphthylation with naphtyhlmethyl bromide and TBAB in DMF. Alcohol **78** was isolated in 83% yield and the remaining C-2 position was protected with a levulinic ester group. Esterification was performed using levulinic acid, DCC and DMAP leading to mannose building block **79** in 90% yield.

[6] Synthesized by Dr. Bo-Young Lee

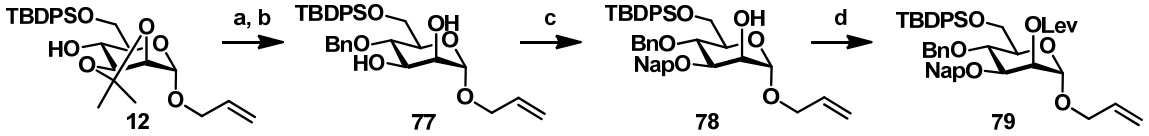

Scheme 28: Synthesis of orthogonal protected Man I building block **79**: a) NaH, BnBr, DMF, 71%; b) 80% AcOH, 84%, c) i) Bu_2SnO, MeOH; ii) TBAI, NapBr, DMF, 83%; d) LevOH, DMAP, DCC, DCM, 90%

C-3 UNPROTECTED MAN I BUILDING BLOCK 81

A second Man I building block was synthesized for glycosylation reactions at the C-3 position. Alcohol **12** was benzylated in 71% yield using sodium hydride and benzyl bromide in DMF. For hydrolysis of the ketal different approaches were evaluated. CSA in a mixture of DCM and methanol gave product **80** in 31% yield. In contrast, performing the reaction by replacing methanol by 100 eq ethanethiol, quantitative amounts of diol **80** were isolated. To install a participating neighboring ester group, an orthoester was formed between the C-2 and the C-3 position using triethylorthoformate and CSA in acetonitrile. Acidic hydrolysis by 80% acetic acid selectively opened the moiety towards the C-2 position gave mannose building block **81** in quantitative yield.

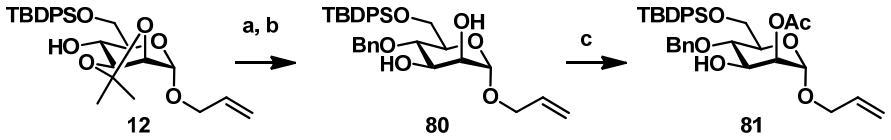

Scheme 29: Synthesis of Man I building block **81**: a) NaH, BnBr, DMF, 71%; b) CSA, MeOH/DCM, 31% or EtSH, CSA quant.; c) i) $CH_3C(OEt)_3$, CSA, ACN; ii) 80% AcOH, quant.

ASSEMBLY OF TETRAGALACTOSE-MAN I WITH THIOLINKER

Tetragalactoside **76**,[7] synthesized by a stepwise glycosylation approach and naphthylmethyl ethers as protecting groups, was used to attach the corresponding linker equipped compounds for conjugation experiments. Removal of the allyl protecting group was accomplished by isomerization with an iridium catalyst and hydrolysis by mercury salts in aqueous acetone solution. Resulting lactol **82** was isolated in 81% and installation of imidate species **83** was performed in DCM using trichloracetonitrile and DBU in DCM at 0°C. **82** showed low reactivity and multiple reaction cycles with the recovered non-reacted lactol were necessary to obtain imidate **83** in 11% yield. In the next reaction glycosylation of **81** was explored. Using TMSOTf in DCM at 0°C product **84** was isolated only in traces, not sufficient for investigations towards attachments of a linker or the synthesis of larger GPI fragments. A possible explanation for low yields observed in the reactions, is steric hindrance

[7] Synthesized by Dr. Bo-Young Lee

at the anomeric position. Additionally, low reactivity was already observed for imidate formation, indicating a low reactivity of the anomeric positions of this tetragalactoside.

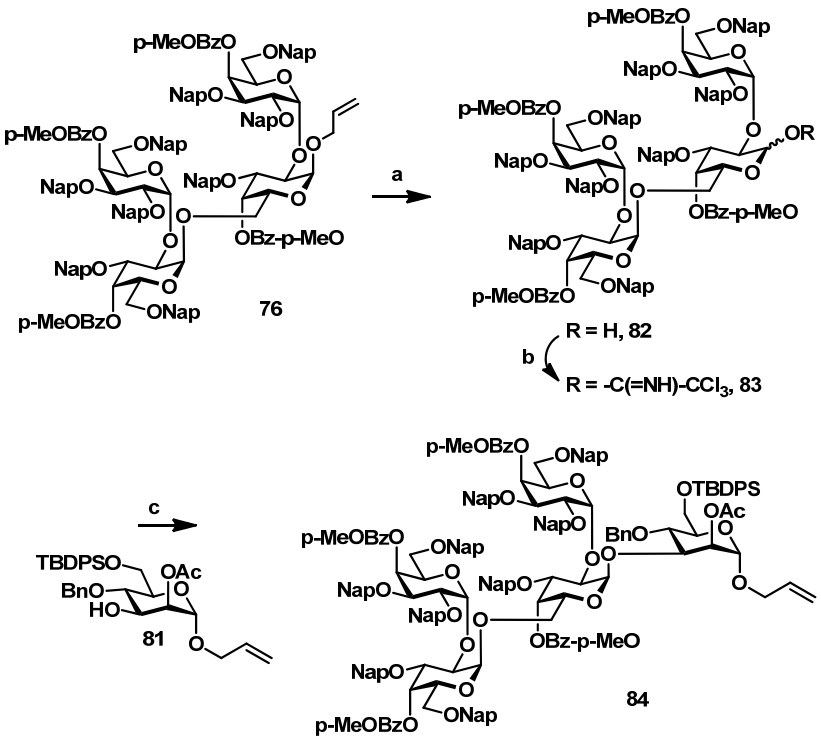

Scheme 30: Summarized efforts in synthesizing **84**: a) i) H_2, $[Ir(COD)(PMePh_2)_2]PF_6$, THF; ii) HgO, $HgCl_2$, acetone, water, 5:1, 81%; b) CCl_3CN, DBU, DCM, 0°C, 11%; c) TMSOTf, DCM, 0°C, traces

However, to investigate the properties of imidate **83**, it was decided to introduce linker **35** directly, since the reactive hydroxyl group is a primary alcohol and remote enough to ensure a reaction. Product **85** was formed in 20% yield using TMSOTf in DCM at 0°C. A Birch reduction was used to remove all protecting groups. Tetragalactoside **86** was purified, using a sephadex G25 size exclusion column using 5% ethanol and water as eluent and by RP-HPLC (hypercarb column 150×10mm, ThermoFisher, 5 µ, acetonitrile in water 0-100% in 60 min). Compound **86** was isolated in 20% yield.

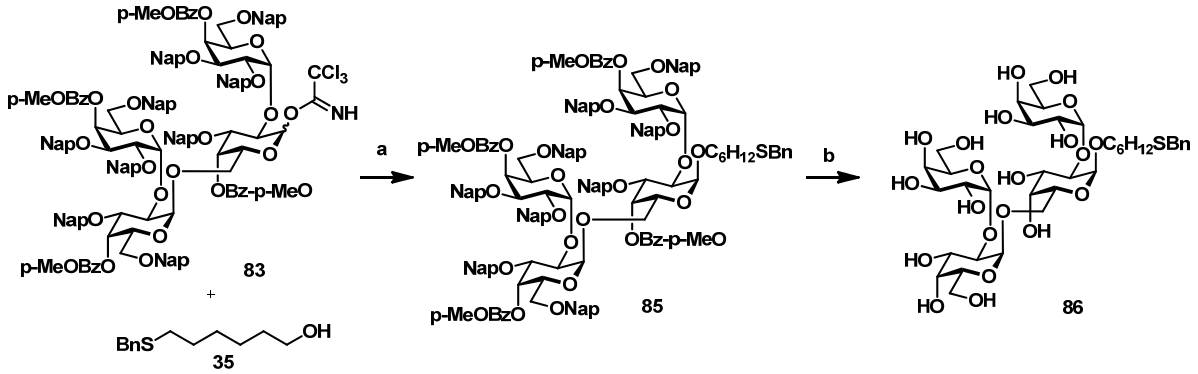

Scheme 31: Synthesis of tetragalactoside **86** equipped with a linker: a) TMSOTf, DCM, 0°C, 20%; b) $NH_{3(l)}$, Na, MeOH, -78%, 20%

4.6 *MYO*-INOSITOL WITH PHOSPHO-THIOLINKER 90

myo-Inositol building block **87**[8] was equipped with the H-phosphonate of 6-Thiobenzylhexanol **88**[9].

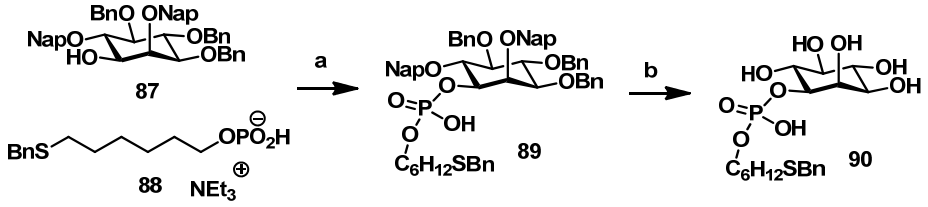

Scheme 32: Synthesis of *myo*-Inositol **90**: a) i) 88, PivCl, pyr; ii) I_2, H_2O, pyr, 43%; b) $NH_{3(l)}$, Na, MeOH, -78°C, 6%

Phosphonylation of **87** and **88** using pivaloylchloride in pyridine was followed by direct oxidation of the intermediate by iodine in aqueous pyridine and gave phosphate **89** in 43% yield. Birch reduction was successfully used to obtain crude compound **90**, which was purified on a sephadex LH20 size exclusion column with 5% ethanol in water as eluent and RP-HPLC (hypercarb column 150×10mm, ThermoFisher, 5 µ, acetonitrile in water 0-100% in 60 min). Pure **90** was isolated as disulfide in 6% yield.

4.7 DISACCHARIDE WITH THIOLINKER 93

Naturally, Man I is bearing the branch of α-galactosides in *T. brucei* GPI. Therefore, Man I building block **81** was used in glycosylations for the synthesis of fragments containing α-galactosides. During the synthesis of tetrasaccharide **31** a significant amount of α-galactosyl-mannoside **91** was accumulated as a sideproduct.

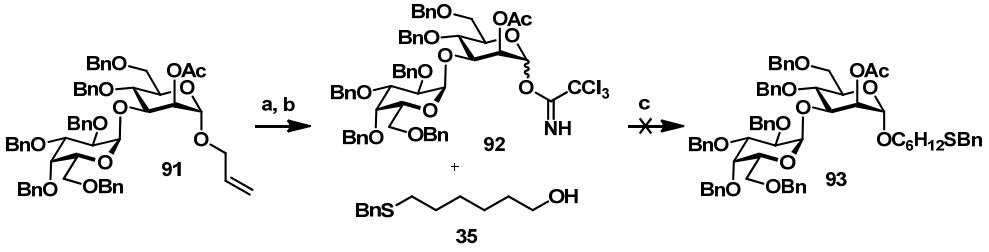

Scheme 33: Summarized efforts of synthesizing **93**: a) i) H_2, $[Ir(COD)(PMePh_2)_2]PF_6$, THF; ii) HgO, $HgCl_2$, acetone, water, 5:1, 17%; b) CCl_3CN, DBU, DCM, 0°C 78%; d) 35, TMSOTf, DCM, 0°C

Disaccharide **91** was submitted to the removal of the allyl group by isomerization with iridium catalyst and hydrogen and hydrolysis by acidic solution of mercury salts in aqueous acetone. Purification by silica column chromatography failed to deliver pure product and therefore isolation of the lactol was examined by supercritical fluid chromatography (Viridis

[8] Synthesized by Dr. Ivan Vilotijević

[9] Synthesized by Monika Garg

2EP-pyridine, semipreparative, 5 µ, ethyl acetate in $CO_{2(sc)}$, 0 to 40% in 60 min). As it can be seen in Figure 24 a mixture of anomers were isolated in 17% yield. The hemiacetal was used for installation of an imidate group using trichloracetonitrile and DBU in DCM at 0°C and gave donor **92** in 78% yield. To synthesize compound **93,** 6-thiobenzylhexanol **35** was used as acceptor in a glycosylation reaction. However, by using TMSOTF in DCM at 0°C, no formation of product **93** and decomposition of employed donor **92** was observed.

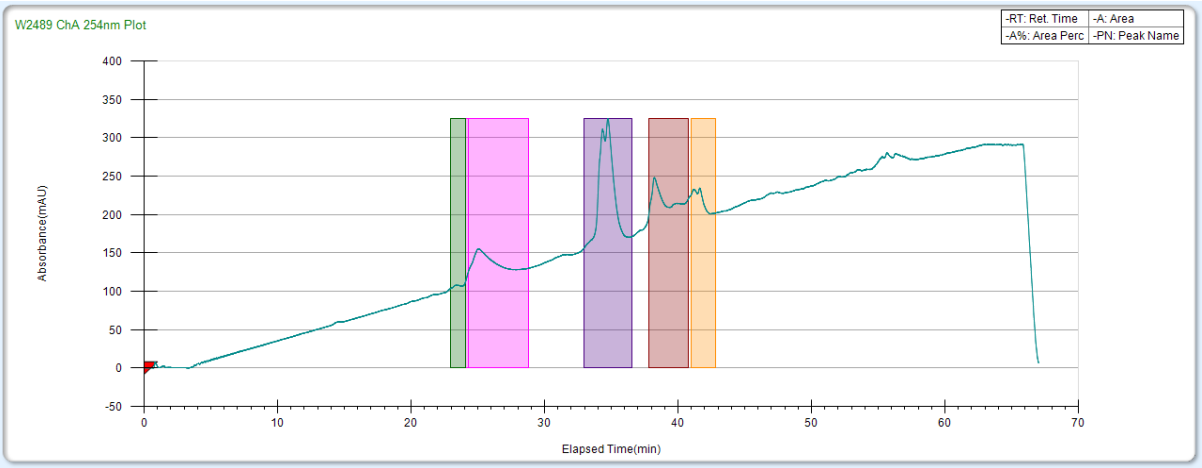

Figure 24: SFC chromatogram of the intermediate lactol: the violet trace indicates a mixture of anomers and was separated from impurities. Viridis 2EP-pyridine, semipreparative, 5 µ, ethyl acetate in $CO_{2(sc)}$, 0 to 40% in 60 min

Since the installation of linker **35** was not accessible by this route, a new synthetic approach was chosen. Man I building block **48** was glycosylated with galactose building block **94**[10]. Although a chloroacetyl group was present in the donor, the optimized conditions for reactive armed thioglycosides were used, *i.e.* -11°C, NIS, TMSOTf, DCM/Ether. Reaction gave disaccharide **95** in quantitative yield as a 1:1 mixture of α- and β-anomer. Isomerization by iridium catalyst and hydrogen and hydrolysis using acidic mercury salt solution in aqueous acetone removed the allyl protecting group in 65% yield. Lactol **96** was used for installation of an imidate leaving group by trichloroacetonitrile and DBU in DCM at 0°C. Resulting donor **97** was isolated in 84% yield and glycosylated with protected linker **35** in quantitative yield using TMSOTf and in DCM at 0°C. Anomeric coupling constants were measured by coupled ^{1}H-^{13}C-HSQC obtaining values of 175.29 Hz for galactose and 169.86 Hz for mannose, indicating presence of both α-glycosidic bonds (Figure 25)

[10] Synthesized by Dr. Yu-Hsuan Tsai

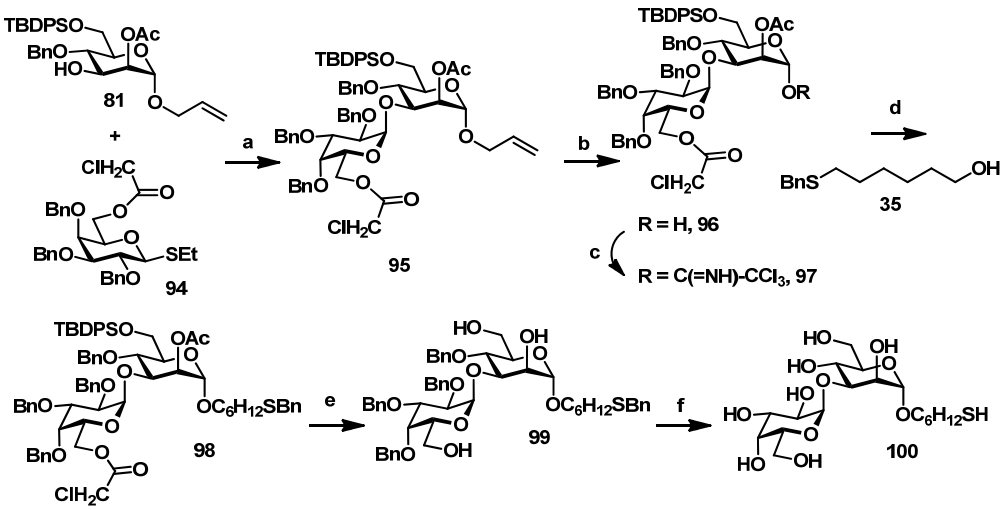

Scheme 34: Synthesis of disaccharide **100**: a) NIS, TMOSTf, DCM/Et_2O, -11°C, 50%; b) i) H_2, $[Ir(COD)(PMePh_2)_2]PF_6$, THF; ii) HgO, $HgCl_2$, acetone, water, 5:1, 65%; c) CCl_3CN, DBU, DCM, 0°C, 84%; d) **35**, TMSOTf, DCM, 0°C, quant.; e) AcCl, DCM/MeOH, 48%; f) $NH_{3(l)}$, Na, MeOH, -78°C, 5%

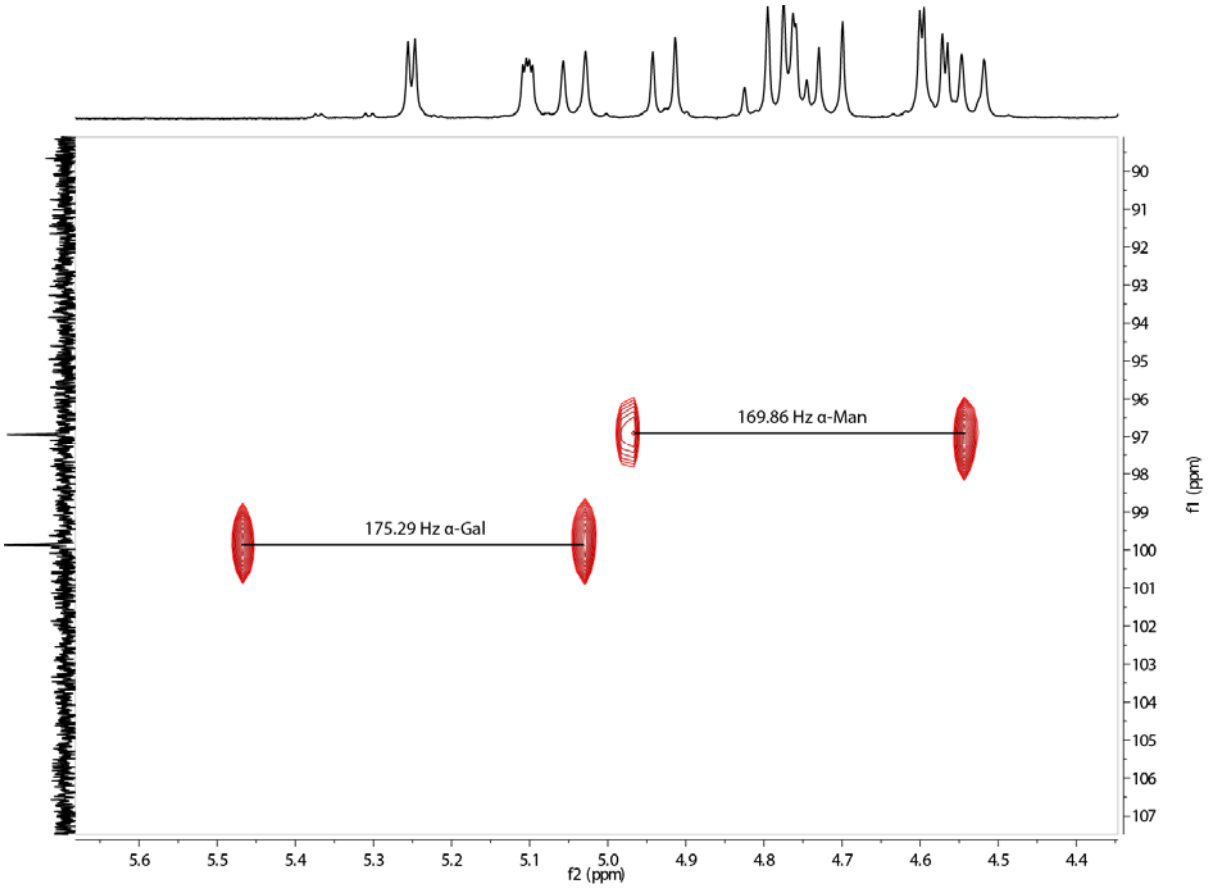

Figure 25: Coupled ^{1}H-^{13}C-HSQC of synthesized disaccharide **97**, J_{CH} is shown for each anomeric position.

All acid labile groups were removed by *in situ* generation of HCl from acetylchloride and methanol in a mixture of DCM and methanol. Triol **99** was isolated in 48% yield. Next, Birch conditions were applied to fully deprotect disaccharide **99**. To separate **100** from side products and remaining salt purification by sephadex G15 size exclusion using 5% ethanol in water as eluent and RP-HPLC (hypercarb column 150×10mm, ThermoFisher, 5 µ, acetonitrile

in water 0-100% in 60 min) was performed. Disaccharide **100** was isolated as disulfide in 5% yield.

4.7 TRISACCHARIDE WITH THIOLINKER 110

The synthesis of corresponding compound trisaccharide **110** with an α1→6 linked galactose requires a galactose building block with an orthogonal protecting group at the C-6 position that can be removed after coupling to Man I building block **81**.

GALACTOSE BUILDING BLOCK 102

To synthesize building block **102**, alcohol **101**[11] was protected with a naphtylmethyl group in 70% yield using sodium hydride and NapBr in DMF.

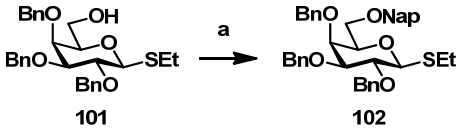

101 102

Scheme 35: Synthesis of galactose building block **102**: a) NaH, NapBr, DMF, 70%

SYNTHESIS OF TRISACCHARIDE WITH THIOLINKER 110

Man I building block **81** was glycosylated with galactose donor **102** using the developed protocol for armed reactive thiodonorsd, *i.e.* -11°C, NIS, TMSOTf, DCM/Ether. Purification of **103** was not successful at this stage. Therefore, the naphtylmethyl protecting group was removed with DDQ in aqueous DCM. Afterwards, eparation of α- and β-anomer was possible and α-anomer **104** was isolated in 20% over two steps. In the following step **104** was reacted with thioglycoside **94** under identical conditions as the glycosylation before. Trisaccharide **105** was isolated in 35% yield.

To introduce the linker moiety, allyl was removed by isomerization using iridium catalyst and hydrogen and hydrolysis by acidic mercury salt in aqueous acetone giving lactol **106** in 45% yield. Next, imidate **107** was synthesized in 95% yield using trichloracetonitrile and DBU in DCM at 0°C. Following glycosylation with linker **35** using TMSOTf in DCM at 0°C gave desired product **108** in 67% yield. Removal of acid labile protecting groups by HCl generated *in situ* from acetylchloride and methanol in DCM, resulted in formation of **109** in 83% yield. Birch reduction gave rise to crude compound **110**. Purification by sephadex G15 size exclusion column using 5% ethanol and water as eluent and RP-HPLC (hypercarb

[11] Synthesized by Dr. Yu-Hsuan Tsai

column 150×10mm, ThermoFisher, 5 µ, acetonitrile in water 0-100% in 60 min) gave **110** as disulfide in 19% yield.

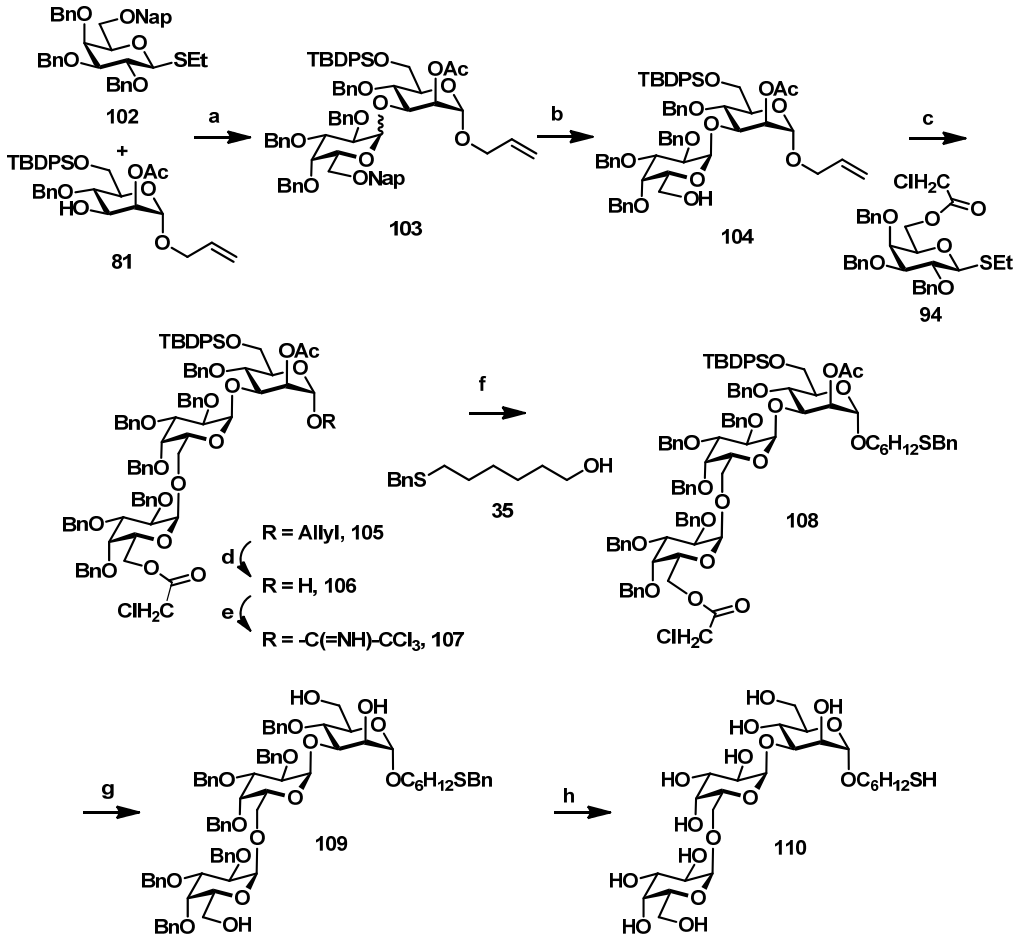

Scheme 36: Synthesis of trisaccharide **110**: a) NIS, TMSOTf, -11°C, DCM/Et_2O; b) DDQ, DCM, H_2O, 20% over two steps; c) **94**, NIS, TMSOTf, -11°C, DCM/Et_2O, 35%; d) i) H_2, $[Ir(COD)(PMePh_2)_2]PF_6$, THF; ii) HgO, $HgCl_2$, acetone, water, 5:1, 45%; e) CCl_3CN, DBU, DCM, 0°C, 95%; f) **35** ,TMSOTf, DCM, 0°C, 67%; g) AcCl, DCM:MeOH, 83%; h) $NH_{3(l)}$, Na, MeOH, -78°C, 19%

4.9 PSEUDOPENTASACCHARIDE PHOSPHO-THIOLINKER 120

To synthesize pseudo pentasaccharide **120** galactose building block **94** was initially used to glycosylate Man I building block **81**. The established conditions for formation of α-selective galactosides, *i.e.* -11°C, NIS, TfOH, DCM/Et_2O, delivered 37% yield of the α-anomer. Next, removal of the chloroacetyl group was achieved by heating the disaccharide and thiourea in chloroform to 50°C. Alcohol **104** was isolated in 81%. To ensure α-selectivity during formation of desired trisaccharide **112** galactose building block **111**[12]**,** having an ester function in the C-4 position, was used. Unfortunately, product and hydrolyzed donor were not separable by silica column chromatography. Therefore, allyl protecting was removed by isomerization using an iridium catalyst and hydrogen and hydrolysis by acidic mercury salt

[12] Synthesized by Dr. Bo-Young Lee

solution in aqueous acetone, giving lactol **113** in 75% over three steps. Installation of the imidate leaving group gave **114** in quantitative yield. Afterwards pseudodisaccharide **115**[13] was used in a glycosylation with imidate **114** delivering pentasaccharide **116** in 48% yield. Following the TBDPS ether in molecule **116** was removed to yield alcohol **117**.

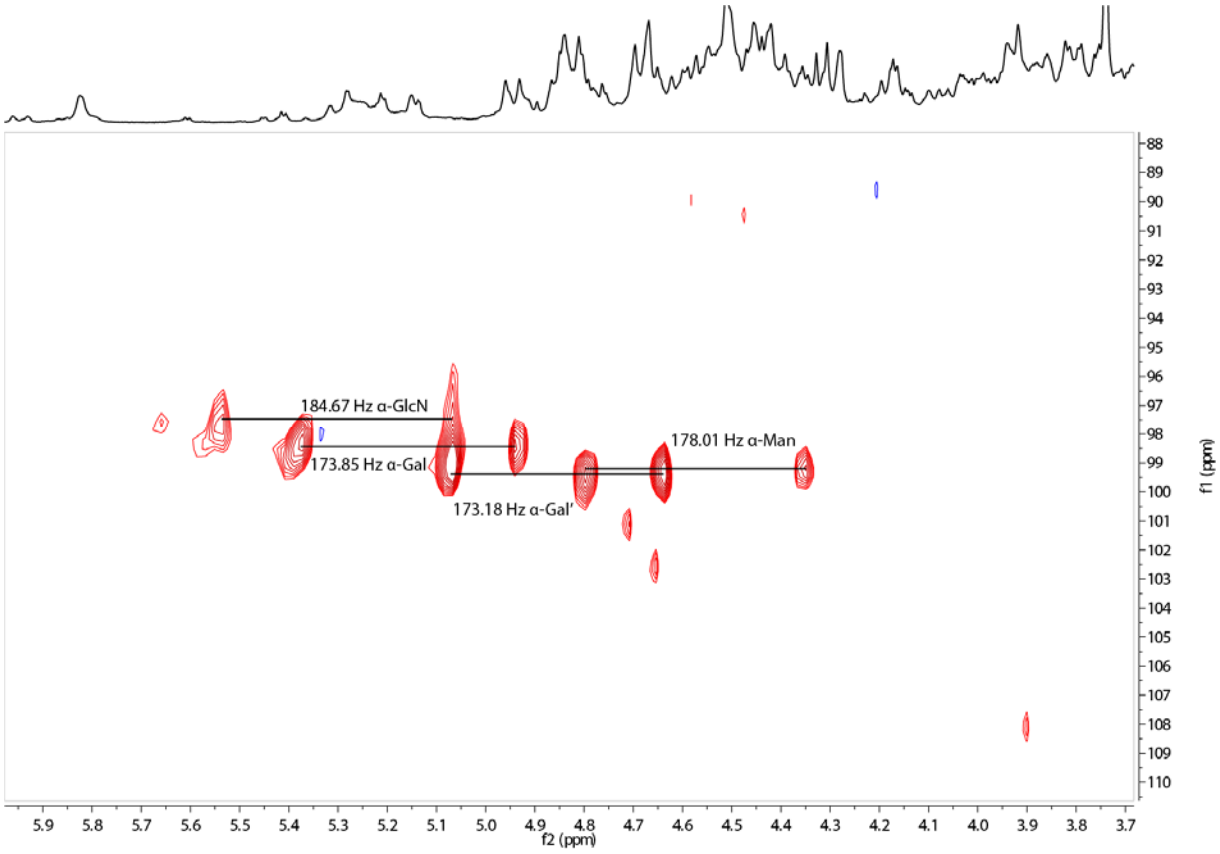

Figure 26: Coupled ^{1}H-^{13}C HSQC of pentasaccharide **117**. J_{CH} are shown in Hz and proof successful synthesis

Anomeric coupling constants were measured by coupled ^{1}H-^{13}C-HSQC and proofed the presence of four α-glycosidic bonds (GlcN - 184.67 Hz, Gal - 173.85 Hz, Gal' - 173.18 Hz, Man - 178.01 Hz). In the next step, removal of remaining ester was performed by sodium methoxide in a mixture of DCM and methanol at 50°C. However cleavage of the *para*-methoxy benzoyl ester remained incomplete. After isolating and resubmitting the reaction product, still an inseparable mixture of ester and alcohol was observed. However, under Birch reduction conditions for global deprotection of final compounds, ester functions are cleaved as well. For this reason, the mixture was subjected to following steps without separation of the compounds. In the next step, benzylation with sodium hydride and benzyl bromide in DMF was conducted in 44% yield. The allyl protecting

[13] Synthesized by Dr. Bo-Young Lee

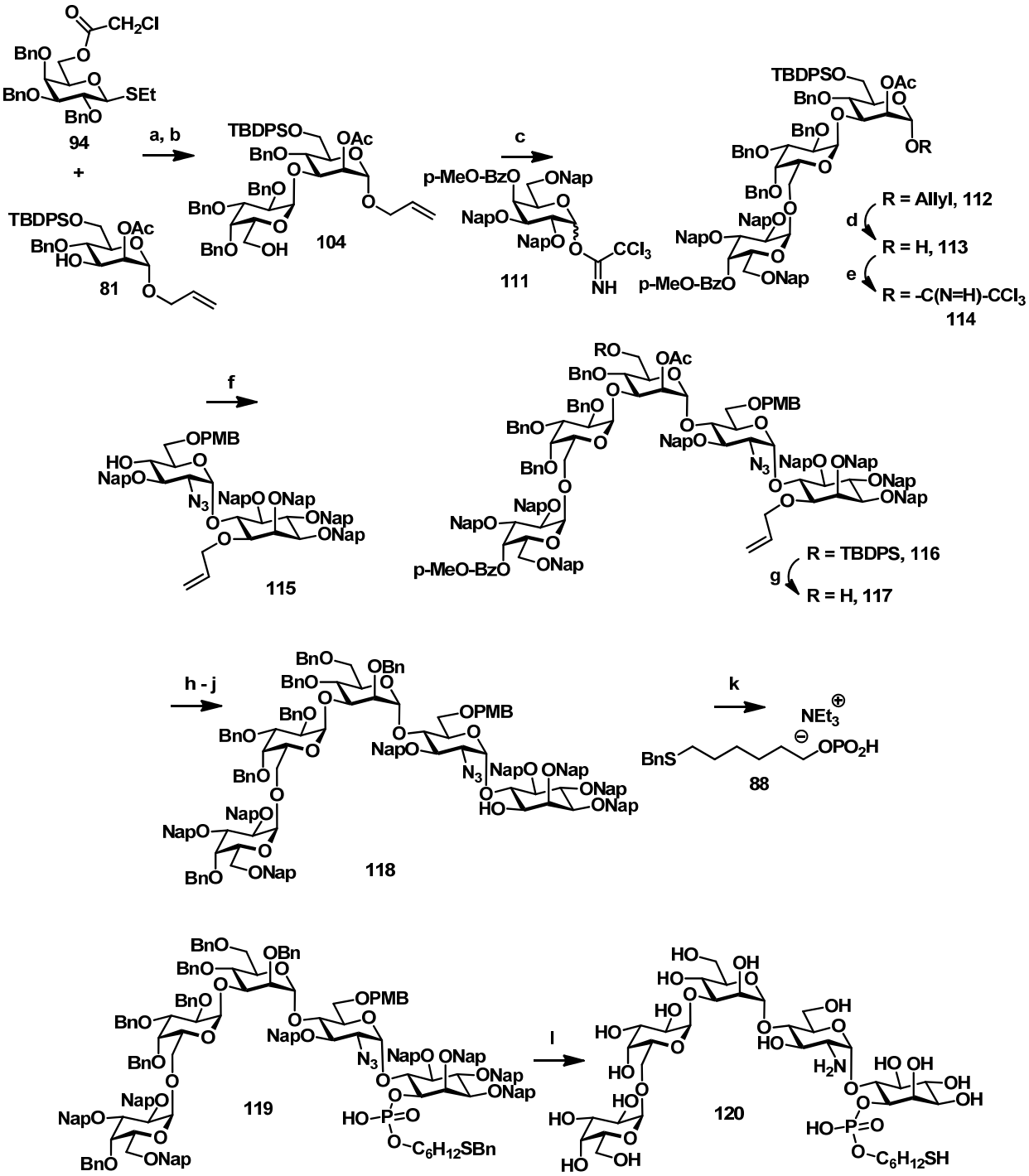

Scheme 37: Synthesis of linker equipped pentasaccharide **120**: a) TfOH, NIS, DCM/Et_2O, -11°C, 37%; b) thiourea, $CHCl_3$, 50°C, 81%; c) **111**, TMSOTf, DCM/Et_2O, 0°C; d) i) H_2, $[Ir(COD)(PMePh_2)_2]PF_6$, THF; ii) HgO, $HgCl_2$, acetone, water, 5:1, 75% over three steps; e) CCl_3CN, DBU, DCM, quant.; f) **115**, TMSOTf, DCM, 0°C, 48%; g) HF-pyridine, THF; h) NaOMe, MeOH/DCM, 78% over two steps; i) NaH, BnBr, DMF, 44%; j) i) H_2, $[Ir(COD)(PMePh_2)_2]PF_6$, THF; ii) HgO, $HgCl_2$, acetone, water, 5:1, quant.; k) i) **88**, PivCl, pyr; ii) I_2, H_2O, pyr, 0°C; l) $NH_{3(l)}$, Na, MeOH, -78°C, 98% over two steps

group was isomerized by using iridium catalyst and hydrogen and hydrolyzed using mercury salts in acidic aqueous acetone. **118** was isolated in quantitative yield and phosphorylation with **88** was approached. Consecutive phosphonylation using pivaloylchloride in pyridine and oxidation by iodine in a mixture of pyridine and water at 0°C gave phosphate **119**. Without

isolation of product **119** Birch reduction was performed. Crude product **120** was purified using a sephadex G25 size exclusion column and RP-HPLC (hypercarb column 150×10mm, ThermoFisher, 5 μ, acetonitrile in water 0-100% in 60 min) and gave **120** in 98% yield.

4.10 PSEUOHEPTASACCHARIDE PHOSPHO-THIOLINKER 129

To start the synthesis of the linker equipped *T. brucei* VSG 117 GPI, imidate **114** and pseudodisaccharide **121**[14] were glycosylated using TMSOTf in DCM at 0°C and desired pseudopentasaccharide **122** was isolated in 78% yield. TBDPS was removed with HF-Pyridine in THF giving alcohol **123** in 33% yield in four days reaction time. In the following reaction, dimannoside donor **124**[15] was used to glycosylate acceptor **123** under conditions[16] that favor formation of the α-product. Pseudoheptasaccharide **125** was isolated in 61% yield by using TBSOTf in a 2:1 mixture of thiophene and toluene at room temperature. Coupled ^{1}H-^{13}C-HSQC showed presence of six α-glycosidic bonds, corresponding to GlcN – 174.70 Hz, Gal – 178.71 Hz, Gal' – 174.70 Hz, Man I – 169.17 Hz, Man II – 170.27 Hz, and Man III'' – 174.01 Hz, as proof of the formation of product **125**.

With the glycan frame in hand, the phosphorylation steps were approached. To attach the phosphate linker moiety, allyl was removed via isomerization by iridium catalyst and hydrogen and hydrolysis by acidic mercury salt solution in aqueous acetone in 82% yield. Afterwards, H-phosphonate **88** and obtained alcohol **126** were employed for the first phosphorylation reaction using activation by pivaloyl chloride. After full conversion was determined by TLC, iodide and a 9:1 mixture of pyridine and water was added at 0°C to oxidize the intermediate phosphonate diester. This procedure resulted in removal of the TIPS ether group as well. Usually the different phosphorylation reactions in GPI synthesis are conducted in a sequence that includes removal of TIPS in the last step. However, under conditions used in this work the side reaction gave pseudoheptasaccharide **127** without TIPS in 18% over two steps.

The second phosphorylation reaction of H-phosphonate **43** and pseudoheptasaccharide **127** using the conditions mentioned in the last step failed to yield **128**. After purification ^{1}H-NMR and ^{31}P-NMR showed, that **128** was not formed, but rather **127** remained unmodified under the applied reaction conditions. In order to investigate the role of the glycan without

[14] Synthesized by Dr. Ivan Vilotijević

[15] Synthesized by Ms. Monika Garg

[16] Communication by Ms. Monika Garg

phosphoethanolamine modification, the compound was subjected to global deprotection using sodium and methanol in liquid ammonia. Product **129** was obtained in 39% yield after purification via size exclusion over a sephadex G25 column using 5% ethanol in water as eluent and RP-HPLC (hypercarb column 150×10mm, ThermoFisher, 5 µ, acetonitrile in water 0-100% in 60 min).

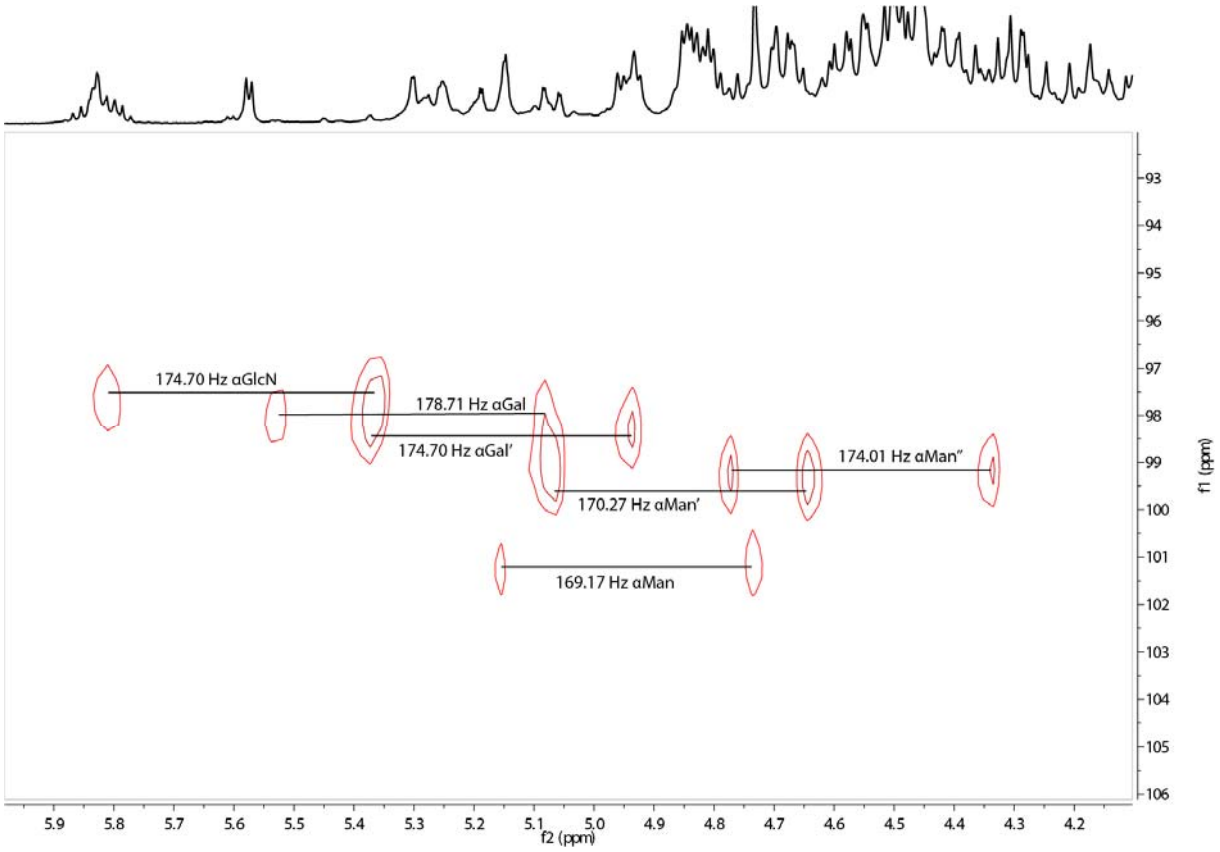

Figure 27: Coupled ^{1}H-^{13}C HSQC of heptasaccharide **125**. J_{CH} are shown in Hz and proof successful synthesis

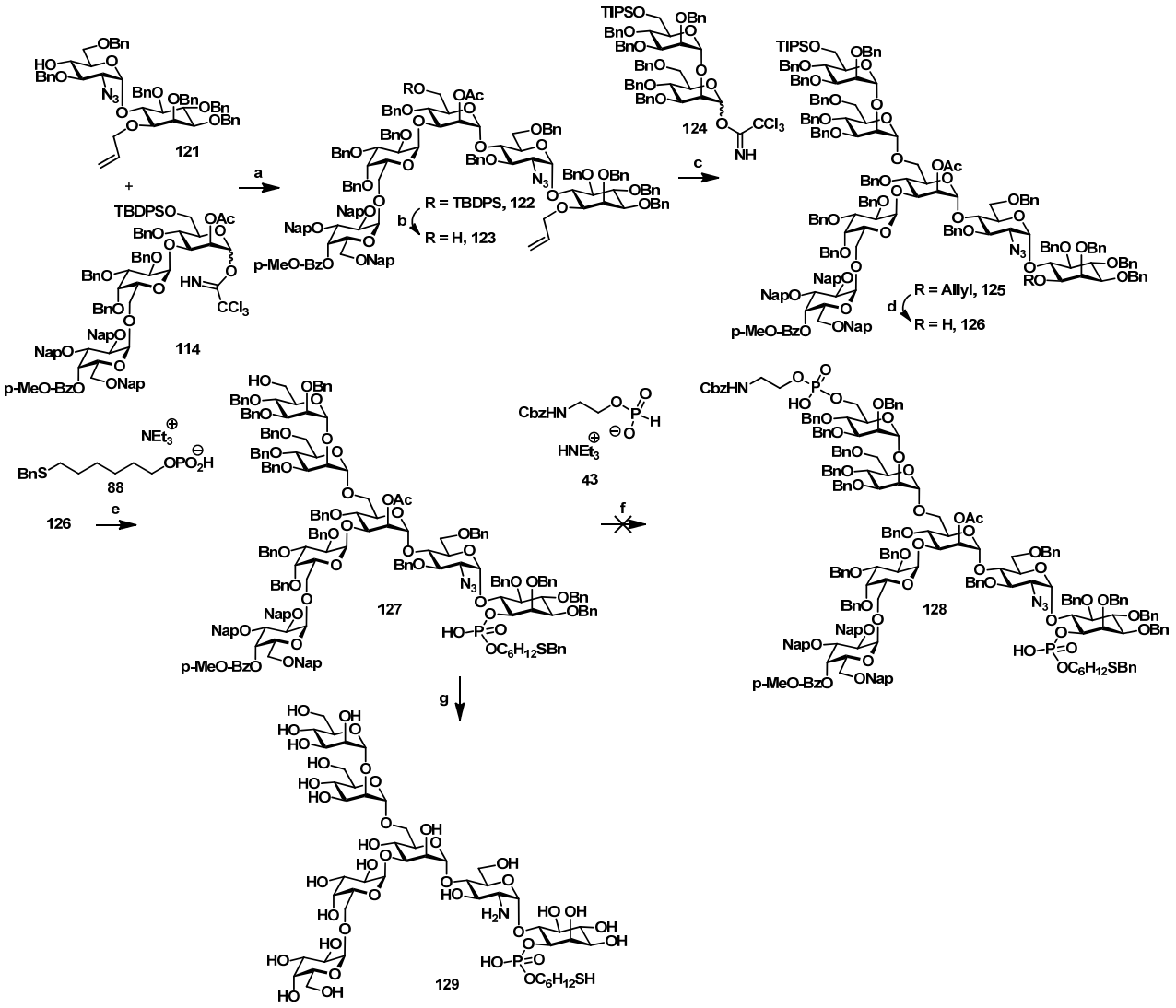

Scheme 38: Synthesis of pseudoheptasaccharide **129**: a) TMSOTf, DCM, 0°C, 78%; b) HF-Pyridine, THF, 33%; c) TBSOTf, thiophene:toluene 2:1,rt, 61%; d) i) H_2, $[Ir(COD)(PMePh_2)_2]PF_6$, THF; ii) HgO, $HgCl_2$, acetone, water, 5:1, 82%; e) i) **88**, PivCl, pyr; ii) I_2, H_2O, pyr, 0°C, 18%; f) i) **43**, PivCl, pyr; ii) I_2, H_2O, pyr, 0°C; g) $NH_{3(l)}$, Na, MeOH, -78°C, 39%

4.11 Conclusion and Outlook: Synthesis of GPIs for Glycan Microarray

In this chapter the synthesis of the *T. brucei* VSG221 GPI anchor was investigated. Therefore, by introducing new galactose (**5**, **8**, **10**, and **64**) and mannose building blocks (**18** and **21**) the established set of building blocks was expanded and broadened towards the assembly of novel GPI fragments. In doing so, required methods were introduced and extensively optimized highlighting the suitability of the introduced building blocks. By this strategy the synthesis of tetrasaccharide **30** was successfully accomplished by two approaches. Assembling of tetragalactoside **75** by a [2+2]-glycosylation approach gave the product only in traces. The use of analogue **76**, synthesized by a stepwise approach, in a glycosylation with Man I building block **81** failed to give the desired pentasaccharide **84**.

These results showed that a synthesis of the *T. brucei* VSG 221 GPI anchor by a convergent strategy[134] is not feasible. Indeed, Boons and coworker showed,[154] that installation of this side branch is possible by stepwise glycosylation, starting from a Man I building block. Additionally the target oriented characteristics were highlighted by using optimized specific conditions for each subsequent reaction.

However, using fragments **30** and **76** and the mentioned building blocks a set of thiol linker equipped GPI fragments comprising important structural modifications of the complex GPI was generated. In the next chapter, analysis of glycan microarrays fabricated using these structures is discussed.

5. Results and Discussion: Glycan Microarray of synthetic GPI structures

5.1 Investigation of *T. brucei* GPI structures

Early on, it was reported that VSGs are shielding the surface of the *T. brucei* parasite.[27b, 44] Due to this fact and the constant recycling of the surface proteins, it is arguable whether antibodies generated during an infection, will be directed against the GPI-Anchor. Additionally, during chronic infection with *T. brucei* B-cell apoptosis as well as depletion of the B-cell repertoire occurs, leading to a lack of antibodies in later infections stages. However, by phagocytosis, VSG and GPI are processed as foreign antigens and, hence, an immune response can occur against these structures. Therefore the question of a specific recognition of *T. brucei* GPIs by anti-GPI-antibodies is explored by using the synthetic structures obtained in the last chapter (Figure 28) for the fabrication of a glycan microarray. As a reference the pseudosaccharide (**D** and compound **13**) was chosen (Figure 29). Additionally *Toxoplasma gondii* (compounds **21**, **23-28**), *Plasmodium falciparum* (compounds **3**, **4** and **6-8**), mammalian (compound **25**) and linear conserved (compounds **1**, **2**, **5**, **19**, **20** and **22**) GPI structures were included in the preparation of this comprehensive glycan microarray.

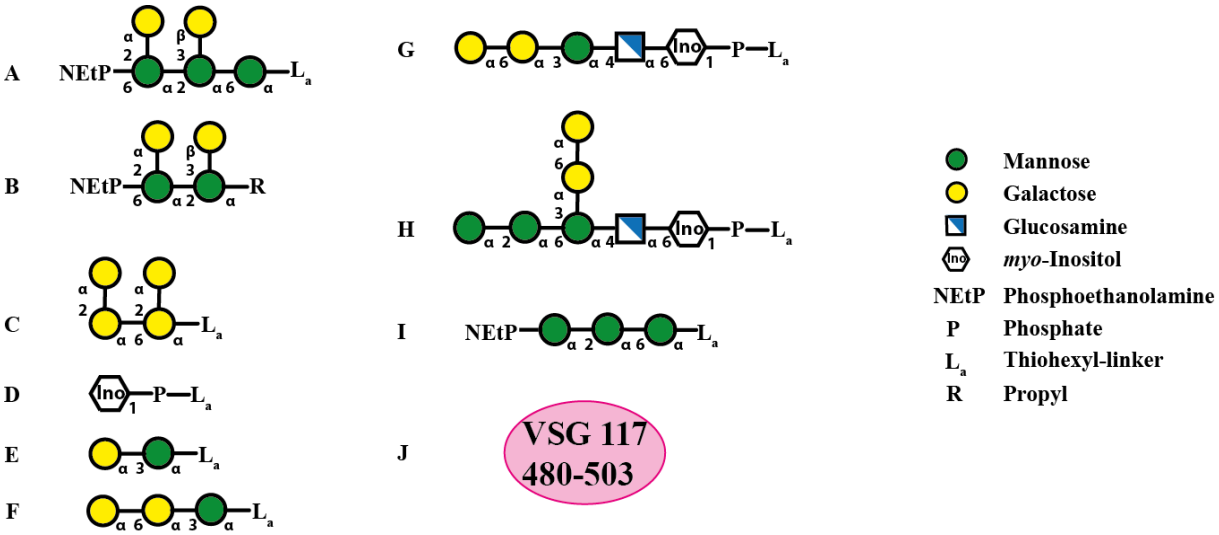

Figure 28: Structures used in glycan microarray fabrication. With exception of **I** and **J**[17], substances were obtained in the previous chapter.

[17] Synthesized by Monika Garg and Dana Michel

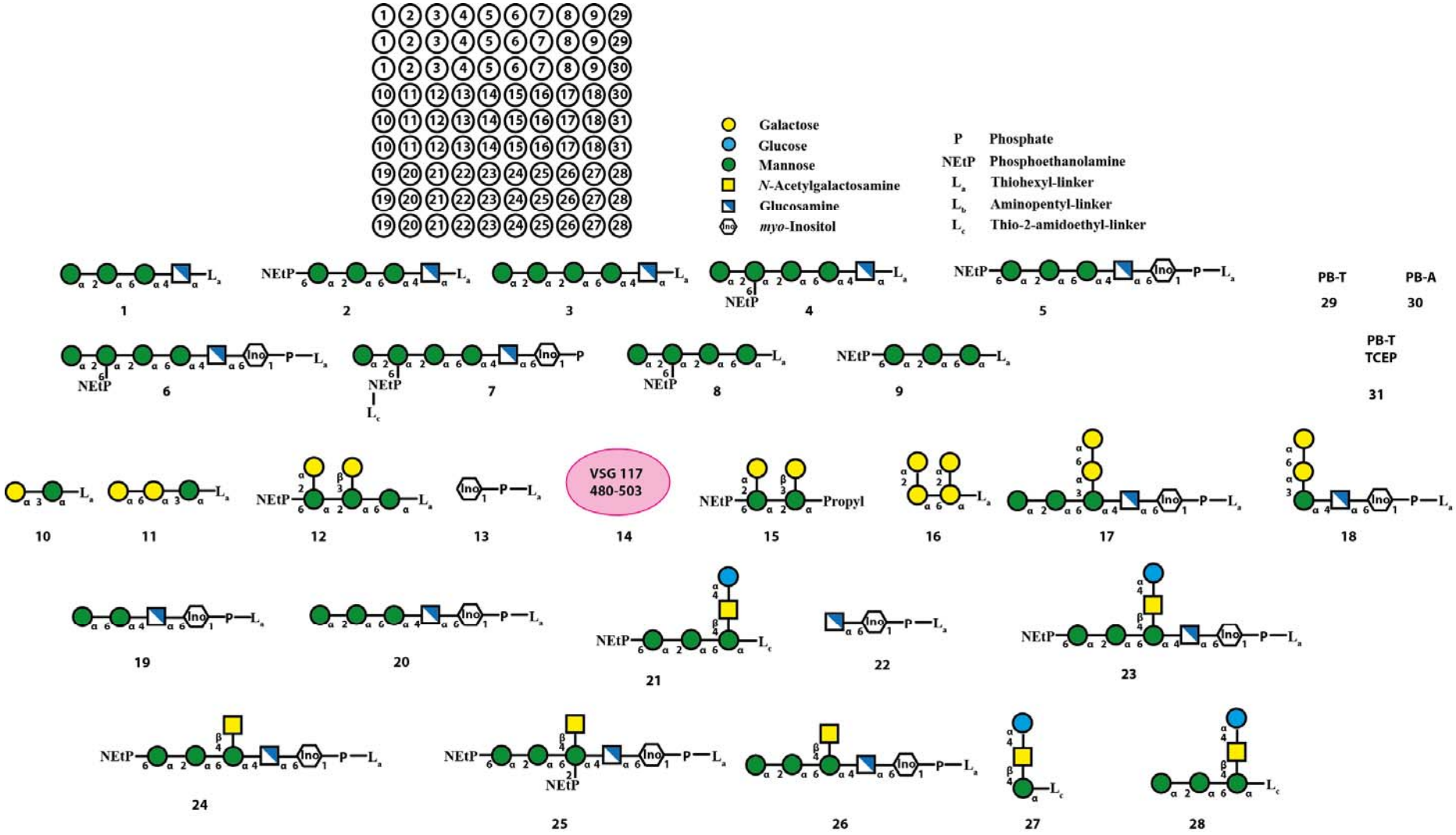

Figure 29: Printing pattern of synthetic GPI structures. Compounds are equipped with thiol or aminolinker at the anomeric position if not stated otherwise. Except for **29 - 31** that are printed as dublicates, all compounds are printed as triplicates in a column below each other

Fabricated glycan microarrays were evaluated against 60 reference sera from human and 50 reference sera from mice. Human sera were received from the WHO HAT specimen database and were divided in 6 groups of 10 samples. For *T. brucei gambiense* and *T. brucei rhodesiense* the groups consisted of patients from stage 1 and 2 and a respective control group from the endemic area. The mice sera were received from the group of Dr. Benoit Stijlemans at the VIB Lab of Myeloid Cell Immunology and were divided in 5 groups of 10 samples. 10 C57Bl/6 mice were infected with *T. brucei* AnTat1.1E and sera were collected prior to infection and after one, two, three and four weeks of infection.

5.2 MICE SERA – INFECTION MODEL *T. BRUCEI* ANTAT1.1E

Representative results (naïve, day 14 p.i. and day 28 p.i.) of immobilized structures in interaction with IgM and IgG from mice sera are shown in Figure 30 and Figure 31. Neither structures of *T. brucei*, nor other synthetic molecules are recognized by IgM and IgG present in sera of naïve mice. For sera samples of 7, 14, 21 and 28 days p.i. the signal strength corresponding to *P. falciparum*, *T. gondii*, mammalian and linear conserved molecules showed no intensification, indicating no binding by produced antibodies. However, GPI structures of *T. brucei* were recognized. As it can be seen in Figure 30, weak binding by IgM is indicated on day 14 p.i. for structures **14-18**. Towards later, chronical, stages indicated binding is reduced until recognition by IgM could not be observed between day 21 p.i. and day 28 p.i. (data not shown).

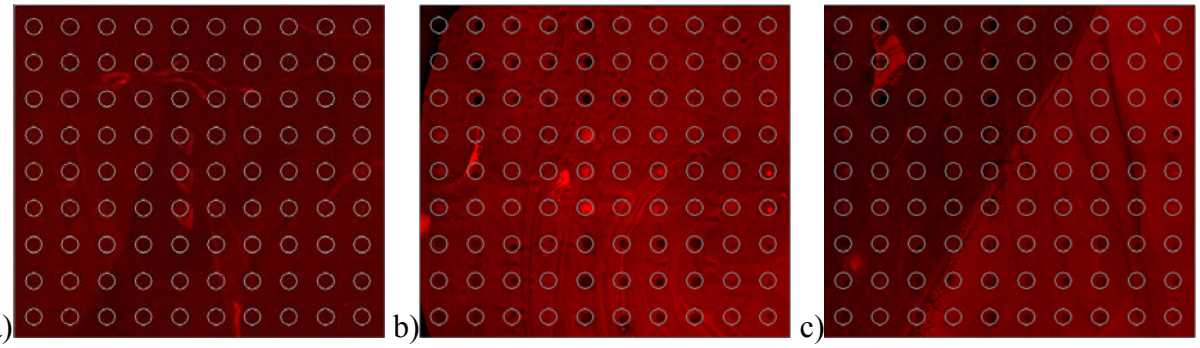

Figure 30: Representative scan of IgM interaction with immobilized structures incubated with serum samples from mice infected by *T. brucei*: a) naïve, b) day 14 p.i., c) day 28 p.i.; structures **14-18** are recognized during early infection

Recognition of immobilized *T. brucei* structures **10** and **14** by IgG from mice sera was observed from day 14 p.i. on and remained, albeit weak present (Figure 31). These results indicate that GPIs are recognized by IgM and IgG produced during a *T. brucei* infection. Noteably, no interaction with other synthetic GPI structures, especially the mammalian GPI **25**, was observed, indicating significance for *T. brucei* derived structures. Furthermore, the results indicate that IgM are only present during early stages, indicating lower titer or

complete absence during chronical stages. In contrast to that, active IgG seem to remain present over the entire monitored infection period.

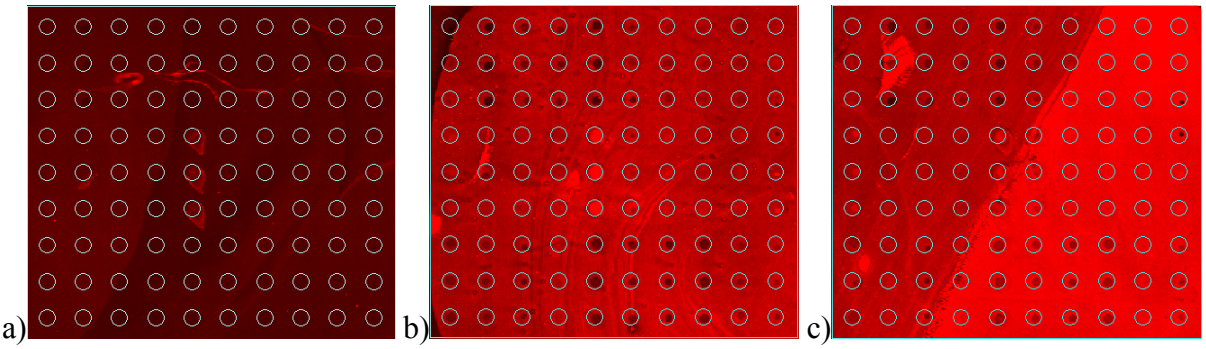

Figure 31: Representative scan of IgG interaction with immobilized structures incubated with serum samples from mice infected by *T. brucei*: a) naïve, b) day 14 p.i., c) day 28 p.i.; weak binding was observed for structures **10** and **14** during infection

To investigate these findings and to examine association of distinct structural features and fluorescence intensity in glycan microarray, a post hoc analysis consisting of analysis of variance with concluding significance tests was conducted (data not shown). Afterwards, the normalized signal strength corresponding to data points of each compound was plotted against the respective infection stage. Thereby significance determined by statistical methods was best illustrated by using a box plot, conveniently comparing data sets by their quartiles including outliers.

As shown in Figure 32 for recognition of IgM, these evaluations indicated a significance of recognition for α-galactosyl branched structures **10** and **16**, especially when the pseudodisaccharide was attached (compounds **17** and **18**). Furthermore, recognition of trimannoside **9** showed significance for the acute infection stage and declining signal strength for later data points. No significance of binding by antibodies was observed for peptide fragment **14**, higher structures with galactoses at Man II and Man III (compounds **12** and **15**) and reference compound, myo-inositol **13**. These results confirm the observation in the fluorescence pattern of the glycan microarray, indicating that a *T. brucei* infection can be observed by interaction with IgM. Finally, the results are suggesting a declining IgM titer during chronic infections after day 21.

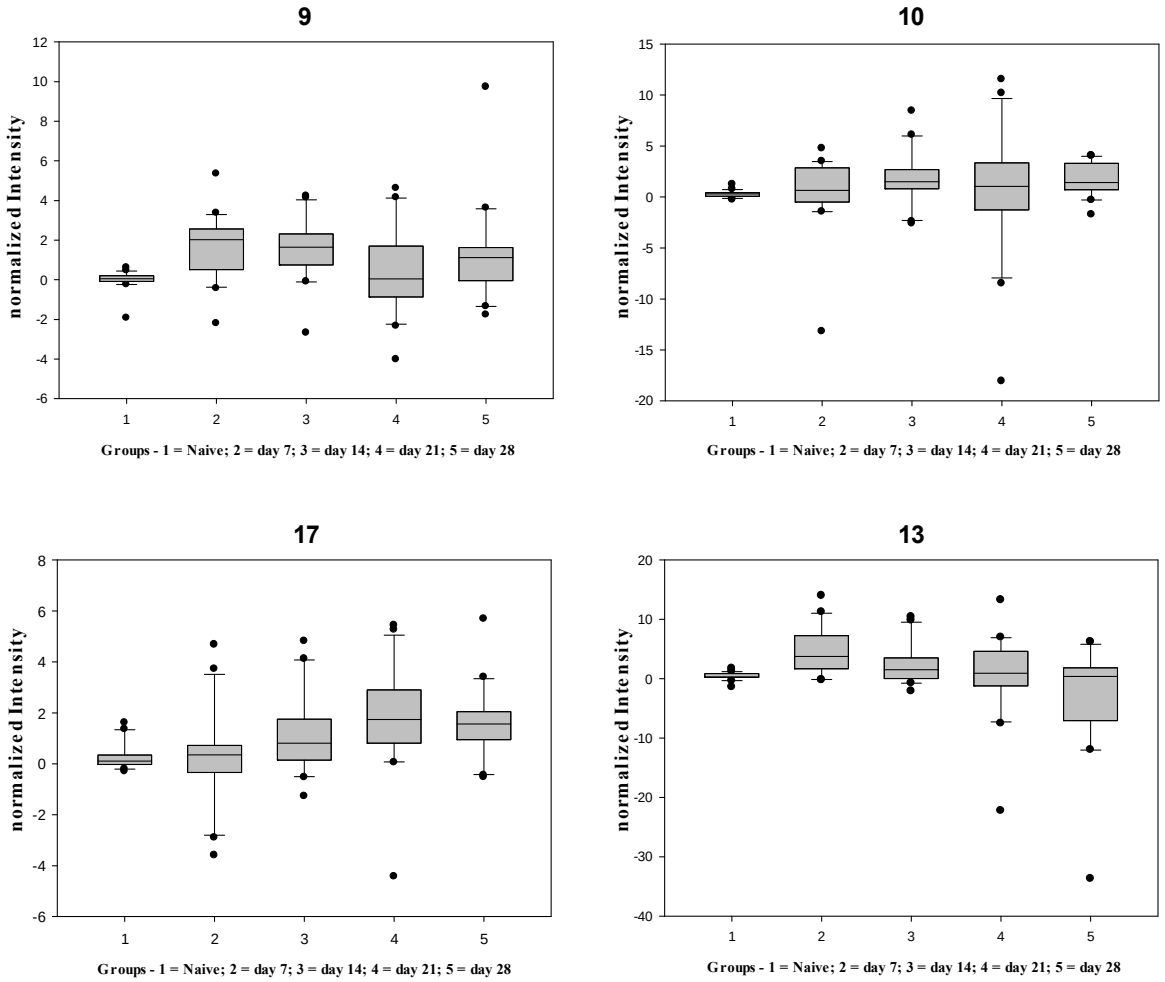

Figure 32: Normalized intensity of fluorescence indicating recognition by IgM is plotted against the five groups of the mouse infection model. Compounds bearing α-galactose **10**, **16-18** and trimannoside **9** show a high significance for infected vs. naïve mice. Details see appendix.

As it can be seen in

Figure 33 recognition by IgG highlights significance of trimannoside **9** in early infection stages (day 7 p.i. and day 14 p.i.). Additionally, branched galactose bearing structures (compounds **10** and **15**) were significantly recognized. In contrast to observations made earlier in this chapter, declining signal strength was observed towards later points of infection, indicating a lack of IgG as well as IgM, after day 21. This is supporting the current work on the matter, where depletion of existing antibodies and loss of immunity was observed during chronic infection stages.[31-32]

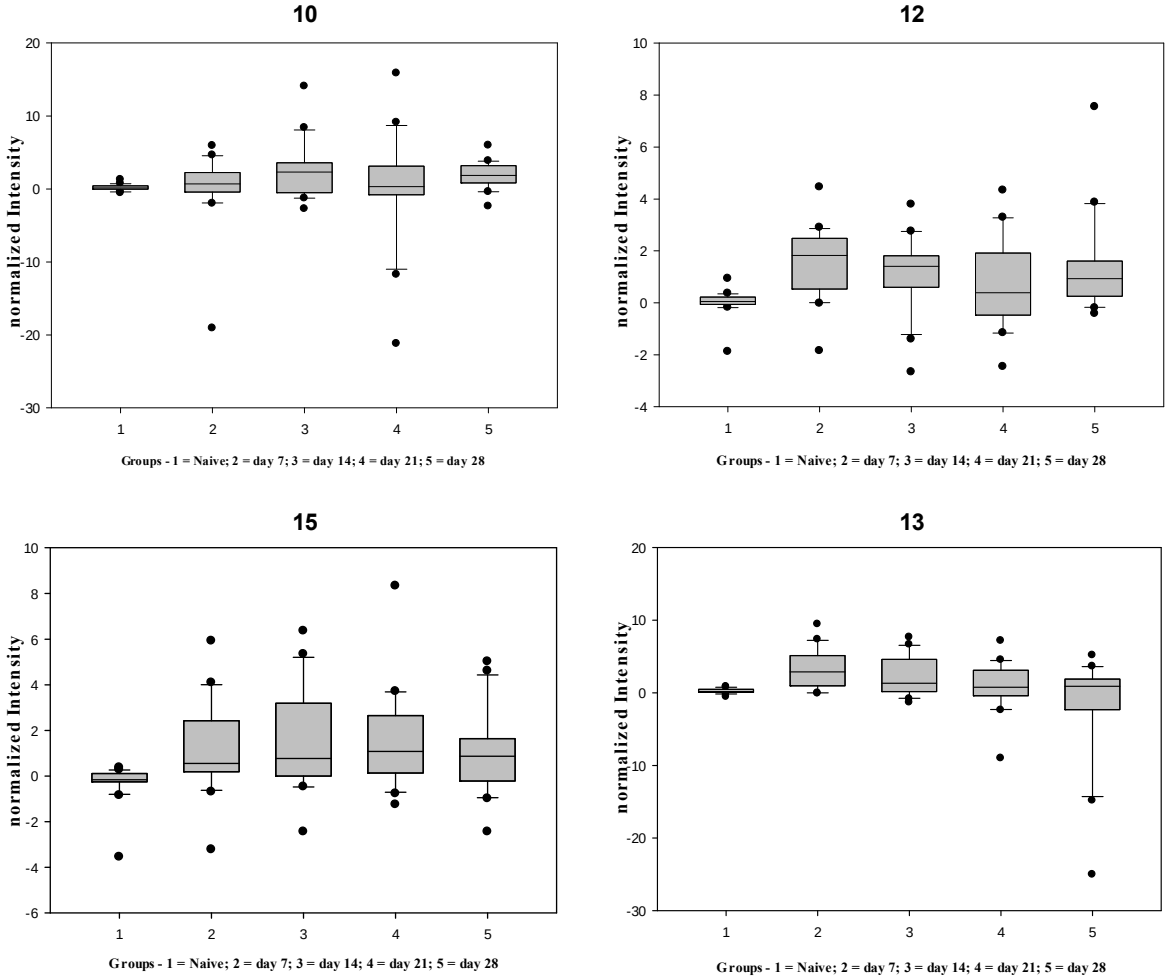

Figure 33: Normalized intensity of fluorescence indicating recognition by IgG is plotted against the five groups of the mouse infection model. Trimannoside **9** and α-galactose structures **10** and **15** are recognized, especially during early infection. Details see appendix.

5.3 CONCLUSION: MICE SERA – INFECTION MODEL *T. BRUCEI* ANTAT1.1E

The investigation of synthetic *T. brucei* GPI structures against sera from an infection mouse model, indicate recognition of synthetic structures by generated IgM and IgG. Furthermore, recognition by IgM was directed against distinct structural pattern, e.g. Galα1→6-Galα1→3-Manα1→4-GlcNα1→6-myo-Ino1, although, observed signal strength was of low intensity and declining towards later infection stages. IgG showed significant binding to the trimannoside backbone and to galactose modified structures and declining signal strength was observed towards chronic infection stage. It is not clear whether this process is a result of increasing parasitemia or modulation of the immune system. However, it is known, that depletion of antibodies and loss of immunity can occur during chronic

infections due to B cell apoptosis.[31-32] Noteworthy, no recognition by IgM and IgG was observed for synthetic GPI structures of other species than *T. brucei*.

5.4 HUMAN SERA – SAMPLES OF HAT PATIENTS

Similarly to the study with mice sera, the presence of anti-GPI antibodies was investigated in sera of HAT patients from Africa and their respective endemic controls. However, in contrast to the basic investigation of mice sera, humans can withstand a *T. brucei* infection for longer time, giving rise to a broader set of antibodies against occurring antigens. Together with possible infections by *Plasmodium falciparum*[107a] and *Toxoplasma gondii*[80] recognition of immobilized structures by IgM and IgG from patients can result in show broader distribution.

Indeed, recognition of immobilized structures derived from *Plasmodium falciparum* and *Toxoplasma gondii* was observed by IgM and IgG as well. Since it was not clear which sample is containing antibodies in response to one of these diseases distribution of recognition was almost completely through endemic controls and infected patients of HAT.

INVESTIGATION OF *T. BRUCEI GAMBIENSE*

At first infection with *T. brucei gambiense* was investigated. As shown in Figure 34, recognition by IgM was observed for *T. brucei* derived structures (compounds **9**, **10**-**12** and **14**-**18**) after infection. By means of shown fluorescence no distinction between the two stages was observed. Recognition observed by IgG showed a broad recognition of structures that is comparable to those in the IgM channel (data not shown).

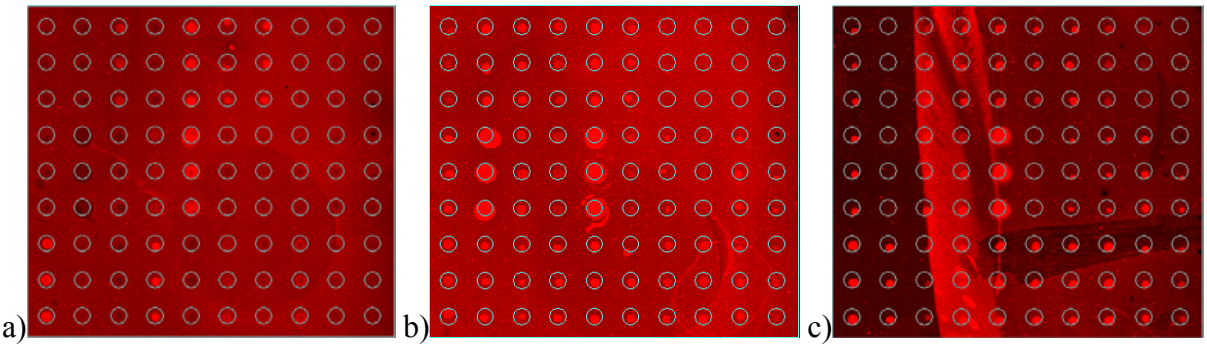

Figure 34: Representative scan of IgM interaction with immobilized structures incubated with serum samples from *T. brucei* gambiense infected humans: a) endemic control, b) stage 1, c) stage 2; broad recognition was observed for *T. brucei* GPI structures **9** and **10**-**18**

A post hoc analysis was performed to investigate significance of these findings. The results of these calculations are shown in Figure 35. For recognition by IgM significance was observed for VSG peptide **14** and α-galactosyl bearing compounds **16** and **17** regarding both

of infections stages. More importantly no general indication for declining antibody titer was found. Broad signal strength range for reference compound myo-inositol **13** was not significant.

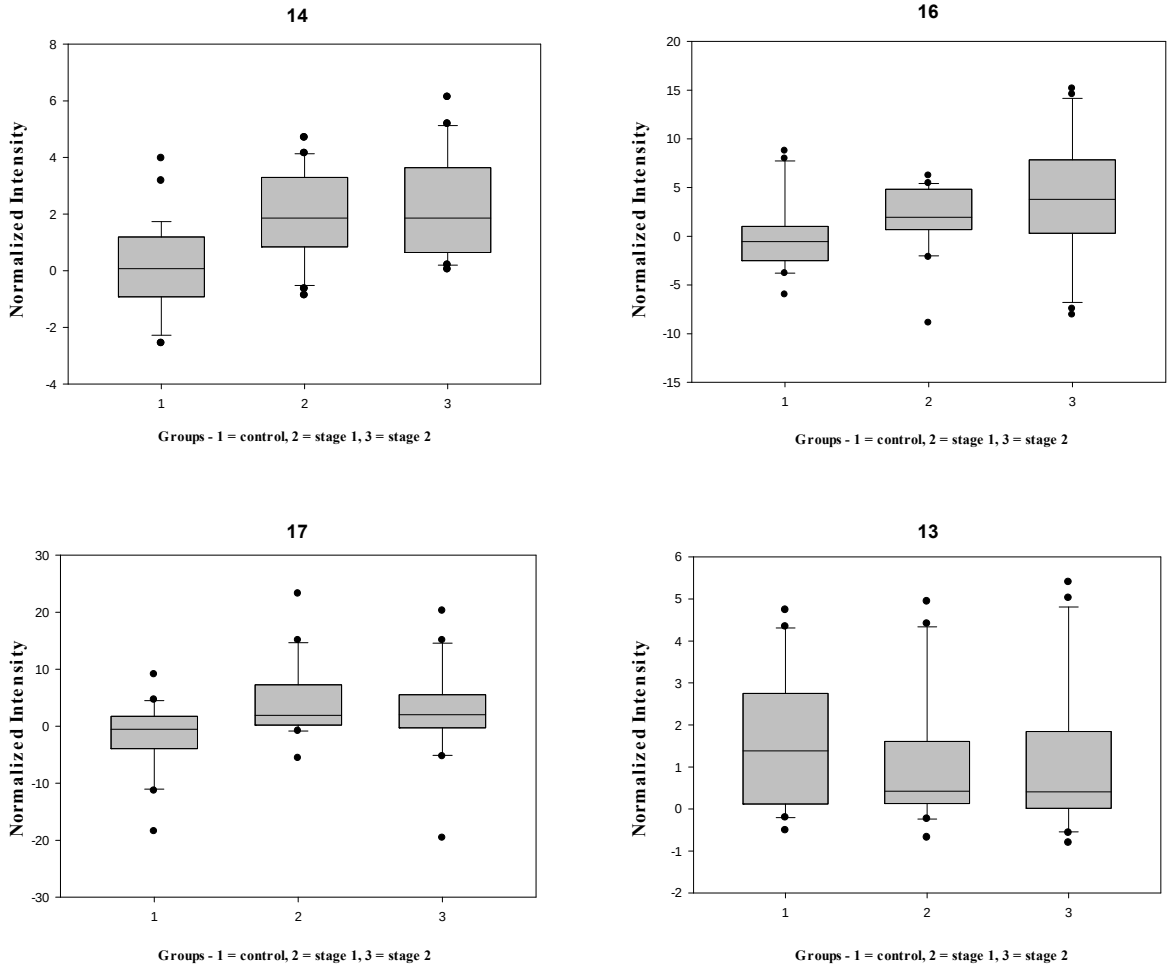

Figure 35: Normalized intensity of fluorescence indicating recognition by IgM is plotted against three groups of a *T. brucei* gambiense investigation. VSG peptide **14** and α-galactosyl compounds **16** and **17** are recognized significantly in infected stages. Details see appendix.

In the detection by IgG, no structure was significantly recognized. The concluded results are shown in Figure 36 and suggest that a *T. brucei gambiense* infection in humans leads to a short lived immune response, generating anit-GPI and anti-VSG specific IgM in both infection stages. However, the immune response was not robust enough to generate long lived anti-GPI and anti-VSG IgG.

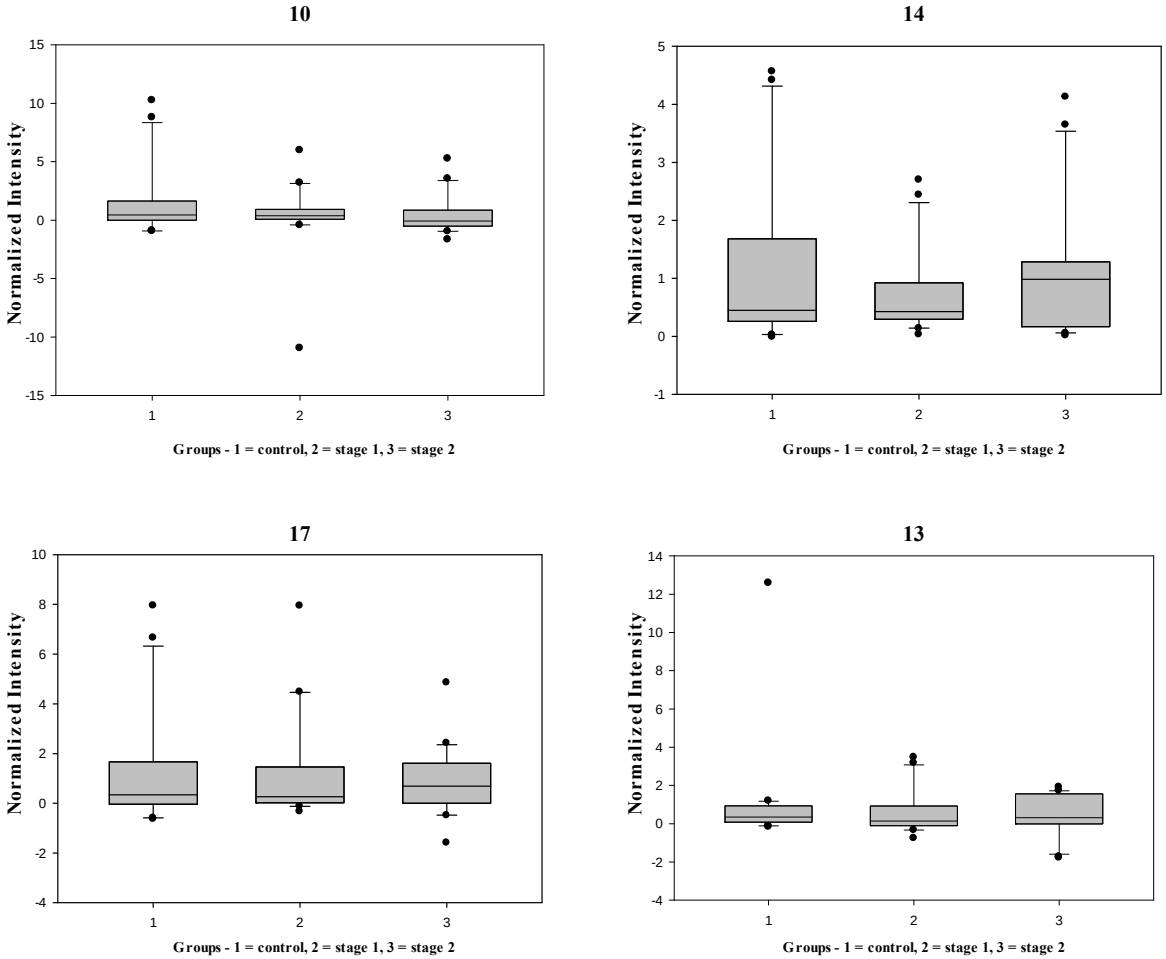

Figure 36: Normalized intensity of fluorescence indicating recognition by IgG is plotted against three groups of a *T. brucei gambiense* investigation. No significance for compounds is observed, indicating no long-lived protection by IgG. Details see appendix.

INVESTIGATION OF *T. BRUCEI RHODESIENSE*

The analysis of sera from patients having an infection with *T. brucei rhodesiense* was carried out in similar manner and a representative array is shown in Figure 37. Similar to the observations described for *T. brucei gambiense*, recognition of a broad range of *T. brucei* GPI structures (compounds **10-12**, **14-16** and **18**) by IgM was determined for both infection stages. In contrast, no specific signals were obtained in the control group. A similar fluorescence pattern concerning infected and healthy state was observed using recognition by IgG (Figure 37). However, more complex structures (compounds **12**, **14**, **16** and **17**) showed a slightly higher fluorescence in the infected stages, while smaller structures (compounds **11**, **13** and **14**) were active in all three groups. For both IgM and IgG recognition of sera of all stages showed no recognition of mammalian GPI **25** indicating no cross-reactivity of present anti-GPI antibodies.

To investigate statistically significance of these findings, post hoc analysis was performed. Calculations for recognition by IgM shown in Figure 38 indicated that

α-galactoside side branched structures **10** and **16** are significantly recognized in infection stages, trimannoside **9** in stage 2. In contrast, VSG peptide 14 was not specific. No indication of a declining IgM titer in sera from patients having the infection was observed.

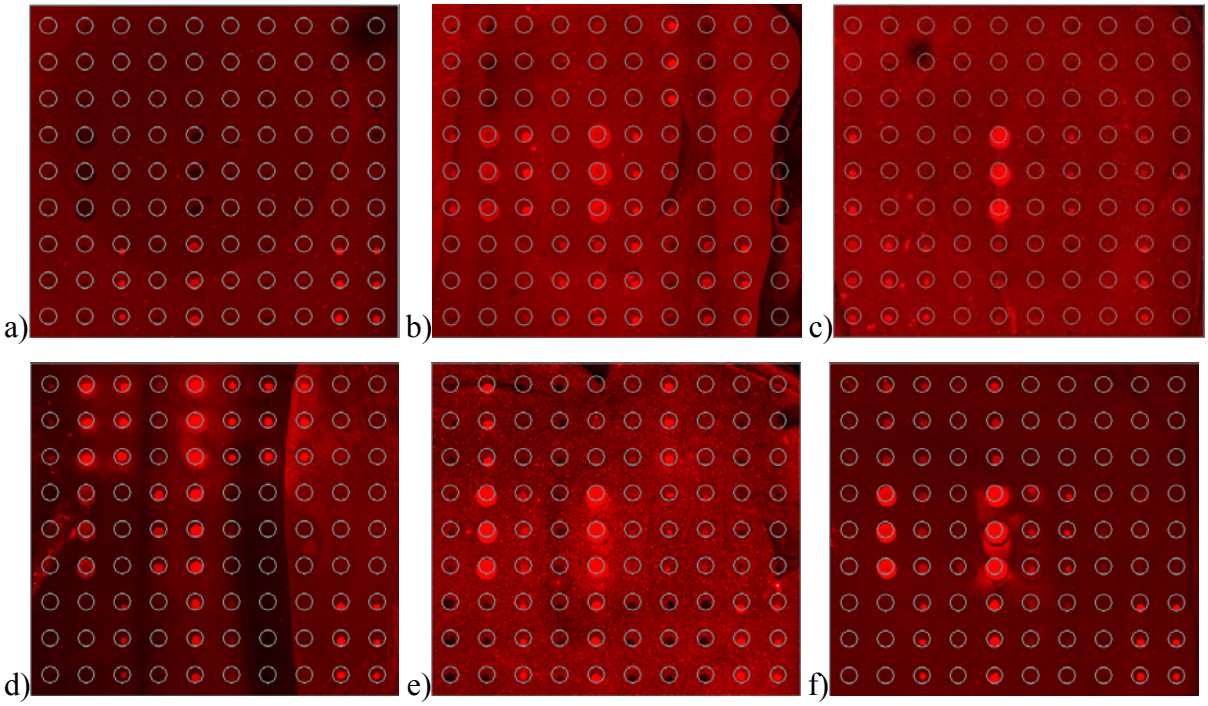

Figure 37: Representative scan of IgM and IgG interaction with immobilized structures incubated with serum samples from *T. brucei rhodesiense* infected humans: IgM: a) endemic control, b) stage 1, c) stage 2; recognition of *T. brucei* GPI structures (compounds **10**-**12**, **14**-**16** and **18**) was observed; IgG: d) endemic control, e) stage 1, f) stage 2; compounds **12**, **14**, **16** and **17**) showed high fluorescence in infected stages, smaller structures (compounds **11**, **13** and **14**) were recognized over all stages

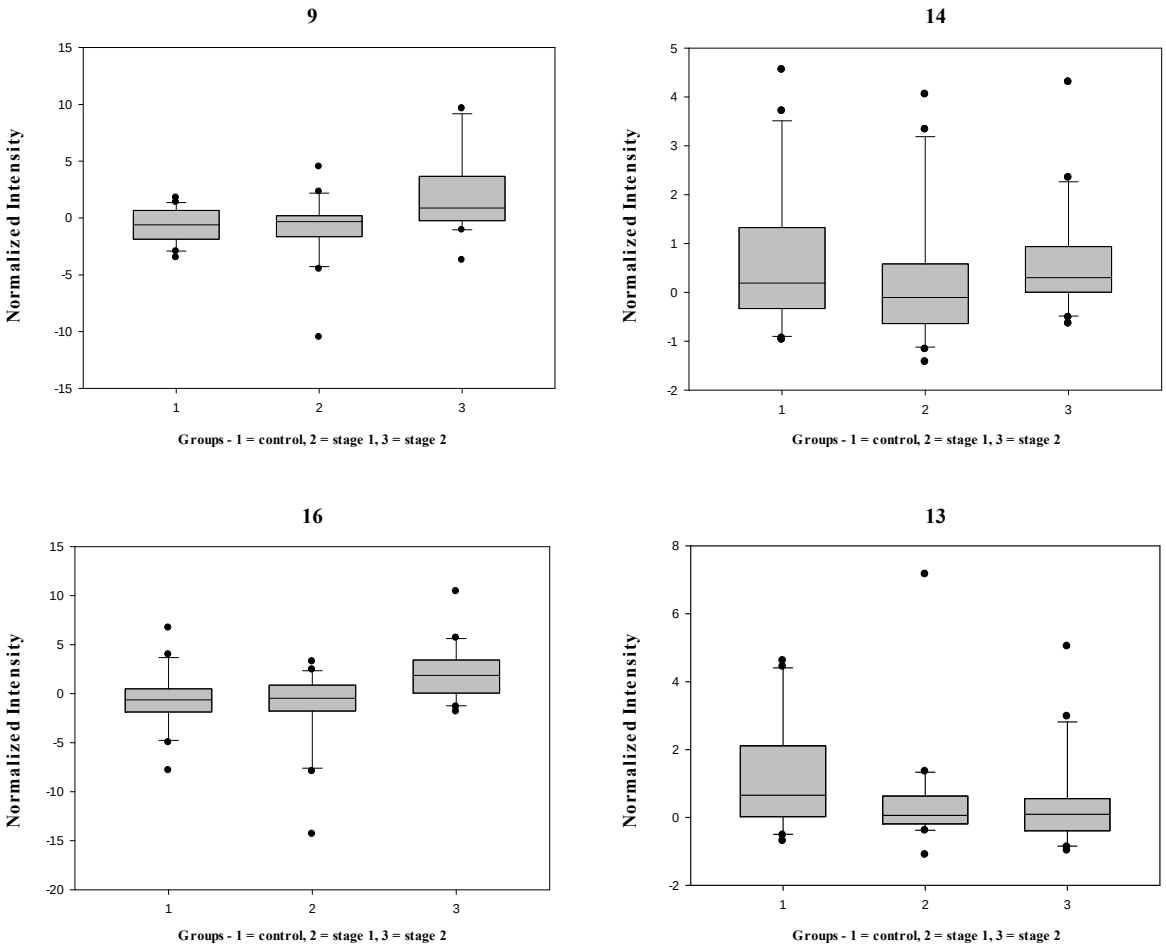

Figure 38: Normalized intensity of fluorescence indicating recognition by IgM against the three groups of a *T. brucei rhodesiense* investigation. α-galactosyl compounds **10** and **16** are recognized significantly in infected stages, trimannoside **9** in stage 2. VSG peptide **14** is not significant. Details see appendix.

The statistic evaluation of recognition by IgG is shown in Figure 39 and resulted in no significant recognition of any structural component. These findings indicate that in both stages of a *T. brucei rhodesiense* infection, short lived IgM are generated against GPI structures. However, in both stages no IgG response was observed, suggesting that no long lived and robust immune response is generated against GPI.

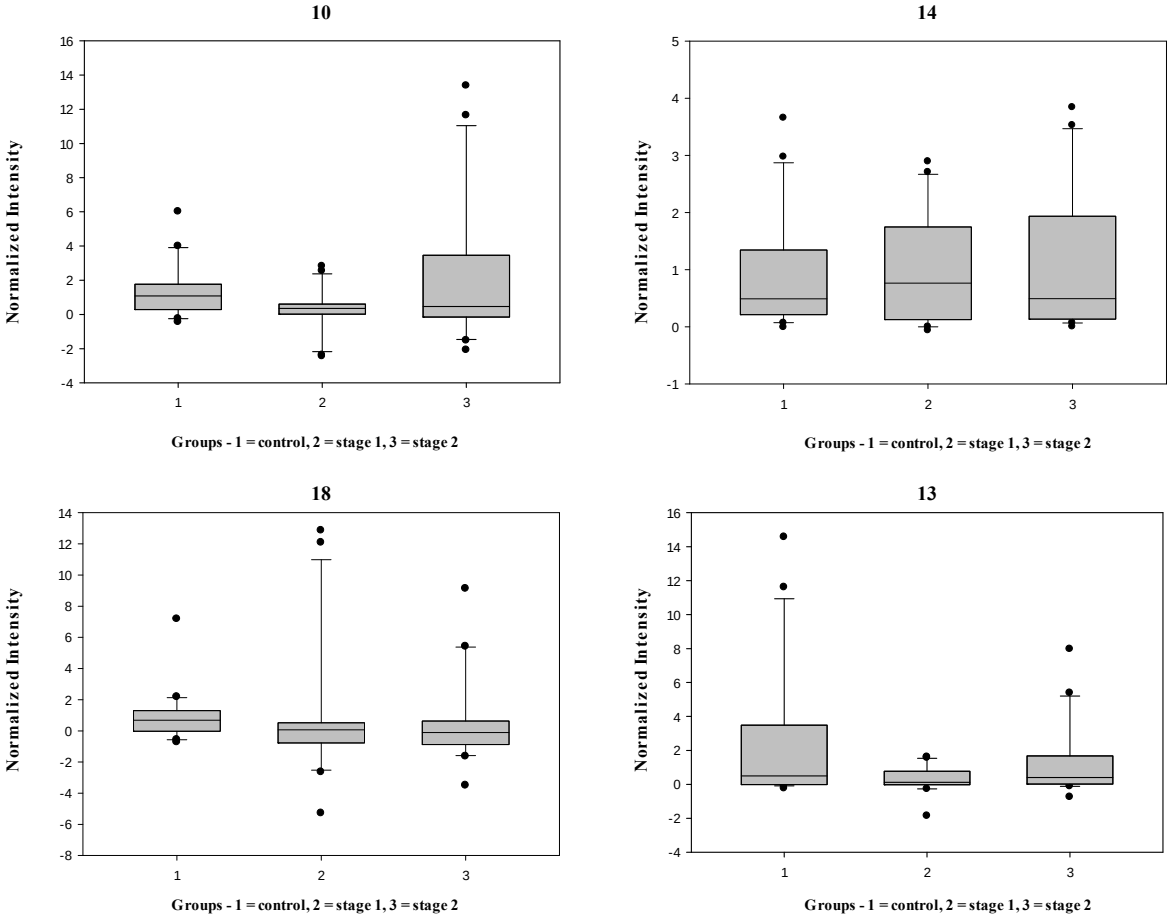

Figure 39: Normalized intensity of fluorescence indicating recognition by IgG against the three groups of a *T. brucei rhodesiense* investigation. No significance by any compound was observed, indicating no long lived protection by IgG. Details see appendix.

5.5 CONCLUSION: GLYCAN MICROARRAY HUMAN

The investigation of synthetic *T. brucei* GPI structures in glycan microarray against sera from human with infections by *T. brucei gambiense* and *T. brucei rhodesiense* showed broad recognition by IgG and IgM for both stages. Due to the source of investigated sera from sub-Saharan Africa, recognition of *Plasmodium falciparum* and *Toxoplasma gondii* GPI structures was observed for IgG and IgM. Although high antibody titers are present in parasitic infections, synthetic mammalian GPI were not significantly recognized by any IgG or IgM, indicating no cross-reactivity with these structures. Evaluation with statistical methods indicated significant binding of a broad range of structures from VSG peptide **14** over trimannoside backbone structure **9** to α-galactoside modified fragments (compounds **15-18**). Interestingly, binding was only significant for IgM, while IgG showed no significantly binding of epitopes. A possible explanation is depletion of existing serum antibodies by soluble VSG-GPI-fragments released by dead parasites, a process that goes well in hand with B-cell apoptosis and subsequent loss of immunity in chronic infections.[31-32] Additionally,

grouping of sera was done by examining the infection stage. Due to the natural way of infection exact dating is impossible. Ongoing investigations with bigger number of samples will allow evaluation of binding specificity by ROC analysis. With these results in hand, the finding of GPI recognition by antibodies can be used in the development of a diagnostic marker for Nagana and human African trypanosomiasis.

5.6 CROSS-REACTIVITY OF ANTI-GPI-ANTIBODIES OF EUROPEAN *T. GONDII* PATIENTS

In 1988, existence of a cross reacting determinant was reported for *T. brucei* GPI.[96] Since then, several studies showed significance of smaller modifications of GPIs in recognition by anti-GPI-antibodies.[80, 107a] Here, synthetic *T. brucei* GPIs (compounds **9-12** and **14-18**) were used in a glycan microarray to investigate recognition by anti-GPI-antibodies. These antibodies are from sera of european toxoplasmosis patients, which have no infection by *T. brucei*. Binding of *T. brucei* GPI structures would therefore indicate cross-reactivity of anti-GPI-antibodies, when binding occurs with sera of acute or latent patients only. Sera received from the University Medical Center Göttingen[18] were divided in five groups: healthy, acute, latent and the two intermediate states of acute/latent and latent/acute. As reference compound myo-inositol **13** was used.

Recognition of immobilized structures by IgM is shown in Figure 40. In all groups, broad signal strength was observed for synthetic GPI structures (compounds **21**, **23**, **24**, and **26-28**) of Toxoplasma gondii. Interestingly, structures of *Plasmodium falciparum* and the conserved core (compounds **2-8**) were recognized as well.[107a] No recognition was observed for mammalian GPI **25**, indicating that anti-GPI-antibodies from toxoplasmosis are not cross-reactive with this structure. Additionally, *T. brucei* derived structures (compounds **11-14**) were recognized from IgM of some patients. Here, statistic evaluation of the obtained signal strength was required to investigate significance in recognition.

[18] Group of Prof. Dr. Uwe Groß

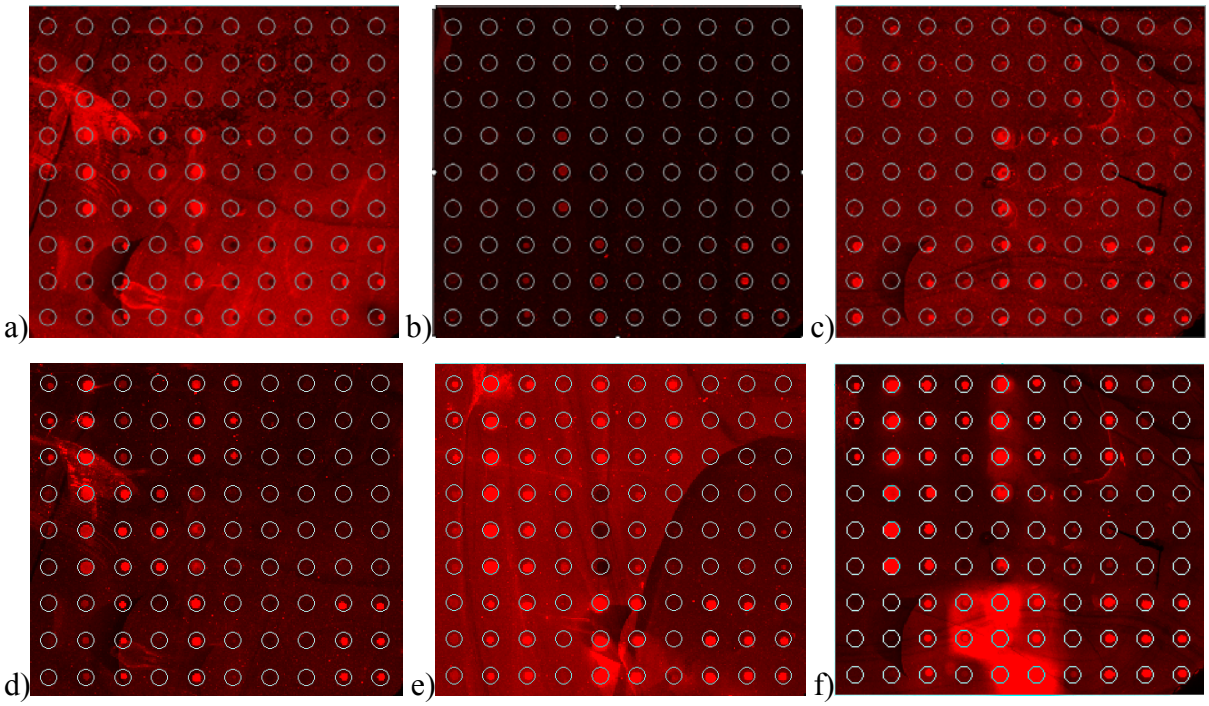

Figure 40: Representative scan of IgM and IgG interaction with immobilized structures incubated with serum samples from *T. gondii* infected humans: IgM: a) endemic control, b) acute, c) chronic; recognition of *T. brucei* VSG-GPI structures **11-14** was observed; IgG: d) endemic control, e) acute, f) chronic; *T. brucei* VSG-GPI **11-14** showed high fluorescence

IgG broadly recognized GPI structures of *Toxoplasma gondii* (compounds **21**, **23**, **24**, and **26-28**) and linear GPI from *Plasmodium falciparum* (compounds **1-9**) in all groups.[107a] Furthermore, GPI structures of *T. brucei* (compounds **11-14**) are bound by antibodies over the entire spectrum of samples.

These results were further evaluated by statistical methods (Figure 41 and Figure 42). For both antibody classes no significance was observed for *T. brucei* compounds **11-14**. This indicates no cross-reactivity of anti-GPI-antibodies of toxoplasmosis patients against synthetic GPI structures of *T. brucei*.

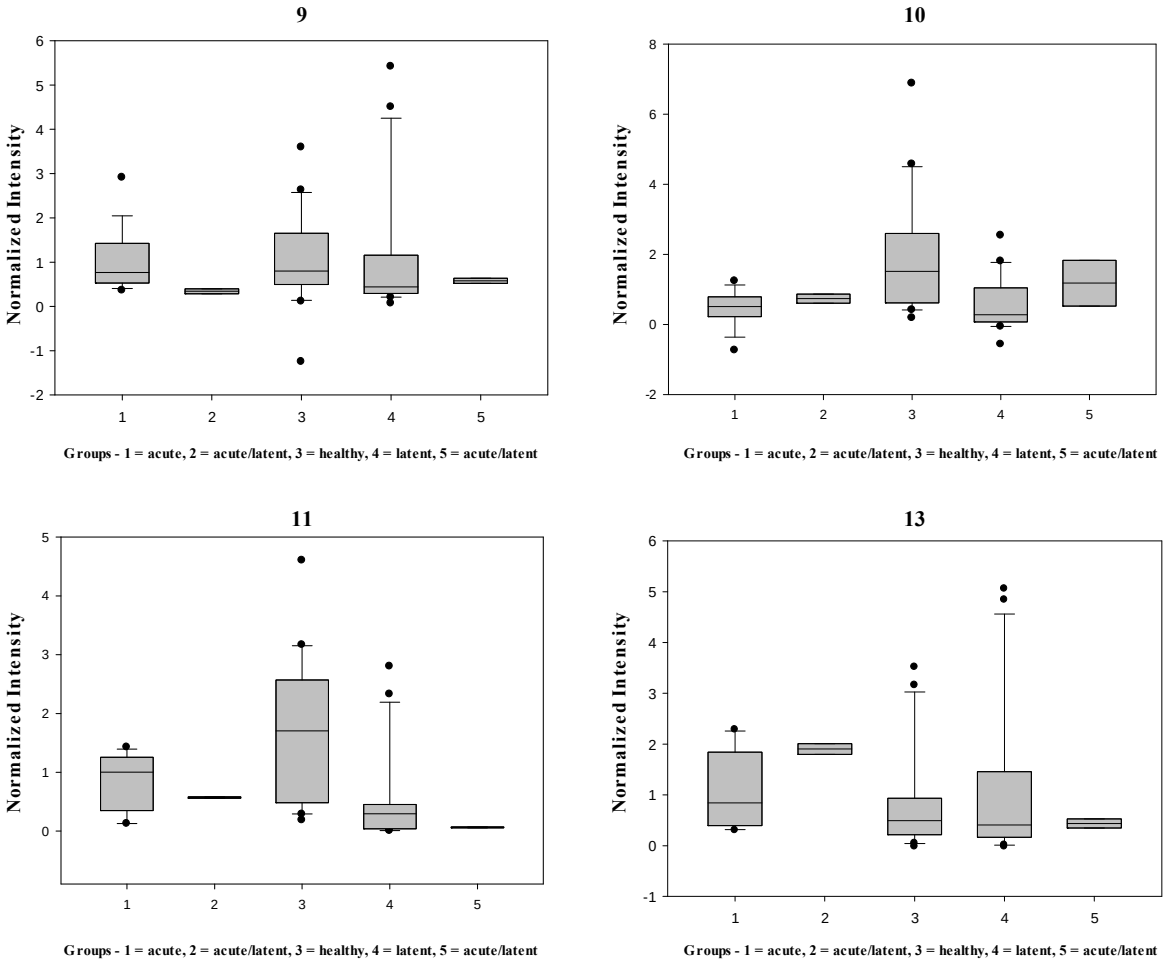

Figure 41: Normalized intensity of fluorescence indicating recognition by IgM against five groups of a *T. gondii* investigation. No structures are significantly recognized, indicating the absence of cross-reactivity of IgM. Details see appendix.

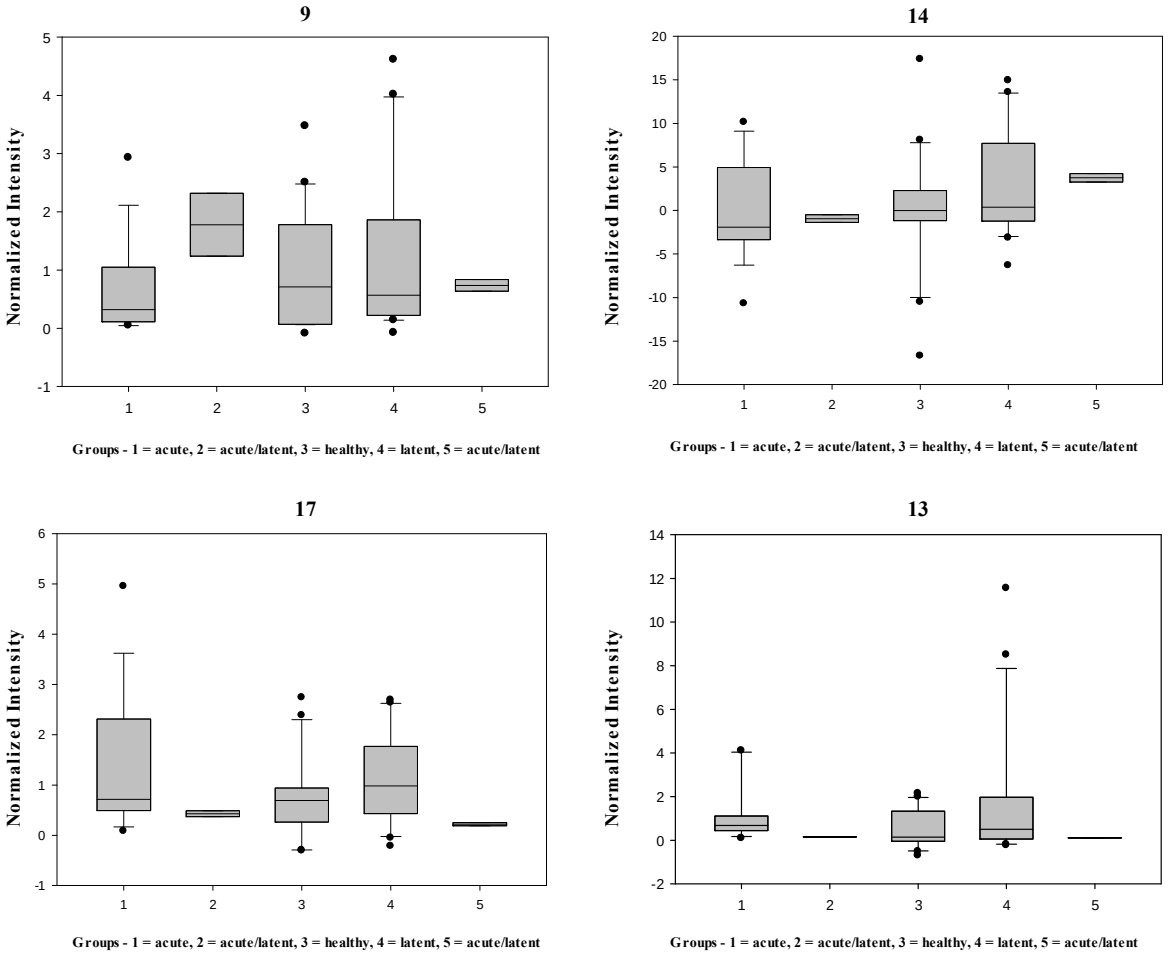

Figure 42: Normalized intensity of fluorescence indicating recognition by IgG against five groups of a *T. gondii* investigation. No structures are significantly recognized, indicating the absence of cross-reactivity of IgG. Details see appendix.

5.7 CONCLUSION: CROSS-REACTIVITY

Examined interaction of synthetic *T. brucei* GPI structures in glycan microarray with anti-GPI-antibodies of sera from toxoplasmosis patients showed no cross-reactivity concerning *T. brucei* GPI structures. Additionally, mammalian GPI **25** was neither recognized by anti-GPI-antibodies from mice or human infected with *T. brucei* nor from IgM and IgG present in sera of toxoplasmosis patients, suggesting selectivity for GPIs of parasites from the corresponding disease and excluding cross-reactivity with GPIs of different origin.

6. RESULTS AND DISCUSSION: SYNTHESIS OF GPI FRAGMENTS FOR MACROPHAGE ACTIVATION

GPIs of parasitic protozoa activate macrophages and lead to release of chemokines and cytokines during an infection process. For *T. brucei* certain structural motifs may be responsible for this release.[40a, 149a, 155] These epitopes contain the phospholipidated inositol glycan and the α-galactoside residues in the side chain of Man I. It was shown, that the VSG is predominantly responsible for release of TNF-α by macrophages. The study indicated that dimyristoyl glycerol plays no crucial role in this induction. On the other hand, release occurred when the lipid moiety was attached to glycosylated inositol and was maximized when α-galactosides were present. However, all these experiments were generated with isolated structures in a macrophage cell line (2C11/12). Pure samples with a defined structure can solve complications and annotate distinct function to each epitope. For this investigation a number of phospholipidated compounds were synthesized. A short alkyl chain was installed at the reducing end when *myo*-inositol was absent. Although synthesis of the *T. brucei* VSG 221 GPI Anchor was not feasible by the used strategy, precursor compounds were derived from intermediate compounds discussed in the previous chapter and therefore comprise all important structural features of the full GPI Anchor. Consecutive synthetic steps as well as the structures that are exclusively synthesized from other starting material are discussed here.

6.1 *MYO*-INOSITOL PHOSPHOLIPID 134

The synthesis of phospholipidated structures started with assembling the required H-phosphonate and subsequent phosphorylation of myo-inositol. Therefore, commercial dimyristoyl glycerol **130** was converted into the corresponding H-phosphonate **131** in quantitative yield, by a phosphonylation reaction using phosphonic acid and pivaloyl chloride in pyridine. In the following reaction *myo*-inositol building block **132**[19] was reacted in a phosphorylation reaction using five equivalents of H-phosphonate **131** and pivaloyl chloride in pyridine. After formation of the intermediate phosphonate diester, oxidation with iodine and a 9:1 mixture of pyridine and water at 0°C enabled isolation of product **133** in 17% yield. To remove all protecting groups of **133**, hydrogenation using Pd/C and hydrogen was conducted under elevated hydrogen pressure in an autoclave. **134** was isolated in 40% yield

[16] synthesized by Fabio Laspiza

after purification with sephadex G15 size exclusion column using a 3:3:1 mixture of chloroform, methanol and water as eluent.

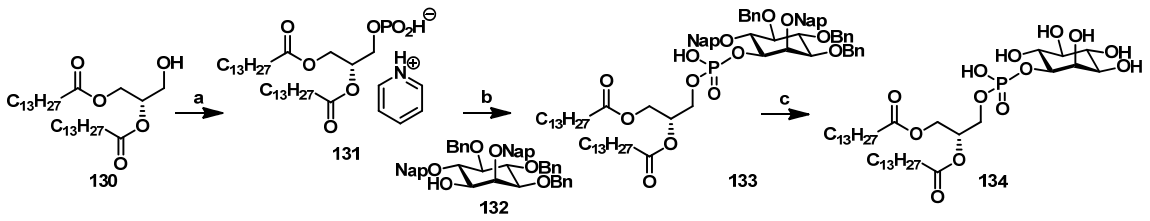

Scheme 39: Synthesis of *myo*-inositol phospholipid **134**: a) H_3PO_3, PivCl, pyr, quant., brsm; b) i) 132, PivCl, pyr; ii) I_2, H_2O, pyr, 0°C, 17%; c) Pd/C, H_2, p↑,MeOH/EtoAc 40%

6.2 PSEUDODISACCHARIDE-PHOSPHOLIPID 137

Corresponding pseudodisaccharide phospholipid **137** was synthesized in 74% yield in a phosphorylation reaction of pseudodisaccharide **135**[20] and designed H-phosphonate **131** using pivaloyl chloride in pyridine for formation of the intermediate phosphonate diester and iodine in a 9:1 mixture of pyridine and water at 0°C. Deprotection under elevated hydrogen pressure and several purification steps using a sephadex G15 size exclusion column with a 3:3:1 mixture of chloroform, methanol and water as eluent gave the pure product **137** in 9% yield.

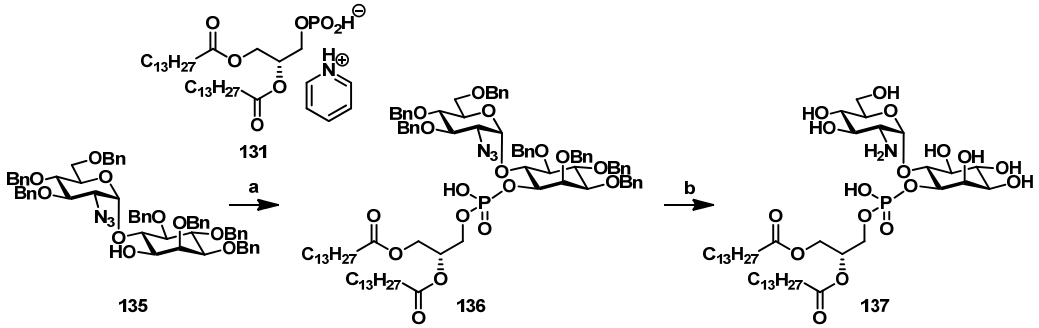

Scheme 40: Synthesis of pseudodisaccharide phospholipid **137**: a) i) 131, PivCl, pyr; ii) I_2, H_2O, pyr, 0°C, 74%; b) Pd/C, H_2, p↑, MeOH/EtOAc, 9%

6.3 DISACCHARIDE 140

Compound **138**, isolated as a sideproduct during the synthesis of tetrasaccharide **30** without stereocontrol, was used to obtain a disaccharide corresponding to an α-galactoside commonly found at the C-3 position of the branch at Man I. Crude compound **138** was subjected to removal of acetyl by potassium carbonate in methanol and DCM giving a mixture of different substances. Purification by silica gel column chromatography was not successful. However, using supercritical fluid chromatography (Viridis 2EP-pyridine, semipreparative, 5 μ, ethyl acetate in $CO_{2(sc)}$, 0 to 40% in 60 min) desired product **139** was

[20] synthesized by Dr. Ivan Vilotijević

obtained in 20% yield. In the following step disaccharide **139** was deprotected by hydrogenation on Pd/C over two days and purified using a sephadex G15 size exclusion column with 5% ethanol in water as eluent to give product **140** in quantitative yield.

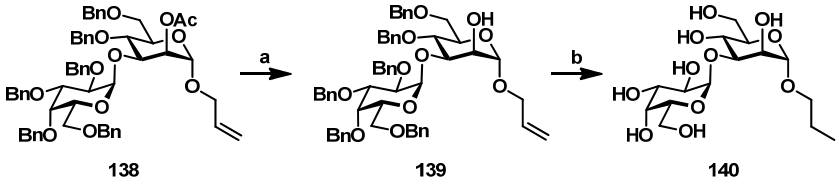

138 139 140

Scheme 41: synthesis of disaccharide **140**: a) K_2CO_3, MeOH/DCM, 20%; b) H_2, Pd/C, MeOH/EtOAc, quant.

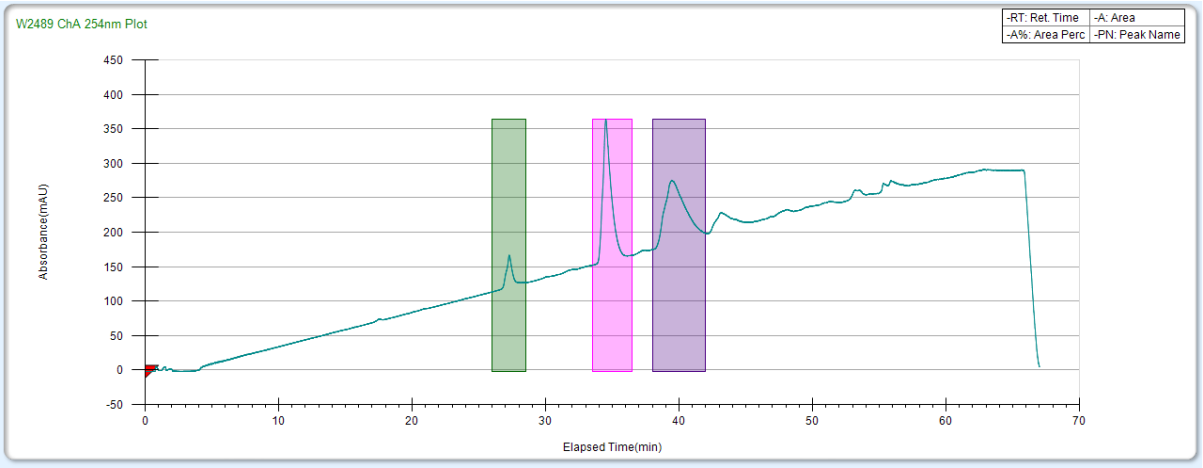

Figure 43: SFC chromatogram of the purification of disaccharide **139**; product is indicated violet, green and pink are main impurities.

6.4 TRISACCHARIDE 142

The corresponding structure with two α-galactosides attached to Man I was synthesized by employing trisaccharide **105** in global deprotection over two steps. Acidic hydrolysis of silyl groups is usually avoided, due to poor selectivity and cleavage of other protecting groups. However, this method can be applied in late synthesis stages, when removal of all protecting groups is desired. Here, *in situ* generated anhydrous HCl from acetyl chloride and methanol cleaved TBDPS and the two small ester protecting groups giving **141** in quantitative yield. During hydrogenolysis on Pd/C, atmospheric pressure of hydrogen showed incomplete cleavage of the protecting groups even after 48 h of reaction. Deprotection of remaining benzyl ethers was only completed in an autoclave. Product **142** was purified in a yield of 78% on sephadex G15 size exclusion column using 5% ethanol in water as eluent.

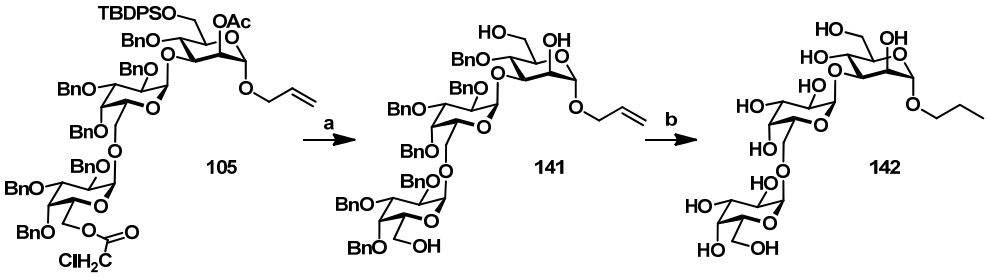

Scheme 42: Synthesis of trisaccharide **142**: a) AcCl, MeOH/DCM, quant.; b) Pd/C, H_2, p↑, MeOH/EtOAc, 78%

6.5 TETRAGALACTOSIDE 144

To complete a set of compounds containing α-galactosides of the side branch of *T. brucei* GPI, deprotection of tetragalactoside **76** was investigated. Removal of aromatic esters in the C-4 positions was initiated by sodium methoxide in methanol and chloroform at elevated temperatures of up to 50°C. The reaction progress, monitored by ^{1}H-NMR, showed that removal of all ester groups was difficult. Refluxing and high concentrations of sodium methoxide were necessary.[21] For this reason, a second deprotection sequence was evaluated. Recently published work suggested removal of naphthylmethyl by a solution of TFA in Toluene.[137] Unfortunately, due to remaining naphthylmethyl groups the desired oxidative cleavage was not successful. Using the protocol of Overkleeft and coworkers,[156] hexafluoroisopropanol and HCl were used to cleave the protecting groups. However, the reaction failed to go to completion, even under prolonged reaction times. Finally, removal of naphthylmethyl was achieved by reductive conditions mediated by H_2 and Pd/C. Resulting compound **143** was subjected to hydrolysis of the esters by sodium methoxide in a mixture of methanol and DCM at 45°C. Purification on a sephadex G15 size exclusion column using 5% ethanol in water as eluent gave product **144** in 33% yield.

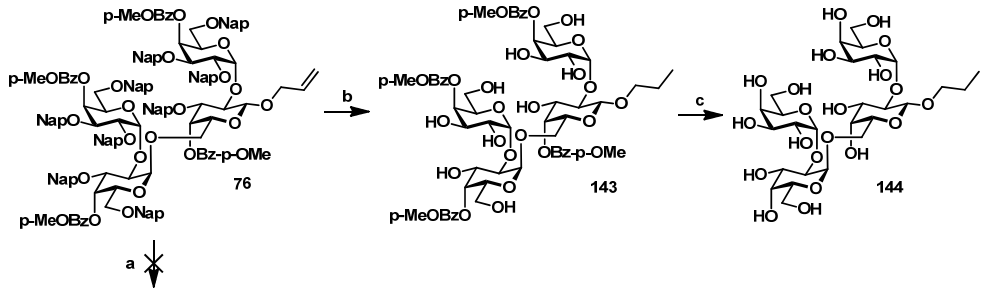

Scheme 43: Synthesis of tetragalactoside **144**: a) i) NaOMe, MeOH/DCM; ii) TFA, toluene; iii) HFIP, HCl; b) Pd/C, H_2, MeOH/EtOAc; c) NaOMe, MeOH, 45°C, 33%

[21] Information by Dr. Bo-Young Lee

6.6 TETRASACCHARIDE 148

Tetrasaccharide **30** was used to synthesize larger fragments. Therefore, the anomeric allyl protecting group was removed via isomerization with an iridium catalyst and hydrogen and consecutive hydrolysis of the enol ether with mercury salts in aqueous acetone. Under these conditions, however, a big fraction of enol ether **145** was isolated. Investigation of hydrolysis with stronger acids, even such as CSA, resulted in cleavage of the TIPS ether giving rise to a compound with enolether and no silyl group **146**. Hydrolysis of these compounds is usually achieved by NBS,[157] but failed to deliver the lactol in this particular reaction.

With these results in hand, it was argued that enol ether **146** would be stable under all conditions necessary in a phosphorylation and deprotection sequence for this GPI fragment. Consequently **145** was subjected to removal of the TIPS group with scandium triflate and water in a 3:1 mixture of refluxing acetonitrile and DCM. The reaction gave desired product **146** in 44% yield. Phosphonylation with H-phosphonate **43** using pivaloyl chloride and consecutive oxidation by iodine and a 9:1 mixture of pyridine and water at 0°C gave corresponding phosphate **147** in 37% yield. Finally, global deprotection was achieved using Pd/C and H_2 in a mixture of methanol and EtOAc under elevated pressure for 6 h and atmospheric pressure for 40 h. Purification on a sephadex G15 size exclusion column using 5% ethanol in water as eluent gave desired product **148** in 62% yield.

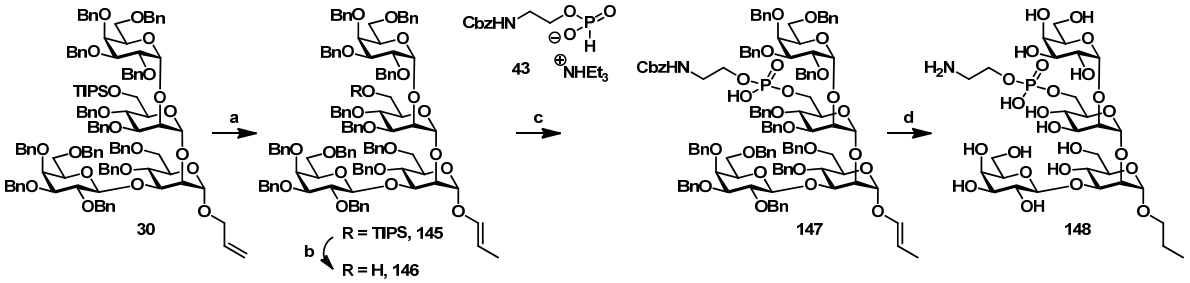

Scheme 44: Synthesis of tetrasaccharide **148**: a) $[Ir(COD)(PMePh_2)_2]PF_6$, H_2, THF b) CSA, DCM or $Sc(OTf)_3$, H_2O, DCM, ACN, reflux, 44%; c) i) **43**, PivCl, pyr; ii) I_2, H_2O, pyr, 37% d) H_2, Pd/C, MeOH/EtOAc, 62%

6.7 TRISACCHARIDE 150

To investigate a potential role played by Gal III attachment to the GPI backbone trisaccharide **33** from the synthesis of tetrasacchraide **30** was subjected to the removal of all acid labile functionalities in quantitative yield by HCl generated *in situ* from acetyl chloride in a mixture of methanol and DCM. Afterwards, diol **149** was exposed to atmospheric reductive conditions mediated by H_2 and Pd/C and delivered trisaccharide **150** in 49% yield over two

steps after purification by sephadex G15 size exclusion column using in 5% ethanol in water as eluent.

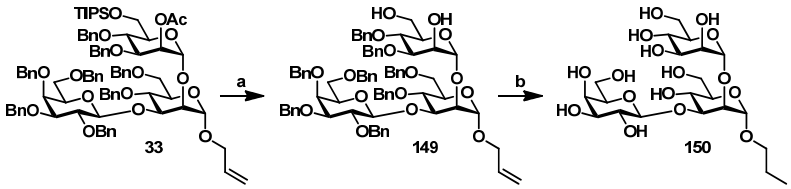

Scheme 45: Synthesis of trisaccharide **150**: a) AcCl, MeOH/DCM quant.; b) Pd/C, H_2, MeOH/EtOAc, 49%

6.8 PSEUDOHEPTASACCHARIDE 152

In the effort of synthesizing the full VSG 117 GPI structure of *T. brucei* **128**, pseudoheptasaccharide **126** was isolated as an intermediate. To investigate the difference in activation of macrophages, when no phosphorylation is present in the molecule, the compound was submitted to the removal of TIPS by scandium triflate and water in a refluxing 5:2 mixture of DCM and acetonitrile. Purification of diol **151** by silica gel column chromatography was followed by reduction using sodium and methanol in liquid ammonia. Purification on a sephadex G25 size exclusion column with 5% ethanol and water as eluent and RP-HPLC ((hypercarb column 150×10mm, ThermoFisher, 5 µ, acetonitrile in water 0-100% in 60 min) delivered product **151** in 44% yield.

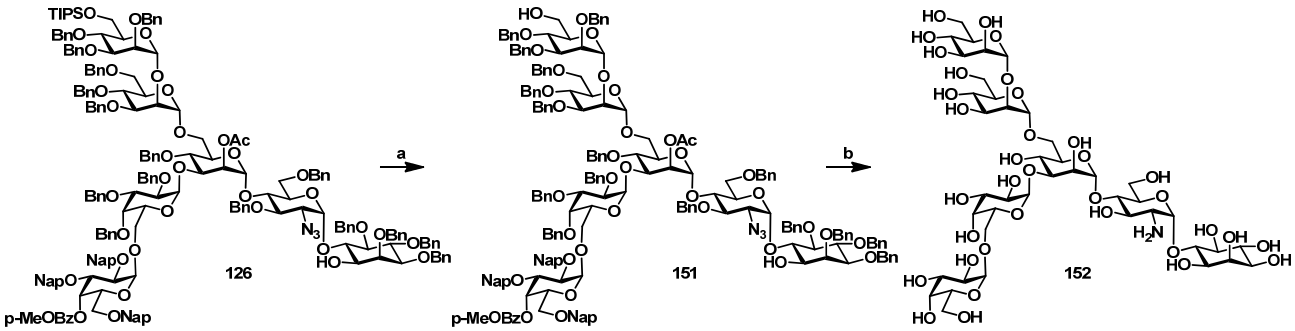

Scheme 46: Synthesis of pseudoheptasaccharide **151**: a) $Sc(OTf)_3$, H_2O, DCM:ACN, reflux, b) $NH_{3(l)}$, Na, MeOH, -78°C, 44 %

6.9 CONCLUSION SYNTHESIS OF GPI FRAGMENTS FOR MACROPHAGE ACTIVATION

In this chapter, synthesis of a library of GPI structures for the investigation in macrophage activation was described. Compounds were synthesized by either employing precursors originating from synthesis described in chapter 4 or by using building blocks specifically used for this purpose.

7. INVESTIGATION OF MACROPHAGE ACTIVATION BY GPI FRAGMENTS

Some reports described the ability of isolated GPIs of *T. brucei* to induce inflammatory effects by activation of Toll-like-receptor 2.[38] Interacting with GPIs, macrophages release IL-12, TNF-α, reactive oxygen species and nitric oxides.[39] Especially the release of TNF-α has been associated to distinct structural features of GPI glycans,[40] and more specifically to unique α-galactosides present in the side branch of *T. brucei* GPI. Other studies showed that the pseudodisaccharide (GlcN-Ino) attached to a phosphodiacylglycerol suppresses the protein tyrosine kinase signal maximizing TNF-α gene expression.[40] These, at some level contradictory, results were obtained in biological assays using isolated GPI structures possibly implying presence of heterogeneous substances and impurities being responsible of false positives. To overcome these limitations and to identify structural features of GPI inducing macrophages activation, a set of highly pure and homogeneous GPI structures (Figure 44) comprising the most important epitopes of *T. brucei* GPI were synthesized and investigated in their potential of macrophage activation.

The GPI derivatives were equipped with a phospholipid having a diacylglycerol for those containing a *myo*-inositol unit or with a short alkyl chain at the reducing end in derivatives lacking this unit. A murine macrophage RAW264.7 cell line (cell count 4×10^4 per 200 µL of RPMI + 5% FCS) was incubated with a 10 µM solution of each compound in DMSO and incubated for 24 h.[22] After this time, TNF-α levels were determined and compared to the value of the assay medium, *i.e.* 200 µL of RPMI + 5% FCS + DMSO (corresponding to 10 µM), in post hoc analysis consisting of analysis of variance and concluding significance test. Figure 44 shows the reproducible levels of TNF-α released by incubation of the RAW264.7 cell line with synthetic GPI structures. The results indicated that phosphorylation plays an important role in the release of TNF-α. Lipidated GPIs of *Trypanosoma brucei* VSG117 **H'**, *Toxoplasma gondii* **O** and *Trypanosoma congolense* **P** are significant in inducing TNF-α, verifying reported observations in other investigations.[39] Moreover, the *T. brucei* phospholipidated pseudodisaccharide **L**, in contrast to *myo*-inositol phospholipid **D'** was able to trigger TNF-α production, confirming the finding of Baetselier and Schofield[40] and indicating that a *myo*-inositol phospholipid triggers TNF-α only when glycosylated further. Interestingly, non-phosphorylated *T. brucei* VSG117 GPI glycan **N** and VSG221

[22] Experiment performed by Group of Dr. Benoit Stijlemans (VIB University, Brussels)

fragment **B** induced also TNF-α production, confirming the important role of α-galactosides in this activity.[40] The VSG 117 C-terminal peptide **J** triggered release of TNF-α underlining the suspected activity[40a, 149a, 155] of the protein part. Finally, the conserved non-mammalian trimannoside GPI backbone **I'** was active in triggering the release of TNF-α.

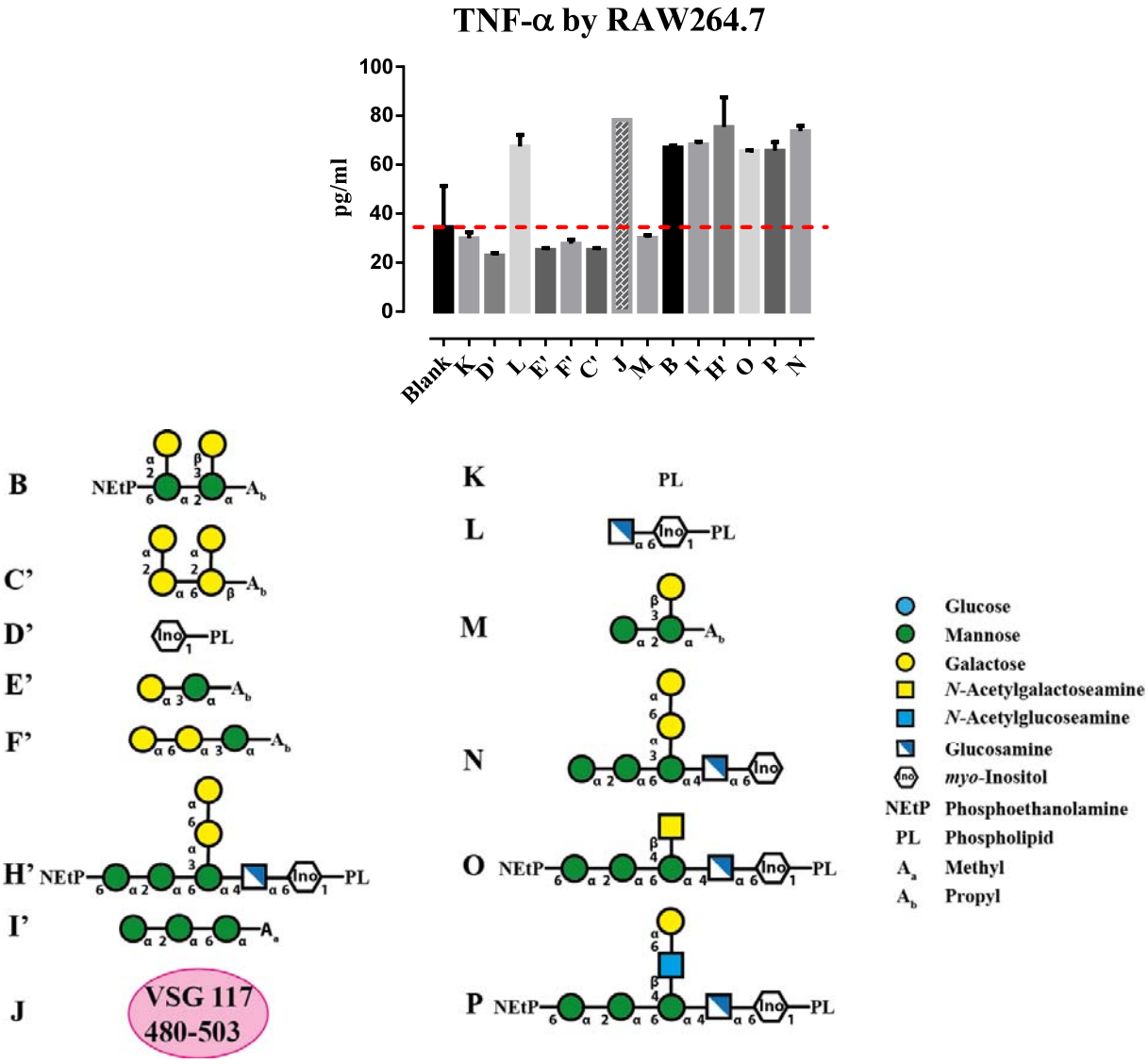

Figure 44: TNF-α release in murine macrophage RAW264.7 activation assay: 4×10^4 cells per 200 µL of RPMI + 5% FCS were incubated with 10 µM compound **B-P** in DMSO for 24 h

To further investigate production of TNF-α induced by GPI derivatives, the activation assay was repeated using a primed murine RAW264.7 cell line (Figure 45). Priming was achieved by incubating the cell line with 100 units/mL of IFN-γ prior to adding the compounds. IFN-γ is a cytokine naturally released in inflammation to stimulate macrophages for activation.

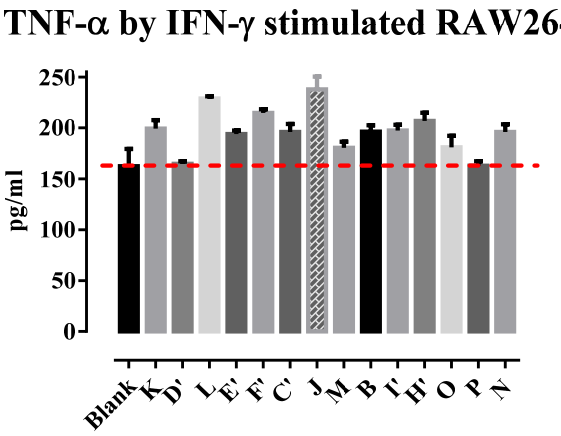

Figure 45: TNF-α release in murine macrophage RAW264.7 activation assay after stimulation by 100 units/mL of IFN-γ

After post hoc analysis the results of this investigation indicate significant activation by all structures with the exception of the *Trypanosoma congolense* GPI **P** and phosphorylated *myo*-inositol **L**.

7.1 Conclusion and Outlook Macrophage Activation

These preliminary findings demonstrated biological activity of fully synthetic GPI structures of parasitic origin. Moreover, it confirmed that *T. brucei* VSG-GPI pose multiple structural components capable of triggering release of different levels of TNF-α on their own These components include: phospholipidated pseudodisaccharide, C-terminal VSG peptide, phosphorylated fragments, α-galactoside containing structures and the non-phosphorylated trimannoside GPI backbone. However, annotation of general activity of non-mammalian GPI backbones is difficult, as the structure is found as well in high-mannose type N-glycans.

Interestingly, stimulated macrophages are triggered to produce TNF-α by the complete set of synthesized *T. brucei* specific structures. Ongoing experiments are evaluating activation of human cell lines and cells isolated from liver and spleen to investigate specificity of the activation effect induced by synthetic structures. Additionally, repeating the reported screening by varying incubation time will deliver insights in the activation kinetics of each compound. By these studies more specific statements concerning a structure-activity relationship will be possible.

8. GPI FRAGMENTS FOR A LIGATION METHOD

According to the synthetic analysis for Peptide-GPI-fragments, three different strategies for assembling these structures are possible. Therefore feasibility of each strategy was investigated, using a standardized building block **153**[23] displaying Man III with possibility of installing the phosphoethanolamine functionality. Furthermore the building block is equipped with naphthyl-methyl groups, enabling deprotection by a broad range of methods, including peptide deprotection protocols.[137, 158]

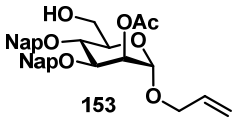

Scheme 47: Man III building block **153**

8.1 STRATEGY 1: FRAGMENT CONDENSATION

The first strategy relied on assembling the GPI fragment with attached phosphoethanolamine moiety, complete deprotection thereafter and consecutive peptide bond formation. Investigation started with a phosphonylation reaction of mannoside **153** and H-phosphonate **43** by activation using pivaloyl chloride in pyridine and subsequent oxidation of the intermediate phosphonate diester by iodine and a 9:1 mixture of pyridine and water. The two stepped sequence delivered product **154** in 45% yield. In the following, removal of naphthylmethyl and Cbz and reduction of allyl using hydrogenolysis on Pd/C gave a mixture of compounds. Purification by sephadex G15 size exclusion column using 5% ethanol in water as eluent resulted in isolation desired product **155** in 8% yield. Additionally, side products **156** bearing one naphthylmethyl group were purified in 10% yield. In the following **156** and an excess of tripeptide **157**[24] were used in a peptide bond formation mediated by DIPEA and PyBOP. After purification by sephadex G15 size exclusion column using 5% ethanol in water as eluent the compound was subjected to cleavage of the peptide protecting groups using a 90:5:5 mixture of TFA, TIPS and water. Sephadex G15 size exclusion column purification delivered product **158** in 51% over two steps.

[23] Synthesized by Dr. Bo-Young Lee

[24] Synthesized by Dana Michel

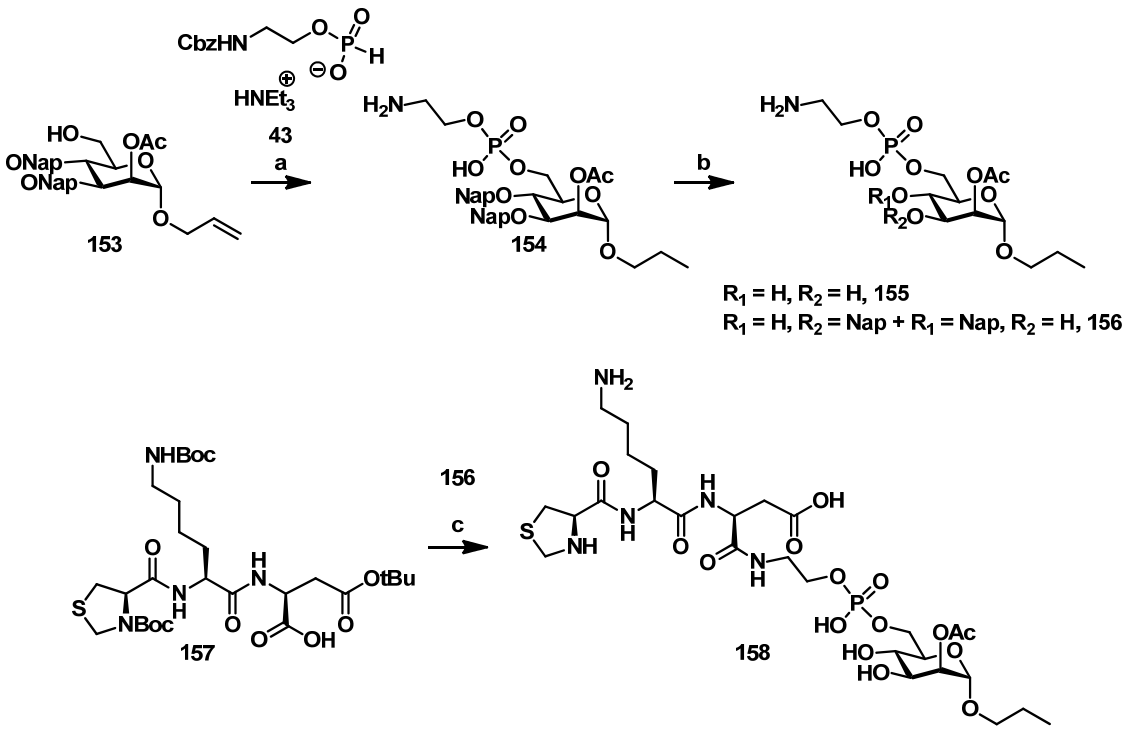

Scheme 48: Investigation of synthesizing **158** by strategy 1: a) i) **43**, PivCl, pyr; ii) I_2, H_2O, pyr, 0°C, 45%; b) Pd/C, H_2, MeOH/EtOAc, 8% (**155**) /10% (**156**); c) i) **156** + **157**, DIPEA, PyBOP; ii) TFA:TIPS:H_2O, 90:5:5, 51% over two steps

8.2 STRATEGY 2: PHOSPHORYLATION OF THE PEPTIDE

For the second strategy, an H-phosphonate of a GPI fragment was required for consecutive phosphorylation with protected tripeptide CKD. Therefore, mannoside **153** was phosphonylated with phosphonic acid in 4% yield using pivaloyl chloride in pyridine. An explanation for the low yield is hygroscopic moisture in the phosphonic acid, which is supported by the isolation of large amounts of starting material. However, in the following, a phosphonylation reaction of mannoside H-phosphonate **159** with an ethanolamine modified version of the tripeptide **160**[25] was conducted using pivaloyl chloride in pyridine. Oxidation by iodine and a 9:1 mixture of pyridine and water delivered intermediate product **161**. Direct removal of naphthylmethyl and reduction of allyl by hydrogenolysis on Pd/C gave a desired product **162**. After purification on sephadex G15 size exclusion column using 5% ethanol in water as eluent CKD-Man III conjugate **162** was dissolved in a 90:5:5 mixture of TFA, TIPS and water. The crude product was purified on sephadex G15 size exclusion column using 5% ethanol in water as eluent giving **158** in 27% yield over three steps.

[25] Synthesized by Dana Michel

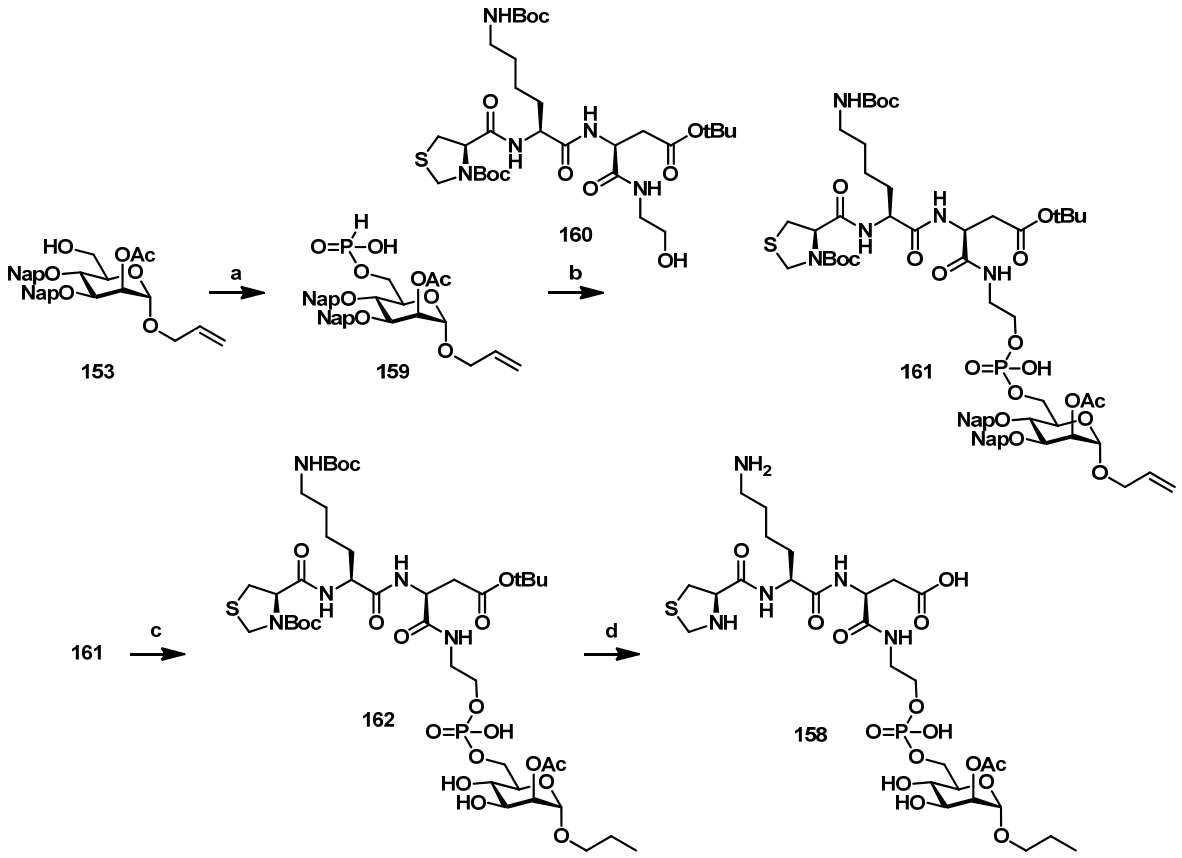

Scheme 49: Investigation of synthesizing **158** by strategy 2: a) H_3PO_3, PivCl, pyr, 4%; b) i) **160**, PivCl, pyr; ii) I_2, H_2O, pyr, 0°C; c) Pd/C, H_2, MeOH/EtOAc; d) TFA:TIPS:H_2O 90:5:5, 27% over three steps

8.3 STRATEGY 3: PHOSPHORYLATION OF THE GLYCAN

The third strategy involves formation of a H-phosphonate of the tripeptide and a phosphorylation reaction with the GPI fragment. Beforehand, this required a phoshonylation reaction of precursor **160** with phosphonic acid. By removing every trace of water from the hygroscopic phosphonic acid, performance of the reaction using pivaloyl chloride in pyridine for activation gave corresponding H-phosphonate **163** in 29% yield. The following phosphonylation of **163** with mannoside **153** using pivaloyl chloride in pyridine and subsequent oxidation by iodine and a 9:1 mixture of pyridine and water at 0°C showed no formation of product **161**. Similar results were obtained when higher mannosides, *i.e.* ManIII-ManII, ManIII-ManII-ManI, were applied in test reactions.

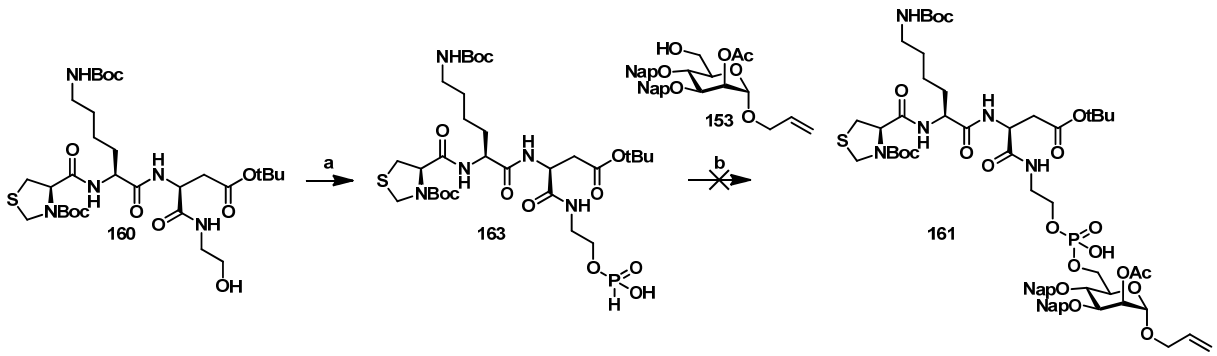

Scheme 50: Investigation of synthesizing **158** by strategy 3: a) H_3PO_3, PivCl, pyr, 29%; b) i) **153**, PivCl, pyr; ii) I_2, H_2O, pyr, 0°C

8.4 Conclusion and Outlook GPI fragments for a Ligation method

Comparing the strategies it is clear that strategy 3 failed to deliver the desired CKD-Man III conjugate. Strategy 1 and 2 were both successful in giving the product. However, strategy 2 requires a phosphonylation reaction with phosphonic acid and thereby optimization for each new protected glycan. In contrast, strategy 1 requires deprotected glycan fragments bearing a phosphoethanolamine, which enables application of conservative GPI glycan synthesis. Eventually, the target structure has to be considered when choosing one of these two promising strategies.

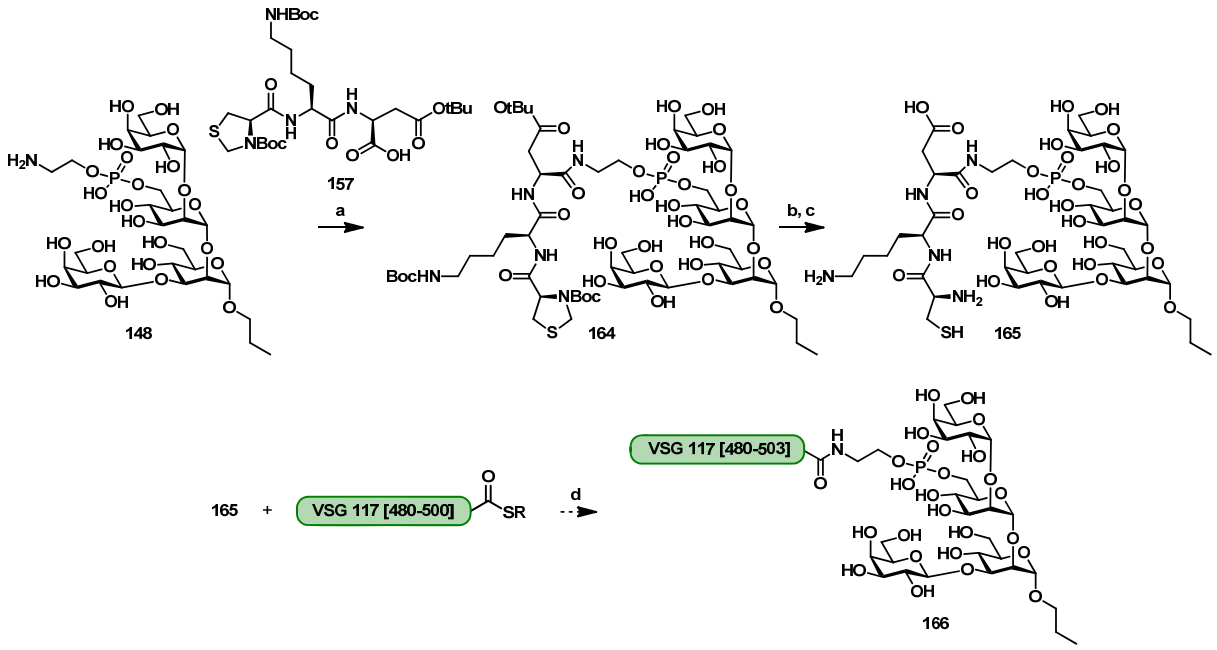

Scheme 51: Outlook: GPI fragment **148** is investigated in a native chemival ligation reaction with **157**: a) DIPEA, PyBOP, DMF, DMSO, 71%; b) 90:5:5, TFA, anisole, TIPS; c) NH_2-OMe; TCEP, guanidine, Na_2HPO_4; d) **165**, MPAA, TCEP, guanidine, Na_2HPO_4

Applying strategy 1 tetrasaccharide **148** was combined with **157** in a fragment condensation mediated by DIEPA and PyBOP giving **164** in 71% yield. Deprotection over

two steps using a 90:5:5 mixture of TFA, anisole and TIPS and methoxyamine delivered **165** which is investigated in a native chemical ligation with a VSG117 (480-500). Successful synthesis of **166** although remained to be investigated would conclude the first assembling of a VSG-GPI-conjugate by this strategy.

9. EXPERIMENTAL PART

9.1 MATERIALS AND METHODS

All chemicals were reagent grade and all solvents anhydrous high-purity grade and used as supplied except where noted otherwise. Reactions were performed in oven-dried glassware under an inert argon atmosphere unless noted otherwise. Reaction molarity was 0.1 molar except where noted otherwise. Reagent grade thiophene was dried over activated molecular sieves prior to use. Pyridine was distilled over CaH_2 prior to use. Sodium hydride suspension was washed with hexane and THF and stored in an anhydrous environment. Benzyl bromide was passed through activated basic aluminum oxide prior to use. Molecular sieves were powdered and activated by heating under high vacuum prior to use. Analytical thin layer chromatography (TLC) was performed on Merck silica gel 60 F_{254} plates (0.25mm). Compounds were visualized by UV irradiation or heating the plate after dipping in staining solution. Those were cerium sulfate-ammonium molybdate (CAM) solution, basic potassium permanganate solution, acidic ninhydrin-acetone solution or a 3-methoxyphenol-sulfuric acid solution. Flash column chromatography was carried out using a forced flow of the indicated solvent on Fluka silica gel 60 (230-400 mesh, for preparative column chromatography).
^{1}H, ^{13}C and ^{31}P-NMR spectra were recorded on a Varian 400 (400 MHz), a Varian 600 (600 MHz), a Bruker 400 (400 MHz) and a Bruker Ascend 400 (400 MHz) spectrometer in $CDCl_3$ (7.26 ppm ^{1}H, 77.1 ppm ^{13}C), D_2O (4.79 ppm ^{1}H), MeOD (4.87 ppm and 3.31 ppm ^{1}H, 49.00 ppm ^{13}C), acetone-d6 (2.05 ppm and 2.84 ppm ^{1}H, 206.26 ppm and 29.84 ppm ^{13}C) unless otherwise stated. Coupling constants are reported in Hertz (Hz). Splitting patterns are indicated as s, singlet; d, doublet; t, triplet; q, quartet; br, broad singlet; dd, doublet of doublets; m, multiplet; dt, doublet of triplets; h, hextet for ^{1}H NMR data. Signals were assigned by means of ^{1}H-^{1}H COSY, ^{1}H-^{1}H TOCSY, ^{1}H-^{1}H NOESY, ^{1}H-^{1}H ROESY, ^{1}H-^{13}C HSQC, ^{1}H-^{13}C HMBC spectra and versions thereof. ESI mass spectral analyses were performed by the MS-service at the Institute for Chemistry and Biochemistry at the Free University of Berlin using a modified MAT 711 spectrometer, the MS-service at the Institute for Chemistry at the University of Potsdam using an ESI-Q-TOF micro spectrometer and a Waters Xevo G2-XS QTof with an Acquity H-class UPLC. Infrared (FTIR) spectra were recorded as thin films on a Perkin Elmer Spectrum 100 FTIR spectrophotometer. Optical rotations were measured with a Schmidt & Haensch UniPol L 1000 at a concentration (c) expressed in g/100 mL. HPLC supported purifications were conducted using Agilent 1100

and Agilent 1200 systems. Supercritical fluid chromatography was carried out using a Waters Investigator System.

9.2 General Synthetic Methods

Method 1: Per-*O*-Acetylation

To a suspension of the compound in pyridine 20 eq acetic anhydride were added at 0°C. The reaction was allowed to warm up to room temperature and stirred for 12-16 hours. The solution was concentrated under reduced pressure and the resulting residue was dissolved in DCM and washed with sat. $NaHCO_3$ solution and brine. The organic phase was dried over Na_2SO_4, filtered and concentrated under reduced pressure. The residue was purified by silica column chromatography using hexane and ethyl acetate as eluent.

Method 2: Introduction of an anomeric group from Acetyl

To a solution of the compound in DCM 0.3 eq BF_3-Et_2O and 3 eq nucleophile were added. The reaction was stirred at room temperature for 12-16 hours and quenched by adding NEt_3 after TLC indicated full conversion. The mixture was diluted with sat. $NaHCO_3$ solution and extracted three times with DCM. The combined organic phases were washed with brine, dried over Na_2SO_4, filtered and concentrated under reduced pressure. The residue was purified by silica column chromatography using hexane and ethyl acetate as eluent.

Method 3: sodium methoxide mediated *O*-Acyl removal

0.1 mL freshly prepared 1 M sodium methoxide solution in methanol was added to a solution of the compound in methanol. The reaction was stirred at room temperature and neutralized with Amberlite H^+ resin after TLC indicated full conversion. The mixture was filtered and concentrated under reduced pressure. The residue was purified by silica column chromatography using hexane and ethyl acetate as eluent.

Method 4: K_2CO_3 mediated *O*-Acyl removal

To a solution of the compound in methanol potassium carbonate was added. The reaction was stirred at room temperature. After TLC indicated full conversion, the suspension was filtered and the filtrate was concentrated under reduced pressure. The residue was purified by silica column chromatography using hexane and ethyl acetate as eluent.

METHOD 5: ACID MEDIATED *O*-ACETYL REMOVAL

To a stirred solution of the compound in a mixture of DCM and methanol 0.1 mL of acetylchloride were added drop wise. The reaction was stirred at room temperature until TLC indicated full conversion. After diluting the green solution with DCM, sat. $NaHCO_3$ solution was added to quench the reaction. The mixture was extracted three times with DCM and the combined organic phases were dried over Na_2SO_4, filtered and concentrated under reduced pressure. The residue was purified by silica column chromatography using hexane and ethyl acetate as eluent.

METHOD 6: TBDPS OR TIPS INSTALLATION

To a solution of the compound in DMF 1.75 eq imidazole, 0.3 eq DMAP and 1.05 eq silylchloride were added. The reaction was stirred at room temperature until TLC indicated full conversion. The reaction was quenched by adding sat. $NaHCO_3$ solution. The mixture was extracted five times with DCM and the combined organic phases were dried over Na_2SO_4, filtered and concentrated under reduced pressure. The residue was purified by silica column chromatography using hexane and ethyl acetate as eluent.

METHOD 7: ISOPROPYLIDENE INSTALLATION

To a solution of the compound in dimethoxypropane 0.3 eq CSA were added and the reaction was stirred at room temperature until TLC indicated full conversion. The reaction was quenched by adding sat. $NaHCO_3$ solution. The mixture was extracted three times with DCM and the combined organic phases were dried over Na_2SO_4, filtered and concentrated under reduced pressure. The residue was purified by silica column chromatography using hexane and ethyl acetate as eluent.

METHOD 8: 2,3-*O*-ORTHOESTER FORMATION AND OPENING

To a solution of the compound in acetonitrile 1.5 eq triethylorthoacetate and 0.3 eq CSA were added and the reaction was stirred at room temperature until TLC indicated full conversion. Acetonitrile was removed under reduced pressure and the residue was suspended in 80% acetic acid. The resulting mixture was stirred for 12-16 hours at room temperature. The obtained clear solution was carefully quenched by adding sat. $NaHCO_3$ solution. The mixture was extracted three times with DCM and the combined organic phases were dried

over Na_2SO_4, filtered and concentrated under reduced pressure. The residue was purified by silica column chromatography using hexane and ethyl acetate as eluent.

METHOD 9: REGIOSELECTIVE ETHER FORMATION VIA STANNYLATION

In a reflux apparatus the compound was dissolved in toluene. 1.2 eq dibutyl stannone were added and the mixture was refluxed for 4 hours. Toluene was evaporated and the residue was dissolved in DMF. 1.2 eq TBAI and 1.2 eq naphthylmethyl bromide or benzyl bromide were added and the reaction was stirred at 50°C for 2 h. The reaction was quenched by adding sat. $NaHCO_3$ solution. The mixture was extracted three times with DCM and the combined organic phases were dried over Na_2SO_4, filtered and concentrated under reduced pressure. The residue was purified by silica column chromatography using hexane and ethyl acetate as eluent.

METHOD 10: WILLIAMSON-ETHER FORMATION – BENZYLATION – METHYL-NAPHTHYLATION

To a stirred solution of the compound in DMF, sodium hydride was added at 0°C. The resulting suspension was stirred for 15 min, then naphthylmethyl bromide or benzyl bromide was added. The reaction mixture was allowed to warm up to room temperature and stirred for 12-16 hours. After completion was indicated by TLC, the reaction was quenched by adding sat. NH_4Cl solution. The resulting mixture was extracted five times with DCM and the combined organic phases were dried over Na_2SO_4, filtered and concentrated under reduced pressure. The residue was purified by silica column chromatography using hexane and ethyl acetate as eluent.

METHOD 11: *O*-ACYLATION WITH ACYLCHLORIDES

To a solution of the compound in pyridine 1.5 eq acylchloride was added. The mixture was stirred at room temperature until TLC indicated full conversion. Afterwards, the reaction was quenched by adding isopropylalcohol and the resulting mixture was concentrated under reduced pressure. The residue was purified by silica column chromatography using hexane and ethyl acetate as eluent.

METHOD 12: TIPS REMOVAL

In a round bottom flask equipped with an air condenser, the compound was dissolved in a 5:2 mixture of acetonitrile and DCM. 10 µL water and 2 eq scandium triflate were added

and the reaction was stirred at 45°C until TLC indicated full conversion. The reaction was quenched by adding sat. $NaHCO_3$ solution. The resulting mixture was extracted five times with DCM and the combined organic phases were dried over Na_2SO_4, filtered and concentrated under reduced pressure. The residue was purified by silica column chromatography using hexane and ethyl acetate as eluent.

METHOD 13: TBDPS REMOVAL

In a 15 ml centrifuge tube, the compound was dissolved in THF. 100 µL of HF-Pyridine were added and the reaction was stirred at room temperature for 12-16 hours. When TLC indicated full conversion the reaction was quenched by adding sat. $NaHCO_3$ solution drop wise. The resulting mixture was extracted three times with DCM and the combined organic phases were dried over Na_2SO_4, filtered and concentrated under reduced pressure. The residue was purified by silica column chromatography using hexane and ethyl acetate as eluent.

METHOD 14: ALLYL-REMOVAL VIA ISOMERIZATION AND HYDROLYSIS

In a round bottom flask, 10 mg of $[IrCOD(PMePh_2)_2]PF_6$ were added to 2 mL THF. Hydrogen was bubbled through the suspension until the catalyst dissolved. This solution was transferred to a second flask, where it dissolved the compound. The reaction was stirred at room temperature overnight. THF was evaporated under reduced pressure and the residue was dissolved in an 8:1 mixture of acetone and water. 0.1 eq mercury oxide and 5 eq mercury chloride were added and the solution was stirred for one hour at room temperature. The reaction was quenched by adding sat. $NaHCO_3$ solution and the resulting mixture was extracted three times with DCM. The combined organic phases were dried over Na_2SO_4, filtered and concentrated under reduced pressure. The residue was purified by silica column chromatography using hexane and ethyl acetate as eluent.

METHOD 15: IMIDATE FORMATION

The compound was dissolved in DCM at 0°C. 8 eq trichloroacetonitrile and 0.1 eq DBU were added and the reaction was stirred until TLC indicated full conversion. The resulting mixture was concentrated under reduced pressure and purified by silica column chromatography using hexane and ethyl acetate as eluent.

METHOD 16: GLYCOSYLATION WITH IMIDATE

Donor and acceptor were co-evaporated three times with toluene and dried under high vacuum. The compound mixture was dissolved in the solvent and 4 Å MS was added. 0.3 eq activator was added and the reaction was stirred until TLC indicated full conversion. The reaction mixture was diluted with DCM and quenched by adding sat. $NaHCO_3$ solution. The mixture was extracted three times with DCM and the combined organic phases were dried over Na_2SO_4, filtered and concentrated under reduced pressure. The residue was purified by silica column chromatography using hexane and ethyl acetate as eluent.

METHOD 17: GLYCOSYLATION WITH THIODONOR

Donor and acceptor were co-evaporated three times with toluene and dried under high vacuum. The compound mixture was solved in the solvent and 4 Å MS was added. 1.7 eq dried NIS and 0.3 eq activator were added. When TLC indicated full conversion the pink solution was diluted with DCM and quenched by adding sat. $NaHCO_3$ solution. The mixture was extracted three times with DCM, washed with sat. $Na_2S_2O_3$ solution and the combined organic phases were dried over Na_2SO_4, filtered and concentrated under reduced pressure. The residue was purified by silica column chromatography using hexane and ethyl acetate as eluent.

METHOD 18: H-PHOSPHONATE FORMATION

Phosphonic acid and the compound were co-evaporated three times with pyridine. After drying the compound mixture under high vacuum, it was dissolved in pyridine. 1.5 eq pivaloylchloride were added and the reaction was stirred at room temperature until TLC indicated full conversion. The reaction was quenched by adding methanol and the solvents were concentrated under reduced pressure. The residue was purified by silica column chromatography using DCM and methanol as eluent.

METHOD 19: PHOSPHATE FORMATION

The H-phosphonate and the compound were co-evaporated three times with pyridine. After drying the compound mixture under high vacuum, it was dissolved in pyridine. 1.5 eq pivaloylchloride were added and the reaction was stirred at room temperature until TLC indicated full conversion. 1.5 eq iodine were added to a 9:1 mixture of pyridine and water. The solution was added to the reaction mixture and stirred at 0°C. When the TLC indicated

full conversion, the reaction was quenched by adding sat. $Na_2S_2O_3$ solution. The mixture was extracted three times with DCM and the combined organic phases were dried over Na_2SO_4, filtered and concentrated under reduced pressure. The residue was purified by silica column chromatography using DCM and methanol as eluent.

METHOD 20: PEPTIDE DEPROTECTION

The compound was dissolved in a 90:5:5 mixture of TFA, TIPS and water. After stirring the mixture for 30 min at room temperature the reaction was diluted with toluene and concentrated under reduced pressure. The residue was purified by G15 size exclusion using 5% ethanol in water as eluent.

METHOD 21: HYDROGENOLYSIS

The compound was suspended in methanol. A few drops of ethyl acetate were added to dissolve the compound. A 0.1 eq of Pd/C were added and the reaction was placed in a hydrogenation chamber. The reaction was stirred for one day at room temperature. The reaction was filtered and concentrated under reduced pressure. The residue was purified by sephadex size exclusion.

METHOD 22: BIRCH REDUCTION

Approximately 10 mL ammonia were condensed in a flask and methanol (2 drops) was added. Sodium was added in small pieces until a dark blue color established. The compound was dissolved in THF and added to the ammonium solution at -78°C. At this temperature the reaction was stirred for 1 h. The reaction was quenched by adding methanol and ammonia was blown off using a stream of nitrogen. The pH of the resulting solution was adjusted with glacial acetic acid to 7-8. The reaction concentrated under reduced pressure and the residue was purified by size exclusion using 5% ethanol in water as eluent.

9.3 PREPARATION OF GLYCAN MICROARRAY

The synthetic glycans were dissolved in phosphate buffer (50 mM NaH_2PO_4, pH 8.5 for amine linker compounds) or PBS buffer (pH 7.4 for thiols, including an equimolar amount of TCEP·HCl). The compounds were immobilized employing a piezoelectric spotting device (S3, Scienion) on maleimide-functionalized slides or on epoxy slides (sciCHIPEPOXY, Scienion), in 50% relative humidity at 23°C. The printed slides were stored for 18 h in a humified chamber to complete the immobilization reaction. Afterwards the slides were stored

in a cooled environment. Prior to the experiment, the slides were washed three times with water and the remaining maleimido or epoxy groups were quenched by incubating the slides in an aqueous solution of 100 mM ethanolamine and 50 mM $Na_2HPO_4 \cdot 12H_2O$ with pH 9.01 for 1 h at 25°C. The slides were rinsed three times with water and dried by centrifugation.

Microarrays were blocked with BSA (2.5%, w/v) in PBS for 1 h at room temperature. Blocked slides were washed twice with PBS, centrifuged and incubated with a 1:15 dilution of mouse or human sera in PBS for 1 h. After washing with PBS, microarrays were incubated with goat anti-mouse IgG H+L Alexa 645 (Molecular Probes, 1:400), donkey anti-mouse IgM Alexa 594 (Dianova, 1:200), goat anti-human IgG-Fc Alexa488 (Dianova, 1:400) or goat anti-human IgM Alexa 594 (Molecular Probes, 1:200) in PBS containing 1% BSA for 1 h. The slides were then washed with PBS and double-distilled water, subsequently dried by centrifugation and analyzed using a fluorescence microarray scanner (Genepix® 4300A, Molecular Devices).

9.4 SYNTHETIC PART FOR CHAPTER 4

Thioethyl-2-*O*-benzoyl-3,4,6-*O*-tri-benzyl-β-D-galactopyranoside (5b)

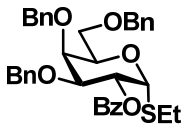

3.400 mmol of alcohol **4** (1.682 g) was reacted according to *O*-Acylation with acylchlorides (Method 11) using benzoyl chloride. β-product **5b** was obtained in 33% yield (1.133 mmol, 0.679 g) as colorless oil.

R_f = 0.4 (6:1, Hex:EA)

^{1}H-NMR (400 MHz, $CDCl_3$): δ = 8.18 – 8.18 (m, 2H, $H_{Ar.}$), 8.04 – 8.02 (m, 2H, $H_{Ar.}$), 7.71 – 7.67 (m, 1H, $H_{Ar.}$), 7.58 – 7.26 (m, 15H, $H_{Ar.}$), 5.82 (d, *J* = 5.5 Hz, 1H, Gal-1), 5.73 (dd, *J* = 10.2 Hz, 5.7 Hz, 1H, Gal-2), 4.96 (d, *J* = 11.5 Hz, 1H, -CH_2-), 4.69 (bs, 2H, -CH_2-), 4.61 (d, *J* = 11.5 Hz, 1H, -CH_2-), 4.51 (d, *J* = 11.7 Hz, 1H, -CH_2-), 4.44 (d, *J* = 11.7 Hz, 1H, -CH_2-), 4.37 (t, *J* = 6.4 Hz, 1H, Gal-5), 4.05 (bs, 1H, Gal-4), 3.97 (d, *J* = 10.2 Hz, 1H, Gal-3), 3.68 – 3.56 (m, 2H, Gal-6, Gal-6), 2.60 – 2.43 (m, 2H, -CH_2-), 1.26 – 1.17 (m, 3H, -CH_3) ppm.

^{13}C-NMR (101 MHz, $CDCl_3$): δ = 165.69 (C=O), 138.38 (C_{Ar}), 137.98 (C_{Ar}), 137.91 (C_{Ar}), 134.54 (C_{Ar}), 133.08 (C_{Ar}), 130.57 (C_{Ar}), 129.94 (C_{Ar}), 129.85 (C_{Ar}), 128.87 (C_{Ar}), 128.40 (C_{Ar}), 128.38 (C_{Ar}), 128.27 (C_{Ar}), 128.24 (C_{Ar}), 127.75 (C_{Ar}), 127.74 (C_{Ar}), 127.69 (C_{Ar}), 127.63 (C_{Ar}), 82.20 (Gal-1), 77.40 (Gal-3), 74.82 (-CH_2-), 74.32 (Gal-4), 73.50 (-CH_2-), 72.64 (-CH_2-), 71.25 (Gal-2), 69.64 (Gal-5), 68.80 (Gal-6), 23.90 (-CH_2-), 14.66 (-CH_3) ppm.

ESI-MS: m/z M_{calcd} for $C_{36}H_{36}O_6S$ = 598.23892; M_{found} = 621.2309 $[M+Na]^+$

Polarimeter: $[\alpha]_D^{20}$ = +86.79 (c = 1.00 g/L in $CHCl_3$)

FTIR: 2871.88, 1788.43, 1723.98, 1601.10, 1453.32, 1317.55, 1268.52, 1213.24, 1174.63, 1097.26, 1071.21, 997.27, 737.80, 699.14 cm^{-1}.

Thioethyl-2-*O*-benzoyl-3,4,6-*O*-tri-benzyl-α-D-galactopyranoside (5a)

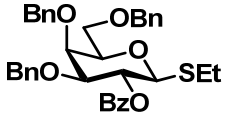

3.400 mmol of alcohol **4** (1.682 g) was reacted according to *O*-Acylation with acylchlorides (Method 11) using benzoyl chloride. α-product **5a** was obtained in 66% (2.267 mmol, 1.357 g) as colorless oil.

$\mathbf{R_f}$ = 0.4 (6:1, Hex:EA)

^{1}H-NMR (400 MHz, $CDCl_3$): δ = 8.13 – 8.11 (m, 1H, $H_{Ar.}$), 8.04 -8.01 (m, 2H, $H_{Ar.}$), 7.62 – 7.56 (m, 2H, $H_{Ar.}$), 7.50 – 7.15 (m, 15H, $H_{Ar.}$), 5.69 (t, *J* = 9.8 Hz, 1H, Gal-2), 5.00 (d, *J* = 11.7 Hz, 1H, -CH_2-), 4.65 (d, *J* = 8.6 Hz, 1H, -CH_2-), 4.62 (d, *J* = 7.9 Hz, 1H, -CH_2-), 4.52 (d, *J* = 6.6 Hz, 1H, -CH_2-), 4.49 (d, *J* = 4.0 Hz, 1H, Gal-1), 4.45 (t, *J* = 8.1 Hz, 2H, -CH_2-, -CH_2-), 4.06 (d, *J* = 2.6 Hz, 1H, Gal-4), 3.70 – 3.60 (m, 4H, Gal-3, Gal-5, Gal-6, Gal-6), 2.79 – 2.63 (m, 2H, -CH_2-), 1.21 (, *J* = 7.5 Hz, 3H, -CH_3) ppm.

^{13}C-NMR (101 MHz, $CDCl_3$): δ = 165.39 (C=O), 138.56 ($C_{Ar.}$), 137.76 ($C_{Ar.}$), 137.65 ($C_{Ar.}$), 133.71 ($C_{Ar.}$), 132.97 ($C_{Ar.}$), 130.17 ($C_{Ar.}$), 130.01 ($C_{Ar.}$), 129.88 ($C_{Ar.}$), 129.69 ($C_{Ar.}$), 128.48 ($C_{Ar.}$), 128.44 ($C_{Ar.}$), 128.29 ($C_{Ar.}$), 128.20 ($C_{Ar.}$), 128.04 ($C_{Ar.}$), 127.97 ($C_{Ar.}$), 127.85 ($C_{Ar.}$), 127.64 ($C_{Ar.}$), 127.50 ($C_{Ar.}$), 83.71 (Gal-1), 81.07 (Gal-3), 77.51 (Gal-5), 74.43 (-CH_2-), 73.58 (-CH_2-), 72.76 (Gal-4), 71.70 (-CH_2-), 70.21 (Gal-2), 68.55 (Gal-6), 23.67 (-CH_2-), 14.83 (-CH_3) ppm.

ESI-MS: m/z M_{calcd} for $C_{36}H_{36}O_6S$ = 598.23892; M_{found} = 621.2304 $[M+Na]^+$

Polarimeter: $[\alpha]_D^{20}$ = +25.90 (c = 1.00 g/L in $CHCl_3$)

FTIR: 3065.60, 3032.41, 2870.16, 1725.86, 1603.64, 1585.78, 1497.45, 1454.09, 1349.19, 1315.83, 1268.57, 1209.28, 1177.44, 1151.45, 1097.93, 1070.11, 1028.18, 999.60, 907.59, 843.14, 735.15, 710.42, 698.13 cm^{-1}.

Thioethyl-2,3,4,6-*O*-tetra-benzyl-α-D-galactopyranoside (8)

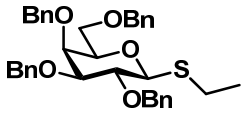

6.870 mmol of thioglycoside **7** (1.514 g) was reacted according to Williamson-ether formation (Method 10) using benzyl bromide. Product **8** was obtained in 74% yield (5.100 mmol, 2.984 g) as colorless oil.

R_f = 0.7 (6:1, Hex:EA)

^{1}H-NMR (400 MHz, $CDCl_3$): δ = 7.45 – 7.20 (m, 20H, $H_{Ar.}$), 4.96 (d, *J* = 11.7 Hz, 1H, -CH_2-), 4.89 (d, *J* = 10.1 Hz, 1H, -CH_2-), 4.80 (d, *J* = 10.1 Hz, 1H, -CH_2-), 4.74 (s, 2H, -CH_2-, -CH_2-), 4.63 (d, *J* = 11.8 Hz, 1H, -CH_2-), 4.52 – 4.39 (m, 3H, -CH_2-, -CH_2-, Gal-1), 3.97 (d, *J* = 2.8 Hz, 1H, Gal-4), 3.83 (t, *J* = 9.5 Hz, 1H, Gal-2), 3.63 – 3.45 (m, 4H, Gal-3, Gal-5, Gal-6, Gal-6), 2.80 – 2.69 (m, 2H, -CH_2-$_{Ethyl}$), 1.35 – 1.27 (m, 3H, -CH_3) ppm.

^{13}C-NMR (101 MHz, $CDCl_3$): δ = 138.72 ($C_{Ar.}$), 138.35 ($C_{Ar.}$), 138.27 ($C_{Ar.}$), 137.84 ($C_{Ar.}$), 128.44 ($C_{Ar.}$), 128.41 ($C_{Ar.}$), 128.39 ($C_{Ar.}$), 128.31 ($C_{Ar.}$), 128.27 ($C_{Ar.}$), 128.24 ($C_{Ar.}$), 128.17 ($C_{Ar.}$), 128.03 ($C_{Ar.}$), 128.00 ($C_{Ar.}$), 127.98 ($C_{Ar.}$), 127.93 ($C_{Ar.}$), 127.91 ($C_{Ar.}$), 127.80 ($C_{Ar.}$), 127.73 ($C_{Ar.}$), 127.63 ($C_{Ar.}$), 127.58 ($C_{Ar.}$), 127.53 ($C_{Ar.}$), 127.50 ($C_{Ar.}$), 127.47 ($C_{Ar.}$), 85.30 (Gal-1), 84.08 (Gal-3), 78.42 (Gal-2), 77.18 (Gal-5), 75.78 (-CH_2-), 74.42 (-CH_2-), 73.55 (-CH_2-), 73.53 (Gal-4), 72.70 (-CH_2-), 68.79 (Gal-6), 24.80 (-CH_2-$_{Ethyl}$), 15.09 (-CH_3) ppm.

ESI-MS: m/z M_{calcd} for $C_{36}H_{40}O_5S$ = 584.2596; M_{found} = 607.2432 $[M+Na]^+$

Polarimeter: $[\alpha]_D^{20}$ = +6.99 (c = 1.00 g/L in $CHCl_3$)

FTIR: 3065.90, 3032.54, 2925.22, 2868.88, 1606.41, 1497.73, 1454.98, 1361.95, 1262.64, 1208.84, 1153.54, 1095.89, 1028.68, 911.53, 807.04, 734.41, 697.08, 664.89 cm^{-1}.

Thiophenyl-2,3,4,6-*O*-tetra-benzyl-α/β-D-galactopyranoside (10)

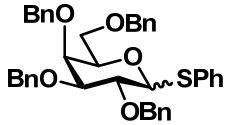

12.170 mmol of thioglycoside **9** (3.313 g) was reacted according to Williamson-ether formation (Method 10) using benzyl bromide. Product **10** was obtained in 85% yield (10.310 mmol, 6.524 g) as colorless oil. The compound was isolated as a mixture of anomers and was characterized accordingly.

R_f = 0.8 (6:1, Hex:EA)

^{1}H-NMR (400 MHz, $CDCl_3$): δ = 7.72 (dd, *J* = 6.6 Hz, 3.0 Hz, 2H), 7.56 – 7.50 (m, 3H), 7.50 – 7.36 (m, 17H), 7.32 – 7.29 (m, 3H), 5.11 (d, *J* = 11.5 Hz, 1H, -CH_2-), 4.96 – 4.72 (m,

6H, -CH_2-, Gal-1α, Gal-1β), 4.57 (q, *J* = 11.7 Hz, 2H, -CH_2-), 4.14 – 4.06 (m, 2H), 3.84 – 3.64 (m, 4H) ppm.

^{13}C-NMR (101 MHz, $CDCl_3$): δ = 138.86 ($C_{Ar.}$), 138.84 ($C_{Ar.}$), 138.44 ($C_{Ar.}$), 138.42 ($C_{Ar.}$), 138.36 ($C_{Ar.}$), 138.33 ($C_{Ar.}$), 137.98 ($C_{Ar.}$), 137.96 ($C_{Ar.}$), 134.26 ($C_{Ar.}$), 134.24 ($C_{Ar.}$), 131.58 ($C_{Ar.}$), 131.57 ($C_{Ar.}$), 128.89 ($C_{Ar.}$), 128.87 ($C_{Ar.}$), 128.52 ($C_{Ar.}$), 128.50 ($C_{Ar.}$), 128.42 ($C_{Ar.}$), 128.40 ($C_{Ar.}$), 128.33 ($C_{Ar.}$), 128.30 ($C_{Ar.}$), 128.28 ($C_{Ar.}$), 128.10 ($C_{Ar.}$), 128.01 ($C_{Ar.}$), 127.99 ($C_{Ar.}$), 127.93 ($C_{Ar.}$), 127.90 ($C_{Ar.}$), 127.88 ($C_{Ar.}$), 127.83 ($C_{Ar.}$), 127.81 ($C_{Ar.}$), 127.78 ($C_{Ar.}$), 127.76 ($C_{Ar.}$), 127.72 ($C_{Ar.}$), 127.66 ($C_{Ar.}$), 127.64 ($C_{Ar.}$), 127.61 ($C_{Ar.}$), 127.57 ($C_{Ar.}$), 127.55 ($C_{Ar.}$), 127.13 ($C_{Ar.}$), 127.11 ($C_{Ar.}$), 97.26, 87.79, 84.27, 79.27, 77.56, 77.52, 77.45, 77.39, 77.24, 77.20, 76.93, 76.88, 76.69, 75.73, 75.32, 74.85, 74.56, 74.54, 73.84, 73.69, 73.66, 73.56, 73.44, 73.35, 72.80, 69.33, 69.15, 68.87, 68.85, 63.42 ppm.

ESI-MS: m/z M_{calcd} for $C_{40}H_{40}O_5S$ = 632.2596; M_{found} = 655.2462 $[M+Na]^+$

FTIR: 3064.73, 3032.44, 2867.08, 1952.85, 1879.91, 1811.04, 1585.34, 1497.51, 1480.09, 1454.71, 1440.51, 1398.60, 1360.85, 1271.70, 1214.84, 1150.91, 1090.13, 1065.32, 1027.50, 1000.76, 910.20, 842.22, 808.84, 732.26, 694.09, 667.34 cm^{-1}.

Allyl-2-*O*-acetyl-4,6-*O*-di-benzyl-α-D-mannopyranoside (14)

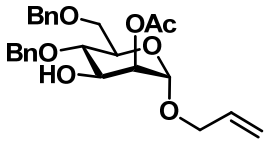

13.780 mmol of diol **13** (5.517 g) was reacted according to 2,3-*O*-orthoester formation and opening (Method 8). Product **14** was obtained in 68% yield (9.370 mmol, 4.150 g) as colorless oil.

R_f = 0.8 (2:1, Hex:EA)

^{1}H-NMR (400 MHz, $CDCl_3$): δ = 7.43 – 7.15 (m, 10H), 5.88 (ddd, *J* = 22.4 Hz, 10.8 Hz, 5.6 Hz, 1H, Allyl-2), 5.28 (dd, *J* = 17.2 Hz, 1.4 Hz, 1H, Allyl-3), 5.19 (d, *J* = 10.4 Hz, 1H, Allyl-3), 5.12 (dd, *J* = 3.5 Hz, 1.4 Hz, 1H, Man-2), 4.91 (d, *J* = 1.1 Hz, 1H, Man-1), 4.79 (d, *J* = 11.0 Hz, 1H, -CH_2-), 4.73 (d, *J* = 12.1 Hz, 1H, -CH_2-), 4.58 – 4.52 (m, 2H, -CH_2-), 4.20 – 4.14 (m, 2H, Gal-3, Allyl-1), 3.99 (dd, *J* = 12.9 Hz, 6.0 Hz, 1H, Allyl-1), 3.85 – 3.77 (m, 3H, Gal-4, Gal-5, Gal-6), 3.72 (d, *J* = 10.0 Hz, 1H, Gal-6), 2.16 (s, 3H, -CH_3) ppm.

^{13}C-NMR (101 MHz, $CDCl_3$): δ = 170.92 (C=O), 138.18 ($C_{Ar.}$), 138.06 ($C_{Ar.}$), 133.38 (Allyl-2), 128.47 ($C_{Ar.}$), 128.35 ($C_{Ar.}$), 127.89 ($C_{Ar.}$), 127.87 ($C_{Ar.}$), 127.84 ($C_{Ar.}$), 127.69 ($C_{Ar.}$), 117.67 (Allyl-3), 96.62 (Man-1), 75.86 (Gal-4), 74.94 (-CH_2-), 73.52 (-CH_2-), 72.62 (Man-2), 71.10 (Gal-5), 70.38 (Gal-3, 68.75 (Gal-6), 68.18 (Allyl-1), 21.12 (-CH_3) ppm.

ESI-MS: m/z M_{calcd} for $C_{25}H_{30}O_7$ = 442.1992; M_{found} = 465.1916 $[M+Na]^+$

Polarimeter: $[\alpha]_D^{20}$ = +36.43 (c = 1.00 g/L in $CHCl_3$)

FTIR: 3066.74, 3032.83, 2917.68, 2868.37, 2326.29, 1743.99, 1648.11, 1497.84, 1455.00, 1371.89, 1235.77, 1134.49, 1058.78, 1028.43, 1018.40, 978.24, 927.78, 847.19, 801.91, 736.94, 698.27, 662.63 cm^{-1}.

2-Methyl-5-*tert*-butyl-thiophenyl-2-*O*-acetyl-3-*O*-benzoyl-4,6-*O*-di-benzyl-β-D-mannopyranoside (18)

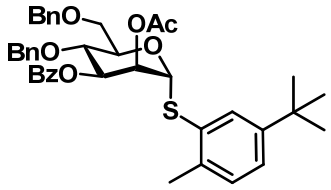

0.982 mmol of alcohol **17** (0.554 g) was reacted according to *O*-Acylation with acylchlorides (Method 11) using benzoyl chloride. Product **18** was obtained in 92% yield (0.901 mmol, 0.603 g) as colorless oil.

$\mathbf{R_f}$ = 0.4 (4:1, Hex:EA)

^{1}H-NMR (400 MHz, $CDCl_3$): δ = 8.07 – 7.97 (m, 2H, $H_{Ar.}$), 7.67 – 7.55 (m, 2H, $H_{Ar.}$), 7.45 (t, *J* = 7.7 Hz, 2H, $H_{Ar.}$), 7.40 – 7.28 (m, 6H, $H_{Ar.}$), 7.23 – 7.04 (m, 6H, $H_{Ar.}$), 5.68 – 5.64 (m, 2H, Gal-2, Gal-3), 5.52 (s, 1H, Gal-1), 4.73 (d, *J* = 12.2 Hz, 1H, -CH_2-), 4.70 (d, *J* = 11.0 Hz, 1H, -CH_2-), 4.55 (d, *J* = 10.8 Hz, 1H, -CH_2-), 4.50 (d, *J* = 12.2 Hz, 1H, -CH_2-), 4.45 (s, 1H, Gal-5), 4.29 (t, *J* = 9.4 Hz, 1H, Gal-4), 3.95 (dd, *J* = 11.0 Hz, 3.4 Hz, 1H, Gal-6), 3.68 (dd, *J* = 11.0 Hz, 1.6 Hz, 1H, Gal-6), 2.41 (s, 1H, Ar-CH_3-), 2.14 (s, 1H, -CH_3), 1.30 (s, 4H, -$C(CH_3)_3$) ppm.

^{13}C-NMR (101 MHz, $CDCl_3$): δ = 169.96 (C=O), 165.31 (C=O), 149.72 ($C_{Ar.}$), 137.95 ($C_{Ar.}$), 137.64 ($C_{Ar.}$), 136.82 ($C_{Ar.}$), 133.27 ($C_{Ar.}$), 132.27 ($C_{Ar.}$), 130.02 ($C_{Ar.}$), 129.79 ($C_{Ar.}$), 129.66 ($C_{Ar.}$), 129.61 ($C_{Ar.}$), 128.50 ($C_{Ar.}$), 128.36 ($C_{Ar.}$), 128.30 ($C_{Ar.}$), 128.03 ($C_{Ar.}$), 127.85 ($C_{Ar.}$), 127.75 ($C_{Ar.}$), 127.73 ($C_{Ar.}$), 125.04 ($C_{Ar.}$), 85.68 (Gal-1), 75.03 (-CH_2-), 73.65 (-CH_2-), 73.23 (Gal-4), 72.76 (Gal-5), 72.68 (Gal-2), 72.21 (Gal-3), 68.46 (Gal-6), 34.47 (-*C*$(CH_3)_3$), 31.33 (-C(*C*$H_3)_3$), 20.99 (-CH_3), 20.34 (Ar-CH_3) ppm.

ESI-MS: m/z M_{calcd} for $C_{40}H_{44}O_7S$ = 668.2808; M_{found} = 691.2682 $[M+Na]^+$

FTIR: 3066.80, 3033.45, 2963.60, 2867.70, 1749.67, 1727.11, 1603.17, 1586.54, 1488.77, 1453.15, 1373.05, 1315.75, 1265.00, 1225.39, 1177.49, 1158.82, 1091.68, 1070.79, 1051.62, 1026.66, 973.04, 935.22, 873.45, 854.02, 821.19, 803.25, 748.82, 711.09, 697.87, 667.71 cm^{-1}.

2-Methyl-5-*tert*-butyl-thiophenyl-2-*O*-acetyl-3,4-*O*-di-benzyl-6-*O*-*tert*-butyldiphenylsilyl-β-D-mannopyranoside (21)

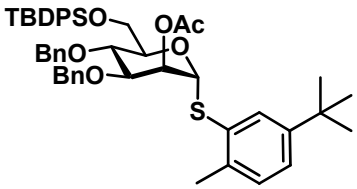

1.646 mmol of alcohol **20** (1.253 g) was reacted according to *O*-Acylation with acylchlorides (Method 11) using acetyl chloride. Product **21** was obtained in quantitative yield (1.646 mmol, 1.322 g) as colorless oil.

R_f = 0.6 (6:1, Hex:EA)

^{1}H-NMR (400 MHz, $CDCl_3$): δ = 7.68 – 7.65 (m, 4H, $H_{Ar.}$), 7.46 (d, *J* = 2.0 Hz, 1H, $H_{Ar.}$), 7.41 – 7.13 (m, 17H, $H_{Ar.}$), 7.11 (d, *J* = 8.0 Hz, 1H, $H_{Ar.}$), 5.64 (dd, *J* = 3.0, 1.7 Hz, 1H, Man-2), 5.43 (d, *J* = 1.7 Hz, 1H, Man-1), 4.97 (d, *J* = 10.7 Hz, 1H, -CH_2-), 4.77 (d, *J* = 11.2 Hz, 1H, -CH_2-), 4.68 (d, *J* = 10.7 Hz, 1H, -CH_2-), 4.61 (d, *J* = 11.2 Hz, 1H, -CH_2-), 4.31 – 4.26 (m, 1H, Man-4), 4.17 – 4.11 (m, 2H, 5-H, Man-6), 4.04 (dd, *J* = 9.4, 3.0 Hz, 1H, Man-3), 3.88 – 3.83 (m, 1H, Man-6), 2.35 (s, 3H, -CH_3), 2.14 (s, 3H, -CH_3), 1.20 (s, 9H, -C(-CH_3)$_3$), 1.06 (s, 9H, -C(-CH_3)$_3$) ppm.

^{13}C-NMR (101 MHz, $CDCl_3$): δ = 170.38 (1C, C=O_{Acetyl}), 149.65 (C_{ar}), 138.51 (C_{ar}), 137.75 (C_{ar}), 136.84 (C_{ar}), 135.84 (C_{ar}), 135.49 (C_{ar}), 133.86 (C_{ar}), 132.97 (C_{ar}), 132.73 (C_{ar}), 129.95 (C_{ar}), 129.89 (C_{ar}), 129.55 (C_{ar}), 129.50 (C_{ar}), 128.44 (C_{ar}), 128.34 (C_{ar}), 128.21 (C_{ar}), 127.84 (C_{ar}), 127.81 (C_{ar}), 127.63 (C_{ar}), 127.58 (C_{ar}), 127.46 (C_{ar}), 125.00 (C_{ar}), 86.24 (Man-1), 78.66 (Man-3), 75.41 (-CH_2-), 73.99 (Man-4), 73.90 (Man-5), 71.96 (-CH_2-), 71.00 (Man-2), 62.56 (Man-6), 34.36 (-C(-CH_3)$_3$), 31.26 (-CH_3), 26.77 (-C(-CH_3)$_3$), 21.09 (-CH_3), 20.38 (-CH_3), 19.42 (-C(-CH_3)$_3$) ppm.

ESI-MS: m/z M_{calcd} for $C_{49}H_{58}O_6SSi$ = 802.3723; M_{found} = 825.3582 $[M+Na]^+$

Polarimeter: $[\alpha]_D^{20}$ = +50.31 (c = 1.00 g/L in $CHCl_3$)

FTIR: 3033.38, 2962.35, 2933.07, 2859.87, 1745.52, 1590.35, 1487.92, 1473.34, 1455.56, 1428.96, 1370.93, 1316.82, 1262.42, 1231.08, 1154.50, 1096.81, 1058.39, 1044.72, 1021.01, 978.18, 938.46, 893.09, 866.93, 822.93, 739.00, 697.82, 665.96 cm^{-1}.

Allyl-2-*O*-acetyl-3,6-*O*-di-benzyl-(2-*O*-benzoyl-3,4,6-*O*-tri-benzyl-D-galactopyranosyl-β1→3)-α-D-mannopyranoside (22)

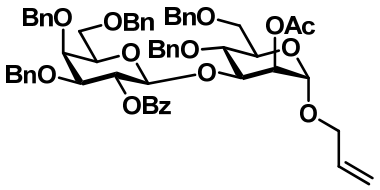

0.339 mmol of thiodonor **5a/5b** (0.203 g) and 0.226 mmol of glycosylacceptor **14** (0.100 g) were dissolved in DCM and reacted according to glycosylation with thiodonor (Method 17) using TMSOTf at 0°C. Product **22** was obtained in quantitative yield (0.226 mmol, 0.221 g) as colorless oil.

R_f = 0.4 (3:1, Hex:EA)

^{1}H-NMR (400 MHz, $CDCl_3$): δ = 8.10 – 8.06 (m, 2H, $H_{Ar.}$), 7.65 – 7.59 (m, 1H, $H_{Ar.}$), 7.50 (t, *J* = 7.7 Hz, 2H, $H_{Ar.}$), 7.42 – 7.12 (m, 23H), 7.07 (t, *J* = 7.4 Hz, 2H), 5.89 – 5.78 (m, 1H, Allyl-1), 5.74 (dd, *J* = 10.1 Hz, 7.8 Hz, 1H, Gal-2), 5.24 (dd, *J* = 17.2 Hz, 1.5 Hz, 1H, Allyl-3), 5.16 (dd, *J* = 10.3 Hz, 1.3 Hz, 1H, Allyl-3), 5.12 – 5.04 (m, 2H, Man-2, -CH_2-), 4.81 (d, *J* = 1.7 Hz, 1H, Man-1), 4.71 – 4.62 (m, 4H, Gal-1, -CH_2-, -CH_2-, -CH_2-), 4.52 (d, *J* = 12.2 Hz, 2H, -CH_2-, -CH_2-), 4.45 (d, *J* = 11.7 Hz, 1H, -CH_2-), 4.40 – 4.35 (m, 3H, Man-3, -CH_2- -CH_2-), 4.14 – 4.08 (m, 2H, Gal-4, Allyl-1), 3.94 (dd, *J* = 12.8 Hz, 6.4 Hz, 1H, Allyl-1), 3.86 – 3.77 (m, 2H, Man-4, Man-5,), 3.77 – 3.65 (m, 5H, Gal-3, Gal-5, Gal-6, Gal-6, Man-6), 3.54 (dd, *J* = 8.1 Hz, 4.3 Hz, 1H, Man-6), 1.38 (s, 1H, -CH_3) ppm.

^{13}C-NMR (101 MHz, $CDCl_3$): δ = 170.34 ($C{=}O_{Acetyl}$), 165.19 ($C{=}O_{Benzoyl}$), 138.78 ($C_{Ar.}$), 138.34 ($C_{Ar.}$), 138.17 ($C_{Ar.}$), 137.87 ($C_{Ar.}$), 137.58 ($C_{Ar.}$), 133.39 (Allyl-2), 133.13 ($C_{Ar.}$), 130.08 ($C_{Ar.}$), 129.90 ($C_{Ar.}$), 128.86 ($C_{Ar.}$), 128.45 ($C_{Ar.}$), 128.35 ($C_{Ar.}$), 128.33 ($C_{Ar.}$), 128.26 ($C_{Ar.}$), 128.06 ($C_{Ar.}$), 128.03 ($C_{Ar.}$), 127.97 ($C_{Ar.}$), 127.91 ($C_{Ar.}$), 127.83 ($C_{Ar.}$), 127.70 ($C_{Ar.}$), 127.62 ($C_{Ar.}$), 127.47 ($C_{Ar.}$), 127.40 ($C_{Ar.}$), 117.98 (Allyl-3), 98.27 (Gal-1), 96.34 (Man-1), 79.72 (Gal-3), 75.25 (-CH_2-), 75.16 (Man-3), 74.81 (-CH_2-), 73.64 (-CH_2-), 73.49 (Gal-5), 73.43 (-CH_2-), 72.79 (Gal-4), 72.74 (Man-4), 72.05 (Gal-2), 71.57 (-CH_2-), 71.23 (Man-5), 68.84 (Man-2), 68.71 (Gal-6), 68.13 (Allyl-1), 68.07 (Man-6), 20.07 (-CH_3) ppm.

ESI-MS: m/z M_{calcd} for $C_{59}H_{62}O_{13}$ = 978.4190; M_{found} = 1001.4110 $[M+Na]^+$

Polarimeter: $[\alpha]_D^{20}$ = +12.72 (c = 1.00 g/L in $CHCl_3$)

FTIR: 3065.94, 3033.00, 2925.00, 2867.58, 1733.71, 1603.96, 1586.21, 1497.58, 1454.59, 1370.51, 1315.50, 1268.77, 1236.76, 1096.65, 1069.93, 1028.50, 999.35, 933.37, 845.31, 805.05, 737.51, 698.80, 664.67 cm^{-1}.

Allyl-3,6-*O*-di-benzyl-(2-*O*-benzoyl-3,4,6-*O*-tri-benzyl-D-galactopyranosyl-β1→3)-α-D-mannopyranoside (23)

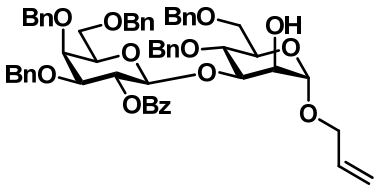

0.245 mmol of disaccharide **22** (0.240 g) was reacted according to acid mediated *O*-Acetyl removal (Method 5). Product **23** was obtained in 67% yield brsm (0.132 mmol, 0.124 g) as colorless oil.

R_f = 0.4 (2:1, Hex:EA)

^{1}H-NMR (400 MHz, $CDCl_3$): δ = 8.04 (d, *J* = 7.0 Hz, 2H, $H_{Ar.}$), 7.63 – 7.59 (m, 1H, $H_{Ar.}$), 7.49 – 7.45 (m, 2H, $H_{Ar.}$), 7.40 – 7.13 (m, 25H), 5.75 (m, 1H), 5.86 – 5.76 (m, 1H, Allyl-2), 5.71 (dd, *J* = 10.0 Hz, 7.9 Hz, 1H, Gal-2), 5.20 (dd, *J* = 17.2 Hz, 1.4 Hz, 1H, Allyl-3), 5.16 – 5.12 (m, 1H, Allyl-3), 5.06 (d, *J* = 11.5 Hz, 1H, -CH_2-), 4.98 (d, *J* = 10.4 Hz, 1H, -CH_2-), 4.80 (d, *J* = 1.4 Hz, 1H, Man-1), 4.72 – 4.61 (m, 4H, Gal-1, -CH_2-, -CH_2-, -CH_2-), 4.52 (dd, *J* = 12.3 Hz, 6.5 Hz, 2H, -CH_2-, -CH_2-), 4.41 (d, *J* = 10.4 Hz, 1H, -CH_2-), 4.41 – 4.31 (m, 2H, -CH_2-, -CH_2-), 4.14 – 4.08 (m, 3H, Gal-4, Allyl-1, Man-3), 3.91 (dd, *J* = 12.8 Hz, 6.2 Hz, 1H, Allyl-1), 3.82 – 3.73 (m, 3H, Man-2, Man-4, Man-5), 3.73 – 3.61 (m, 5H, Man-6, Man-6, Gal-3, Gal-5, Gal-6), 3.43 (dd, *J* = 8.0 Hz, 4.2 Hz, 1H, Gal-6) ppm.

^{13}C-NMR (101 MHz, $CDCl_3$): δ = 165.79 (C=O), 138.64 ($C_{Ar.}$), 138.51 ($C_{Ar.}$), 138.28 ($C_{Ar.}$), 137.76 ($C_{Ar.}$), 137.53 ($C_{Ar.}$), 133.67 (Allyl-2), 133.30 ($C_{Ar.}$), 129.81 ($C_{Ar.}$), 129.67 ($C_{Ar.}$), 128.52 ($C_{Ar.}$), 128.47 ($C_{Ar.}$), 128.36 ($C_{Ar.}$), 128.31 ($C_{Ar.}$), 128.25 ($C_{Ar.}$), 128.07 ($C_{Ar.}$), 128.00 ($C_{Ar.}$), 127.94 ($C_{Ar.}$), 127.87 ($C_{Ar.}$), 127.83 ($C_{Ar.}$), 127.75 ($C_{Ar.}$), 127.73 ($C_{Ar.}$), 127.52 ($C_{Ar.}$), 127.34 ($C_{Ar.}$), 117.60 (Allyl-3), 100.33 (Gal-1), 98.02 (Man-1), 80.01 (Man-3), 79.61 (Gal-3), 74.86 (-CH_2-), 74.73 (-CH_2-), 73.59 (Gal-5), 73.59 (-CH_2-), 73.35 (-CH_2-), 73.08 (Man-4), 72.67 (Gal-2), 72.47 (Gal-4), 71.52 (-CH_2-), 71.12 (Man-5), 68.88 (Man-6), 68.84 (Man-2), 67.93 (Gal-6), 67.85 (Allyl-1) ppm.

ESI-MS: m/z M_{calcd} for $C_{57}H_{60}O_{12}$ = 936.4085; M_{found} = 959.3939 $[M+Na]^+$

Polarimeter: $[\alpha]_D^{20}$ = +39.97 (c = 1.00 g/L in $CHCl_3$)

FTIR: 3570.32, 3065.64, 3032.37, 2924.53, 2866.53, 2371.20, 2327.03, 1727.60, 1603.68, 1586.11, 1497.41, 1454.10, 1365.39, 1315.66, 1267.09, 1210.20, 1094.82, 1060.31, 1027.76, 992.34, 914.25, 843.99, 804.50, 734.69, 710.82, 696.08, 665.69 cm^{-1}.

Allyl-4,6-*O*-di-benzyl-(acetyl-3,4-*O*-di-benzyl-6-*O*-tri-*iso*-propylsilyl-D-mannopyranosyl-α1→2)-(2-*O*-benzoyl-3,4,6-*O*-tri-benzyl-D-galactopyranosyl-β1→3)-α-D-mannopyranoside (26)

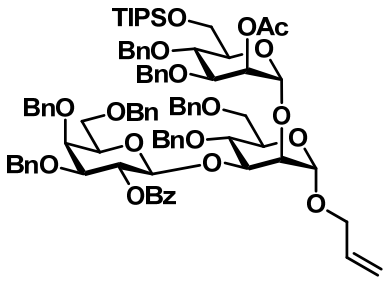

1.226 mmol of imidatedonor **24** (0.862 g) and 0.245 mmol of glycosylacceptor **23** (0.230 g) were dissolved in DCM and reacted according to glycosylation with imidate (Method 16) using TMSOTf at 0°C. Product **26** was obtained in 95% yield (0.232 mmol, 0.344 g) as colorless oil.

$\mathbf{R_f}$ = 0.6 (2:1, Hex:EA)

^{1}H-NMR (400 MHz, $CDCl_3$): δ = 8.07 – 8.05 (m, 2H, $H_{Ar.}$), 7.50 (t, *J* = 7.3 Hz, 1H, $H_{Ar.}$), 7.42 – 7.07 (m, 37H, $H_{Ar.}$), 5.78 – 5.68 (m, 2H, Allyl-2, Gal-2), 5.31 (s, 1H, Man'-2), 5.15 (d, *J* = 17.2 Hz, 1H, Allyl-3), 5.08 (d, *J* = 10.2 Hz, 1H, Allyl-3), 5.02 (d, *J* = 11.4 Hz, 1H, -CH_2-), 4.88 – 4.79 (m, 3H, Man-1, Man'-1, -CH_2-), 4.76 (d, *J* = 7.7 Hz, 1H, Gal-1), 4.66 – 4.40 (m, 9H, -CH_2-, -CH_2-, -CH_2-, -CH_2-, -CH_2-), 4.36 (d, *J* = 11.7 Hz, 1H, -CH_2-), 4.32 – 4.23 (m, 1H, -CH_2-), 4.20 (d, *J* = 10.9 Hz, 1H, -CH_2-), 4.07 - 4.03 (m, 2H, Allyl-1, Gal-4), 3.93 – 3.57 (m, 15H, Allyl-1, Man-2, Man-3, Man-4, Man-5, Man-6, Man-6, Gal-3, Gal-5, Gal-6, Man'-3, Man'-4, Man'-5, Man'-6, Man'-6), 3.38 (s, 1H, Gal-6), 1.94 (s, 3H, -CH_3), 1.12 – 1.03 (m, 21H, (-CH(-CH_3)$_2$)$_3$) ppm.

^{13}C-NMR (101 MHz, $CDCl_3$): δ = 169.88 ($C{=}O_{Acetyl}$), 165.27 ($C{=}O_{Benzoyl}$), 138.82 ($C_{Ar.}$), 138.77 ($C_{Ar.}$), 138.60 ($C_{Ar.}$), 138.51 ($C_{Ar.}$), 138.18 ($C_{Ar.}$), 137.90 ($C_{Ar.}$), 137.49 ($C_{Ar.}$), 133.81 (Allyl-2), 132.81 ($C_{Ar.}$), 130.22 ($C_{Ar.}$), 130.01 ($C_{Ar.}$), 128.40 ($C_{Ar.}$), 128.27 ($C_{Ar.}$), 128.24 ($C_{Ar.}$), 128.20 ($C_{Ar.}$), 128.11 ($C_{Ar.}$), 128.06 ($C_{Ar.}$), 127.96 ($C_{Ar.}$), 127.83 ($C_{Ar.}$), 127.77 ($C_{Ar.}$), 127.72 ($C_{Ar.}$), 127.59 ($C_{Ar.}$), 127.50 ($C_{Ar.}$), 127.48 ($C_{Ar.}$), 127.45 ($C_{Ar.}$), 127.41 ($C_{Ar.}$), 127.32 ($C_{Ar.}$), 127.20 ($C_{Ar.}$), 117.14 (Allyl-3), 100.34 (Gal-1), 98.82 (Man'-1), 97.34 (Man1-1), 80.27 (Gal-3), 78.06 (Man'-3), 75.52 (Man1-2), 74.99 (-CH_2-), 74.56 (-CH_2-), 73.78 (Man1-3), 73.76 (Man1-5), 73.51 (Man'-4), 73.16 (Gal-5), 73.14 (Man1-4), 72.50 (Gal-2), 72.48 (Gal-4), 72.10 (Man'-5), 71.66 (-CH_2-), 71.55 (-CH_2-), 69.24 (Man1-6), 68.71 (Man'-2), 68.24 (Gal-6), 67.79 (Allyl-1), 62.59 (Man'-6), 20.92 (-CH_3), 18.08 ((-CH(-CH_3)$_2$)$_3$), 18.01 ((-CH(-CH_3)$_2$)$_3$), 12.03 (-CH_3) ppm.

ESI-MS: m/z M_{calcd} for $C_{88}H_{104}O_{18}Si$ = 1476.6992; M_{found} = 1500.6911 $[M+Na]^+$

Polarimeter: $[\alpha]_D^{20}$ = +19.81 (c = 1.00 g/L in $CHCl_3$)

FTIR: 3993.80, 3965.16, 3934.91, 3898.74, 3875.26, 3835.29, 3791.96, 3741.58, 3707.53, 3641.82, 3623.67, 3582.96, 3555.95, 3479.76, 3457.45, 3353.97, 3301.81, 3178.36, 3090.97, 3066.09, 3032.77, 3009.21, 2941.81, 2892.77, 2867.19, 2729.76, 2570.98, 2443.43, 2373.49, 2360.38, 2335.89, 2316.40, 2272.90, 2258.64, 2229.47, 2207.74, 2196.91, 2176.12, 2166.21, 2157.08, 2148.97, 2124.11, 2095.18, 2079.31, 2064.93, 2044.98, 2030.56, 2019.56, 2010.74, 1995.82, 1955.52, 1947.41, 1874.94, 1812.46, 1733.31, 1649.81, 1603.66, 1587.38, 1497.79, 1455.16, 1368.12, 1329.76, 1316.02, 1268.41, 1239.33, 1210.55, 1097.36, 1028.99, 1012.68, 917.19, 883.74, 824.72, 736.40, 697.94 cm^{-1}.

Allyl-4,6-*O*-di-benzyl-(3,4-*O*-di-benzyl-D-mannopyranosyl-α1→2)-(2-*O*-benzoyl-3,4,6-*O*-tri-benzyl-D-galactopyranosyl-β1→3)-α-D-mannopyranoside (27)

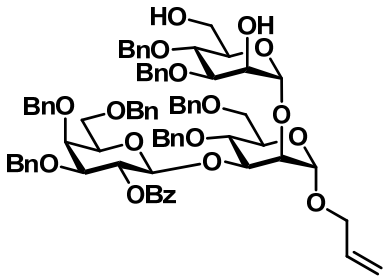

0.148 mmol of trisaccharide **26** (0.219 g) was reacted according to acid mediated *O*-Acetyl removal (Method 5). Product **27** was obtained in 88% yield (0.130 mmol, 0.166 g) as colorless oil.

R_f = 0.35 (2:1, Hex:EA)

^{1}H-NMR (400 MHz, $CDCl_3$): δ = 8.01 – 7.94 (m, 2H, $H_{Ar.}$), 7.53 – 7.00 (m, 38H, $H_{Ar.}$), 5.76 – 5.58 (m, 2H, Allyl-2, Gal-2), 5.13 – 5.07 (m, 1H, Allyl-3), 5.04 (dd, *J* = 10.3 Hz, 1.6 Hz, 1H, Allyl-3), 4.97 – 4.93 (m, 2H, -CH_2-), 4.77 (d, *J* = 2.0 Hz, 1H, Man-1), 4.72 (d, *J* = 11.1 Hz, 1H, -CH_2-), 4.64 – 4.28 (m, 12H, Gal-1, Man‘-1), 4.27 – 4.15 (m, 2H), 4.08 (dd, *J* = 9.0 Hz, 2.9 Hz, 1H), 4.01 – 3.94 (m, 2H), 3.83 – 3.75 (m, 1H), 3.68 – 3.43 (m, 15H), 3.26 – 3.18 (m, 1H) ppm.

^{13}C-NMR (101 MHz, $CDCl_3$): δ = 165.44 (C=O), 138.76 ($C_{Ar.}$), 138.66 ($C_{Ar.}$), 138.47 ($C_{Ar.}$), 138.42 ($C_{Ar.}$), 138.03 ($C_{Ar.}$), 137.84 ($C_{Ar.}$), 137.43 ($C_{Ar.}$), 133.67 (Allyl-2), 133.34 ($C_{Ar.}$), 129.98 ($C_{Ar.}$), 129.92 ($C_{Ar.}$), 128.61 ($C_{Ar.}$), 128.54 ($C_{Ar.}$), 128.48 ($C_{Ar.}$), 128.44 ($C_{Ar.}$), 128.40 ($C_{Ar.}$), 128.32 ($C_{Ar.}$), 128.30 ($C_{Ar.}$), 128.28 ($C_{Ar.}$), 128.26 ($C_{Ar.}$), 128.12 ($C_{Ar.}$), 128.07 ($C_{Ar.}$), 128.00 ($C_{Ar.}$), 127.92 ($C_{Ar.}$), 127.90 ($C_{Ar.}$), 127.85 ($C_{Ar.}$), 127.76 ($C_{Ar.}$), 127.71 ($C_{Ar.}$), 127.62 ($C_{Ar.}$), 127.55 ($C_{Ar.}$), 127.51 ($C_{Ar.}$), 127.39 ($C_{Ar.}$), 127.25 ($C_{Ar.}$), 117.62 (Allyl-3), 101.04 (Gal-1), 100.89 (Man’-1), 97.29 (Man-1), 79.78, 79.44, 79.28, 77.36, 77.24, 77.04, 76.72,

76.50, 75.01, 74.93, 74.75, 73.98, 73.52, 73.48, 73.18, 72.65, 72.33, 72.06, 71.96, 71.56, 71.34, 69.00, 67.98, 67.91, 67.83, 62.05 ppm.

ESI-MS: m/z M_{calcd} for $C_{77}H_{82}O_{17}$ = 1278.5552; M_{found} = 1301.6082 $[M+Na]^+$

Allyl-4,6-*O*-di-benzyl-(3,4-*O*-di-benzyl-6-*O*-tri-*iso*-propylsilyl-D-mannopyranosyl-α1→2)-(2-*O*-benzoyl-3,4,6-*O*-tri-benzyl-D-galactopyranosyl-β1→3)-α-D-mannopyranoside (28)

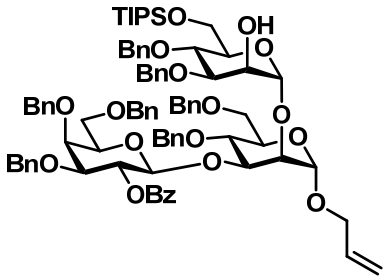

0.596 mmol of diol **27** (0.762 g) was reacted according to TBDPS or TIPS installation (Method 6) at 80°C. Product **28** was obtained in 96% yield (0.571 mmol, 0.820 g) as colorless oil.

R_f = 0.5 (3:1, Hex:EA)

^{1}H-NMR (400 MHz, $CDCl_3$): δ = 8.14 (d, *J* = 7.6 Hz, 2H, $H_{Ar.}$), 7.60 (t, *J* = 7.3 Hz, 1H, $H_{Ar.}$), 7.51 – 7.13 (m, 37H, $H_{Ar.}$), 5.83 (ddd, *J* = 17.8 Hz, 10.4 Hz, 6.5 Hz, 2H, Allyl-2, Gal-2), 5.23 (d, *J* = 17.2 Hz, 1H, Allyl-3), 5.16 (d, *J* = 10.4 Hz, 1H, Allyl-3), 5.12 – 5.08 (m, 2H, -CH_2-, -CH_2-), 4.95 (s, 1H, Man-1), 4.87 (d, *J* = 11.0 Hz, 1H, -CH_2-), 4.76 (d, *J* = 7.8 Hz, 1H, Gal-1), 4.73 – 4.62 (m, 5H, Man'-1, -CH_2-, -CH_2-, -CH_2-, -CH_2-), 4.58 – 4.51 (m, 2H, -CH_2-, -CH_2-), 4.51 – 4.46 (m, 2H, -CH_2-, -CH_2-), 4.46 – 4.41 (m, 2H, -CH_2-,-CH_2-), 4.35 (d, *J* = 11.8 Hz, 1H, -CH_2-), 4.32 (d, *J* = 5.2 Hz, 1H, Man-3), 4.17 – 4.10 (m, 2H, Allyl-1, Gal-4), 3.95 – 3.65 (m, 15H, Allyl-1, Man-2, Man-4, Man-5, Man-6, Man-6, Gal-3, Gal-5, Gal-6, Man'-2, Man'-3, Man'-4, Man'-5, Man'-6, Man'-6), 3.47 (dd, *J* = 7.2 Hz, 3.2 Hz, 1H, Gal-6), 1.14 – 1.06 (m, 21H, (-CH(-CH_3)$_2$)$_3$) ppm.

^{13}C-NMR (101 MHz, $CDCl_3$): δ = 165.38 (C=O), 138.82 ($C_{Ar.}$), 138.81 ($C_{Ar.}$), 138.75 ($C_{Ar.}$), 138.69 ($C_{Ar.}$), 138.22 ($C_{Ar.}$), 137.94 ($C_{Ar.}$), 137.52 ($C_{Ar.}$), 133.93 (Allyl-2), 133.25 ($C_{Ar.}$), 130.06 ($C_{Ar.}$), 129.92 ($C_{Ar.}$), 128.56 ($C_{Ar.}$), 128.47 ($C_{Ar.}$), 128.40 ($C_{Ar.}$), 128.35 ($C_{Ar.}$), 128.33 ($C_{Ar.}$), 128.29 ($C_{Ar.}$), 128.27 ($C_{Ar.}$), 128.11 ($C_{Ar.}$), 128.08 ($C_{Ar.}$), 128.05 ($C_{Ar.}$), 127.94 ($C_{Ar.}$), 127.91 ($C_{Ar.}$), 127.85 ($C_{Ar.}$), 127.78 ($C_{Ar.}$), 127.73 ($C_{Ar.}$), 127.62 ($C_{Ar.}$), 127.55 ($C_{Ar.}$), 127.47 ($C_{Ar.}$), 127.31 ($C_{Ar.}$), 127.29 ($C_{Ar.}$), 117.25 (Allyl-3), 101.64 (Man'-1), 99.70 (Gal-1), 97.60 (Man-1), 79.99 (Gal-3), 79.45 (Man'-3), 77.92 (Man-3), 76.48 (Man-2), 75.04 (-CH_2-), 75.00 (-CH_2-), 74.79 (-CH_2-), 73.97 (Man'-4), 73.60 (Gal-5), 73.47 (Man-4), 73.23 (Man'-5), 73.14

(-CH_2-), 72.61 (Gal-4), 72.55 (Gal-2), 72.09 (Man-5), 71.54 (-CH_2-), 71.45 (-CH_2-), 69.36 (Man-6), 68.11 (Gal-6), 67.90 (Man'-2), 67.86 (Allyl-1), 62.96 (Man'-6), 18.16 (-CH(-CH_3)$_2$)$_3$) 18.11 (-CH(-CH_3)$_2$)$_3$), 12.04 (-CH_3) ppm.

ESI-MS: m/z M_{calcd} for $C_{86}H_{102}O_{17}Si$ = 1434.6886; M_{found} = 1457.6771 $[M+Na]^+$

Polarimeter: $[\alpha]_D^{20}$ = +16.98 (c = 1.00 g/L in $CHCl_3$)

FTIR: 3065.54, 3032.64, 2926.91, 2867.05, 1732.87, 1604.35, 1497.74, 1455.02, 1365.53, 1268.22, 1210.23, 1099.51, 1069.56, 1029.22, 998.05, 916.96, 884.00, 804.78, 736.15, 698.01 cm^{-1}.

Allyl-4,6-*O*-di-benzyl-(3,4-*O*-di-benzyl-6-*O*-tri-*iso*-propylsilyl-(2,3,4,6-*O*-tetra-benzyl-D-galactopyranosyl-α1→2)-D-mannopyranosyl-α1→2)-(2-*O*-benzoyl-3,4,6-*O*-tri-benzyl-D-galactopyranosyl-β1→3)-α-D-mannopyranoside (29)

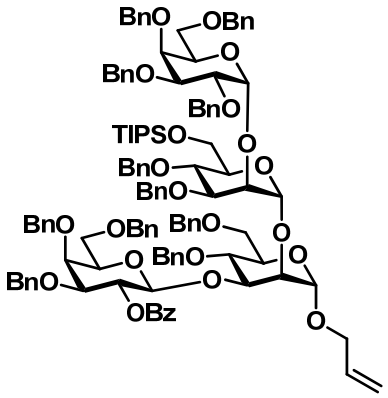

0.020 mmol of thiodonor **8** (0.011 g) and 0.014 mmol of glycosylacceptor **28** (0.020 g) were dissolved in a 1:1 mixture of DCM and ether and reacted according to glycosylation with thiodonor (Method 17) using TMSOTf at -11°C. Product **29** was obtained in 81% yield (0.011 mmol, 0.022 g) as colorless oil.

$\mathbf{R_f}$ = 0.5 (6:1, Hex:EA)

^{1}H-NMR (400 MHz, $CDCl_3$): δ = 8.05 (d, *J* = 7.8 Hz, 2H), 7.54 – 6.98 (m, 58H), 5.80 – 5.53 (m, 2H, Allyl-2, βGal-2), 5.32 (s, 1H, Man-1), 5.11 – 3.42 (m, 53H), 1.04 (s, 21H, (-CH(-CH_3)$_2$)$_3$) ppm.

^{13}C-NMR (101 MHz, $CDCl_3$): δ = 165.34 (C=O), 139.37 ($C_{Ar.}$), 139.34 ($C_{Ar.}$), 139.18 ($C_{Ar.}$), 139.13 ($C_{Ar.}$), 139.04 ($C_{Ar.}$), 138.85 ($C_{Ar.}$), 138.71 ($C_{Ar.}$), 138.67 ($C_{Ar.}$), 138.62 ($C_{Ar.}$), 138.55 ($C_{Ar.}$), 138.50 ($C_{Ar.}$), 138.45 ($C_{Ar.}$), 138.19 ($C_{Ar.}$), 137.81 ($C_{Ar.}$), 137.56 ($C_{Ar.}$), 134.11 ($C_{Ar.}$), 133.93 (Ally-3), 132.79 ($C_{Ar.}$), 130.29 ($C_{Ar.}$), 130.00 ($C_{Ar.}$), 129.76 ($C_{Ar.}$), 129.07 ($C_{Ar.}$), 129.00 ($C_{Ar.}$), 128.59 ($C_{Ar.}$), 128.39 ($C_{Ar.}$), 128.38 ($C_{Ar.}$), 128.35 ($C_{Ar.}$), 128.32 ($C_{Ar.}$), 128.29 ($C_{Ar.}$), 128.26 ($C_{Ar.}$), 128.23 ($C_{Ar.}$), 128.18 ($C_{Ar.}$), 128.11 ($C_{Ar.}$), 128.09 ($C_{Ar.}$), 128.06 ($C_{Ar.}$), 128.02 ($C_{Ar.}$), 127.98 ($C_{Ar.}$), 127.96 ($C_{Ar.}$), 127.92 ($C_{Ar.}$), 127.89 ($C_{Ar.}$), 127.82 ($C_{Ar.}$), 127.79

($C_{Ar.}$), 127.75 ($C_{Ar.}$), 127.70 ($C_{Ar.}$), 127.66 ($C_{Ar.}$), 127.61 ($C_{Ar.}$), 127.47 ($C_{Ar.}$), 127.44 ($C_{Ar.}$), 127.37 ($C_{Ar.}$), 127.34 ($C_{Ar.}$), 127.30 ($C_{Ar.}$), 127.28 ($C_{Ar.}$), 127.21 ($C_{Ar.}$), 127.14 ($C_{Ar.}$), 127.11 ($C_{Ar.}$), 127.01 ($C_{Ar.}$), 126.72 ($C_{Ar.}$), 126.49 ($C_{Ar.}$), 116.69 ($C_{Ar.}$), 116.25 ($C_{Ar.}$), 102.33 (βGal-1), 97.97 (Man-1), 97.47 (Man'-1), 93.56 (α-Gal-1), 80.25, 79.70, 78.68, 78.52, 77.37, 77.26, 77.05, 76.74, 76.51, 76.00, 75.69, 74.97, 74.82, 74.68, 74.61, 73.70, 73.47, 73.34, 73.15, 73.09, 72.98, 72.75, 72.46, 72.25, 72.17, 71.40, 71.02, 69.69, 69.25, 69.06, 68.82, 67.92, 67.73, 62.80, 60.42, 18.13, 18.05, 18.03 ppm.

ESI-MS: m/z M_{calcd} for $C_{120}H_{136}O_{22}Si$ = 1956.9293; M_{found} = 1979.9196 $[M+Na]^+$

FTIR: 3065.16, 3032.45, 2924.09, 2866.75, 1949.18, 1730.38, 1604.59, 1497.65, 1454.65, 1363.87, 1314.41, 1268.23, 1209.19, 1098.12, 1062.79, 1028.74, 997.39, 914.30, 883.82, 842.53, 734.99, 697.11 cm^{-1}.

Allyl-4,6-*O*-di-benzyl-(3,4-*O*-di-benzyl-6-*O*-tri-*iso*-propylsilyl-(2,3,4,6-*O*-tetra-benzyl-D-galactopyranosyl-α1→2)-D-mannopyranosyl-α1→2)-(2,3,4,6-*O*-tetra-benzyl-D-galactopyranosyl-β1→3)-α-D-mannopyranoside (30)

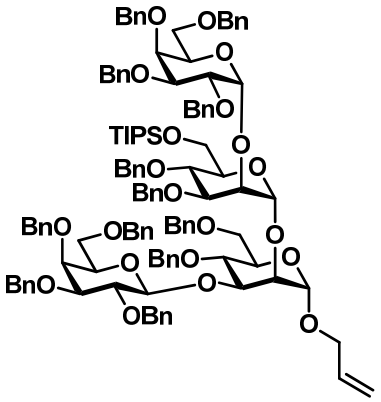

0.038 mmol of tetrasaccharide **29** (0.071 g) was reacted according to NaOMe mediated *O*-Acyl removal (Method 3) at 45°C and Williamson-ether formation (Method 10) using benzyl bromide. Product **30** was obtained in 44% yield over two steps (0.017 mmol, 0.033 g) as colorless oil.

R_f = 0.55 (6:1, Hex:EA)

^{1}H-NMR (400 MHz, $CDCl_3$): δ = 7.43 – 6.93 (m, 60H, $H_{Ar.}$), 5.86 (ddd, *J* = 17.0 Hz, 10.9 Hz, 5.7 Hz, 1H, Allyl-2), 5.57 (d, *J* = 3.3 Hz, 1H, Man-1), 5.41 – 3.29 (m, 55H), 1.29 (s, 21H, $(-CH(-CH_3)_2)_3$) ppm.

^{13}C-NMR (101 MHz, $CDCl_3$): δ = 139.13 ($C_{Ar.}$), 138.96 ($C_{Ar.}$), 138.89 ($C_{Ar.}$), 138.83 ($C_{Ar.}$), 138.75 ($C_{Ar.}$), 138.66 ($C_{Ar.}$), 138.53 ($C_{Ar.}$), 133.96 (Allyl-2), 130.00 ($C_{Ar.}$), 128.92 ($C_{Ar.}$), 128.75 ($C_{Ar.}$), 128.40 ($C_{Ar.}$), 128.40 ($C_{Ar.}$), 128.29 ($C_{Ar.}$), 128.17 ($C_{Ar.}$), 127.94 ($C_{Ar.}$), 127.70

($C_{Ar.}$), 127.67 ($C_{Ar.}$), 127.63 ($C_{Ar.}$), 127.32 ($C_{Ar.}$), 127.22 ($C_{Ar.}$), 127.02 ($C_{Ar.}$), 125.98 ($C_{Ar.}$), 124.80 ($C_{Ar.}$), 124.48 ($C_{Ar.}$), 124.01 ($C_{Ar.}$), 119.09 ($C_{Ar.}$), 117.20 (Allyl-3), 100.30 (βGal-1), 98.13 (αGal-1), 97.39 (Man'-1), 93.55 (Man-1), 77.35, 77.25, 77.04, 76.72, 76.01, 75.22, 75.00, 74.81, 74.65, 74.36, 73.39, 73.28, 73.13, 72.73, 72.27, 71.73, 71.58, 71.30, 70.97, 70.69, 70.45, 69.61, 69.39, 68.96, 68.75, 68.50, 68.24, 67.88, 18.14 ((-CH(-CH_3)$_2$)$_3$) ppm.

ESI-MS: m/z M_{calcd} for $C_{120}H_{138}O_{21}Si$ = 1942.9500; M_{found} = 1965.9371 $[M+Na]^+$

FTIR: 3064.83, 3031.39, 2922.32, 2866.43, 1605.10, 1497.17, 1454.72, 1363.81, 1209.08, 1093.48, 1057.90, 1028.82, 915.76, 883.82, 734.36, 696.75 cm^{-1}.

Allyl-2-*O*-acetyl-3,6-*O*-di-benzyl-(2,3,4,6-*O*-tetra-benzyl-D-galactopyranosyl-β1→3)-α-D-mannopyranoside (31)

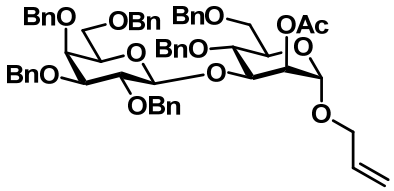

0.169 mmol of thiodonor **8** (0.099 g) and 0.113 mmol of glycosylacceptor **14** (0.050 g) were dissolved in DCM and reacted according to glycosylation with thiodonor (Method 17) using TMSOTf at 0°C. Product **31** was obtained in 66% yield (0.075 mmol, 0.072 g) as colorless oil.

$\mathbf{R_f}$ = 0.35 (6:1, Hex:EA)

^{1}H-NMR (400 MHz, $CDCl_3$): δ = 7.37 – 7.03 (m, 30H, $H_{Ar.}$), 5.84 (ddt, *J* = 16.4 Hz, 11.0 Hz, 5.7 Hz, 1H, Allyl-2), 5.24 (dd, *J* = 17.3 Hz, 1.7 Hz, 1H, Allyl-3), 5.20 – 5.14 (m, 2H, Gal-2, Allyl-3), 5.12 (d, *J* = 3.5 Hz, Gal-1), 5.08 (d, *J* = 11.1 Hz, 1H, -CH_2-), 4.92 – 4.89 (m, 2H, Man-1, -CH_2-), 4.76 (d, *J* = 5.4 Hz, 2H, , -CH_2-), 4.70 (d, *J* = 12.4 Hz, 2H, -CH_2-), 4.65 – 4.59 (m, 2H, -CH_2-), 4.54 (d, *J* = 11.4 Hz, 1H, -CH_2-), 4.51 – 4.45 (m, 2H, -CH_2-), 4.42 – 4.36 (m, 2H, -CH_2-), 4.21 – 3.89 (m, 8H, Allyl-1, Gal-3, Gal-4, Gal-5, Man-2, Man-4, Man-5), 3.84 – 3.72 (m, 2H, Man-3, Gal-6), 3.65 (dd, *J* = 10.8 Hz, 2.0 Hz, 1H, Gal-6), 3.58 (t, *J* = 8.6 Hz, 1H, Man-6), 3.39 (dd, *J* = 8.9 Hz, 5.1 Hz, 1H, Man-6), 2.08 (s, 3H, -CH_3) ppm.

ESI-MS: m/z M_{calcd} for $C_{59}H_{64}O_{12}$ = 964.4398; M_{found} = 987.4717 $[M+Na]^+$

Allyl-4,6-*O*-di-benzyl-(2,3,4,6-*O*-tetra-benzyl-D-galactopyranosyl-β1→3)-α-D-mannopyranoside (32)

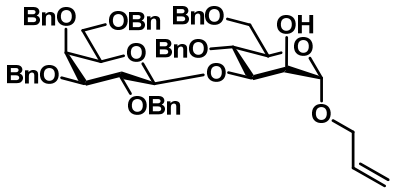

0.920 mmol of disaccharide **31** (0.888 g) was reacted according to NaOMe mediated *O*-Acyl removal (Method 3) at 40°C. Product **32** was obtained in 71% yield (0.650 mmol, 0.600 g) as colorless oil.

R_f = 0.25 (6:1, Hex:EA)

^{1}H-NMR (400 MHz, $CDCl_3$): δ = 7.32 – 7.03 (m, 30H, $H_{Ar.}$), 5.77 (dddd, *J* = 16.9 Hz, 10.3 Hz, 6.4 Hz, 5.2 Hz, 1H, Allyl-2), 5.16 (dq, *J* = 17.2 Hz, 1.6 Hz, 1H, Allyl-3), 5.08 (dq, *J* = 10.4 Hz, 1.4 Hz, 1H, Allyl-3), 4.92 (d, *J* = 11.5 Hz, 1H, -CH_2-), 4.86 – 4.46 (m, 10H, Man-1, -CH_2-), 4.41 (d, *J* = 7.7 Hz, 1H, Gal-1), 4.36 – 4.25 (m, 3H), 4.13 – 4.03 (m, 2H), 3.95 – 3.78 (m, 4H), 3.71 – 3.39 (m, 9H) ppm.

^{13}C-NMR (101 MHz, $CDCl_3$): δ = 138.94 ($C_{Ar.}$), 138.47 ($C_{Ar.}$), 138.43 ($C_{Ar.}$), 138.18 ($C_{Ar.}$), 138.01 ($C_{Ar.}$), 137.81 ($C_{Ar.}$), 133.72 (Allyl-2), 128.54 ($C_{Ar.}$), 128.49 ($C_{Ar.}$), 128.47 ($C_{Ar.}$), 128.46 ($C_{Ar.}$), 128.45 ($C_{Ar.}$), 128.33 ($C_{Ar.}$), 128.26 ($C_{Ar.}$), 128.23 ($C_{Ar.}$), 128.12 ($C_{Ar.}$), 127.98 ($C_{Ar.}$), 127.88 ($C_{Ar.}$), 127.87 ($C_{Ar.}$), 127.83 ($C_{Ar.}$), 127.70 ($C_{Ar.}$), 127.68 ($C_{Ar.}$), 127.54 ($C_{Ar.}$), 127.44 ($C_{Ar.}$), 127.41 ($C_{Ar.}$), 117.74 (Allyl-3), 99.68 (Gal-1), 98.31 (Man-1), 83.07, 78.87, 78.23, 77.37, 77.25, 77.05, 76.73, 75.64, 74.69, 73.60, 73.41, 73.39, 73.29, 73.20, 72.44, 70.86, 69.08, 68.10, 67.90, 67.81 ppm.

ESI-MS: m/z M_{calcd} for $C_{57}H_{62}O_{11}$ = 922.4292; M_{found} = 945.4626 $[M+Na]^+$

Polarimeter: $[\alpha]_D^{20}$ = +86.79 (c = 1.00 g/L in $CHCl_3$)

FTIR: 3446.24, 3065.15, 3032.51, 2922.45, 2867.03, 1737.71, 1606.64, 1497.63, 1454.78, 1364.49, 1309.27, 1210.33, 1093.28, 1063.85, 1028.86, 992.51, 915.74, 807.06, 734.72, 697.19 cm^{-1}.

Allyl-4,6-*O*-di-benzyl-(2-*O*-acetyl-3,4-*O*-di-benzyl-6-*O*-tri-*iso*-propylsilyl-D-mannopyranosyl-α1→2)-(2,3,4,6-*O*-tetra-benzyl-D-galactopyranosyl-β1→3)-α-D-mannopyranoside (33)

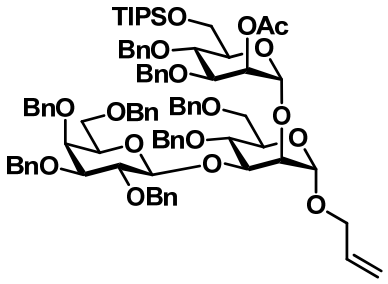

1.950 mmol of imidatedonor **24** (1.371 g) and 0.650 mmol of glycosylacceptor **32** (0.600 g) were dissolved in DCM and reacted according to glycosylation with imidate (Method 16) using TMSOTf at 0°C. Product **33** was obtained in 82% yield (0.533 mmol, 0.780 g) as colorless oil.

R_f = 0.6 (4:1, Hex:EA)

^{1}H-NMR (400 MHz, $CDCl_3$): δ = 7.31 – 6.97 (m, 40H, $H_{Ar.}$), 5.81 – 5.71 (m, 1H, Allyl-2), 5.41 (t, *J* = 2.1 Hz, 1H, Man'-2), 5.15 (dq, *J* = 17.2 Hz, 1.6 Hz, 1H, Allyl-3), 5.05 (dq, *J* = 10.4 Hz, 1.4 Hz, 1H, Allyl-3), 5.01 (d, *J* = 1.7 Hz, 1H, Man'-1), 4.90 – 4.83 (m, 4H, Man-1, -CH_2-), 4.81 – 4.74 (m, 2H, -CH_2-), 4.61 – 4.33 (m, 9H, Gal-1, -CH_2-), 4.30 – 4.02 (m, 5H), 4.00 – 3.93 (m, 2H), 3.89 – 3.64 (m, 10H), 3.62 – 3.56 (m, 1H), 3.53 – 3.44 (m, 3H), 3.32 – 3.25 (m, 1H), 1.79 (s, 3H, -CH_3), 1.01 – 0.99 (m, 21H, (-CH-(CH_3)$_2$)$_3$) ppm.

^{13}C-NMR (101 MHz, $CDCl_3$): δ = 170.14 (C=O), 138.91 ($C_{Ar.}$), 138.68 ($C_{Ar.}$), 138.58 ($C_{Ar.}$), 138.40 ($C_{Ar.}$), 138.27 ($C_{Ar.}$), 137.98 ($C_{Ar.}$), 133.93 (Allyl-2), 128.38 ($C_{Ar.}$), 128.29 ($C_{Ar.}$), 128.25 ($C_{Ar.}$), 128.19 ($C_{Ar.}$), 128.17 ($C_{Ar.}$), 128.15 ($C_{Ar.}$), 128.12 ($C_{Ar.}$), 128.06 ($C_{Ar.}$), 127.99 ($C_{Ar.}$), 127.94 ($C_{Ar.}$), 127.89 ($C_{Ar.}$), 127.71 ($C_{Ar.}$), 127.69 ($C_{Ar.}$), 127.50 ($C_{Ar.}$), 127.47 ($C_{Ar.}$), 127.42 ($C_{Ar.}$), 127.40 ($C_{Ar.}$), 127.36 ($C_{Ar.}$), 127.26 ($C_{Ar.}$), 127.16 ($C_{Ar.}$), 117.25 (Allyl-3), 102.12 (Gal-1), 98.98 (Man'-1), 97.63 (Man-1), 82.94, 78.90, 78.34, 77.35, 77.24, 77.04, 76.72, 75.51, 75.16, 74.64, 74.55, 73.77, 73.55, 73.47, 73.38, 73.25, 73.19, 72.70, 71.90, 71.65, 69.40, 68.80, 68.36, 67.90, 62.49, 20.79 (-CH_3), 18.08 ((-CH(-CH_3)$_2$)$_3$), 18.05 ((-CH-CH_3)$_2$)$_3$), 18.01 ((-CH(-CH_3)$_2$)$_3$) ppm.

Allyl-4,6-*O*-di-benzyl-(3,4-*O*-di-benzyl-6-*O*-tri-*iso*-propylsilyl-D-mannopyranosyl-α1→2)-(2,3,4,6-*O*-tetra-benzyl-D-galactopyranosyl-β1→3)-α-D-mannopyranoside (34)

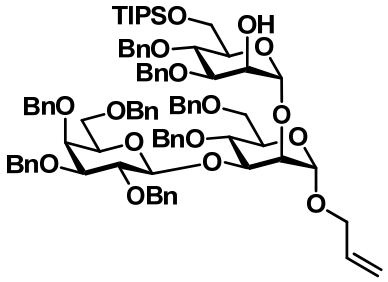

0.628 mmol of trisaccharide **33** (0.920 g) was reacted according to NaOMe mediated *O*-Acyl removal (Method 3). Product **34** was obtained in quantitative yield (0.628 mmol, 0.894 g) as colorless oil.

R_f = 0.45 (4:1, Hex:EA)

^{1}H-NMR (400 MHz, $CDCl_3$): δ = 7.32 – 6.97 (m, 40H, $H_{Ar.}$), 5.81 – 5.68 (m, 1H, Allyl-2), 5.13 (dq, *J* = 17.2 Hz, 1.7 Hz, 1H, Allyl-3), 5.03 (dq, *J* = 10.4 Hz, 1.4 Hz, 1H, Allyl-3), 4.98 (d, *J* = 1.6 Hz, Man'-1), 4.92 – 4.83 (m, 4H, Man-1, -CH_2-), 4.78 – 4.74 (m, 2H, -CH_2-), 4.65 – 4.58 (m, 3H, -CH_2-), 4.55 (d, *J* = 11.2 Hz, 1H, -CH_2-), 4.50 – 4.43 (m, 3H, Gal-1, -CH_2-), 4.39 – 4.27 (m, 5H, -CH_2-), 4.23 (d, *J* = 11.7 Hz, 1H, -CH_2-), 4.09 – 3.99 (m, 1H), 3.96 (t, *J* = 2.6 Hz, 1H), 3.90 – 3.58 (m, 14H), 3.58 – 3.44 (m, 3H), 3.34 (dd, *J* = 8.7 Hz, 4.9 Hz, 1H), 0.99 – 0.97 (m, 21H, (-CH(-CH_3)$_2$)$_3$) ppm.

^{13}C-NMR (101 MHz, $CDCl_3$): δ = 138.98 ($C_{Ar.}$), 138.92 ($C_{Ar.}$), 138.76 ($C_{Ar.}$), 138.73 ($C_{Ar.}$), 138.64 ($C_{Ar.}$), 138.37 ($C_{Ar.}$), 138.23 ($C_{Ar.}$), 137.95 ($C_{Ar.}$), 133.94 (Allyl-2), 128.40 ($C_{Ar.}$), 128.36 ($C_{Ar.}$), 128.33 ($C_{Ar.}$), 128.31 ($C_{Ar.}$), 128.29 ($C_{Ar.}$), 128.24 ($C_{Ar.}$), 128.21 ($C_{Ar.}$), 128.19 ($C_{Ar.}$), 128.17 ($C_{Ar.}$), 127.98 ($C_{Ar.}$), 127.94 ($C_{Ar.}$), 127.91 ($C_{Ar.}$), 127.75 ($C_{Ar.}$), 127.68 ($C_{Ar.}$), 127.54 ($C_{Ar.}$), 127.50 ($C_{Ar.}$), 127.48 ($C_{Ar.}$), 127.39 ($C_{Ar.}$), 127.35 ($C_{Ar.}$), 127.32 ($C_{Ar.}$), 117.17 (Allyl-3), 101.03 (Man'-1), 100.94 (Gal-1), 97.83 (Man-1), 82.79, 79.89, 79.03, 77.37, 77.26, 77.06, 76.74, 75.03, 74.87, 74.76, 74.52, 74.08, 73.66, 73.51, 73.34, 73.27, 73.20, 72.69, 71.96, 71.86, 69.43, 68.55, 68.21, 67.86, 62.89, 60.45, 18.09 (-CH(CH_3)$_2$)$_3$, 18.06 (-CH(-CH_3)$_2$)$_3$) ppm.

ESI-MS: m/z M_{calcd} for $C_{86}H_{104}O_{16}Si$ = 1420.7094; M_{found} = 1443.7714 $[M+Na]^+$

FTIR: 3570.53, 3065.54, 3033.11, 2924.66, 2866.75, 1606.87, 1497.74, 1454.99, 1363.40, 1309.33, 1286.40, 1219.66, 1097.34, 1063.07, 1029.05, 995.90, 916.03, 883.50, 805.82, 772.95, 734.35, 696.96 cm^{-1}.

Allyl-4,6-*O*-di-benzyl-(-(2,3,4,6-*O*-tetra-benzyl-D-galactopyranosyl-α1→2)-3,4-*O*-di-benzyl-6-*O*-tri-*iso*-propylsilyl-α-D-mannopyranosyl-α1→2)-(2-3,4,6-*O*-tetra-benzyl-D-galactopyranosyl-β1→3)-α-D-mannopyranoside (30)

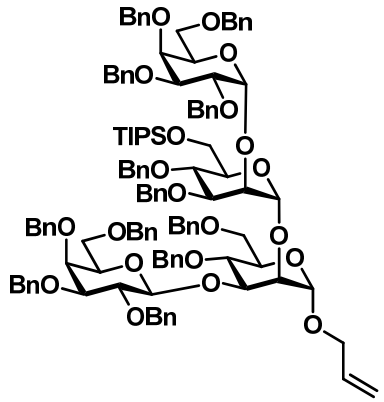

0.158 mmol of thiodonor **10** (0.100 g) and 0.113 mmol of glycosylacceptor **34** (0.160 g) were dissolved in a 1:1 mixture of DCM and ether and reacted according to glycosylation with thiodonor (Method 17) using TfOH at -11°C. Product **30** was obtained in 60% yield brsm (0.057 mmol, 0.112 g) as colorless oil.

R_f = 0.4 (6:1, Hex:EA)

^{1}H-NMR (400 MHz, $CDCl_3$): δ = 7.44 – 6.92 (m, 60H, $H_{Ar.}$), 5.81 – 5.65 (m, 1H, Allyl-1), 5.23 – 3.16 (m, 56H), 1.01 – 0.97 (m, 21H, $(-CH(-CH_3)_2)_3$) ppm.

^{13}C-NMR (101 MHz, $CDCl_3$): δ = 139.25 ($C_{Ar.}$), 139.18 ($C_{Ar.}$), 139.16 ($C_{Ar.}$), 138.98 ($C_{Ar.}$), 138.89 ($C_{Ar.}$), 138.81 ($C_{Ar.}$), 138.76 ($C_{Ar.}$), 138.74 ($C_{Ar.}$), 138.53 ($C_{Ar.}$), 138.49 ($C_{Ar.}$), 138.30 ($C_{Ar.}$), 138.06 ($C_{Ar.}$), 134.10 (Allyl-2), 128.43 ($C_{Ar.}$), 128.40 ($C_{Ar.}$), 128.35 ($C_{Ar.}$), 128.30 ($C_{Ar.}$), 128.27 ($C_{Ar.}$), 128.20 ($C_{Ar.}$), 128.19 ($C_{Ar.}$), 128.17 ($C_{Ar.}$), 128.15 ($C_{Ar.}$), 128.07 ($C_{Ar.}$), 127.93 ($C_{Ar.}$), 127.89 ($C_{Ar.}$), 127.87 ($C_{Ar.}$), 127.80 ($C_{Ar.}$), 127.72 ($C_{Ar.}$), 127.55 ($C_{Ar.}$), 127.49 ($C_{Ar.}$), 127.47 ($C_{Ar.}$), 127.44 ($C_{Ar.}$), 127.36 ($C_{Ar.}$), 127.33 ($C_{Ar.}$), 127.30 ($C_{Ar.}$), 127.28 ($C_{Ar.}$), 127.24 ($C_{Ar.}$), 127.17 ($C_{Ar.}$), 126.83 ($C_{Ar.}$), 117.18 (Allyl-3), 101.89 (Man'-1), 101.64 (β-Gal-1), 98.75 (α-Gal-1), 97.64 (Man-1), 82.76, 80.14, 78.61, 78.46, 77.82, 77.43, 77.31, 77.11, 76.79, 76.57, 76.35, 75.48, 75.09, 74.94, 74.85, 74.65, 74.62, 74.27, 73.76, 73.62, 73.48, 73.40, 73.28, 73.25, 73.11, 72.85, 72.49, 71.86, 71.03, 69.52, 69.36, 68.97, 68.33, 67.99, 62.81, 18.22 ($(-CH(CH_3)_2)_3$), 18.21 ($(-CH(CH_3)_2)_3$), ppm.

6-Thiobenzyl-hexyl-3,4-*O*-di-benzyl-6-*O*-tri-*iso*-propylsilyl-α-D-mannopyranoside (36)

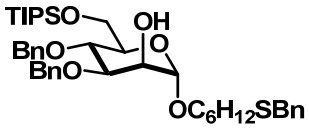

0.067 mmol of phosphate donor **25** (0.050 g) and 0.087 mmol of alcohol **35** (19.420 mg) were dissolved in DCM and reacted according glycosylation with imidate (Method 16) using TMSOTf at 0°C. Afterwards sodium methoxide mediated *O*-Acyl removal (Method 3) was performed. Product **36** was obtained in 41% yield (0.028 mmol, 0.020 g) over two steps as colorless oil.

R_f = 0.45 (4:1, Hex:EA)

^{1}H-NMR (600 MHz, $CDCl_3$): δ = 7.30 – 7.15 (m, 15H, $H_{Ar.}$), 4.80 (d, *J* = 10.9 Hz, 1H, -CH_2-), 4.74 (s, 1H, Man-1), 4.63 (q, *J* = 11.5 Hz, 2H, -CH_2-), 4.56 (d, *J* = 10.9 Hz, 1H, -CH_2-), 3.93 (s, 1H, Man-2), 3.86 (d, *J* = 10.7 Hz, 1H, -CH_2-), 3.83 – 3.77 (m, 2H, -CH_2-, Man-3), 3.68 (t, *J* = 9.5 Hz, 1H, Man-4), 3.64 – 3.54 (m, 3H, -OH, Man-5, Man-6), 3.28 (dd, *J* = 16.0 Hz, 6.6 Hz, 1H, Man-6), 1.52 – 1.41 (m, 4H, -CH_2-), 1.31 – 1.17 (m, 4H, -CH_2-), 1.05 – 0.96 (m, 25H, -CH_2-, (-$CH(CH_3)_2)_3$) ppm.

^{13}C-NMR (151 MHz, $CDCl_3$): δ = 138.59 ($C_{Ar.}$), 138.20 ($C_{Ar.}$), 128.95 ($C_{Ar.}$), 128.65 ($C_{Ar.}$), 128.58 ($C_{Ar.}$), 128.54 ($C_{Ar.}$), 128.20 ($C_{Ar.}$), 128.01 ($C_{Ar.}$), 127.99 ($C_{Ar.}$), 127.86 ($C_{Ar.}$), 127.01 ($C_{Ar.}$), 98.98 (Man-1), 80.62 (Man-3), 75.35 (-CH_2-), 74.52 (Man-4), 72.81 (Man-5), 72.16 (-CH_2-), 68.69 (Man-2), 67.35 (Man-6), 63.17 (-CH_2-), 36.45 (-CH_2-**)**, 31.47 (-CH_2-), 29.41 (-CH_2-), 29.28 (-CH_2-), 28.83 (-CH_2-), 25.96 (-CH_2-), 18.17 ((-$CH(CH_3)_2)_3$), 18.14 ((-$CH(-CH_3)_2)_3$), 12.16 ((-$CH(CH_3)_2)_3$) ppm.

ESI-MS: m/z M_{calcd} for $C_{42}H_{62}O_6SSi$ = 722.4036; M_{found} = 723.4091 $[M+Na]^+$

Polarimeter: $[\alpha]_D^{20}$ = +22.04 (c = 0.10 g/L in $CHCl_3$)

FTIR: 3545.96, 3350.80, 2942.71, 2226.41, 2191.11, 2134.74, 2017.46, 1958.86, 1455.13, 1106.63, 774.58, 698.69, 673.84, 666.27 cm^{-1}.

6-Thiobenzly-hexyl-2,3,4-*O*-tri-benzyl-6-*O*-tri-*iso*-propylsilyl-α-D-mannopyranoside (36)

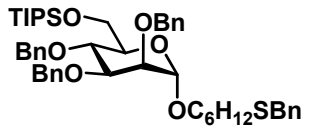

0.028 mmol of alcohol **36** (0.020 g) was reacted according to Williamson ether formation (Method 10) using benzyl bromide. Product **37** was obtained in quantitative yield (0.028 mmol, 0.022 g) as colorless oil.

R_f = 0.7 (6:1, Hex:EA)

^{1}H-NMR (600 MHz, $CDCl_3$): δ = 7.34 – 7.06 (m, 20H, $H_{Ar.}$), 4.84 (d, *J* = 10.8 Hz, 1H, -CH_2-), 4.71 (s, 1H, Man-1), 4.66 (d, *J* = 12.4 Hz, 1H, -CH_2-), 4.62 – 4.54 (m, 4H, -CH_2-), 3.89 – 3.79 (m, 4H, Man-2, Man-3, -CH_2-, -CH_2-), 3.67 (s, 1H, Man-4), 3.59 – 3.50 (m, 2H, Man-5, Man-6), 3.24 – 3.20 (m, 1H, Man-6), 1.48 – 1.38 (m, 4H, -CH_2-, -CH_2-, -CH_2-, -CH_2-), 1.29 – 1.15 (m, 8H, -CH_2-, -CH_2-, -CH_2-, -CH_2-, -CH_2-, -CH_2-, -CH_2-, -CH_2-), 0.99 (s, 21H, -(-$CH(CH_3)_2)_3$) ppm.

^{13}C-NMR (151 MHz, $CDCl_3$): δ = 138.84 ($C_{Ar.}$), 138.83 ($C_{Ar.}$), 138.76 ($C_{Ar.}$), 138.74 ($C_{Ar.}$), 138.42 ($C_{Ar.}$), 128.94 ($C_{Ar.}$), 128.57 ($C_{Ar.}$), 128.54 ($C_{Ar.}$), 128.47 ($C_{Ar.}$), 128.44 ($C_{Ar.}$), 128.36 ($C_{Ar.}$), 128.24 ($C_{Ar.}$), 127.92 ($C_{Ar.}$), 127.78 ($C_{Ar.}$), 127.76 ($C_{Ar.}$), 127.72 ($C_{Ar.}$), 127.61 ($C_{Ar.}$), 127.57 ($C_{Ar.}$), 127.00 ($C_{Ar.}$), 97.56 (Man-1), 80.59 (Man-3), 75.40 (-CH_2-), 75.31 (-CH_2-), 75.22 (Man-4), 73.65 (Man-2), 72.65 (-CH_2-), 72.30 (Man-5), 67.20 (Man-6), 63.46 (-CH_2-), 36.45 (-CH_2-), 31.47 (-CH_2-), 29.44 (-CH_2-), 29.27 (-CH_2-), 28.83 (-CH_2-), 25.95 (-CH_2-), 18.18 ((-$CH(CH_3)_2)_3$), 18.15 ((-$CH(CH_3)_2)_3$), 12.18 ((-$CH(CH_3)_2)_3$) ppm.

6-Thiobenzyl-hexyl-2,3,4-tri-*O*-benzyl-α-D-mannopyranoside (38)

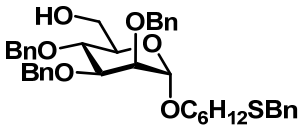

0.028 mmol of mannoside **37** (0.022 g) was reacted according to TIPS removal (Method 12). Product **38** was obtained in 71% yield (0.020 mmol, 0.013 g) as colorless oil.

R_f = 0.1 (6:1, Hex:EA)

^{1}H-NMR (400 MHz, $CDCl_3$): δ = 7.31 – 7.146 (m, 20H, $H_{Ar.}$), 4.87 (d, *J* = 10.8 Hz, 1H, -CH_2-), 4.73 – 4.70 (m, 2H, Man-1, -CH_2-), 4.63 – 4.56 (m, 4H, -CH_2-), 3.96 – 3.67 (m, 5H, Man-2, Man-3, Man-4, -CH_2-, -CH_2-), 3.58 – 3.49 (m, 2H, Man-5, Man-6), 3.26 – 3.20 (m, 1H, Man-6), 1.70 – 0.79 (m, 12H, , -CH_2-, -CH_2-, -CH_2-, -CH_2-, -CH_2-, -CH_2-) ppm.

ESI-MS: m/z M_{calcd} for $C_{40}H_{48}O_6S$ = 656.3172; M_{found} = 657.3232 $[M+H]^+$

Polarimeter: $[\alpha]_D^{20}$ = +23.04 (c = 0.10 g/L in $CHCl_3$)

FTIR: 3524.97, 3030.94, 2927.69, 2164.48, 2130.38, 1955.07, 1497.23, 1455.39, 1363.25, 1096.57, 736.06, 699.19 cm^{-1}.

H-4,6-*O*-di-benzyl-(-(2,3,4,6-*O*-tetra-benzyl-D-galactopyranosyl-α1→2)-3,4-*O*-di-benzyl-6-*O*-tri-*iso*-propylsilyl-D-mannopyranosyl-α1→2)-(2-3,4,6-*O*-tetra-benzyl-D-galactopyranosyl-β1→3)-α/β-D-mannopyranoside (39)

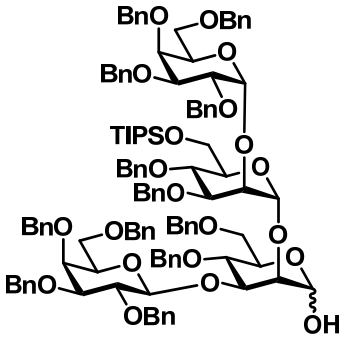

10.290 µmol of tetrasaccharide **30** (0.020 g) was reacted according to allyl removal via isomerization and hydrolysis (Method 14). Product **39** was obtained in 61% yield (6.300 µmol, 0.012 g) as colorless oil. The product was isolated as a mixture of the anomers and was characterized accordingly

$\mathbf{R_f}$ = 0.2 (4:1, Hex:EA)

^{1}H-NMR (400 MHz, $CDCl_3$): δ = 7.35 – 6.88 (m, 60H, $H_{Ar.}$), 5.42 (d, *J* = 2.6 Hz, 0.5H, α-Man), 5.19 (d, *J* = 2.9 Hz, 0.5H, α-Gal), 5.14 (t, *J* = 2.6 Hz, 0.5H, α-Man), 5.10 (d, *J* = 1.9 Hz, 0.5H, α-Man), 4.97 – 4.74 (m, 6H, -CH_2-), 4.68 – 4.00 (m, 25H, β-Gal, β-Man), 3.97 – 3.24 (m, 22H), 1.01 – 0.97 (m, 21H, (-CH(-CH_3)$_2$)$_3$) ppm.

^{13}C-NMR (101 MHz, $CDCl_3$): δ = 139.10 ($C_{Ar.}$), 139.03 ($C_{Ar.}$), 138.92 ($C_{Ar.}$), 138.90 ($C_{Ar.}$), 138.79 ($C_{Ar.}$), 138.77 ($C_{Ar.}$), 138.58 ($C_{Ar.}$), 138.54 ($C_{Ar.}$), 138.53 ($C_{Ar.}$), 138.49 ($C_{Ar.}$), 138.35 ($C_{Ar.}$), 138.27 ($C_{Ar.}$), 138.05 ($C_{Ar.}$), 138.03 ($C_{Ar.}$), 137.97 ($C_{Ar.}$), 128.41 ($C_{Ar.}$), 128.40 ($C_{Ar.}$), 128.39 ($C_{Ar.}$), 128.36 ($C_{Ar.}$), 128.31 ($C_{Ar.}$), 128.29 ($C_{Ar.}$), 128.26 ($C_{Ar.}$), 128.23 ($C_{Ar.}$), 128.21 ($C_{Ar.}$), 128.17 ($C_{Ar.}$), 128.16 ($C_{Ar.}$), 128.13 ($C_{Ar.}$), 128.05 ($C_{Ar.}$), 128.02 ($C_{Ar.}$), 127.94 ($C_{Ar.}$), 127.91 ($C_{Ar.}$), 127.89 ($C_{Ar.}$), 127.88 ($C_{Ar.}$), 127.85 ($C_{Ar.}$), 127.78 ($C_{Ar.}$), 127.76 ($C_{Ar.}$), 127.72 ($C_{Ar.}$), 127.67 ($C_{Ar.}$), 127.58 ($C_{Ar.}$), 127.51 ($C_{Ar.}$), 127.47 ($C_{Ar.}$), 127.44 ($C_{Ar.}$), 127.41 ($C_{Ar.}$), 127.39 ($C_{Ar.}$), 127.35 ($C_{Ar.}$), 127.32 ($C_{Ar.}$), 127.30 ($C_{Ar.}$), 127.28 ($C_{Ar.}$), 127.25 ($C_{Ar.}$), 127.23 ($C_{Ar.}$), 127.22 ($C_{Ar.}$), 127.18 ($C_{Ar.}$), 126.89 ($C_{Ar.}$), 126.86 ($C_{Ar.}$), 101.79 (β-Gal-1), 101.77 (α-Man-1), 101.49 (α-Man-1), 98.76 (β-Gal-1), 92.92 (β-Man-1), 92.57 (α-Man-1), 82.63, 79.97, 78.68, 78.46, 78.35, 77.54, 77.24, 76.30, 75.73, 75.57, 75.54, 75.38, 75.15, 74.92, 74.84, 74.76, 74.70, 74.64, 74.59, 74.41, 74.34, 74.18, 74.14, 74.05, 73.78, 73.72, 73.63, 73.45, 73.38, 73.32, 73.29, 73.26, 73.22, 73.13, 73.07, 72.91, 72.48, 72.36, 72.14, 71.88, 71.12, 69.77, 69.72, 69.41, 68.41, 68.32, 18.16 ((-CH(-CH_3)$_2$)$_3$), 18.12 ((-CH(-CH_3)$_2$)$_3$) ppm.

ESI-MS: m/z M_{calcd} for $C_{117}H_{134}O_{21}Si$ = 1902.9187; M_{found} = 1925.8992 $[M+Na]^+$

6-Thiobenzyl-hexyl-2,3,4-*O*-tri-benzyl-(-(-(2,3,4,6-*O*-tetra-benzyl-D-galactopyranosyl-α1→2)-3,4-*O*-di-benzyl-6-*O*-tri-*iso*-propylsilyl-D-mannopyranosyl-α1→2)-(2,3,4,6-*O*-tetra-benzyl-D-galactopyranosyl-β1→3)-4,6-*O*-di-benzyl-D-mannopyranosyl-α/β1→6)-α-D-mannopyranoside (41)

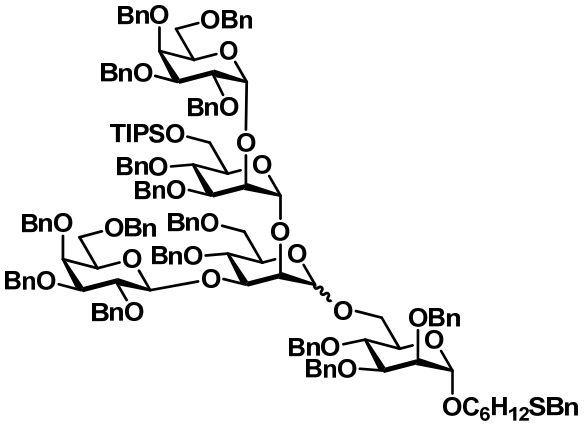

9.270 µmol of imidatedonor **40** (0.019 g) and 0.014 mmol of glycosylacceptor **38** (0.009 g) were dissolved in DCM and reacted according to glycosylation with imidate (Method 16) using TMSOTf at 0°C. Product **41** was obtained in 47% yield (4.330 µmol, 0.011 g) as colorless oil. The product was isolated as a mixture of the anomers and was characterized accordingly.

R_f = 0.6 (6:1, Hex:EA)

^{1}H-NMR (400 MHz, $CDCl_3$): δ = 7.36 – 6.97 (m, 80H, $H_{Ar.}$), 5.67 – 3.13 (m, 67H), 1.95 – 1.11 (m, 12H, $-CH_2-$, $-CH_2-$, $-CH_2-$, $-CH_2-$, $-CH_2-$, $-CH_2-$), 1.11 – 0.89 (m, 21H, $(-CH(-CH_3)_2)_3$) ppm.

6-Thiobenzyl-hexyl-2,3,4-*O*-tri-benzyl-(-(-(2,3,4,6-*O*-tetra-benzyl-D-galactopyranosyl-α1→2)-3,4-*O*-di-benzyl-D-mannopyranosyl-α1→2)-(2,3,4,6-*O*-tetra-benzyl-D-galactopyranosyl-β1→3)-4,6-*O*-di-benzyl-D-mannopyranosyl-α1→6)-α-D-mannopyranoside (42)

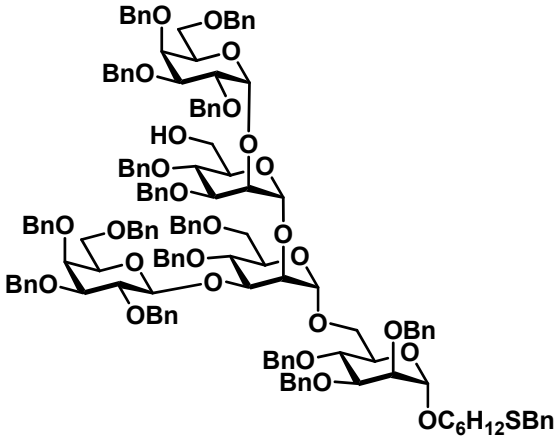

4.330 µmol of pentasaccharide **41** (0.011 g) was reacted according to TIPS removal (Method 12). After purification by preparative TLC product **42** was obtained in 24% yield (1.047 µmol, 2.500 mg) as colorless oil.

R_f = 0.2 (6:1, Hex:EA)

^{1}H-NMR (600 MHz, $CDCl_3$): δ = 7.30 – 7.18 (m, 80H, $H_{Ar.}$), 5.32 – 5.18 (m, 4H, Gal-1, Man-1, Man-1, Gal-1_α), 4.87 – 4.33 (m, 37H), 4.10 – 3.38 (s, 26H), 1.26 – 1.12 (m, 12H, -CH_2-) ppm.

6-Thiobenzyl-hexyl-2,3,4-*O*-tri-benzyl-(-(-(2,3,4,6-*O*-tetra-benzyl-D-galactopyranosyl-α1→2)-3,4-*O*-di-benzyl-6-*O*-(2-benzyloxycarbonylamino-phosphatidyl)-D-mannopyranosyl-α1→2)-(2,3,4,6-*O*-tetra-benzyl-D-galactopyranosyl-β1→3)-4,6-*O*-di-benzyl-D-mannopyranosyl-α1→6)-α-D-mannopyranoside (44)

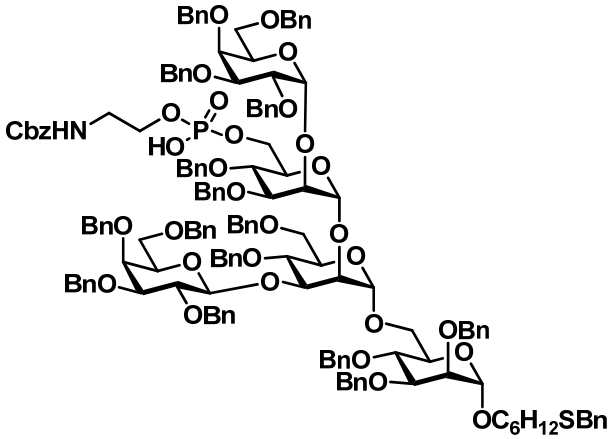

1.047 µmol of alcohol **42** (2.500 mg) and 10.470 µmol H-phosphonate **43** (3.770 mg) were reacted according to phosphate formation (Method 19). Product **44** was obtained in 97% yield (1.021 µmol, 2.700 mg) as colorless oil.

R_f = 0.5 (10% MeOH in DCM)

^{1}H-NMR (600 MHz, $CDCl_3$): δ = 7.73 – 7.19 (m, 90H, $H_{Ar.}$), 5.53 – 5.18 (m, 4H, Gal-1, Man-1, Man-1, Gal-1), 4.88 – 4.33 (m, 39H), 4.12 – 3.37 (m, 34H), 1.58 – 1.26 (m, 12H, -CH_2-) ppm.

^{13}C-NMR (151 MHz, $CDCl_3$): δ = 164.17, 138.70, 138.69, 138.68, 138.66, 138.31, 138.05, 137.88, 137.25, 128.82, 128.76, 128.58, 128.56, 128.55, 128.54, 128.50, 128.48, 128.40, 128.39, 128.37, 128.37, 128.35, 128.33, 128.26, 128.24, 128.15, 128.12, 128.09, 128.05, 127.99, 127.97, 127.89, 127.81, 127.79, 127.76, 127.73, 127.71, 127.65, 101.93, 97.94, 92.10, 82.33, 80.86, 78.87, 76.75, 76.27, 75.69, 75.25, 74.82, 74.76, 74.73, 74.64, 73.92, 73.91, 73.83, 73.76, 73.74, 73.71, 73.63, 73.11, 73.03, 71.58, 69.73, 69.05, 66.60, 33.39, 32.08, 29.86, 29.81, 29.75, 29.74, 29.60, 29.52, 29.40, 29.22, 24.89, 22.85, 14.28 ppm.

^{31}P-NMR (162 MHz, $CDCl_3$): δ = -22.47 ppm.

ESI-MS: m/z M_{calcd} for $C_{158}H_{172}NO_{31}PS$ = 2641.1373; M_{found} = 887.3750 $[M+NH_4]^{3+}$

Polarimeter: $[\alpha]_D^{20}$ = -0.51 (c = 0.19 g/L in $CHCl_3$)

FTIR: 3398.51, 2919.33, 2851.78, 1710.59, 1498.04, 1455.42, 1368.34, 1099.88, 741.28, 697.62 cm^{-1}.

6-Thio-hexyl-(-(D-galactopyranosyl-α1→2)-6-*O*-(2-amino-phosphatidyl)-D-mannopyranosyl-α1→2)-D-galactopyranosyl-β1→3)-D-mannopyranosyl-α1→6)-α-D-mannopyranoside (45)

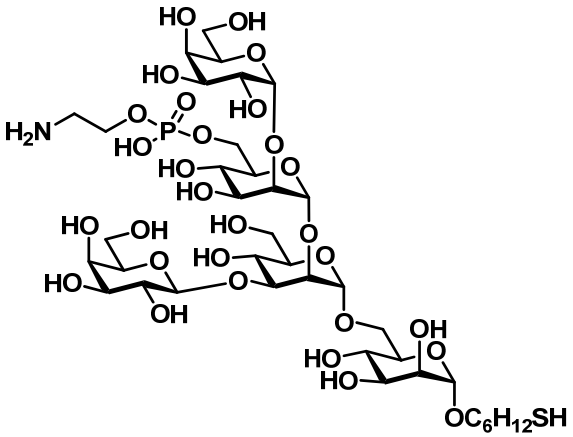

0.794 µmol of phosphate **44** (2.100 mg) was reacted according to Birch reduction (Method 22). Product **45** was obtained in 10% yield (1.021 µmol, 2.700 mg) as white powder by using sephadex G15 size exclusion chromatography using 5% ethanol in water as eluent.

^{1}H-NMR (400 MHz, D_2O): δ = 5.13 (d, *J* = 4.0 Hz), 4.02 – 3.38 (m) , 2.64 (t, *J* = 7.2 Hz), 1.61 – 1.22 (m) ppm.

^{13}C-NMR (101 MHz, D_2O): δ = 101.92, 101.53, 101.13, 100.57, 99.45, 78.48, 72.67, 71.30, 69.77, 69.19, 68.61, 67.68, 67.04, 65.94, 61.48, 61.19, 38.08, 28.23, 28.13, 27.13, 24.86, 21.03 ppm.

^{31}P-NMR (162 MHz, D_2O): δ = 75.00 ppm.

ESI-MS: m/z M_{calcd} for $C_{38}H_{70}NO_{29}PS$ = 1067.3492; M_{found} = 1261.4429 $[M+2Et_3N]^+$

1-*O*-Allyl-2,3,4,5-*O*-tetra-benzyl-(-(4-*O*-benzyl-6-*O*-*tert*-butyldiphenylsilyl-2-*O*-levulinoyl-3-*O*-2-methyl-naphthyl-D-mannopyranosyl-α1→4)-2-azido-3,6-*O*-di-benzyl-2-deoxy-4-*O*-D-glucopyranosyl-α1→6)-*myo*-inositol (48)

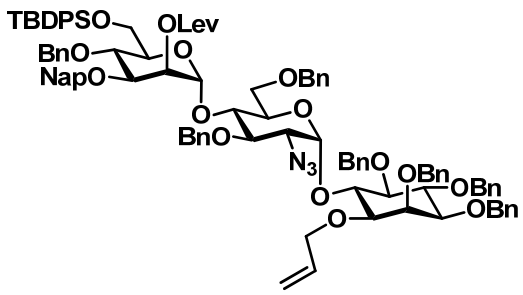

0.221 mmol of thiodonor **46** (0.201 g) and 0.158 mmol of glycosylacceptor **47** (0.150 g) were dissolved in DCM and reacted according to glycosylation with thiodonor (Method 17) using TfOH at 0°C. Product **48** was obtained in 89% yield (0.140 mmol, 0.235 g) as colorless oil.

$\mathbf{R_f}$ = 0.30 (6:1, Hex:EA)

^{1}H-NMR (400 MHz, $CDCl_3$): δ = 7.69 – 6.79 (m, 52H, $H_{Ar.}$), 5.85 (ddt, *J* = 16.4 Hz, 10.8 Hz, 5.4 Hz, 1H, Allyl-2), 5.64 (d, *J* = 3.5 Hz, 1H, Glu-1), 5.37 (s, 1H, Man-2), 5.28 (s, 1H, Man-1), 5.19 (d, *J* = 17.1 Hz, 1H, Allyl-3), 5.10 (d, *J* = 10.3 Hz, 1H, Allyl-3), 4.91 (d, *J* = 11.1 Hz, 1H, -CH_2-), 4.85 – 4.72 (m, 7H, Man-1, -CH_2-), 4.63 – 4.51 (m, 8H, -CH_2-, -CH_2-, -CH_2-, -CH_2-, -CH_2-, -CH_2-, -CH_2-, -CH_2-), 4.43 (d, *J* = 11.4 Hz, 1H, -CH_2-), 4.17 – 3.70 (m, 10H, Allyl-1), 3.47 (d, *J* = 11.0 Hz, 1H), 3.35 – 3.28 (m, 4H), 3.18 – 3.14 (m, 2H), 3.05 (d, *J* = 10.0 Hz, 1H), 2.50 – 2.48 (m, 4H, Lev), 1.96 (s, 3H, Lev), 0.95 (s, 9H, -C(-CH_3)$_3$) ppm.

^{13}C-NMR (101 MHz, $CDCl_3$): δ = 218.21 ($C{=}O_{Ketone}$), 172.01 ($C{=}O_{Ester}$), 139.15 ($C_{Ar.}$), 138.88 ($C_{Ar.}$), 138.63 ($C_{Ar.}$), 138.60 ($C_{Ar.}$), 138.42 ($C_{Ar.}$), 138.35 ($C_{Ar.}$), 138.19 ($C_{Ar.}$), 138.02 ($C_{Ar.}$), 136.04 ($C_{Ar.}$), 135.65 ($C_{Ar.}$), 134.32 ($C_{Ar.}$), 133.35 ($C_{Ar.}$), 133.07 ($C_{Ar.}$), 129.67 ($C_{Ar.}$), 128.55 ($C_{Ar.}$), 128.50 ($C_{Ar.}$), 128.39 ($C_{Ar.}$), 128.35 ($C_{Ar.}$), 128.15 ($C_{Ar.}$), 128.00 ($C_{Ar.}$), 127.83 ($C_{Ar.}$), 127.76 ($C_{Ar.}$), 127.70 ($C_{Ar.}$), 127.63 ($C_{Ar.}$), 127.57 ($C_{Ar.}$), 127.49 ($C_{Ar.}$), 127.35 ($C_{Ar.}$), 127.28 ($C_{Ar.}$), 126.84 ($C_{Ar.}$), 126.24 ($C_{Ar.}$), 126.11 ($C_{Ar.}$), 125.94 ($C_{Ar.}$), 117.16 (Allyl-3), 99.14 (Glu-1), 96.74 (Man-1), 82.06, 81.92, 81.28, 80.93, 77.48, 77.16, 76.84, 75.91, 75.56, 75.25, 75.13, 74.87, 74.17, 74.04, 73.63, 73.23, 73.09, 72.94, 71.70, 70.88 (Allyl-1), 69.77, 69.34, 68.36 (C-6), 63.43, 62.44 (C-6), 38.15 (Lev-3), 29.89 (Lev-5), 28.21 (Lev-2), 26.92 (-C(-CH_3)$_3$), 19.53 (-C(-CH_3)$_3$) ppm.

ESI-MS: m/z M_{calcd} for $C_{102}H_{109}N_3O_{17}Si$ = 1675.7526; M_{found} = 1698.7422 $[M+Na]^+$

Allyl-3,4,5,6-*O*-tetra-benzyl-(-(4-*O*-benzyl-6-*O*-*tert*-butyldiphenylsilyl-3-*O*-2-methyl-naphthyl-D-mannopyranosyl-α1→4)-2-azido-3,6-*O*-di-benzyl-2-deoxy-4-*O*-D-glucopyranosyl-α1→6)-*myo*-inositol (49)

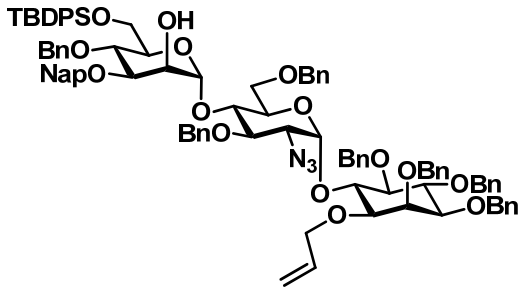

0.130 mmol of trisaccharide **48** (0.218 g) was reacted according to sodium methoxide mediated *O*-Acyl removal (Method 3) at 40°C. Product **49** was obtained in 93% yield (0.120 mmol, 0.190 g) as colorless oil.

$\mathbf{R_f}$ = 0.70 (4:1, Hex:EA)

^{1}H NMR (400 MHz, $CDCl_3$): δ = 7.67 – 6.79 (m, 52H, $H_{Ar.}$), 5.88 – 5.79 (m, 1H, Allyl-2), 5.66 (d, *J* = 3.6 Hz, 1H, Glu-1), 5.19 (d, *J* = 17.3 Hz, 1H, Allyl-3), 5.15 (s, 1H, Man-1), 5.10 (d, *J* = 10.5 Hz, 1H, Allyl-3), 4.89 (d, *J* = 11.0 Hz, 1H, -CH_2-), 4.82 (d, *J* = 10.6 Hz, 1H, -CH_2-), 4.79 – 4.76 (m, 1H, -CH_2-), 4.76 – 4.72 (m, 3H, -CH_2-, -CH_2-, -CH_2-), 4.67 – 4.46 (m, 8H, , -CH_2-, -CH_2-, -CH_2-, -CH_2-, -CH_2-, -CH_2-, -CH_2-, -CH_2-), 4.44 (d, *J* = 10.8 Hz, 1H, -CH_2-), 4.22 – 3.80 (m, 10H, , -CH_2-), 3.74 – 3.67 (m, 4H), 3.50 (d, *J* = 11.1 Hz, 1H), 3.41 (s, 1H), 3.35 – 3.01 (m, 6H), 0.94 (s, 9H, -C(-CH_3)$_3$) ppm.

^{13}C-NMR (101 MHz, $CDCl_3$): δ = 139.14 ($C_{Ar.}$), 138.87 ($C_{Ar.}$), 138.69 ($C_{Ar.}$), 138.39 ($C_{Ar.}$), 138.35 ($C_{Ar.}$), 138.30 ($C_{Ar.}$), 137.77 ($C_{Ar.}$), 136.00 ($C_{Ar.}$), 135.76 ($C_{Ar.}$), 135.61 ($C_{Ar.}$), 134.31 (Allyl-2), 133.87 ($C_{Ar.}$), 133.29 ($C_{Ar.}$), 133.22 ($C_{Ar.}$), 133.11 ($C_{Ar.}$), 131.15 ($C_{Ar.}$), 129.64 ($C_{Ar.}$), 129.62 ($C_{Ar.}$), 129.26 ($C_{Ar.}$), 128.65 ($C_{Ar.}$), 128.52 ($C_{Ar.}$), 128.43 ($C_{Ar.}$), 128.39 ($C_{Ar.}$), 128.38 ($C_{Ar.}$), 128.36 ($C_{Ar.}$), 128.32 ($C_{Ar.}$), 128.16 ($C_{Ar.}$), 128.10 ($C_{Ar.}$), 127.98 ($C_{Ar.}$), 127.81 ($C_{Ar.}$), 127.77 ($C_{Ar.}$), 127.75 ($C_{Ar.}$), 127.74 ($C_{Ar.}$), 127.66 ($C_{Ar.}$), 127.63 ($C_{Ar.}$), 127.60 ($C_{Ar.}$), 127.57 ($C_{Ar.}$), 127.55 ($C_{Ar.}$), 127.34 ($C_{Ar.}$), 127.26 ($C_{Ar.}$), 126.94 ($C_{Ar.}$), 126.80 ($C_{Ar.}$), 126.34 ($C_{Ar.}$), 126.13 ($C_{Ar.}$), 125.97 ($C_{Ar.}$), 121.39 ($C_{Ar.}$), 117.16 (Allyl-3), 102.09 (Man-1), 97.58 (Glu-1), 81.99, 81.54, 80.95, 80.13, 79.57, 77.48, 77.16, 76.84, 75.88, 75.32, 75.10, 74.32, 74.14, 73.69, 73.20, 73.05, 72.90, 72.83, 72.10, 70.88, 69.79, 69.08, 68.50, 63.38, 62.67, 50.38, 31.37, 27.00, 19.46 (-C(-CH_3)$_3$), 17.54 (-C(-CH_3)$_3$) ppm.

ESI-MS: m/z M_{calcd} for $C_{97}H_{103}N_3O_{15}Si$ = 1577.7158; M_{found} = 1601.7108 $[M+Na]^+$

Polarimeter: $[\alpha]_D^{20}$ = 41.23 (c = 0.1 g/L in $CHCl_3$)

FTIR: 2929.97, 2161.79, 2107.54, 1455.20, 1359.08, 1101.39, 1029.16, 738.48, 699.50 cm^{-1}.

Allyl-3,4,5,6-*O*-tetra-benzyl-(-(2,4-*O*-di-benzyl-6-*O*-*tert*-butyldiphenylsilyl-3-*O*-2-methyl-naphthyl-D-mannopyranosyl-α1→4)-2-azido-3,6-*O*-di-benzyl-2-deoxy-4-*O*-D-glucopyranosyl-α1→6)-*myo*-inositol (50)

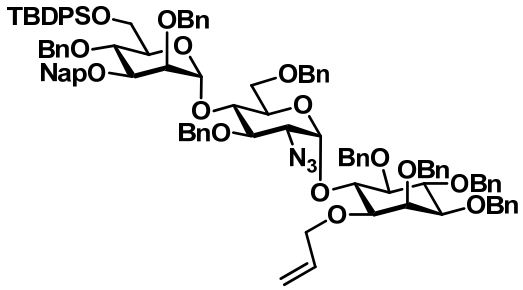

0.035 mmol of alcohol **49** (0.056 g) was reacted according to Williamson ether formation (Method 10). Product **50** was obtained in 93% yield (0.034 mmol, 0.057 g) as colorless oil.

R_f = 0.80 (4:1, Hex:EA)

^{1}H-NMR (600 MHz, $CDCl_3$): δ = 7.84 – 6.74 (m, 57H, $H_{Ar.}$), 5.84 (ddt, *J* = 15.8 Hz, 10.5 Hz, 5.3 Hz, 1H, Allyl-2), 5.67 (d, *J* = 3.5 Hz, 1H, GlcN-1), 5.19 (d, *J* = 17.2 Hz, 1H, Allyl-3), 5.15 (s, 1H, Man-1), 5.09 (d, *J* = 10.1 Hz, 1H, Allyl-3), 4.94 (d, *J* = 11.0 Hz, 1H, -CH_2-), 4.81 (d, *J* = 10.6 Hz, 1H, -CH_2-), 4.80 - 4.78 (m, 1H -CH_2-), 4.76 -4.74 (m, 3H, -CH_2-), 4.68 – 4.48 (m, 9H, -CH_2-), 4.43 (d, *J* = 11.2 Hz, 1H, -CH_2-), 4.31 (d, *J* = 12.2 Hz, 1H, -CH_2-), 4.28 (dd, *J* = 12.2 Hz, 7.0 Hz, 1H, -CH_2-), 4.21 – 4.09 (m, 3H), 4.07 – 3.99 (m, 2H), 3.96 – 3.86 (m, 5H), 3.77 (d, *J* = 10.7 Hz, 2H), 3.74 – 3.67 (m, 2H), 3.63 (s, 1H), 3.51 (d, *J* = 11.1 Hz, 1H), 3.29 (t, *J* = 9.3 Hz, 4H), 3.24 (d, *J* = 10.4 Hz, 1H), 3.12 (dd, *J* = 16.4, 6.7 Hz, 2H), 0.92 (s, 9H, -C(-CH_3)$_3$) ppm.

^{13}C-NMR (151 MHz, $CDCl_3$): δ = 139.40 ($C_{Ar.}$), 138.94 ($C_{Ar.}$), 138.91 ($C_{Ar.}$), 138.70 ($C_{Ar.}$), 138.40 ($C_{Ar.}$), 138.36 ($C_{Ar.}$), 138.06 ($C_{Ar.}$), 136.29 ($C_{Ar.}$), 136.06 ($C_{Ar.}$), 135.80 ($C_{Ar.}$), 134.34 ($C_{Ar.}$), 134.05 ($C_{Ar.}$), 133.39 (Allyl-3), 133.36 ($C_{Ar.}$), 133.06 ($C_{Ar.}$), 129.61 ($C_{Ar.}$), 129.56 ($C_{Ar.}$), 129.54 ($C_{Ar.}$), 129.21 ($C_{Ar.}$), 128.60 ($C_{Ar.}$), 128.55 ($C_{Ar.}$), 128.51 ($C_{Ar.}$), 128.36 ($C_{Ar.}$), 128.19 ($C_{Ar.}$), 128.16 ($C_{Ar.}$), 128.15 ($C_{Ar.}$), 128.01 ($C_{Ar.}$), 127.96 ($C_{Ar.}$), 127.85 ($C_{Ar.}$), 127.83 ($C_{Ar.}$), 127.82 ($C_{Ar.}$), 127.77 ($C_{Ar.}$), 127.73 ($C_{Ar.}$), 127.63 ($C_{Ar.}$), 127.60 ($C_{Ar.}$), 127.45 ($C_{Ar.}$), 127.37 ($C_{Ar.}$), 127.30 ($C_{Ar.}$), 127.12 ($C_{Ar.}$), 126.87 ($C_{Ar.}$), 126.51 ($C_{Ar.}$), 126.27 ($C_{Ar.}$), 126.04 ($C_{Ar.}$), 126.00 ($C_{Ar.}$), 117.17 (Allyl-2), 100.93 (Man-1), 97.66 (GlcN-1), 82.05, 82.02, 81.57, 80.98, 79.84, 77.53, 77.37, 77.16, 76.95, 76.70, 75.93, 75.38, 75.31, 75.06, 74.23, 74.17, 73.73, 73.67, 73.21, 72.94, 72.87, 72.36, 72.30, 70.90, 69.93, 68.55, 63.26, 62.77, 26.95 (-C(-CH_3)$_3$), 19.48 (-C(-CH_3)$_3$) ppm.

ESI-MS: m/z M_{calcd} for $C_{104}H_{109}N_3O_{15}Si$ = 1667.7628; M_{found} = 1690.7478 $[M+Na]^+$

Polarimeter: $[\alpha]_D^{20}$ = 44.39 (c = 0.1 g/L in $CHCl_3$)

FTIR: 2874.98, 2184.25, 2107.85, 1497.89, 1455.49, 1359.03, 1101.99, 1029.15, 820.55, 736.82, 698.11 cm^{-1}.

Allyl-3,4,5,6-*O*-tetra-benzyl-(-(2,4-*O*-di-benzyl-3-*O*-2-methyl-naphthyl-D-mannopyranosyl-α1→4)-2-azido-3,6-*O*-di-benzyl-2-deoxy-4-*O*-D-glucopyranosyl-α1→6)-*myo*-inositol (51)

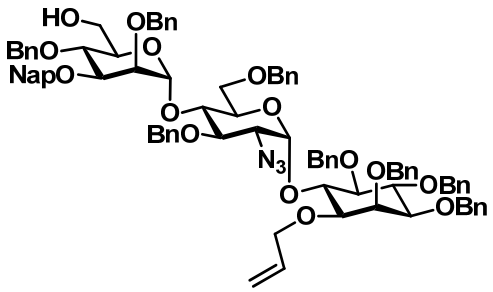

0.034 mmol of trisaccharide **50** (0.057 g) was reacted according to TBDPS removal (Method 13). Product **51** was obtained in 68% yield (0.023 mmol, 0.033 g) as colorless oil.

$\mathbf{R_f}$ = 0.20 (4:1, Hex:EA)

^{1}H-NMR (400 MHz, $CDCl_3$): δ = 7.79 – 7.04 (m, 47H, $H_{Ar.}$), 6.01 (ddd, *J* = 16.4 Hz, 11.0 Hz, 5.5 Hz, 1H, Allyl-2), 5.82 (t, *J* = 4.5 Hz, 1H, GlcN-1), 5.35 (dd, *J* = 17.3 Hz, 6.6 Hz, 1H, Allyl-3), 5.26 (d, *J* = 10.0 Hz, 1H, Allyl-3), 5.13 - 5.02 (m, 2H), 4.98 – 4.85 (m, 7H), 4.81 – 4.55 (m, 18H), 4.48 – 4.42 (m, 1H), 4.37 – 4.17 (m, 4H), 4.13 – 3.98 (m, 6H), 3.80 (t, *J* = 9.3 Hz, 1H), 3.53 – 3.14 (m, 8H), 2.98 (d, *J* = 4.6 Hz, 1H) ppm.

ESI-MS: m/z M_{calcd} for $C_{88}H_{91}N_3O_{15}$ = 1429.6450; M_{found} = 1452.6240 $[M+Na]^+$

Polarimeter: $[\alpha]_D^{20}$ = 17.75 (c = 0.1 g/L in $CHCl_3$)

FTIR: 3059.48, 1659.07, 1598.66, 1568.66, 1490.26, 1447.63, 1362.19, 1318.54, 1276.95, 1195.58, 1177.70, 1150.65, 1073.41, 1029.17, 1000.73, 920.46, 882.55, 788.47, 760.71, 720.29, 692.97 cm^{-1}.

Allyl-3,4,5,6-*O*-tetra-benzyl-(-(-(2-*O*-acetyl-3-*O*-benzoyl-4,6-*O*-di-benzyl-D-mannopyranosyl-α1→6)-2,4-*O*-di-benzyl-3-*O*-2-methyl-naphthyl-6-*O*-D-mannopyranosyl-α1→4)-2-azido-3,6-*O*-di-benzyl-2-deoxy-4-*O*-D-glucopyranosyl-α1→6)-*myo*-inositol (53)

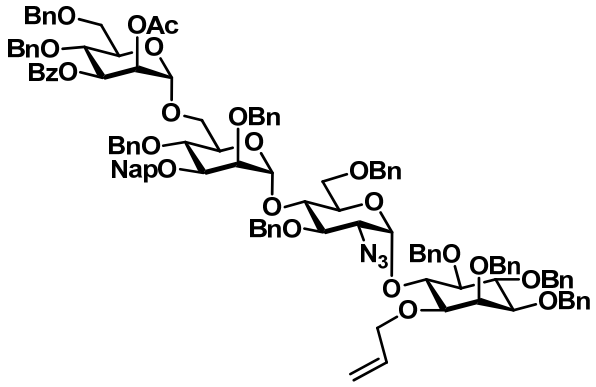

0.071 mmol of thiodonor **18** (0.048 g) and 0.048 mmol of glycosylacceptor **51** (0.068 g) were dissolved in DCM and reacted according to glycosylation with thiodonor (Method 17) using TfOH at 0°C. Product **53** was obtained in 93% yield (0.044 mmol, 0.084 g) as colorless oil.

$\mathbf{R_f}$ = 0.40 (6:1, Hex:EA)

^{1}H-NMR (400 MHz, $CDCl_3$): δ = 7.93 (d, *J* = 7.8 Hz, 2H, $H_{Ar.}$), 7.79 – 7.74 (m, 1H, $H_{Ar.}$), 7.72 (d, *J* = 8.5 Hz, 1H, $H_{Ar.}$), 7.65 (d, *J* = 5.4 Hz, 2H, $H_{Ar.}$), 7.52 (t, *J* = 7.4 Hz, 1H, $H_{Ar.}$), 7.45 – 7.03 (m, 53H), 7.00 – 6.96 (m, 2H, $H_{Ar.}$), 5.91 (ddt, *J* = 16.4 Hz, 10.8 Hz, 5.3 Hz, 1H; Allyl-2), 5.75 (d, *J* = 3.7 Hz, 1H, GlcN-1), 5.63 (dd, *J* = 10.0 Hz, 3.4 Hz, 1H, Man'-3), 5.43 (d, *J* = 3.4 Hz, 1H, Man'-2), 5.26 (d, *J* = 17.2 Hz, 1H, Allyl-3), 5.22 (s, 1H, Man-1), 5.16 (d,

J = 10.5 Hz, 1H, Allyl-3), 5.02 (d, J = 11.4 Hz, 1H, -CH_2-), 4.92 – 4.76 (m, 7H, Man'-1, -CH_2-), 4.74 – 4.47 (m, 12H, -CH_2-), 4.42 – 4.35 (m, 2H), 4.31 – 4.18 (m, 4H), 4.14 – 3.93 (m, 8H), 3.87 – 3.72 (m, 6H), 3.65 – 3.60 (m, 2H), 3.55 – 3.23 (m, 10H), 2.01 (s, 3H, -CH_3) ppm.

^{13}C-NMR (101 MHz, $CDCl_3$): δ = 169.42 (C=O), 164.90 (C=O), 138.96 ($C_{Ar.}$), 138.75 ($C_{Ar.}$), 138.56 ($C_{Ar.}$), 138.51 ($C_{Ar.}$), 138.34 ($C_{Ar.}$), 138.24 ($C_{Ar.}$), 138.15 ($C_{Ar.}$), 137.89 ($C_{Ar.}$), 137.86 ($C_{Ar.}$), 135.99 ($C_{Ar.}$), 134.19 ($C_{Ar.}$), 133.20 (Allyl-2), 132.86 ($C_{Ar.}$), 130.06 ($C_{Ar.}$), 129.54 ($C_{Ar.}$), 128.39 ($C_{Ar.}$), 128.38 ($C_{Ar.}$), 128.36 ($C_{Ar.}$), 128.30 ($C_{Ar.}$), 128.26 ($C_{Ar.}$), 128.23 ($C_{Ar.}$), 128.18 ($C_{Ar.}$), 128.10 ($C_{Ar.}$), 128.05 ($C_{Ar.}$), 128.00 ($C_{Ar.}$), 127.97 ($C_{Ar.}$), 127.89 ($C_{Ar.}$), 127.86 ($C_{Ar.}$), 127.82 ($C_{Ar.}$), 127.73 ($C_{Ar.}$), 127.65 ($C_{Ar.}$), 127.63 ($C_{Ar.}$), 127.60 ($C_{Ar.}$), 127.56 ($C_{Ar.}$), 127.50 ($C_{Ar.}$), 127.46 ($C_{Ar.}$), 127.45 ($C_{Ar.}$), 127.42 ($C_{Ar.}$), 127.27 ($C_{Ar.}$), 127.06 ($C_{Ar.}$), 126.97 ($C_{Ar.}$), 126.83 ($C_{Ar.}$), 126.21 ($C_{Ar.}$), 126.05 ($C_{Ar.}$), 125.78 ($C_{Ar.}$), 125.76 ($C_{Ar.}$), 117.01 (Allyl-3), 100.01 (Man-1), 98.02 (Man'-1), 97.50 (GlcN-1), 81.91, 81.87, 81.43, 80.82, 79.67, 77.30, 77.18, 76.98, 76.66, 76.27, 75.90, 75.77, 75.12, 74.85, 74.70, 74.41, 73.97, 73.49, 73.17, 73.13, 73.00, 72.76, 72.76, 72.33, 72.33, 72.29, 72.01, 72.01, 71.22, 70.78, 70.11, 69.91, 68.44, 62.72, 20.81 (-CH_3) ppm.

ESI-MS: m/z M_{calcd} for $C_{117}H_{119}N_3O_{22}$ = 1917.8285; M_{found} = 1940.8161 $[M+Na]^+$

Polarimeter: $[\alpha]_D^{20}$ = 34.88 (c = 0.1 g/L in $CHCl_3$)

FTIR: 2925.08, 2106.29, 1728.88, 1497.82, 1454.71, 1362.29, 1270.91, 1095.76, 736.97, 698.02 cm^{-1}.

Allyl-3,4,5,6-*O*-tetra-benzyl-(-(-(4,6-*O*-di-benzyl-D-mannopyranosyl-α1→6)-2,4-*O*-di-benzyl-3-*O*-2-methyl-naphthyl-6-*O*-D-mannopyranosyl-α1→4)-2-azido-3,6-*O*-di-benzyl-2-deoxy-4-*O*-D-glucopyranosyl-α1→6)- *myo*-inositol (54)

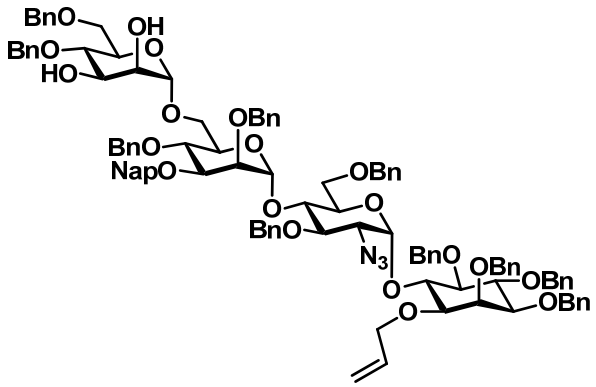

0.042 mmol of diester **53** (0.080 g) was reacted according to potassium carbonate mediated *O*-Acyl removal (Method 4). Product **54** was obtained in 95% yield (0.039 mmol, 0.070 g) as colorless oil.

$\mathbf{R_f}$ = 0.30 (4:1, Hex:EA)

^{1}H-NMR (600 MHz, $CDCl_3$): δ = 7.82 – 7.61 (m, 8H, $H_{Ar.}$), 7.52 – 6.98 (m, 49H, $H_{Ar.}$), 5.90 (dd, *J* = 11.9 Hz, 6.7 Hz, 1H, Allyl-2), 5.73 (d, *J* = 3.9 Hz, 1H, GlcN-1), 5.26 (d, *J* = 17.3 Hz, 1H, Allyl-3), 5.18 – 5.15 (m, 2H, Allyl-3, Man-1), 4.97 (d, *J* = 11.2 Hz, 1H, -CH_2-), 4.91 (t, *J* = 11.4 Hz, 2H, -CH_2-), 4.84 - 4.81 (m, 7H), 4.73 – 4.54 (m, 24H), 4.49 – 4.19 (m, 17H), 4.10 (t, *J* = 9.5 Hz, 2H), 4.03 – 3.94 (m, 13H), 3.84 – 3.73 (m, 13H), 3.67 – 3.55 (m, 11H), 3.51 – 3.43 (m, 7H), 3.40 – 3.33 (m, 3H), 3.22 – 3.17 (m, 4H) ppm.

Allyl-3,4,5,6-*O*-tetra-benzyl-(-(-(2-*O*-acetyl-4,6-*O*-di-benzyl-D-mannopyranosyl-α1→6)-2,4-*O*-di-benzyl-3-*O*-2-methyl-naphthyl-6-*O*-D-mannopyranosyl-α1→4)-2-azido-3,6-*O*-di-benzyl-2-deoxy-4-*O*-D-glucopyranosyl-α1→6)- *myo*-inositol (55)

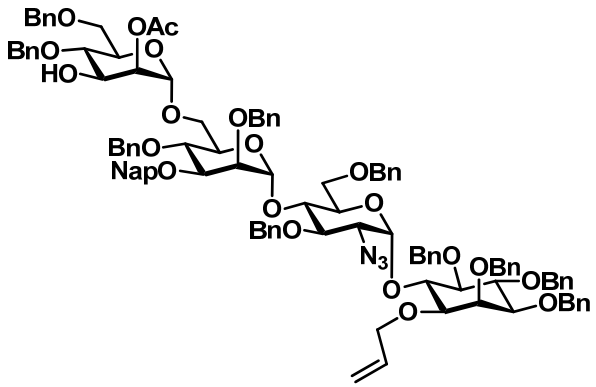

0.039 mmol of diol **54** (0.070 g) was reacted according to 2,3-*O*-orthoester formation and opening (Method 8). Product **55** was obtained in 70% yield (0.028 mmol, 0.050 g) as colorless oil.

$\mathbf{R_f}$ = 0.35 (4:1, Hex:EA)

^{1}H-NMR (600 MHz, acetone-d_6): δ = 7.85 – 7.74 (m, 4H, $H_{Ar.}$), 7.49 – 7.37 (m, 14H, $H_{Ar.}$), 7.36 – 7.13 (m, 38H, $H_{Ar.}$), 7.07 - 7.04(m, 1H, $H_{Ar.}$), 6.07 (ddt, *J* = 17.4 Hz, 10.8 Hz, 5.6 Hz, 1H, Allyl-2), 5.75 (d, *J* = 3.6 Hz, 1H, GlcN-1), 5.35 (dd, *J* = 17.2 Hz, 1.8 Hz, 1H, Allyl-3), 5.26 (d, *J* = 2.2 Hz, 1H, Man-1), 5.20 – 5.15 (m, 2H, Allyl-3, Man'-2), 5.03 (d, *J* = 11.1 Hz, 1H, -CH_2-), 4.96 (d, *J* = 10.9 Hz, 1H, -CH_2-), 4.92 – 4.87 (m, 6H), 4.82 – 4.65 (m, 12H, Man'1), 4.59 – 4.54 (m, 2H, -CH_2-), 4.45 – 4.41 (m, 2H), 4.37 (s, 2H), 4.33 (d, *J* = 6.9 Hz, 1H), 4.30 (d, *J* = 12.1 Hz, 1H), 4.27 – 4.09 (m, 7H), 4.06 (t, *J* = 9.6 Hz, 1H), 4.02 – 3.88 (m, 4H), 3.88 – 3.83 (m, 2H), 3.83 – 3.80 (m, 2H), 3.78 – 3.76 (m, 2H), 3.70 (dd, *J* = 9.9 Hz, 2.4 Hz, 1H), 3.66 (dd, *J* = 9.8 Hz, 2.2 Hz, 1H), 3.64 – 3.58 (m, 4H), 3.50 (dd, *J* = 11.2 Hz, 1.9 Hz, 1H), 3.44 (t, *J* = 9.4 Hz, 1H), 3.37 (dd, *J* = 11.4 Hz, 2.0 Hz, 1H), 3.34 – 3.30 (m, 2H), 2.04 (s, 3H, -CH_3) ppm.

^{13}C-NMR (151 MHz, acetone-d_6): δ = 172.36 (C=O), 142.07 ($C_{Ar.}$), 141.88 ($C_{Ar.}$), 141.82 ($C_{Ar.}$), 141.74 ($C_{Ar.}$), 141.67 ($C_{Ar.}$), 141.58 ($C_{Ar.}$), 141.26 ($C_{Ar.}$), 141.11 ($C_{Ar.}$), 139.06 ($C_{Ar.}$), 137.67 ($C_{Ar.}$), 136.01 ($C_{Ar.}$), 135.70 (Allyl-2), 131.01 ($C_{Ar.}$), 131.00 ($C_{Ar.}$), 130.94 ($C_{Ar.}$), 130.89 ($C_{Ar.}$), 130.79 ($C_{Ar.}$), 130.75 ($C_{Ar.}$), 130.75 ($C_{Ar.}$), 130.68 ($C_{Ar.}$), 130.66 ($C_{Ar.}$), 130.65 ($C_{Ar.}$), 130.44 ($C_{Ar.}$), 130.33 ($C_{Ar.}$), 130.30 ($C_{Ar.}$), 130.29 ($C_{Ar.}$), 130.25 ($C_{Ar.}$), 130.21 ($C_{Ar.}$), 130.19 ($C_{Ar.}$), 130.17 ($C_{Ar.}$), 130.15 ($C_{Ar.}$), 130.04 ($C_{Ar.}$), 130.02 ($C_{Ar.}$), 129.90 ($C_{Ar.}$), 129.89 ($C_{Ar.}$), 129.86 ($C_{Ar.}$), 129.85 ($C_{Ar.}$), 129.84 ($C_{Ar.}$), 129.79 ($C_{Ar.}$), 129.65 ($C_{Ar.}$), 129.62 ($C_{Ar.}$), 129.58 ($C_{Ar.}$), 129.56 ($C_{Ar.}$), 129.54 ($C_{Ar.}$), 128.91 ($C_{Ar.}$), 128.81 ($C_{Ar.}$), 128.63 ($C_{Ar.}$), 128.54 ($C_{Ar.}$), 118.83 (Allyl-3), 102.85 (Man-1), 100.43 (Man'-1), 100.07 (GlcN-1), 84.68, 84.37, 83.98, 83.51, 82.42, 82.15, 79.53, 78.88, 78.75, 77.87, 77.85, 77.23, 77.20, 77.07, 76.95, 76.24, 75.50, 75.48, 75.38, 75.28, 74.72, 74.61, 74.46, 74.15, 74.05, 73.16, 72.92, 72.54, 71.94, 71.56, 68.97, 65.46, 22.78 (-CH_3) ppm.

ESI-MS: m/z M_{calcd} for $C_{110}H_{115}N_3O_{21}$ = 1813.8023; M_{found} = 1836.7967 $[M+Na]^+$

Allyl-3,4,5,6-*O*-tetra-benzyl-(-(-(-(2,3,4,6-*O*-tetra-benzyl-D-galactopyranosyl-β1→3)-2-*O*-acetyl-4,6-*O*-di-benzyl-D-mannopyranosyl-α1→6)-2,4-*O*-di-benzyl-3-*O*-2-methyl-naphthyl-6-*O*-D-mannopyranosyl-α1→4)-2-azido-3,6-*O*-di-benzyl-2-deoxy-4-*O*-D-glucopyranosyl-α1→6)- *myo*-inositol (56)

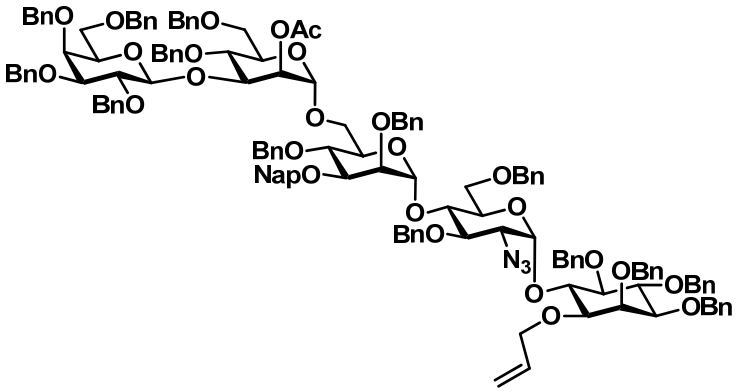

0.036 mmol of alcohol **55** (0.023 g) and 7.160 µmol of glycosylacceptor **10** (0.013 g) were dissolved in a 5:2 mixture of acetonitrile and DCM and reacted according to glycosylation with thiodonor (Method 17) using TfOH at 0°C. Product **56** was obtained in 63% yield (4.490 µmol, 0.011 g) as colorless oil.

R_f = 0.6 (6:1, Hex:EA)

^{1}H-NMR (400 MHz, $CDCl_3$): δ = 7.90 – 7.60 (m, 8H, $H_{Ar.}$), 7.52 – 7.01 (m, 69H, $H_{Ar.}$), 5.92 (ddt, *J* = 16.1 Hz, 10.4 Hz, 5.4 Hz, 1H, Allyl-2), 5.75 (d, *J* = 4.0 Hz, 1H, GlcN-1), 5.31 – 5.15 (m, 4H, Allyl-3, Man-1), 5.12 (s, 1H, Man'-2), 5.06 – 3.14 (m, 76H), 2.07 (s, 3H, -CH_3) ppm.

Allyl-3-*O*-benzyl-2-*O*-*para*-methoxy-benzyl-6-*O*-*tert*-butyl-diphenyl-silyl-β-D-galactopyranoside (62)

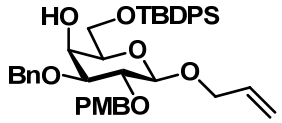

2.870 mmol of diol **61** (1.660 g) was reacted according to regioselective ether formation via stannylation (Method 9) using methanol as substitute for toluene. Product **62** was obtained in 71% yield (2.870 mmol, 1.980 g) as colorless oil.

R_f = 0.3 (6:1, Hex:EA)

^{1}H-NMR (400 MHz, $CDCl_3$): δ = 7.66 (tt, *J* = 7.9 Hz, 1.2 Hz, 4H, $H_{Ar.}$), 7.44 – 7.23 (m, 13H, $H_{Ar.}$), 6.86 – 6.82 (m, 2H, $H_{Ar.}$), 5.93 (ddt, *J* = 16.4 Hz, 10.8 Hz, 5.5 Hz, 1H, Allyl-2), 5.34 – 5.26 (m, 1H, Allyl-3), 5.21 – 5.14 (m, 1H, Allyl-3), 4.83 (d, *J* = 10.5 Hz, 1H, -CH_2-), 4.77 – 4.67 (m, 2H, -CH_2-), 4.65 (d, *J* = 10.5 Hz, 1H, -CH_2-), 4.40 – 4.31 (m, 2H, Allyl-3, Gal-1), 4.12 – 4.05 (m, 1H, Allyl-3), 4.00 (d, *J* = 3.3 Hz, 1H, Gal-4), 3.93 (dd, *J* = 10.4 Hz, 6.3 Hz, 1H, Gal-6), 3.85 (dd, *J* = 10.4 Hz, 5.7 Hz, 1H, Gal-6), 3.79 (s, 1H, -CH_3), 3.69 – 3.63 (m, 1H, Gal-2), 3.45 – 3.35 (m, 2H, Gal-3, Gal-5), 1.03 (s, 9H, -C(-CH_3)$_3$) ppm.

^{13}C-NMR (101 MHz, $CDCl_3$): δ = 159.16 ($C_{Ar.}$), 138.09 ($C_{Ar.}$), 135.61 ($C_{Ar.}$), 135.53 ($C_{Ar.}$), 134.12 (Allyl-2), 133.32 ($C_{Ar.}$), 133.13 ($C_{Ar.}$), 130.79 ($C_{Ar.}$), 129.83 ($C_{Ar.}$), 129.72 ($C_{Ar.}$), 128.42 ($C_{Ar.}$), 127.81 ($C_{Ar.}$), 127.76 ($C_{Ar.}$), 127.69 ($C_{Ar.}$), 127.67 ($C_{Ar.}$), 117.11 (Allyl-3), 113.68 ($C_{Ar.}$), 102.64 (Gal-1), 80.64 (Gal-3), 78.76 (Gal-2), 74.87 (-CH_2-), 74.21 (Gal-5), 72.46 (-CH_2-), 69.88 (Allyl-1), 66.72 (Gal-4), 62.83 (Gal-6), 55.26 (-CH_3), 26.78 (-CH_3), 19.18 (-C(-CH_3)$_3$) ppm.

Allyl-4-*O*-benzoyl-3-*O*-benzyl-2-*O*-*para*-methoxy-benzyl-6-*O*-*tert*-butyl-diphenyl-silyl-β-D-galactopyranoside (63)

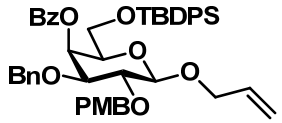

2.950 mmol of alcohol **62** (1.971 g) was reacted according to *O*-Acylation with acylchlorides (Method 11) using benzoyl chloride at 50°C. Product **63** was obtained in 86% yield (2.520 mmol, 1.950 g) as colorless oil.

R_f = 0.7 (6:1, Hex:EA)

^{1}H-NMR (400 MHz, $CDCl_3$): δ = 8.10 (d, *J* = 7.4 Hz, 2H, $H_{Ar.}$), 7.66 (d, *J* = 6.9 Hz, 2H, $H_{Ar.}$), 7.63 – 7.55 (m, 1H, $H_{Ar.}$), 7.53 (d, *J* = 7.1 Hz, 2H, $H_{Ar.}$), 7.49 – 7.36 (m, 7H, $H_{Ar.}$), 7.32

– 7.25 (m, 6H, $H_{Ar.}$), 7.15 (t, *J* = 7.5 Hz, 2H, $H_{Ar.}$), 6.84 (d, *J* = 8.5 Hz, 2H, $H_{Ar.}$), 5.98 (ddd, *J* = 22.5 Hz, 10.8 Hz, 5.6 Hz, 1H, Allyl-2), 5.91 – 5.90 (m, Gal-4), 5.36 (d, *J* = 17.2 Hz, 1H, Allyl-3), 5.23 (d, *J* = 10.4 Hz, 1H, Allyl-3), 4.93 (d, *J* = 11.6 Hz, 1H, -CH_2-), 4.82 (d, *J* = 10.3 Hz, 1H, -CH_2-), 4.67 (d, *J* = 10.5 Hz, 1H, -CH_2-), 4.63 (d, *J* = 11.8 Hz, 1H, -CH_2-), 4.46 (d, *J* = 6.7 Hz, 1H, Gal-1), 4.44 – 4.39 (m, 1H, Allyl-1), 4.15 (dd, *J* = 12.9 Hz, 5.9 Hz, 1H, Allyl-1), 3.80 (s, 3H, -CH_3), 3.78 (d, *J* = 6.9 Hz, 2H, Gal-6, Gal-6), 3.72 - 3.66 (m, 3H, Gal-2, Gal-3, Gal-5), 1.05 (s, 9H, -C(-CH_3)$_3$) ppm.

^{13}C-NMR (101 MHz, $CDCl_3$): δ = 165.64 (C=O), 159.17 ($C_{Ar.}$), 138.08 ($C_{Ar.}$), 135.56 ($C_{Ar.}$), 135.50 ($C_{Ar.}$), 134.03 (Allyl-2), 133.13 ($C_{Ar.}$), 132.97 ($C_{Ar.}$), 132.72 ($C_{Ar.}$), 130.77 ($C_{Ar.}$), 130.05 ($C_{Ar.}$), 129.85 ($C_{Ar.}$), 129.73 ($C_{Ar.}$), 129.65 ($C_{Ar.}$), 128.33 ($C_{Ar.}$), 128.23 ($C_{Ar.}$), 128.05 ($C_{Ar.}$), 127.72 ($C_{Ar.}$), 127.59 ($C_{Ar.}$), 127.53 ($C_{Ar.}$), 117.44 (Allyl-3), 113.65 ($C_{Ar.}$), 102.87 (Gal-1), 79.57 (Gal-2), 78.87 (Gal-3), 75.15 (-CH_2-), 73.55 (Gal-5), 72.03 (-CH_2-), 70.51 (Allyl-1), 66.95 (Gal-4), 61.70 (Gal-6), 55.27 (-CH_3), 26.72 (-C(CH_3)$_3$), 19.05 (-C(-CH_3)$_3$) ppm.

Allyl-4-*O*-benzoyl-3-*O*-benzyl-6-*O*-*tert*-butyl-diphenyl-silyl-β-D-galactopyranoside (64)

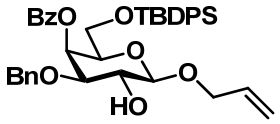

To a solution of **63** (2.520 mmol, 1.950 g) in DCM 10 v/v% TFA was added. After 15 min, NEt_3 was added and solvents were evaporated to dryness. The residue was dissolved in DCM and washed with sat. $NaHCO_3$ solution and brine. The combined organic phases were dried using Na_2SO_4, filtered and evaporated. The residue was purified by column chromatography. Product **64** was obtained in 90% yield (2.270 mmol, 1.482 g) as colorless oil.

R_f = 0.4 (6:1, Hex:EA)

^{1}H-NMR (600 MHz, $CDCl_3$): δ = 8.11 – 8.09 (m, 2H, H_{Ar}), 7.69 – 7.68 (m, 2H, H_{Ar}), 7.60 – 7.55 (m, 3H, H_{Ar}), 7.47 – 7.43 (m, 3H, H_{Ar}), 7.41 – 7.38 (m, 4H, H_{Ar}), 7.34 – 7.26 (m, 4H, H_{Ar}), 7.18 – 7.16 (m, 2H, H_{Ar}), 6.03 – 5.93 (m, 2H, Allyl-2, Gal-4), 5.34 (d, *J* = 17.2 Hz, 1H, Allyl-3), 5.24 (d, *J* = 10.3 Hz, 1H, Allyl-3), 4.98 (d, *J* = 11.5 Hz, 1H, -CH_2-), 4.61 (d, *J* = 11.4 Hz, 1H, -CH_2-), 4.40 (dd, *J* = 14.6 Hz, 5.9 Hz, 1H, Allyl-1), 4.16 (dd, *J* = 12.6 Hz, 6.3 Hz, 1H, Allyl-1), 3.89 (t, *J* = 8.0 Hz, 1H, Gal-2), 3.83 – 3.77 (m, 3H, Gal-6, Gal-6, Gal-5), 3.60 (d, *J* = 9.6 Hz, 1H, Gal-3), 1.07 (s, 9H, -C(-CH_3)$_3$) ppm.

^{13}C-NMR (151 MHz, $CDCl_3$): δ = 168.29 (C=O), 140.25 (C_{Ar}), 138.23 (C_{Ar}), 138.16 (C_{Ar}), 136.45 (Allyl-2), 135.79 (C_{Ar}), 135.73 (C_{Ar}), 135.40 (C_{Ar}), 132.67 (C_{Ar}), 132.58 (C_{Ar}), 132.43 (C_{Ar}), 132.35 (C_{Ar}), 131.12 (C_{Ar}), 131.03 (C_{Ar}), 130.87 (C_{Ar}), 130.52 (C_{Ar}), 130.42 (C_{Ar}),

130.29 (C_{Ar}), 120.75 (Allyl-3), 104.58 (Gal-1), 82.08 (Gal-3), 76.58 (Gal-5), 74.38 (-CH_2-), 73.55 (Gal-2), 72.89 (Allyl-1), 68.96 (Gal-4), 64.38 (Gal-6), 29.41 (-CH_3), 21.74 (-C(-CH_3)$_3$) ppm.

ESI-MS: m/z M_{calcd} for $C_{39}H_{44}O_7Si$ = 652.2856; M_{found} = 675.2751 $[M+Na]^+$

Allyl-3,4-*O*-di-benzyl-2-*O*-*para*-methoxy-benzyl-6-*O*-*tert*-butyl-diphenyl-silyl-β-D-galactopyranoside (65)

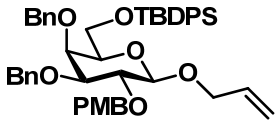

0.741 mmol of diol **61** (0.429 g) was reacted according to Williamson ether formation (Method 10) using benzyl bromide. Product **65** was obtained in 60% yield (0.442 mmol, 0.336 g) as colorless oil.

R_f = 0.8 (6:1, Hex:EA)

^{1}H-NMR (400 MHz, $CDCl_3$): δ = 7.62 – 7.59 (m, 4H, $H_{Ar.}$), 7.44 – 7.21 (m, 18H, $H_{Ar.}$), 6.87 – 6.81 (m, 2H, $H_{Ar.}$), 5.98 – 5.86 (m, 1H, Allyl-2), 5.29 (dqd, *J* = 17.3 Hz, 1.7 Hz, 0.6 Hz, 1H, Allyl-3), 5.16 (dtd, *J* = 10.3 Hz, 1.7 Hz, 1.1 Hz, 1H, Allyl-3), 4.97 (d, *J* = 11.4 Hz, 1H, -CH_2-), 4.87 – 4.79 (m, 2H, -CH_2-), 4.74 – 4.66 (m, 2H, -CH_2-), 4.62 (d, *J* = 11.4 Hz, 1H, -CH_2-), 4.39 – 4.31 (m, 2H, Gal-1, Allyl-1), 4.10 – 4.03 (m, 1H, Allyl-1), 3.89 (d, *J* = 2.9 Hz, 1H, Gal-2), 3.81 – 3.76 (m, 6H, Gal-6, Gal-6, -CH_3, Gal-3), 3.47 (dd, *J* = 9.8 Hz, 2.9 Hz, 1H, Gal-5), 3.37 – 3.32 (m, 1H, Gal-4), 1.04 (s, 9H, -C(-CH_3)$_3$) ppm.

^{13}C-NMR (101 MHz, $CDCl_3$): δ = 159.12 ($C_{Ar.}$), 138.75 ($C_{Ar.}$), 138.70 ($C_{Ar.}$), 135.54 ($C_{Ar.}$), 135.53 ($C_{Ar.}$), 134.23 (Allyl-2), 133.35 ($C_{Ar.}$), 133.24 ($C_{Ar.}$), 130.96 ($C_{Ar.}$), 129.90 ($C_{Ar.}$), 129.73 ($C_{Ar.}$), 129.71 ($C_{Ar.}$), 128.35 ($C_{Ar.}$), 128.04 ($C_{Ar.}$), 128.02 ($C_{Ar.}$), 127.98 ($C_{Ar.}$), 127.70 ($C_{Ar.}$), 127.55 ($C_{Ar.}$), 127.52 ($C_{Ar.}$), 127.29 ($C_{Ar.}$), 116.99 (Allyl-3), 113.66 ($C_{Ar.}$), 102.86 (Gal-1), 82.15 (Gal-5), 79.33 (Gal-3), 74.86 (-CH_2-), 74.72 (Gal-4), 74.53 (-CH_2-), 73.76 (Gal-2), 73.13 (-CH_2-), 69.98 (Allyl-2), 62.43 (Gal-6), 55.27 (-CH_3), 26.87 (-CH_3), 19.17 (-C(-CH_3)$_3$) ppm.

Thioethyl-3,4,6-*O*-tri-benzyl-2-*O*-*para*-methoxy-benzyl-α/β-D-galactopyranoside (69)

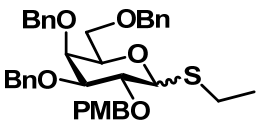

0.262 mmol of imidatedonor **68** (0.187 g) and 0.392 mmol of ethanethiol (0.024 g) were dissolved in DCM and reacted according to glycosylation with imidate (Method 16) using

TMSOTf at 0°C. Product **69** was obtained in 77% yield (0.200 mmol, 0.123 g) as colorless oil. The product was isolated as a mixture of anomeres and was characterized accordingly.

$\mathbf{R_f}$ = 0.8 (6:1, Hex:EA)

^{1}H-NMR (400 MHz, $CDCl_3$): δ = 7.43 – 7.21 (m, 17H, $H_{Ar.}$), 6.91 – 6.79 (m, 2H, $H_{Ar.}$), 5.45 (d, *J* = 5.5 Hz, 1H, Gal-1), 4.95 (d, *J* = 11.5 Hz, 1H, -CH_2-), 4.84 (d, *J* = 11.9 Hz, 1H, -CH_2-), 4.69 (dd, *J* = 11.6 Hz, 6.3 Hz, 2H, -CH_2-), 4.62 (d, *J* = 11.4 Hz, 1H, -CH_2-), 4.58 (d, *J* = 11.5 Hz, 1H, -CH_2-), 4.47 (d, *J* = 11.8 Hz, 1H, -CH_2-), 4.40 (d, *J* = 11.8 Hz, 1H, -CH_2-), 4.32 – 4.24 (m, 2H, Gal-2, Gal-5), 3.93 (d, *J* = 2.0 Hz, 1H, Gal-4), 3.80 (s, 3H, -CH_3), 3.78 (d, *J* = 15.5 Hz, 1H, Gal-3), 3.54 (dd, *J* = 6.4 Hz, 2.3 Hz, 2H, Gal-6, Gal-6), 2.61 – 2.45 (m, 2H, -CH_2-), 1.26 (t, *J* = 7.4 Hz, 3H, -CH_3) ppm.

^{13}C-NMR (101 MHz, $CDCl_3$): δ = 159.17 ($C_{Ar.}$), 138.83 ($C_{Ar.}$), 138.62 ($C_{Ar.}$), 138.03 ($C_{Ar.}$), 130.35 ($C_{Ar.}$), 129.68 ($C_{Ar.}$), 129.61 ($C_{Ar.}$), 128.43 ($C_{Ar.}$), 128.41 ($C_{Ar.}$), 128.35 ($C_{Ar.}$), 128.32 ($C_{Ar.}$), 128.26 ($C_{Ar.}$), 128.20 ($C_{Ar.}$), 127.89 ($C_{Ar.}$), 127.65 ($C_{Ar.}$), 127.56 ($C_{Ar.}$), 127.45 ($C_{Ar.}$), 127.44 ($C_{Ar.}$), 127.40 ($C_{Ar.}$), 113.84 ($C_{Ar.}$), 113.67 ($C_{Ar.}$), 83.28 (Gal-1), 79.53 (Gal-3), 75.76 (Gal-2), 75.09 (Gal-4), 74.77 (-CH_2-), 73.38 (-CH_2-)73.37 (-CH_2-), 72.10 (-CH_2-), 69.59 (Gal-5), 69.01 (Gal-6), 55.27 (-CH_3), 23.47 (-CH_2-), 14.65 (-CH_3) ppm.

Allyl-4-*O*-benzoyl-3-*O*-benzyl-6-*O*-*tert*-butyldiphenylsilyl-(2,3,4,6-*O*-tetra-benzyl-D-galactopyranosyl-α1→2)-β-D-galactopyrannoside (70)

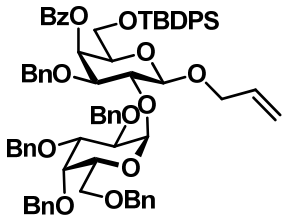

0.043 mmol of thiodonor **8** (0.025 g) and 0.031 mmol of glycosylacceptor **64** (0.020 g) were dissolved in ether and reacted according to glycosylation with thiodonor (Method 17) using TMSOTf at -11°C. Product **70** was obtained in 59% yield (0.018 mmol, 0.021 g) as colorless oil.

$\mathbf{R_f}$ = 0.45 (6:1, Hex:EA)

^{1}H-NMR (400 MHz, $CDCl_3$): δ = 8.11 – 8.00 (m, 2H, $H_{Ar.}$), 7.73 – 6.74 (m, 38H, $H_{Ar.}$), 6.01 - 5.71(m, 2H, Allyl-2, Gal-4), 5.36 – 5.24 (m, 1H, Allyl-3), 5.19 – 5.12 (m, 2H, Allyl-3, Gal'-1, Gal-1), 5.05 (d, *J* = 3.4 Hz, 1H, Gal'-1), 4.89 (d, *J* = 11.2 Hz, 1H, -CH_2-), 4.83 (d, *J* = 11.5 Hz, 1H, -CH_2-), 4.77 (d, *J* = 7.8 Hz, 1H, , -CH_2-), 4.74 (d, *J* = 6.4 Hz, 1H, -CH_2-), 4.71 (d, *J* = 11.6 Hz, 1H, , -CH_2-), 4.66 (d, *J* = 6.9 Hz, 1H, Gal-1), 4.62 (d, *J* = 6.6 Hz, 1H, , -CH_2-), 4.54 (d, *J* = 11.2 Hz, 1H, -CH_2-), 4.47 (d, *J* = 11.4 Hz, 1H, -CH_2-), 4.40 (d,

J = 9.5 Hz, 1H, -CH_2-), 4.26 (dd, *J* = 10.3, 3.4 Hz, 1H), 4.21 – 4.09 (m, 4H), 4.08 – 3.99 (m, 2H), 3.95 (dd, *J* = 10.0, 2.6 Hz, 1H), 3.86 (d, *J* = 12.0 Hz, 1H), 3.81 (dd, *J* = 12.0, 6.1 Hz, 1H), 3.73 (dd, *J* = 13.5, 6.7 Hz, 3H), 3.64 – 3.38 (m, 3H), 3.36 – 3.08 (m, 1H), 1.27 (s, 9H, -C(-CH_3)$_3$) ppm.

^{13}C-NMR (101 MHz, $CDCl_3$): δ = 165.51 (C=O), 138.85 ($C_{Ar.}$), 138.83 ($C_{Ar.}$), 138.76 ($C_{Ar.}$), 138.24 ($C_{Ar.}$), 138.12 ($C_{Ar.}$), 135.56 ($C_{Ar.}$), 135.47 ($C_{Ar.}$), 133.86 (Allyl-2), 133.14 ($C_{Ar.}$), 132.89 ($C_{Ar.}$), 130.14 ($C_{Ar.}$), 129.81 ($C_{Ar.}$), 129.71 ($C_{Ar.}$), 129.64 ($C_{Ar.}$), 129.63 ($C_{Ar.}$), 128.41 ($C_{Ar.}$), 128.34 ($C_{Ar.}$), 128.32 ($C_{Ar.}$), 128.30 ($C_{Ar.}$), 128.22 ($C_{Ar.}$), 128.15 ($C_{Ar.}$), 128.14 ($C_{Ar.}$), 128.11 ($C_{Ar.}$), 128.08 ($C_{Ar.}$), 128.04 ($C_{Ar.}$), 128.02 ($C_{Ar.}$), 128.00 ($C_{Ar.}$), 127.97 ($C_{Ar.}$), 127.93 ($C_{Ar.}$), 127.83 ($C_{Ar.}$), 127.78 ($C_{Ar.}$), 127.70 ($C_{Ar.}$), 127.68 ($C_{Ar.}$), 127.61 ($C_{Ar.}$), 127.58 ($C_{Ar.}$), 127.49 ($C_{Ar.}$), 127.44 ($C_{Ar.}$), 127.42 ($C_{Ar.}$), 127.37 ($C_{Ar.}$), 127.36 ($C_{Ar.}$), 127.29 ($C_{Ar.}$), 127.21 ($C_{Ar.}$), 118.44 (Allyl-3), 104.08 (Gal-1β), 98.33 (Gal'-1α), 94.62 (Gal-1α), 94.36 (Gal'-1α), 78.94, 77.35, 77.03, 76.71, 75.77, 75.05, 74.76, 74.69, 72.85, 72.67, 72.62, 71.91, 70.14, 69.50, 68.56, 68.41, 68.23, 68.18, 62.12, 29.71, 26.71, 26.68, 19.08 ppm.

ESI-MS: m/z M_{calcd} for $C_{73}H_{78}O_{12}Si$ = 1174.5263; M_{found} = 1197.5147 $[M+Na]^+$

Allyl-4-*O*-benzoyl-3-*O*-benzyl-(2,3,4,6-*O*-tetra-benzyl-D-galactopyranosyl-α1→2)-β-D-galactopyrannoside (71)

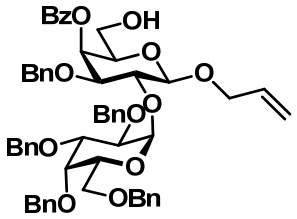

0.111 mmol of disaccharide **70** (0.130 g) was reacted according to TBDPS removal (Method 13). Product **71** was obtained in 69% yield (0.076 mmol, 0.072 g) as colorless oil.

R_f = 0.2 (6:1, Hex:EA)

^{1}H-NMR (400 MHz, $CDCl_3$): δ = 8.09 (d, *J* = 7.8 Hz, 2H, $H_{Ar.}$), 7.55 (t, *J* = 7.4 Hz, 1H, $H_{Ar.}$), 7.44 – 7.04 (m, 25H, $H_{Ar.}$), 6.97 (dd, *J* = 6.4 Hz, 2.9 Hz, 1H, $H_{Ar.}$), 5.90 (ddt, *J* = 16.3 Hz, 10.7 Hz, 5.4 Hz, 1H, Allyl-2), 5.68 -5.62 (m, 2H, Gal-4, Gal'-1), 5.28 (dd, *J* = 17.3 Hz, 1.9 Hz, 1H, Allyl-3), 5.16 (d, *J* = 10.5 Hz, 1H, Allyl-3), 4.87 (d, *J* = 11.4 Hz, 1H, -CH_2-), 4.81 – 4.62 (m, 3H, -CH_2-, Gal-1), 4.53 – 4.34 (m, 4H), 4.18 (t, *J* = 8.9 Hz, 1H), 4.12 – 3.98 (m, 5H), 3.89 (dd, *J* = 10.1 Hz, 2.8 Hz, 1H), 3.81 (dd, *J* = 10.3 Hz, 3.1 Hz, 2H), 3.76 – 3.67 (m, 3H), 3.56 (td, *J* = 10.5 Hz, 6.9 Hz, 1H), 3.41 (t, *J* = 8.6 Hz, 1H), 3.28 (dd, *J* = 9.2 Hz, 5.5 Hz, 1H) ppm.

^{13}C-NMR (101 MHz, $CDCl_3$): δ = 167.27 (C=O), 138.89 ($C_{Ar.}$), 138.84 ($C_{Ar.}$), 138.47 ($C_{Ar.}$), 138.18 ($C_{Ar.}$), 137.25 ($C_{Ar.}$), 133.64 (Allyl-2), 133.58 ($C_{Ar.}$), 130.15 ($C_{Ar.}$), 129.13 ($C_{Ar.}$), 128.48 ($C_{Ar.}$), 128.38 ($C_{Ar.}$), 128.33 ($C_{Ar.}$), 128.25 ($C_{Ar.}$), 128.21 ($C_{Ar.}$), 128.08 ($C_{Ar.}$), 128.05 ($C_{Ar.}$), 128.03 ($C_{Ar.}$), 128.01 ($C_{Ar.}$), 127.97 ($C_{Ar.}$), 127.80 ($C_{Ar.}$), 127.52 ($C_{Ar.}$), 127.43 ($C_{Ar.}$), 127.34 ($C_{Ar.}$), 127.32 ($C_{Ar.}$), 127.24 ($C_{Ar.}$), 117.28 (Allyl-3), 103.18 (Gal-1), 96.19 (Gal'-1), 78.79, 78.17, 77.36, 77.24, 77.04, 76.72, 76.12, 74.97, 74.71, 73.48, 72.82, 72.80, 71.92, 71.73, 70.32, 68.49, 68.24, 67.52, 60.63 ppm.

ESI-MS: m/z M_{calcd} for $C_{57}H_{60}O_{12}$ = 936.4085; M_{found} = 959.3981 $[M+Na]^+$

Allyl-4-*O*-benzoyl-3,6-*O*-di-benzyl-(2,3,4,6-*O*-tetra-benzyl-D-galactopyranosyl-α1→2)-β-D-galactopyrannoside (72)

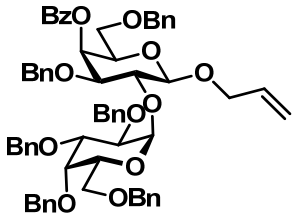

0.107 mmol of alcohol **71** (0.100 g) was reacted according to Williamson ether formation (Method 10) using benzyl bromide. Product **72** was obtained in 54% yield (0.057 mmol, 0.059 g) as colorless oil.

R_f = 0.8 (6:1, Hex:EA)

^{1}H-NMR (600 MHz, $CDCl_3$): δ = 8.12 – 8.06 (m, 2H, $H_{Ar.}$), 7.55 (td, *J* = 7.4 Hz, 1.4 Hz, 1H, $H_{Ar.}$), 7.45 – 7.05 (m, 30H, $H_{Ar.}$), 6.99 – 6.95 (m, 2H, $H_{Ar.}$), 5.90 (ddt, *J* = 17.3 Hz, 10.8 Hz, 5.5 Hz, 1H, Allyl-2), 5.66 (d, *J* = 3.7 Hz, 1H, Gal'-1), 5.63 (d, *J* = 3.3 Hz, 1H, Gal-4), 5.28 (dq, *J* = 17.3 Hz, 1.8 Hz, 1H, Allyl-3), 5.16 (dq, *J* = 10.5 Hz, 1.5 Hz, 1H, Allyl-3), 4.87 (d, *J* = 11.3 Hz, 1H, -CH_2-), 4.80 – 4.35 (m, 6H, -CH_2-, Gal-1), 4.18 (dd, *J* = 9.9 Hz, 7.9 Hz, 1H), 4.15 – 3.98 (m, 5H), 3.89 (td, *J* = 10.1 Hz, 2.9 Hz, 1H), 3.82 – 3.79 (m, 3H), 3.75 – 3.68 (m, 3H), 3.58 – 3.49 (m, 2H), 3.41 (dd, *J* = 9.2 Hz, 8.1 Hz, 1H), 3.28 (dd, *J* = 9.1 Hz, 5.5 Hz, 1H) ppm.

^{13}C-NMR (101 MHz, $CDCl_3$): δ = 168.02 (C=O), 138.44 ($C_{Ar.}$), 138.71 ($C_{Ar.}$), 138.69 ($C_{Ar.}$), 138.63 ($C_{Ar.}$), 138.56 ($C_{Ar.}$), 137.21 ($C_{Ar.}$), 133.61 (Allyl-2), 130.13 ($C_{Ar.}$), 128.46 ($C_{Ar.}$), 128.31 ($C_{Ar.}$), 128.23 ($C_{Ar.}$), 128.06 ($C_{Ar.}$), 128.04 ($C_{Ar.}$), 128.00 ($C_{Ar.}$), 127.78 ($C_{Ar.}$), 127.42 ($C_{Ar.}$), 127.32 ($C_{Ar.}$), 119.52 (Allyl-3), 105.08 (Gal-1), 98.90 (Gal'-1), 81.44, 80.82, 78.13, 77.68, 77.31, 77.20, 76.99, 76.67, 75.58, 74.47, 74.39, 72.81, 71.18, 70.97, 70.21, 63.36 ppm.

ESI-MS: m/z M_{calcd} for $C_{64}H_{66}O_{12}$ = 1026.4554; M_{found} = 1049.4331 $[M+Na]^+$

FTIR: 3493.90, 3065.51, 3032.84, 2923.92, 2871.49, 1953.78, 1721.73, 1603.01, 1586.20, 1497.58, 1454.28, 1358.46, 1314.89, 1271.26, 1209.75, 1095.75, 1038.86, 1026.83, 933.95, 867.48, 821.12, 735.36, 711.63, 697.01, 667.11 cm^{-1}.

H-*O*-benzoyl-3,6-*O*-di-benzyl-(2,3,4,6-*O*-tetra-benzyl-D-galactopyranosyl-α1→2)-β-D-galactopyrannoside (73)

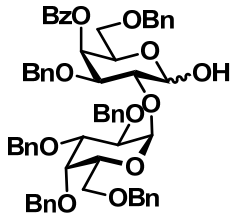

0.047 mmol of disaccharide **72** (0.048 g) was reacted according to allyl removal via isomerization and hydrolysis (Method 14). Product **73** was obtained in 95% yield (0.044 mmol, 0.044 g) as colorless oil. The compound was isolated as a mixture of anomers and was characterized accordingly.

R_f = 0.1 (6:1, Hex:EA)

^{1}H-NMR (400 MHz, $CDCl_3$): δ = 7.40 – 7.14 (m, 35H, $H_{Ar.}$), 5.32 – 5.27 (m, 1H, Gal-1), 4.98 – 4.13 (m, 20H), 4.09 – 3.79 (m, 5H), 3.62 – 3.33 (m, 4H) ppm.

^{13}C-NMR (101 MHz, $CDCl_3$): δ = 138.65 ($C_{Ar.}$), 138.54 ($C_{Ar.}$), 138.51 ($C_{Ar.}$), 138.35 ($C_{Ar.}$), 138.11 ($C_{Ar.}$), 137.92 ($C_{Ar.}$), 137.75 ($C_{Ar.}$), 137.59 ($C_{Ar.}$), 128.53 ($C_{Ar.}$), 128.46 ($C_{Ar.}$), 128.45 ($C_{Ar.}$), 128.43 ($C_{Ar.}$), 128.39 ($C_{Ar.}$), 128.36 ($C_{Ar.}$), 128.33 ($C_{Ar.}$), 128.24 ($C_{Ar.}$), 128.22 ($C_{Ar.}$), 128.19 ($C_{Ar.}$), 128.17 ($C_{Ar.}$), 128.16 ($C_{Ar.}$), 128.13 ($C_{Ar.}$), 128.05 ($C_{Ar.}$), 128.01 ($C_{Ar.}$), 127.95 ($C_{Ar.}$), 127.92 ($C_{Ar.}$), 127.89 ($C_{Ar.}$), 127.85 ($C_{Ar.}$), 127.79 ($C_{Ar.}$), 127.70 ($C_{Ar.}$), 127.64 ($C_{Ar.}$), 127.60 ($C_{Ar.}$), 127.56 ($C_{Ar.}$), 127.51 ($C_{Ar.}$), 127.48 ($C_{Ar.}$), 127.44 ($C_{Ar.}$), 127.43 ($C_{Ar.}$), 127.38 ($C_{Ar.}$), 127.36 ($C_{Ar.}$), 98.76, 96.31, 90.53, 81.38, 79.25, 78.95, 77.42, 77.32, 77.20, 77.00, 76.68, 75.55, 74.86, 74.78, 74.57, 74.46, 74.35, 74.34, 73.83, 73.75, 73.59, 73.54, 73.40, 73.19, 73.13, 72.71, 72.54, 72.49, 72.42, 70.00, 69.64, 69.48, 68.60, 68.46, 68.34 ppm.

ESI-MS: m/z M_{calcd} for $C_{61}H_{62}O_{12}$ = 986.4241; M_{found} = 1009.4025 $[M+Na]^+$

FTIR: 3430.29, 3065.88, 3032.19, 2922.02, 2869.34, 1953.36, 1726.08, 1684.82, 1605.96, 1497.58, 1454.81, 1361.01, 1216.81, 1155.23, 1077.49, 1053.60, 1027.83, 911.64, 819.88, 747.59, 733.52, 695.61, 666.80 cm^{-1}.

Allyl-2-*O*-levulinoyl-4-*O*-benzyl-6-*O*-*tert*-butyldiphenylsilyl-3-*O*-2-methyl-naphthyl-α-D-mannopyranoside (79)

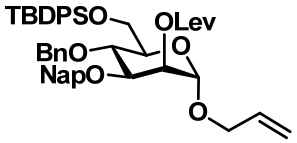

To a solution of **78** (0.890 mmol, 0.613 g) in DCM 0.712 mmol (0.087 g) DMAP, 1.345 mmol (0.155 g) levulinic acid and 1.335 mmol (0.275 g) DCC were added. After 1 hour sat. $NaHCO_3$ solution was added and the mixture was extracted three times with DCM. The combined organic phases were dried using Na_2SO_4, filtered and evaporated. The residue was purified by column chromatography. Product **79** was obtained in 90% yield (0.801 mmol, 0.630 g) as colorless oil.

R_f = 0.35 (6:1, Hex:EA)

^{1}H-NMR (400 MHz, $CDCl_3$): δ = 8.02 (s, 1H, $H_{Ar.}$), 7.86 – 7.66 (m, 9H, $H_{Ar.}$), 7.52 – 7.29 (m, 9H, $H_{Ar.}$), 7.29 – 7.11 (m, 6H, $H_{Ar.}$), 5.94 – 5.75 (m, 1H, Allyl-1), 5.46 (dd, *J* = 3.2 Hz, 1.8 Hz, 1H, Man-2), 5.22 (dq, *J* = 17.2 Hz, 1.5 Hz, 1H, Allyl-3), 5.16 (dd, *J* = 10.4 Hz, 1.3 Hz, 1H, Allyl-3), 4.93 (d, *J* = 10.7 Hz, 1H, -CH_2-), 4.89 – 4.84 (m, 2H, -CH_2-, Man-1), 4.69 (d, *J* = 11.4 Hz, 1H, -CH_2-), 4.61 (d, *J* = 10.7 Hz, 1H, -CH_2-), 4.13 (ddt, *J* = 12.8 Hz, 5.2 Hz, 1.4 Hz, 1H), 4.08 (dd, *J* = 9.4 Hz, 3.3 Hz, 1H), 4.02 – 3.89 (m, 4H), 3.73 (dd, *J* = 9.7 Hz, 2.7 Hz, 1H), 2.81 – 2.62 (m, 4H), 2.11 (s, 3H), 1.07 (s, 9H) ppm.

^{13}C-NMR (101 MHz, $CDCl_3$): δ = 206.32 (C=O), 172.19 (C=O), 162.55 ($C_{Ar.}$), 138.39 ($C_{Ar.}$), 135.90 ($C_{Ar.}$), 135.55 ($C_{Ar.}$), 135.53 ($C_{Ar.}$), 133.78 (Allyl-3), 133.48 ($C_{Ar.}$), 133.26 ($C_{Ar.}$), 133.17 ($C_{Ar.}$), 132.97 ($C_{Ar.}$), 129.59 ($C_{Ar.}$), 129.59 ($C_{Ar.}$), 128.34 ($C_{Ar.}$), 128.06 ($C_{Ar.}$), 127.94 ($C_{Ar.}$), 127.86 ($C_{Ar.}$), 127.66 ($C_{Ar.}$), 127.63 ($C_{Ar.}$), 127.59 ($C_{Ar.}$), 127.54 ($C_{Ar.}$), 126.85 ($C_{Ar.}$), 126.19 ($C_{Ar.}$), 125.96 ($C_{Ar.}$), 125.82 ($C_{Ar.}$), 117.75 (Allyl-2), 96.60 (Man-1), 78.26, 75.31, 74.18, 72.63, 71.72, 69.05, 67.83, 62.88, 38.00, 29.81, 28.12, 26.76, 19.36 ppm.

ESI-MS: m/z M_{calcd} for $C_{48}H_{54}O_8Si$ = 786.3588; M_{found} = 809.3419 $[M+Na]^+$

Polarimeter: $[\alpha]_D^{20}$ = -0.76 (c = 0.5 g/L in $CHCl_3$)

FT-IR: 3489.40, 3051.68, 2955.00, 2926.26, 2855.69, 2287.99, 2212.35, 2169.09, 2051.14, 2024.79, 1980.23, 1961.84, 1741.96, 1720.90, 1602.43, 1589.26, 1509.14, 1487.84, 1462.24, 1427.98, 1405.18, 1361.51, 1313.34, 1271.75, 1154.83, 1138.36, 1111.53, 1059.09, 1028.28, 996.73, 937.15, 858.76, 822.36 cm^{-1}.

Allyl-2-*O*-acetyl-4-*O*-benzyl-6-*O*-*tert*-butyldiphenylsilyl-α-D-mannopyranoside (81)

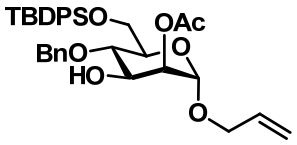

0.491 mmol of diol **80** (0.269 g) was reacted according to 2,3-*O*-orthoester formation and opening (Method 8). Product **81** was obtained in quantitative yield (0.491 mmol, 0.290 g) as colorless oil.

R_f = 0.4 (2:1, Hex:EA)

^{1}H-NMR (600 MHz, $CDCl_3$): δ = 7.82 – 7.63 (m, 4H, $H_{Ar.}$), 7.47 – 7.19 (m, 11H, $H_{Ar.}$), 5.85 (m, 1H, Allyl-2), 5.24 (dd, *J* = 17.2 Hz, 1.4 Hz, 1H, Allyl-3), 5.16 (dd, *J* = 10.4 Hz, 1.4 Hz, 1H, Allyl-3), 5.12 (dd, *J* = 3.1 Hz, 1.3 Hz, 1H, Man-2), 4.88 (d, *J* = 1.3 Hz, 1H, Man-1), 4.85 (d, *J* = 11.1 Hz, 1H, -CH_2-), 4.68 (d, *J* = 11.1 Hz, 1H, -CH_2-), 4.20 (dd, *J* = 9.3 Hz, 3.1 Hz, 1H, Man-3), 4.12 (m, 1H, -CH_2-), 4.00 (dd, *J* = 11.3 Hz, 4.0 Hz, 1H, Man-6), 3.97 – 3.89 (m, 3H, Man-4, Man-6, Allyl-1), 3.68 (dd, *J* = 9.7 Hz, 2.4 Hz, 1H, Man-5), 2.14 (s, 3H, -CH_3), 1.09 (s, -C(-CH_3)$_3$) ppm.

^{13}C-NMR (151 MHz, $CDCl_3$): δ = 170.81 (C=O), 138.33 ($C_{Ar.}$), 135.92 ($C_{Ar.}$), 135.52 ($C_{Ar.}$), 133.84 ($C_{Ar.}$), 133.51 (Allyl-2), 133.11 ($C_{Ar.}$), 129.61 ($C_{Ar.}$), 129.59 ($C_{Ar.}$), 128.43 ($C_{Ar.}$), 127.78 ($C_{Ar.}$), 127.74 ($C_{Ar.}$), 127.65 ($C_{Ar.}$), 127.51 ($C_{Ar.}$), 117.53 (Allyl-3), 96.28 (Man-1), 75.84 (Man-4), 75.05 (-CH_2-), 72.86 (Man-2), 72.37 (Man-5), 70.28 (Man-3), 67.87 (Allyl-1), 62.82 (Man-6), 26.76 (-CH_3), 21.01 (-CH_3), 19.38 (-C(-CH_3)$_3$) ppm.

ESI-MS: m/z M_{calcd} for $C_{34}H_{42}O_7Si$ = 590.270; M_{found} = 613.2598 $[M+Na]^+$

Poalrimeter: $[\alpha]_D^{20}$ = 31.1 (*c* = 1.00, $CHCl_3$)

FTIR: 3475, 3071, 2931, 2858, 1746, 1473, 1455, 1428, 1372, 1238, 1137, 1112, 1077, 982, 926, 824, 741, 702 cm^{-1}.

H-3-*O*-methyl-2-naphthyl-4-*O*-*para*-methoxy-benzoyl-(-(2,3,6-*O*-tri-2-methyl-napthyl-4-*O*-*para*-methoxy-benzoyl-D-galactopyranosyl-α1→2)-3,6-*O*-di-2-methyl-naphthyl-4-*O*-*para*-methoxy-benzoyl-D-galactopyranosy-α1→6)-(2,3,6-*O*-tri-2-methyl-napthyl-4-*O*-*para*-methoxy-benzoyl-D-galactopyranosyl-α1→2)-α/β-D-galactopyranoside (82)

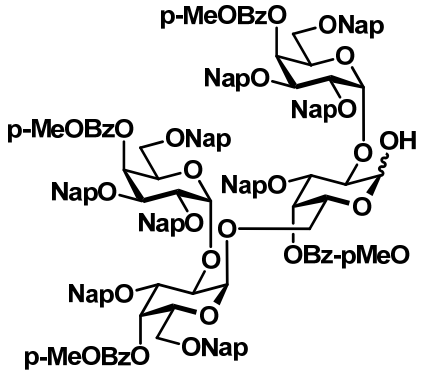

0.080 mmol of tetrasaccharide **76** (0.200 g) were reacted according to allyl removal via isomerization and hydrolysis (Method 14). Product **82** was obtained in 81% yield (0.064 mmol, 0.159 g) as colorless oil.

R_f = 0.1 (3:1, Hex:EA)

^{1}H-NMR (400 MHz, $CDCl_3$): δ = 7.93 – 6.53 (m, 77H, $H_{Ar.}$), 5.88 – 5.03 (m, 4H), 4.95 – 3.01 (m, 58H) ppm.

Trichloracetamido-3-*O*-methyl-2-naphthyl-4-*O*-*para*-methoxy-benzoyl-(-(2,3,6-*O*-tri-2-methyl-napthyl-4-*O*-*para*-methoxy-benzoyl-D-galactopyranosyl-α1→2)-3,6-*O*-di-2-methyl-naphthyl-4-*O*-*para*-methoxy-benzoyl-D-galactopyranosy-α1→6)-(2,3,6-*O*-tri-2-methyl-napthyl-4-*O*-*para*-methoxy-benzoyl-D-galactopyranosyl-α1→2)-α/β-D-galactopyranoside (83)

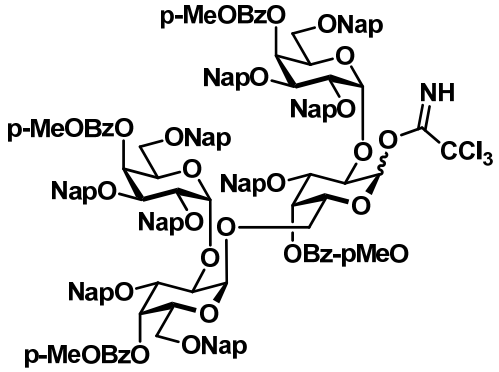

0.024 mmol of lactol **82** (0.059 g) were reacted according to imidate formation (Method 15). Product **83** was obtained in 11% yield (2.680 µmol, 7.000 mg) as colorless oil.

R_f = 0.6 (3:1, Hex:EA)

^{1}H-NMR (400 MHz, $CDCl_3$): δ = 7.85 – 7.02 (m, 77H, $H_{Ar.}$), 5.75 – 3.33 (m, 58 H) ppm.

6-Thiobenzyl-hexyl--3-*O*-methyl-2-naphthyl-4-*O*-*para*-methoxy-benzoyl-(-(2,3,6-*O*-tri-2-methyl-napthyl-4-*O*-*para*-methoxy-benzoyl-D-galactopyranosyl-α1→2)-3,6-*O*-di-2-methyl-naphthyl-4-*O*-*para*-methoxy-benzoyl-D-galactopyranosy-α1→6)-(2,3,6-*O*-tri-2-methyl-napthyl-4-*O*-*para*-methoxy-benzoyl-D-galactopyranosyl-α1→2)-α-D-galactopyranoside (85)

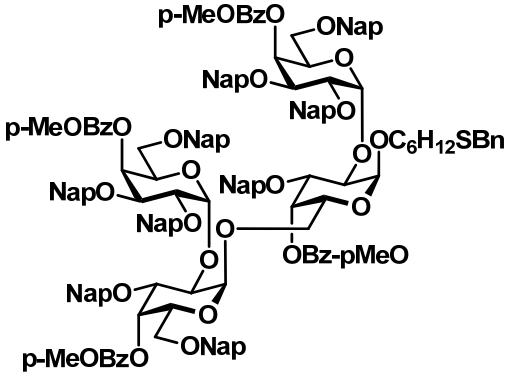

0.019 mmol of imidate **83** (0.050 g) and 0.057 mmol of 6-Thiobenzylhexanol **35** (0.013 g) were dissolved in DCM and reacted according to glycosylation with imidate donor (Method 16) using TMSOTf at 0°C. Product **85** was obtained in 20% yield (3.740 µmol, 10.000 mg) as colorless oil.

$\mathbf{R_f}$ = 0.55 (4:1, Hex:EA)

^{1}H-NMR (400 MHz, $CDCl_3$): δ = 7.89 – 6.56 (m, 82H, $H_{Ar.}$), 5.85 – 5.77 (m, 2H), 5.52 – 5.46 (m, 2H), 5.16 – 5.04 (m, 5H), 4.95 – 3.03 (m, 53H), 2.30 -2.25 (m, 2H), 1.50 -1.13 (m, 8H) ppm.

6-Thio-hexyl-(-(D-galactopyranosyl-α1→2)-D-galactopyranosyl-α1→6)-(α-D-galactopyranosyl-α1→2)-α-D-galactopyranoside (86)

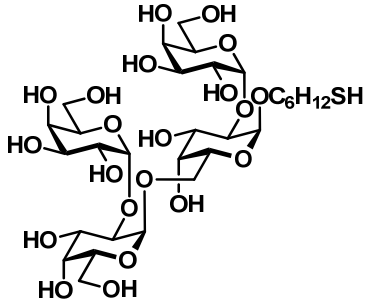

3.740 µmol of tetrasaccharide **85** (10.000 mg) was reacted according to Birch reduction (Method 22). Product **86** was obtained in 20% (7.480 µmol, 5.860 mg) as white solid.

^{1}H-NMR (400 MHz, D_2O): δ = 5.14 – 4.99 (m, 4H), 4.07 – 3.44 (m, 26H), 2.82 – 2.77 (m, 2H), 1.68 – 1.28 (m, 8H) ppm.

ESI-MS: m/z M_{calcd} for $C_{30}H_{54}O_{21}S$ = 782.2878; M_{found} = 1581.6877 $[2M+NH_4]^+$

1-*O*-(6-Thiobenzyl-hexyl-phosphatidyl)-3,4,5-*O*-tri-benzyl-2,6-*O*-di-2-methyl-naphthyl-*myo*-inositol (89)

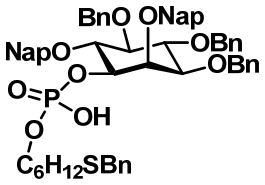

0.021 mmol of *myo*-inositol **87** (0.015 g) and 0.031 mmol of H-phosphonate **88** (0.012 g) were reacted according to phosphate formation (Method 19). Product **89** was obtained in 43% yield (8.750 µmol, 0.009 g) as colorless oil.

R_f = 0.5 (10% MeOH in DCM)

^{1}H-NMR (600 MHz, $CDCl_3$): δ = 11.69 (s, 1H, phosphate), 7.83 – 7.63 (m, 7H, $H_{Ar.}$), 7.52 – 7.05 (m, 22H, $H_{Ar.}$), 5.12 – 5.03 (m, 2H, -CH_2-), 4.93 (d, *J* = 11.4 Hz, 1H, -CH_2-), 4.88 – 4.79 (m, 2H, -CH_2-), 4.74 (d, *J* = 10.8 Hz, 1H, -CH_2-), 4.66 – 4.55 (m, 3H), 4.18 – 4.01 (m, 3H), 3.82 - 3.74 (m, 1H), 3.63 – 3.46 (m, 6H), 2.14 (t, *J* = 7.6 Hz, 2H), 1.57 – 1.28 (m, 4H), 1.27 – 1.17 (m, 8H) ppm.

^{13}C-NMR (151 MHz, $CDCl_3$): δ = 139.01 ($C_{Ar.}$), 138.79 ($C_{Ar.}$), 138.73 ($C_{Ar.}$), 137.32 ($C_{Ar.}$), 137.01 ($C_{Ar.}$), 133.40 ($C_{Ar.}$), 133.35 ($C_{Ar.}$), 132.88 ($C_{Ar.}$), 128.92 ($C_{Ar.}$), 128.55 ($C_{Ar.}$), 128.41 ($C_{Ar.}$), 128.23 ($C_{Ar.}$), 128.06 ($C_{Ar.}$), 127.96 ($C_{Ar.}$), 127.80 ($C_{Ar.}$), 127.74 ($C_{Ar.}$), 127.54 ($C_{Ar.}$), 126.96 ($C_{Ar.}$), 126.19 ($C_{Ar.}$), 125.98 ($C_{Ar.}$), 125.92 ($C_{Ar.}$), 125.76 ($C_{Ar.}$), 125.60 ($C_{Ar.}$), 83.53, 81.78, 81.14, 81.04, 76.06, 75.96, 75.35, 75.05, 72.55, 45.89, 36.32, 31.35, 29.84, 29.14, 28.72, 25.32 ppm.

^{31}P-NMR (162 MHz, $CDCl_3$): δ = -0.95 ppm.

ESI-MS: m/z M_{calcd} for $C_{62}H_{65}O_9PS$ = 1016.4087; M_{found} = 1015.4209 $[M]^-$

Polarimeter: $[\alpha]_D^{20}$ = 12.22 (c = 0.1 g/L in $CHCl_3$)

FT-IR: 3411.52, 2929.16, 2854.26, 2172.49, 2143.00, 1984.45, 1724.55, 1455.02, 1363.14, 1205.15, 1070.42, 824.77, 738.60, 698.07 cm^{-1}.

1-*O*-(6-Thio-hexyl-phosphatidyl)-*myo*-inositol (90)

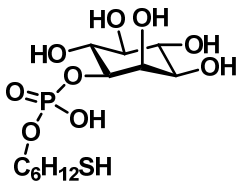

8.750 µmol of phosphate **89** (8.900 mg) was reacted according to Birch reduction (Method 22). Product **90** was obtained in 6% yield (0.531 µmol, 0.2 mg) as white powder by using sephadex G15 size exclusion chromatography using 5% ethanol in water as eluent.

^{1}H-NMR (400 MHz, D_2O): δ = 4.05 (d, *J* = 2.9 Hz, 1H), 3.73 (d, *J* = 7.6 Hz, 3H), 3.56 (t, *J* = 9.6 Hz, 1H), 3.46 (t, *J* = 9.6 Hz, 1H), 3.36 (dd, *J* = 9.9 Hz, 2.8 Hz, 1H), 3.14 (t, *J* = 9.4 Hz, 1H), 2.58 (t, *J* = 7.2 Hz, 2H), 1.55 - 1.42 (m, 4H), 1.23 (s, 4H) ppm.

^{13}C-NMR (151 MHz, D_2O): δ = 78.71, 76.56, 74.82, 73.97, 73.85, 73.36, 68.97, 40.78, 32.29, 30.88, 29.87, 27.11 ppm.

^{31}P-NMR (162 MHz, D_2O): δ = -0.05 ppm.

ESI-MS: m/z M_{calcd} for $C_{12}H_{25}O_9PS$ = 376.0957; M_{found} = 749.1682 $[2M]^-$

Allyl-2-*O*-acetyl-4-*O*-benzyl-6-*O*-*tert*-butyldiphenylsilyl-(2,3,4-*O*-tri-benzyl-6-*O*-chloroacetyl-D-galactopyranosyl-α1→3)-α-D-mannopyranoside (95)

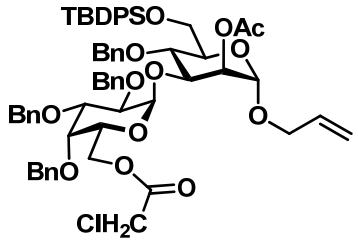

0.127 mmol of thiodonor **94** (0.073 g) and 0.085 mmol of glycosylacceptor **81** (0.050 g) were dissolved in ether and reacted according to glycosylation with thiodonor (Method 17) using TMSOTf at -11°C. Product **95** was obtained in 59% yield (0.050 mmol, 0.055 g) as colorless oil.

R_f = 0.45 (4:1, Hex:EA)

^{1}H-NMR (400 MHz, $CDCl_3$): δ = 7.72 – 7.61 (m, 2H, $H_{Ar.}$), 7.60 – 7.50 (m, 2H, $H_{Ar.}$), 7.39 – 7.14 (m, 10H), 7.15 – 7.04 (m, 14H, $H_{Ar.}$), 6.98 (dd, *J* = 6.7 Hz, 2.8 Hz, 2H, $H_{Ar.}$), 5.79 (dddd, *J* = 17.1 Hz, 10.3 Hz, 6.7 Hz, 5.3 Hz, 1H, Allyl-2), 5.23 (d, *J* = 3.6 Hz, 1H, Gal-1), 5.18 (dq, *J* = 17.1 Hz, 1.5 Hz, 1H, Allyl-3), 5.13 (dd, *J* = 10.3 Hz, 1.5 Hz, 1H, Allyl-3), 5.09 (dd, *J* = 3.4 Hz, 1.8 Hz, 1H, Man-2), 4.96 (d, *J* = 11.5 Hz, 1H, -CH_2-), 4.86 (d, *J* = 11.6 Hz, 1H, -CH_2-), 4.77 (d, *J* = 1.7 Hz, 1H, Man-1), 4.76 – 4.67 (m, 1H, -CH_2-), 4.65 (d, *J* = 12.0 Hz, 1H, -CH_2-), 4.53 (d, *J* = 4.3 Hz, 1H, , -CH_2-), 4.52 – 4.46 (m, 1H, -CH_2-), 4.23 – 4.13 (m, 3H), 4.08 – 3.93 (m, 8H), 3.91 – 3.72 (m, 6H), 3.61 (ddd, *J* = 9.8 Hz, 3.9 Hz, 1.7 Hz, 1H), 2.01 (s, 3H, -CH_3), 1.00 (s, 9H, -C(-CH_3)$_3$) ppm.

^{13}C-NMR (101 MHz, $CDCl_3$): δ = 170.72 (C=O), 167.16 (C=O), 138.71 ($C_{Ar.}$), 138.55 ($C_{Ar.}$), 138.40 ($C_{Ar.}$), 138.15 ($C_{Ar.}$), 136.06 ($C_{Ar.}$), 135.63 ($C_{Ar.}$), 133.90 (Allyl-2), 133.44 ($C_{Ar.}$), 133.17 ($C_{Ar.}$), 129.73 ($C_{Ar.}$), 129.69 ($C_{Ar.}$), 128.59 ($C_{Ar.}$), 128.55 ($C_{Ar.}$), 128.54 ($C_{Ar.}$), 128.52 ($C_{Ar.}$), 128.49 ($C_{Ar.}$), 128.44 ($C_{Ar.}$), 128.33 ($C_{Ar.}$), 128.31 ($C_{Ar.}$), 128.26 ($C_{Ar.}$), 128.02 ($C_{Ar.}$), 127.76 ($C_{Ar.}$), 127.74 ($C_{Ar.}$), 127.66 ($C_{Ar.}$), 127.63 ($C_{Ar.}$), 127.59 ($C_{Ar.}$), 127.45 ($C_{Ar.}$), 127.31

($C_{Ar.}$), 127.01 ($C_{Ar.}$), 118.65 (Allyl-3), 99.78 (Gal-1, J = 170.6 Hz), 96.28 (Man-1), 78.81, 77.48, 77.16, 76.84, 75.81, 75.64, 74.84, 74.59, 74.43, 74.35, 73.52, 73.03, 72.93, 72.41, 69.18, 67.94, 65.69, 62.74, 40.97, 26.89, 21.22, 19.50 ppm.

ESI-MS: m/z M_{calcd} for $C_{63}H_{71}ClO_{13}Si$ = 1098.4352; M_{found} = 1121.4280 $[M+Na]^+$

Polarimeter: $[\alpha]_D^{20}$ = 63.62 (c = 0.1 g/L in $CHCl_3$)

FTIR: 3032.85, 2932.53, 2859.53, 1746.71, 1497.87, 1455.37, 1429.11, 1361.32, 1287.92, 1238.44, 1134.26, 1103.38, 1065.93, 1028.84, 992.14, 932.15, 863.08, 824.28, 738.19, 699.66 cm^{-1}.

H-2-*O*-acetyl-4-*O*-benzyl-6-*O*-*tert*-butyldiphenylsilyl-(2,3,4-*O*-tri-benzyl-6-*O*-chloroacetyl-D-galactopyranosyl-α1→3)-α-D-mannopyranoside (96)

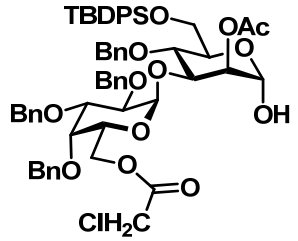

0.050 mmol of disaccharide **95** (0.055 g) was reacted according to allyl removal via isomerization and hydrolysis (Method 14). Product **96** was obtained in 65% yield (0.032 mmol, 0.034 g) as colorless oil.

$\mathbf{R_f}$ = 0.1 (4:1, Hex:EA)

^{1}H-NMR (400 MHz, $CDCl_3$): δ = 7.66 – 7.62 (m, 2H, $H_{Ar.}$), 7.55 (dt, J = 6.8 Hz, 1.4 Hz, 2H, $H_{Ar.}$), 7.35 – 7.17 (m, 16H, $H_{Ar.}$), 7.16 – 6.98 (m, 10H, $H_{Ar.}$), 5.25 (d, J = 3.6 Hz, 1H, Gal-1), 5.13 – 5.09 (m, 2H, Man-1, Man-2), 5.00 (d, J = 11.6 Hz, 1H, -CH_2-), 4.86 (d, J = 11.6 Hz, 1H, -CH_2-), 4.77 – 4.67 (m, 2H, -CH_2-), 4.62 (d, J = 12.0 Hz, 1H, -CH_2-), 4.57 – 4.48 (m, 3H, -CH_2-), 4.27 – 4.17 (m, 2H), 4.10 – 4.04 (m, 2H), 4.01 – 3.96 (m, 4H), 3.93 – 3.78 (m, 5H), 3.73 (dd, J = 11.4, 1.7 Hz, 1H), 2.02 (s, 3H, -CH_3), 1.01 (s, 9H, -C(-CH_3)$_3$) ppm.

^{13}C-NMR (101 MHz, $CDCl_3$): δ = 170.77 (C=O), 167.26 (C=O), 138.84 ($C_{Ar.}$), 138.56 ($C_{Ar.}$), 138.37 ($C_{Ar.}$), 138.14 ($C_{Ar.}$), 136.08 ($C_{Ar.}$), 135.62 ($C_{Ar.}$), 133.95 ($C_{Ar.}$), 133.20 ($C_{Ar.}$), 129.77 ($C_{Ar.}$), 129.72 ($C_{Ar.}$), 128.61 ($C_{Ar.}$), 128.55 ($C_{Ar.}$), 128.34 ($C_{Ar.}$), 128.26 ($C_{Ar.}$), 128.03 ($C_{Ar.}$), 127.78 ($C_{Ar.}$), 127.74 ($C_{Ar.}$), 127.67 ($C_{Ar.}$), 127.63 ($C_{Ar.}$), 127.61 ($C_{Ar.}$), 127.46 ($C_{Ar.}$), 127.27 ($C_{Ar.}$), 126.85 ($C_{Ar.}$), 126.73 ($C_{Ar.}$), 99.71 (Gal-1), 92.37 (Man-1), 78.78, 77.48, 77.36, 77.16, 76.84, 75.62, 75.04, 74.72, 74.53, 74.46, 74.33, 73.45, 73.05, 72.98, 72.55, 69.17, 65.64, 62.80, 40.93, 26.95, 21.23, 19.55 ppm.

ESI-MS: m/z M_{calcd} for $C_{60}H_{67}ClO_{13}Si$ = 1058.4039; M_{found} = 1081.3901 $[M+Na]^+$

Polarimeter: $[\alpha]_D^{20} = 40.07$ (c = 0.1 g/L in $CHCl_3$)

FTIR: 2934.63, 1745.15, 1455.60, 1241.04, 1061.56 cm^{-1}.

Trichloracetamido-2-*O*-acetyl-4-*O*-benzyl-6-*O*-*tert*-butyldiphenylsilyl-(2,3,4-*O*-tri-benzyl-6-*O*-chloroacetyl-D-galactopyranosyl-α1→3)-α-D-mannopyranoside (97)

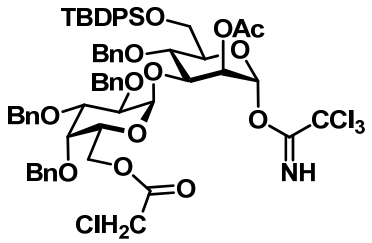

0.032 mmol of lactol **96** (0.034 g) was reacted according to imidate formation (Method 15). Product **97** was obtained in 84% yield (0.027 mmol, 0.033 g) as colorless oil.

$\mathbf{R_f}$ = 0.45 (4:1, Hex:EA)

^{1}H-NMR (400 MHz, $CDCl_3$): δ = 8.62 (s, 1H, =NH), 7.63 (dt, *J* = 6.9 Hz, 1.5 Hz, 2H, $H_{Ar.}$), 7.58 – 7.53 (m, 2H, $H_{Ar.}$), 7.37 – 7.01 (m, 26H), 6.29 (d, *J* = 2.0 Hz, 1H, Man-1), 5.24 (d, *J* = 2.3 Hz, 1H, Gal-1), 5.13 – 5.07 (m, 2H, Man-2, $-CH_2-$), 4.89 (d, *J* = 11.4 Hz, 1H, $-CH_2-$), 4.82 – 4.63 (m, 4H, $-CH_2-$), 4.58 – 4.50 (m, 3H), 4.19 – 4.16 (m, 2H), 4.10 – 3.75 (m, 11H), 2.05 (s, 3H, $-CH_3$), 1.00 (s, 9H, $-C(-CH_3)_3$) ppm.

6-(Thiobenzyl-hexyl)-2-*O*-acetyl-4-*O*-benzyl-6-*O*-*tert*-butyldiphenylsilyl-(2,3,4-*O*-tri-benzyl-6-*O*-chloroacetyl-D-galactopyranosyl-α1→3)-α-D-mannopyranoside (98)

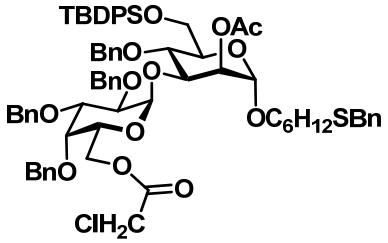

0.027 mmol of imidate **97** (0.033 g) and 0.054 mmol of 6-Thiobenzylhexanol **35** (0.012 g) were dissolved in DCM and reacted according to glycosylation with imidate donor (Method 16) using TMSOTf at 0°C. Product **98** was obtained in quantitative yield (0.027 mmol, 0.034 g) as colorless oil.

$\mathbf{R_f}$ = 0.45 (4:1, Hex:EA)

^{1}H-NMR (400 MHz, $CDCl_3$): δ = 7.64 (dt, *J* = 6.7 Hz, 1.5 Hz, 2H, $H_{Ar.}$), 7.57 (dt, *J* = 6.8 Hz, 1.4 Hz, 2H, $H_{Ar.}$), 7.35 – 7.06 (m, 29H, $H_{Ar.}$), 7.00 – 6.96 (m, 2H, $H_{Ar.}$), 5.19 (d, *J* = 3.6 Hz, 1H, Gal-1), 5.04 (dd, *J* = 3.4 Hz, 1.7 Hz, 1H, Man-1), 4.98 (d, *J* = 11.4 Hz, 1H, $-CH_2-$), 4.87 (d, *J* = 11.6 Hz, 1H, $-CH_2-$), 4.77 – 4.68 (m, 4H, $-CH_2-$, Man-1), 4.66 (d, *J* = 12.1 Hz,

1H, -CH_2-), 4.55 – 4.50 (m, 2H, -CH_2-), 4.47 (d, *J* = 11.5 Hz, 1H, -CH_2-), 4.22 – 4.08 (m, 2H), 4.04 – 3.73 (m, 13H), 3.66 – 3.40 (m, 2H), 3.29 (dt, *J* = 9.7 Hz, 6.8 Hz, 1H), 2.37 – 2.27 (m, 4H, -CH_2-), 2.00 (s, 3H, -CH_3), 1.57 – 1.12 (m, 8H), 0.99 (s, 9H) ppm.

^{13}C-NMR (101 MHz, $CDCl_3$): δ = 170.75 (C=O), 167.04 (C=O), 138.75 ($C_{Ar.}$), 138.57 ($C_{Ar.}$), 138.42 ($C_{Ar.}$), 138.19 ($C_{Ar.}$), 136.06 ($C_{Ar.}$), 135.65 ($C_{Ar.}$), 133.92 ($C_{Ar.}$), 133.23 ($C_{Ar.}$), 129.73 ($C_{Ar.}$), 129.69 ($C_{Ar.}$), 128.94 ($C_{Ar.}$), 128.58 ($C_{Ar.}$), 128.56 ($C_{Ar.}$), 128.54 ($C_{Ar.}$), 128.34 ($C_{Ar.}$), 128.28 ($C_{Ar.}$), 128.25 ($C_{Ar.}$), 128.00 ($C_{Ar.}$), 127.76 ($C_{Ar.}$), 127.74 ($C_{Ar.}$), 127.71 ($C_{Ar.}$), 127.63 ($C_{Ar.}$), 127.57 ($C_{Ar.}$), 127.47 ($C_{Ar.}$), 127.34 ($C_{Ar.}$), 127.14 ($C_{Ar.}$), 127.03 ($C_{Ar.}$), 126.98 ($C_{Ar.}$), 100.03 (Gal-1), 97.10 (Man-1), 78.80, 77.48, 77.36, 77.16, 76.84, 76.62, 75.72, 74.79, 74.69, 74.45, 74.29, 73.54, 73.06, 72.78, 72.60, 69.11, 67.68, 65.41, 64.61, 62.85, 40.87, 36.44, 36.38, 31.37, 29.85, 29.37, 29.19, 28.75, 28.60, 28.58, 26.91, 25.84, 25.68, 21.24, 19.51 ppm.

ESI-MS: m/z M_{calcd} for $C_{73}H_{85}ClO_{13}SSi$ = 1264.5169; M_{found} = 1287.5035 $[M+Na]^+$

Polarimeter: $[\alpha]_D^{20}$ = 65.75 (c = 0.1 g/L in $CHCl_3$)

FTIR: 3032.53, 2932.25, 2859.17, 2211.79, 2162.52, 1743.16, 1496.93, 1454.99, 1429.28, 1364.17, 1239.58, 1135.16, 1101.34, 1059.38, 1028.84, 824.05, 798.05, 737.48, 700.11 cm^{-1}.

6-(Thiobenzyl-hexyl)-4-*O*-benzyl-(2,3,4-*O*-tri-benzyl-D-galactopyranosyl-α1→3)-α-D-mannopyranoside (99)

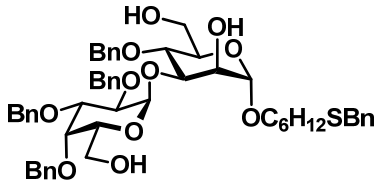

0.027 mmol of diester **98** (0.034 g) was reacted according to acid mediated *O*-acetyl removal (Method 5). Product **99** was obtained in 48% (0.013 mmol, 0.012 g) as colorless oil.

R_f = 0.2 (2:1, Hex:EA)

^{1}H-NMR (400 MHz, $CDCl_3$): δ = 7.34 – 7.07 (m, 25H, $H_{Ar.}$), 5.06 – 5.01 (m, 2H, -CH_2-, Gal-1), 4.86 (d, *J* = 11.7 Hz, 1H, -CH_2-), 4.77 – 4.58 (m, 5H, -CH_2-, Man-1), 4.53 – 4.48 (m, 2H, -CH_2-), 4.09 – 3.99 (m, 3H), 3.90 – 3.79 (m, 3H), 3.78 – 3.65 (m, 3H), 3.62 (s, 2H), 3.60 – 3.43 (m, 3H), 3.32 – 3.21 (m, 2H), 2.33 (t, *J* = 7.3 Hz, 2H), 1.52 – 1.41 (m, 4H), 1.31 -1.17 (m, 4H) ppm.

^{13}C-NMR (101 MHz, $CDCl_3$): δ = 138.52 ($C_{Ar.}$), 138.41 ($C_{Ar.}$), 138.40 ($C_{Ar.}$), 138.20 ($C_{Ar.}$), 128.79 ($C_{Ar.}$), 128.48 ($C_{Ar.}$), 128.42 ($C_{Ar.}$), 128.37 ($C_{Ar.}$), 128.34 ($C_{Ar.}$), 128.32 ($C_{Ar.}$), 127.91 ($C_{Ar.}$), 127.83 ($C_{Ar.}$), 127.67 ($C_{Ar.}$), 127.58 ($C_{Ar.}$), 127.57 ($C_{Ar.}$), 127.47 ($C_{Ar.}$), 126.84 ($C_{Ar.}$), 100.04 (Gal-1), 98.65 (Man-1), 82.45, 78.52, 77.32, 77.20, 77.00, 76.91, 76.68, 75.25, 74.88,

74.28, 73.32, 73.21, 73.11, 71.65, 71.41, 69.69, 67.70, 63.10, 61.92, 36.23, 31.24, 29.23, 29.04, 28.57, 25.74 ppm.

ESI-MS: m/z M_{calcd} for $C_{53}H_{64}O_{11}S$ = 908.4169; M_{found} = 931.4075 $[M+Na]^+$

Polarimeter: $[\alpha]_D^{20}$ = 30.76 (c = 0.1 g/L in $CHCl_3$)

FTIR: 3393.73, 3032.10, 2930.62, 2163.30, 2036.82, 1497.01, 1454.56, 1352.26, 1096.52, 1068.04, 1043.31, 738.63, 698.46, 682.08, 660.41 cm^{-1}.

6-(Thio-hexyl)-D-galactopyranosyl-α1→3-α-D-mannopyranoside (100)

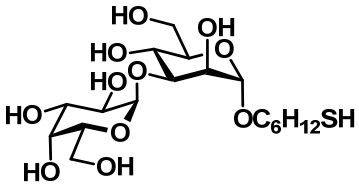

0.013 mmol of triol **99** (0.012 g) was reacted according to Birch reduction (Method 22). Product **100** was obtained in 5% (0.654 µmol, 0.030 mg) as white solid by using sephadex G15 size exclusion chromatography using 5% ethanol in water as eluent.

^{1}H-NMR (400 MHz, D_2O): δ = 5.12 (d, *J* = 4.1 Hz, 1H, Gal-1), 4.72 (1H, Man-1), 4.01 – 3.21 (m, 16H), 1.51 – 1.42 (m, 4H), 1.24 – 1.05 (m, 4H) ppm.

^{13}C-NMR (151 MHz, D_2O): δ = 99.98 (Gal-1), 99.42 (Man-1), 72.69, 71.22, 69.07, 68.55, 66.39, 65.96, 64.64, 30.71, 21.94 ppm.

ESI-MS: m/z M_{calcd} for $C_{18}H_{34}O_{11}S$ = 458.1822; M_{found} = 937.3439 $[2M+Na]^+$

Thioethyl-2,3,4-tri-*O*-benzyl-6-*O*-2-methyl-naphthyl-α-D-galactopyranoside (102)

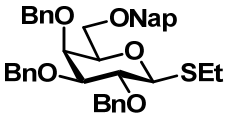

1.213 mmol of alcohol **101** (0.600 g) was reacted according to Williamson ether formation (Method 9) using naphthylmethyl bromide. Product **102** was obtained in 70% (0.851 mmol, 0.540 g) as colorless oil.

R_f = 0.8 (6:1, Hex:EA)

^{1}H-NMR (600 MHz, acetone-d_6): δ = 7.92 – 7.82 (m, 4H, $H_{Ar.}$), 7.53 – 7.46 (m, 3H, $H_{Ar.}$), 7.45 – 7.39 (m, 4H, $H_{Ar.}$), 7.35 – 7.20 (m, 11H, $H_{Ar.}$), 4.96 (d, *J* = 11.4 Hz, 1H, -CH_2-), 4.86 – 4.81 (m, 3H, -CH_2-, -CH_2-, -CH_2-), 4.74 (d, *J* = 11.9 Hz, 1H, -CH_2-), 4.72 (d, *J* = 12.2 Hz, 1H, -CH_2-), 4.65 (d, *J* = 12.1 Hz, 1H, -CH_2-), 4.61 (d, *J* = 11.4 Hz, 1H, -CH_2-), 4.52 (d, *J* = 9.3 Hz, 1H, Gal-1), 4.13 (d, *J* = 2.5 Hz, 1H, Gal-4), 3.83 – 3.75 (m, 2H, Gal-2, Gal-5),

3.73 – 3.71 (m, 2H, Gal-6, Gal-3), 3.68 (dd, *J* = 9.4, 6.1 Hz, 1H, Gal-6), 2.78 – 2.72 (m, 1H, -CH_2-), 2.69 -2.63 (m, 1H, -CH_2-), 1.25 (t, *J* = 7.4 Hz, 3H, -CH_3) ppm.

^{13}C-NMR (151 MHz, acetone-d_6): δ = 140.28 ($C_{Ar.}$), 140.06 ($C_{Ar.}$), 139.96 ($C_{Ar.}$), 137.23 ($C_{Ar.}$), 134.40 ($C_{Ar.}$), 134.08 ($C_{Ar.}$), 129.25 ($C_{Ar.}$), 129.08 ($C_{Ar.}$), 129.02 ($C_{Ar.}$), 128.99 ($C_{Ar.}$), 128.92 ($C_{Ar.}$), 128.84 ($C_{Ar.}$), 128.72 ($C_{Ar.}$), 128.67 ($C_{Ar.}$), 128.58 ($C_{Ar.}$), 128.39 ($C_{Ar.}$), 128.32 ($C_{Ar.}$), 128.26 ($C_{Ar.}$), 127.33 ($C_{Ar.}$), 127.13 ($C_{Ar.}$), 126.95 ($C_{Ar.}$), 126.86 ($C_{Ar.}$), 85.71 (Gal-1), 85.01 (Gal-3), 79.54 (Gal-2), 77.95 (Gal-5), 75.98 (-CH_2-), 75.49 (-CH_2-), 75.43 (Gal-4), 73.98 (-CH_2-), 73.15 (-CH_2-), 70.05 (Gal-6), 24.94 (-CH_2-), 15.86 (-CH_3) ppm.

ESI-MS: m/z M_{calcd} for $C_{40}H_{42}O_5S$ = 634.2753; M_{found} = 657.2623 $[M+Na]^+$

Polarimeter: $[\alpha]_D^{20}$ = -32.58 (c = 0.1 g/L in $CHCl_3$)

FTIR: 2864.93, 1741.59, 1455.13, 1362.19, 1211.26, 1095.14, 817.33, 734.31, 698.62 cm^{-1}.

Allyl-2-*O*-acetyl-4-*O*-benzyl-6-*O*-*t*ert-butyldiphenylsilyl-(2,3,4-*O*-tri-benzyl-6-*O*-2-methyl-naphthyl-D-galactopyranosyl-α/β1→3)-α-D-mannopyranoside (103)

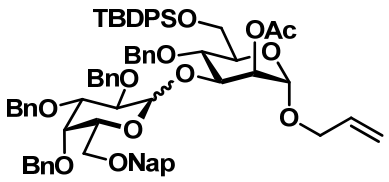

0.237 mmol of thiodonor **102** (0.150 g) and 0.169 mmol of glycosylacceptor **81** (0.100 g) were dissolved in ether and reacted according to glycosylation with thiodonor (Method 17) using TMSOTf at -11°C. Product **103** was obtained in quantitative yield (0.169 mmol, 0.197 g) as colorless oil. The product was isolated as a mixture of anomeres and was characterized accordingly.

R_f = 0.45 (6:1, Hex:EA)

^{1}H-NMR (400 MHz, $CDCl_3$): δ = 8.08 – 7.60 (m, 7H, $H_{Ar.}$), 7.60 – 6.92 (m, 30H, $H_{Ar.}$), 5.83 (dq, *J* = 10.6 Hz, 5.7 Hz, 1H, Allyl-2), 5.35 (s, β-H-Gal-1), 5.31 (s, 1H), 5.22 (d, *J* = 17.3 Hz, 1H), 5.13 (d, *J* = 10.2 Hz, 1H), 5.09 – 4.91 (m, 5H), 4.88 – 4.78 (m, 2H), 4.74 (s, 2H), 4.15 – 3.85 (m), 3.77 – 3.48 (m), 1.85 (s, 3H, -CH_3), 1.12 (s, 9H, -C(-CH_3)$_3$) ppm.

^{13}C-NMR (101 MHz, $CDCl_3$): δ = 170.64 (C=O), 139.00 ($C_{Ar.}$), 138.91 ($C_{Ar.}$), 138.71 ($C_{Ar.}$), 138.59 ($C_{Ar.}$), 138.53 ($C_{Ar.}$), 135.97 ($C_{Ar.}$), 135.63 ($C_{Ar.}$), 135.47 ($C_{Ar.}$), 133.96 ($C_{Ar.}$), 133.61 (Allyl-2), 133.27 ($C_{Ar.}$), 133.07 ($C_{Ar.}$), 129.64 ($C_{Ar.}$), 128.36 ($C_{Ar.}$), 128.32 ($C_{Ar.}$), 128.25 ($C_{Ar.}$), 128.17 ($C_{Ar.}$), 127.98 ($C_{Ar.}$), 127.92 ($C_{Ar.}$), 127.85 ($C_{Ar.}$), 127.74 ($C_{Ar.}$), 127.72 ($C_{Ar.}$), 127.59 ($C_{Ar.}$), 127.54 ($C_{Ar.}$), 127.43 ($C_{Ar.}$), 127.38 ($C_{Ar.}$), 127.29 ($C_{Ar.}$), 126.86 ($C_{Ar.}$), 126.64 ($C_{Ar.}$), 126.14 ($C_{Ar.}$), 126.04 ($C_{Ar.}$), 125.96 ($C_{Ar.}$), 125.92 ($C_{Ar.}$), 117.81 (Allyl-3), 100.77

(β-Gal-1), 96.11 (Man-1), 93.69 (α-Gal-1), 82.36, 79.50, 78.75, 77.43, 77.11, 76.79, 76.06, 75.18, 75.05, 74.85, 74.77, 74.67, 73.81, 73.71, 73.53, 73.39, 72.87, 72.80, 72.59, 69.79, 69.67, 69.06, 68.27, 67.97, 62.91, 46.74, 42.78, 42.58, 26.82, 24.90, 20.86, 19.76, 19.47 ppm.

Allyl-2-*O*-acetyl-4-*O*-benzyl-6-*O*-*t*ert-butyldiphenylsilyl-(2,3,4-*O*-tri-benzyl-D-galactopyranosyl-α1→3)-α-D-mannopyranoside (104)

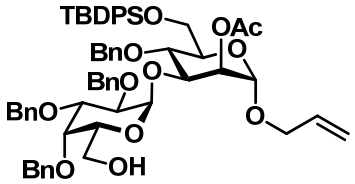

To as solution of disaccharide **103** (0.327 mmol, 0.380 g) in a 10:1 mixture of DCM and water was added DDQ (0.490 mmol, 0.111 g). After 3 h sat. $NaHCO_3$ solution was added and the organic layer was washed with water, dried over Na_2SO_4, filtered and concentrated. The residue was purified by silica gel column chromatography to give product **104** in 20% (0.065 mmol, 0.067 g) as colorless oil.

R_f = 0.45 (4:1, Hex:EA)

^{1}H-NMR (400 MHz, $CDCl_3$): δ = 7.62 (dd, *J* = 26.5 Hz, 7.2 Hz, 4H, $H_{Ar.}$), 7.37 – 6.99 (m, 26H, $H_{Ar.}$), 5.78 (ddd, *J* = 15.8 Hz, 10.5 Hz, 5.1 Hz, 1H, Allyl-2), 5.18 – 5.14 (m, 2H, Man-1, Man-2), 5.11 – 5.04 (m, 3H, -CH_2-), 4.88 (d, *J* = 11.6 Hz, 1H, -CH_2-), 4.81 – 4.63 (m, 5H, Gal-1), 4.59 - 4.54 (m, 2H, -CH_2-, -CH_2-), 4.48 (d, *J* = 11.3 Hz, 1H, -CH_2-), 4.14 (d, *J* = 9.7 Hz, 1H), 4.08 – 3.94 (m, 3H), 3.92 - 3.75 (m, 7H), 3.64 -3.57 (m, 2H), 3.48 – 3.45 (m, 1H), 2.02 (s, 3H), 1.00 (s, 9H) ppm.

^{13}C-NMR (101 MHz, $CDCl_3$): δ = 171.14 (C=O), 138.85 ($C_{Ar.}$), 138.75 ($C_{Ar.}$), 138.49 ($C_{Ar.}$), 138.35 ($C_{Ar.}$), 136.06 ($C_{Ar.}$), 135.64 ($C_{Ar.}$), 133.96 ($C_{Ar.}$), 133.69 (Allyl-2), 133.22 ($C_{Ar.}$), 129.71 ($C_{Ar.}$), 129.67 ($C_{Ar.}$), 128.62 ($C_{Ar.}$), 128.58 ($C_{Ar.}$), 128.51 ($C_{Ar.}$), 128.31 ($C_{Ar.}$), 128.05 ($C_{Ar.}$), 127.86 ($C_{Ar.}$), 127.75 ($C_{Ar.}$), 127.66 ($C_{Ar.}$), 127.63 ($C_{Ar.}$), 127.53 ($C_{Ar.}$), 127.39 ($C_{Ar.}$), 127.33 ($C_{Ar.}$), 117.79 (Allyl-3), 100.20 (Man-1), 96.23 (Gal-1), 78.82, 77.79, 77.48, 77.16, 76.84, 76.12, 74.93, 74.87, 74.54, 74.34, 73.41, 73.04, 72.91, 72.58, 71.47, 68.12, 62.82, 62.40, 26.89, 21.34, 19.50 ppm.

ESI-MS: m/z M_{calcd} for $C_{61}H_{70}O_{12}Si$ = 1022.4637; M_{found} = 1045.4498 $[M+Na]^+$

Polarimeter: $[\alpha]_D^{20}$ = 54.18 (c = 0.1 g/L in $CHCl_3$)

FTIR: 3449.45, 3032.05, 2930.51, 2164.95, 2130.63, 2012.18, 1743.78, 1497.81, 1455.35, 1429.14, 1366.13, 1235.98, 1105.92, 1056.53, 1029.72, 823.05, 740.02, 699.91, 671.70 cm^{-1}.

Allyl-2-*O*-acetyl-4-*O*-benzyl-6-*O*-*t*ert-butyldiphenylsilyl-(-(2,3,4-*O*-tri-benzyl-6-*O*-chloroacetyl-D-galactopyranosyl-α1→6)-2,3,4-*O*-tri-benzyl-D-galactopyranosyl-α1→3)-α-D-mannopyranoside (105)

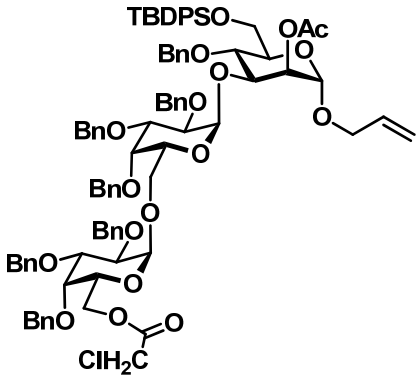

0.095 mmol of thiodonor **94** (0.054 g) and 0.064 mmol of glycosylacceptor **104** (0.065 g) were dissolved in a 1:1 mixture of DCM and ether and reacted according to glycosylation with thiodonor (Method 17) using TMSOTf at -11°C. Product **105** was obtained in 35% yield (0.022 mmol, 0.034 g) as colorless oil.

$\mathbf{R_f}$ = 0.55 (6:1, Hex:EA)

^{1}H-NMR (400 MHz, $CDCl_3$): δ = 7.61 (dd, *J* = 24.0, 6.7 Hz, 4H, $H_{Ar.}$), 7.44 – 6.93 (m, 41H, $H_{Ar.}$), 5.85 – 5.66 (m, 1H, Allyl-2), 5.23 – 4.98 (m, 5H), 4.97 – 4.33 (m, 20H), 4.24 – 3.41 (m, 27H), 1.95 (s, 3H, -CH_3), 0.99 (s, 9H, -C(-CH_3)$_3$) ppm.

^{13}C-NMR (101 MHz, $CDCl_3$): δ = 170.50 (C=O), 167.23 (C=O), 139.02 ($C_{Ar.}$), 138.97 ($C_{Ar.}$), 138.93 ($C_{Ar.}$), 138.71 ($C_{Ar.}$), 138.61 ($C_{Ar.}$), 138.34 ($C_{Ar.}$), 136.08 ($C_{Ar.}$), 135.67 ($C_{Ar.}$), 134.00 ($C_{Ar.}$), 133.73 (Allyl-2), 133.25 ($C_{Ar.}$), 129.72 ($C_{Ar.}$), 129.68 ($C_{Ar.}$), 128.76 ($C_{Ar.}$), 128.64 ($C_{Ar.}$), 128.57 ($C_{Ar.}$), 128.53 ($C_{Ar.}$), 128.49 ($C_{Ar.}$), 128.47 ($C_{Ar.}$), 128.43 ($C_{Ar.}$), 128.42 ($C_{Ar.}$), 128.37 ($C_{Ar.}$), 128.35 ($C_{Ar.}$), 128.31 ($C_{Ar.}$), 128.29 ($C_{Ar.}$), 128.11 ($C_{Ar.}$), 127.97 ($C_{Ar.}$), 127.90 ($C_{Ar.}$), 127.82 ($C_{Ar.}$), 127.76 ($C_{Ar.}$), 127.74 ($C_{Ar.}$), 127.73 ($C_{Ar.}$), 127.65 ($C_{Ar.}$), 127.59 ($C_{Ar.}$), 127.58 ($C_{Ar.}$), 127.51 ($C_{Ar.}$), 127.48 ($C_{Ar.}$), 127.46 ($C_{Ar.}$), 127.33 ($C_{Ar.}$), 127.31 ($C_{Ar.}$), 127.28 ($C_{Ar.}$), 126.51 ($C_{Ar.}$), 117.80 (Allyl-3), 100.79 (Man-1), 98.64 (Gal'-1), 95.98 (Gal-1), 79.11, 79.04, 78.51, 77.37, 77.16, 76.95, 76.44, 76.07, 75.06, 74.91, 74.88, 74.59, 74.25, 73.63, 73.33, 73.28, 72.80, 72.41, 69.84, 68.85, 67.98, 66.61, 65.31, 62.88, 41.04 (-$CClCH_2$), 40.74 (-$CClCH_2$), 26.93 (-*C*(-CH_3)$_3$), 21.27 (-CH_3), 19.50 (-C(-*C*H_3)$_3$) ppm.

ESI-MS: m/z M_{calcd} for $C_{90}H_{99}ClO_{18}Si$ = 1530.6289; M_{found} = 1553.6170 $[M+Na]^+$

Polarimeter: $[\alpha]_D^{20}$ = 24.51 (c = 0.1 g/L in $CHCl_3$)

FTIR: 3033.45, 2931.30, 1743.95, 1497.87, 1455.32, 1360.77, 1240.03, 1136.06, 1102.87, 1058.91, 1028.82, 823.30, 739.62, 699.33 cm^{-1}.

H-2-*O*-acetyl-4-*O*-benzyl-6-*O*-*t*ert-butyldiphenylsilyl-(-(2,3,4-*O*-tri-benzyl-6-*O*-chloroacetyl-D-galactopyranosyl-α1→6)-2,3,4-*O*-tri-benzyl-D-galactopyranosyl-α1→3)-α-D-mannopyranoside (106)

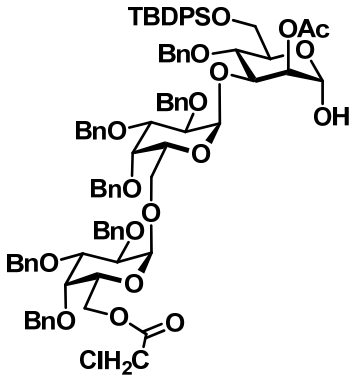

0.014 mmol of trisaccharide **105** (0.022 g) was reacted according to allyl removal via isomerization and hydrolysis (Method 14). Product **106** was obtained in 45% yield (6.430 µmol, 9.600 mg) as colorless oil.

$\mathbf{R_f}$ = 0.1 (4:1, Hex:EA)

^{1}H-NMR (400 MHz, $CDCl_3$): δ = 7.64 (d, *J* = 7.3 Hz, 2H, $H_{Ar.}$), 7.55 (d, *J* = 7.3 Hz, 2H, $H_{Ar.}$), 7.39 – 6.99 (m, 41H, $H_{Ar.}$), 5.29 (s, 1H, Gal-1), 5.06 (s, 1H, Man-1), 4.95 (d, *J* = 11.8 Hz, 1H, Gal'-1), 4.88 – 4.80 (m, 3H, Gal-1, Gal'-6, -CH_2-), 4.76 – 4.42 (m, 13H, -CH_2-), 4.36 – 4.22 (m, 2H), 4.11 (s, 1H, Man-1), 4.06 – 3.61 (m, 16H), 3.08 (d, *J* = 10.1 Hz, Man-6), 2.00 (s, 3H, -CH_3), 0.98 (s, 9H, -C(-CH_3)$_3$) ppm.

^{13}C-NMR (101 MHz, $CDCl_3$): δ = 170.77 (C=O), 167.15 (C=O), 138.92 ($C_{Ar.}$), 138.68 ($C_{Ar.}$), 138.59 ($C_{Ar.}$), 138.46 ($C_{Ar.}$), 138.28 ($C_{Ar.}$), 138.17 ($C_{Ar.}$), 138.05 ($C_{Ar.}$), 137.49 ($C_{Ar.}$), 136.15 ($C_{Ar.}$), 135.66 ($C_{Ar.}$), 129.62 ($C_{Ar.}$), 128.61 ($C_{Ar.}$), 128.57 ($C_{Ar.}$), 128.52 ($C_{Ar.}$), 128.49 ($C_{Ar.}$), 128.39 ($C_{Ar.}$), 128.28 ($C_{Ar.}$), 128.21 ($C_{Ar.}$), 128.15 ($C_{Ar.}$), 128.06 ($C_{Ar.}$), 127.95 ($C_{Ar.}$), 127.82 ($C_{Ar.}$), 127.72 ($C_{Ar.}$), 127.69 ($C_{Ar.}$), 127.67 ($C_{Ar.}$), 127.61 ($C_{Ar.}$), 127.56 ($C_{Ar.}$), 127.38 ($C_{Ar.}$), 127.30 ($C_{Ar.}$), 126.91 ($C_{Ar.}$), 99.10 (Gal-1), 97.28 (Gal-1), 91.96 (Man-1), 79.04, 78.58, 77.48, 77.36, 77.16, 76.84, 75.68, 75.24, 74.90, 74.59, 74.45, 73.89, 73.42, 73.38, 73.34, 73.13, 72.77, 72.60, 69.95, 67.95, 64.89, 62.86, 40.84 (-$CClH_2$), 26.93 (-*C*(-CH_3)$_3$), 21.36 (-C(-*C*H_3)$_3$), 19.57 (-CH_3) ppm.

ESI-MS: m/z M_{calcd} for $C_{87}H_{95}ClO_{18}Si$ = 1490.5976; M_{found} = 1513.5905 $[M+Na]^+$

Polarimeter: $[\alpha]_D^{20}$ = 54.35 (c = 0.1 g/L in $CHCl_3$)

FTIR: 3453.56, 3033.13, 2930.22, 2172.92, 2128.27, 2037.40, 1966.26, 1738.57, 1497.85, 1455.58, 1429.05, 1361.71, 1241.71, 1103.51, 1059.90, 1028.48, 825.28, 739.79, 698.76, 664.27 cm^{-1}.

Trichloracetamido-2-*O*-acetyl-4-*O*-benzyl-6-*O*-*t*ert-butyldiphenylsilyl-(-(2,3,4-*O*-tri-benzyl-6-*O*-chloroacetyl-D-galactopyranosyl-α1→6)-2,3,4-*O*-tri-benzyl-D-galactopyranosyl-α1→3)-α-D-mannopyranoside (107)

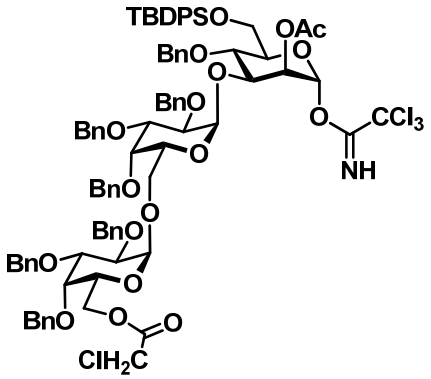

6.430 µmol of lactol **106** (9.600 mg) was reacted according to imidate formation (Method 15). Product **107** was obtained in 95% yield (6.110 µmol, 10.000 mg) as colorless oil.

$\mathbf{R_f}$ = 0.6 (4:1, Hex:EA)

^{1}H-NMR (400 MHz, $CDCl_3$): δ = 8.58 (s, 1H, =NH), 7.67 – 7.55 (m, 5H), 7.38 – 7.01 (m, 40H), 6.25 (s, 1H, Man-1), 5.24 – 5.13 (m, 2H), 4.94 – 4.38 (m, 22H), 4.18 – 3.76 (m, 24H), 3.60 – 3.43 (m, 3H), 1.99 (s, 3H, $-CH_3$), 1.00 (s, 9H, $-C(-CH_3)_3$) ppm.

6-(Thiobenzyl-hexyl)-2-*O*-acetyl-4-*O*-benzyl-6-*O*-*t*ert-butyldiphenylsilyl-(-(2,3,4-*O*-tri-benzyl-6-*O*-chloroacetyl-D-galactopyranosyl-α1→6)-2,3,4-*O*-tri-benzyl-D-galactopyranosyl-α1→3)-α-D-mannopyranoside (108)

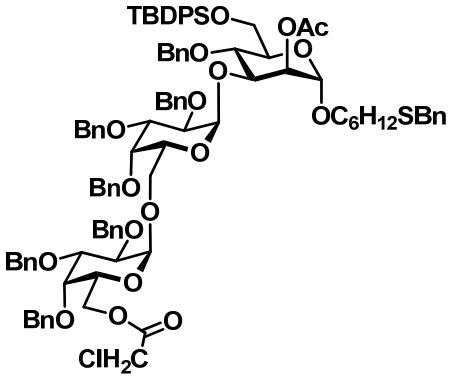

6.110 µmol of imidate **107** (10.000 mg) and 0.031 mmol of 6-Thiobenzylhexanol **35** (0.007 g) were dissolved in DCM and reacted according to glycosylation with imidate donor (Method 16) using TMSOTf at 0°C. Product **108** was obtained in 67% yield (4.120 µmol, 7.000 mg) as colorless oil.

$\mathbf{R_f}$ = 0.50 (4:1, Hex:EA)

^{1}H-NMR (400 MHz, $CDCl_3$): δ = 7.74 – 7.60 (m, 4H, $H_{Ar.}$), 7.42 – 7.07 (m, 46H, $H_{Ar.}$), 5.45 – 4.44 (m, 18H), 4.25 – 3.25 (m, 23H), 2.41 – 2.31 (m, 2H), 2.02 (s, 1.5H, $-CH_3$), 1.99 (s, 1.5H, $-CH_3$), 1.63 – 1.18 (m, 8H), 1.04 (s, 9H, $-C(-CH_3)_3$) ppm.

6-(Thiobenzyl-hexyl)-4-*O*-benzyl-(-(2,3,4-*O*-tri-benzyl-D-galactopyranosyl-α1→6)-2,3,4-*O*-tri-benzyl-D-galactopyranosyl-α1→3)-α-D-mannopyranoside (109)

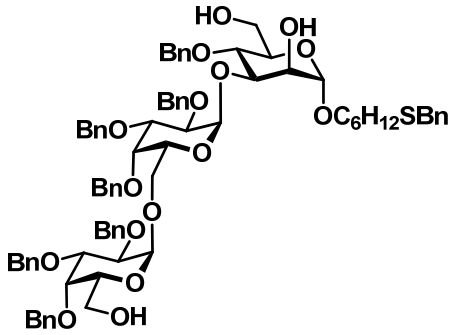

4.120 µmol of trisaccharide **108** (7.000 mg) was reacted according to acid mediated *O*-acetyl removal (Method 5). Product **109** was obtained in 83% (3.430 µmol, 4.600 mg) as colorless oil.

R_f = 0.2 (2:1, Hex:EA)

^{1}H-NMR (400 MHz, $CDCl_3$): δ = 7.72 – 7.69 (m, 1H, $H_{Ar.}$), 7.53 - 7.51 (m, 1H, $H_{Ar.}$), 7.42 – 7.18 (m, 38H, $H_{Ar.}$), 5.12 – 3.08 (m, 39H), 2.36 – 2.33 (m, 2H), 1.42 – 1.19 (m, 8H) ppm.

ESI-MS: m/z M_{calcd} for $C_{80}H_{92}O_{16}S$ = 1340.6106; M_{found} = 1363.5980 $[M+Na]^+$

Polarimeter: $[\alpha]_D^{20}$ = 10.54 (c = 0.1 g/L in $CHCl_3$)

FTIR: 3400.89, 2925.13, 2855.51, 2310.45, 2219.20, 2196.67, 2163.72, 2143.15, 2053.58, 2024.55, 1986.08, 1941.06, 1725.99, 1455.76, 1376.12, 1096.72, 826.02, 737.91, 698.77, 663.35 cm^{-1}.

6-(Thio-hexyl)-(-(-D-galactopyranosyl-α1→6)-D-galactopyranosyl-α1→3)-α-D-mannopyranoside (110)

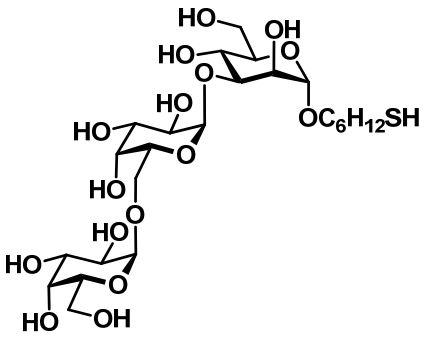

3.430 µmol of triol **109** (4.600 mg) was reacted according to Birch reduction (Method 22). Product **110** was obtained in 19% (0.644 µmol, 0.400 mg) as white solid by using sephadex G15 size exclusion chromatography using 5% ethanol in water as eluent.

^{1}H-NMR (600 MHz, D_2O): δ = 5.12 (d, *J* = 4.1 Hz, 1H, Gal-1), 4.71 (s, 1H, Gal'-1), 4.65 (d, *J* = 1.9 Hz, 1H, Man-1), 4.02 – 3.18 (m, 14H), 2.64 (t, *J* = 7.2 Hz, 2H), 1.60 - 1.45 (m, 4H), 1.31 – 1.23 (m, 4H) ppm.

^{13}C-NMR (151 MHz, D_2O): δ = 100.66, 99.46, 78.43, 72.58, 71.25, 69.67, 69.15, 68.63, 67.70, 65.92, 61.44, 61.21, 60.69, 37.97, 28.06, 27.01, 24.92 ppm.

ESI-MS: m/z M_{calcd} for $C_{24}H_{44}O_{16}S$ = 620.2350; M_{found} = 1261.4429 $[2M+Na]^+$

H-2-*O*-acetyl-4-*O*-benzyl-6-*O*-*tert*-butyldiphenylsilyl-(-(2,3,6-*O*-tri-2-methyl-naphthyl-4-*O*-*para*-methoxy-benzoyl-D-galactopyranosyl-α1→6)-2,3,4-*O*-tri-benzyl-D-galactopyranosyl-α1→3)-α-D-mannopyranoside (113)

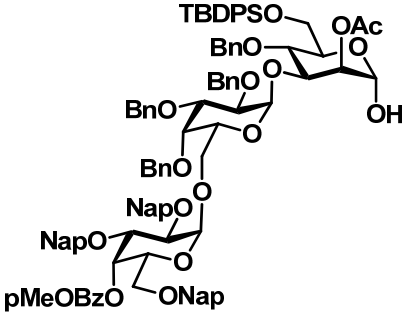

0.137 mmol of compound **112** (0.238 g) was reacted according to allyl removal via isomerization and hydrolysis (Method 14). Product **113** was obtained in 56% yield (0.076 mmol, 0.130 g) as colorless oil.

R_f = 0.1 (4:1, Hex:EA)

^{1}H-NMR (400 MHz, $CDCl_3$): δ = 7.86 – 7.81 (m, 2H, $H_{Ar.}$), 7.75 – 7.49 (m, 17H, $H_{Ar.}$), 7.44 – 6.98 (m, 34H), 6.71 – 6.67 (m, 2H, $H_{Ar.}$), 5.89 – 5.86 (m, 1H, Gal'-4), 5.33 (d, *J* = 3.5 Hz, 1H, Gal'-1, J_{CH} = 172.23 Hz), 5.13 (dd, *J* = 3.3 Hz, 1.9 Hz, 1H, Man-2), 4.95 (d, *J* = 2.2 Hz,

1H, Gal-1, J_{CH} = 170.40 Hz), 4.91 (dd, *J* = 7.7 Hz, 3.5 Hz, 2H, -CH_2-), 4.82 – 4.78 (m, 1H, -CH_2-), 4.74 (d, *J* = 10.9 Hz, 1H, -CH_2-), 4.70 – 4.65 (m, 2H, -CH_2-), 4.64 (d, *J* = 10.6 Hz, 1H, -CH_2-), 4.60 – 4.54 (m, 3H, -CH_2-), 4.53 – 4.45 (m, 3H), 4.37 (dd, *J* = 9.8 Hz, 3.2 Hz, 1H, -CH_2-), 4.28 (dt, *J* = 12.7 Hz, 5.8 Hz, 2H), 4.18 (dd, *J* = 10.1, 3.3 Hz, 1H), 4.12 (t, *J* = 1.9 Hz, 1H, Man-1, J_{CH} = 170.40 Hz), 4.06 – 3.84 (m, 8 H), 3.81 – 3.71 (m, 5H), 3.63 (dd, *J* = 11.4 Hz, 1.6 Hz, 1H), 3.50 (dd, *J* = 6.4 Hz, 3.7 Hz, 2H), 3.20 (dd, *J* = 10.0 Hz, 3.3 Hz, 1H), 1.94 (s, 3H), 0.93 (s, 9H, -C(-CH_3)$_3$) ppm.

^{13}C-NMR (101 MHz, $CDCl_3$): δ = 171.24 (C=O), 170.73 (C=O), 165.59 ($C_{Ar.}$), 163.42 ($C_{Ar.}$), 163.37 ($C_{Ar.}$), 163.33 ($C_{Ar.}$), 138.95 ($C_{Ar.}$), 138.63 ($C_{Ar.}$), 138.42 ($C_{Ar.}$), 138.40 ($C_{Ar.}$), 136.04 ($C_{Ar.}$), 135.86 ($C_{Ar.}$), 135.52 ($C_{Ar.}$), 135.22 ($C_{Ar.}$), 134.83 ($C_{Ar.}$), 134.06 ($C_{Ar.}$), 133.32 ($C_{Ar.}$), 133.15 ($C_{Ar.}$), 133.12 ($C_{Ar.}$), 132.95 ($C_{Ar.}$), 132.94 ($C_{Ar.}$), 131.87 ($C_{Ar.}$), 129.68 ($C_{Ar.}$), 129.49 ($C_{Ar.}$), 128.67 ($C_{Ar.}$), 128.42 ($C_{Ar.}$), 128.35 ($C_{Ar.}$), 128.33 ($C_{Ar.}$), 128.29 ($C_{Ar.}$), 128.27 ($C_{Ar.}$), 128.24 ($C_{Ar.}$), 128.16 ($C_{Ar.}$), 128.11 ($C_{Ar.}$), 128.06 ($C_{Ar.}$), 128.02 ($C_{Ar.}$), 127.96 ($C_{Ar.}$), 127.82 ($C_{Ar.}$), 127.80 ($C_{Ar.}$), 127.74 ($C_{Ar.}$), 127.72 ($C_{Ar.}$), 127.65 ($C_{Ar.}$), 127.62 ($C_{Ar.}$), 127.60 ($C_{Ar.}$), 127.54 ($C_{Ar.}$), 127.52 ($C_{Ar.}$), 127.44 ($C_{Ar.}$), 127.26 ($C_{Ar.}$), 127.13 ($C_{Ar.}$), 127.10 ($C_{Ar.}$), 126.81 ($C_{Ar.}$), 126.70 ($C_{Ar.}$), 126.66 ($C_{Ar.}$), 126.62 ($C_{Ar.}$), 126.34 ($C_{Ar.}$), 126.14 ($C_{Ar.}$), 126.11 ($C_{Ar.}$), 125.98 ($C_{Ar.}$), 125.94 ($C_{Ar.}$), 125.87 ($C_{Ar.}$), 125.83 ($C_{Ar.}$), 125.72 ($C_{Ar.}$), 125.69 ($C_{Ar.}$), 125.65 ($C_{Ar.}$), 122.50 ($C_{Ar.}$), 113.59 ($C_{Ar.}$), 99.10 (Gal'-1), 97.73 (Gal-1), 91.94 (Man-1), 78.91, 77.40, 77.29, 77.09, 76.77, 76.03, 75.99, 75.67, 75.02, 74.87, 74.37, 74.24, 73.71, 73.62, 73.46, 73.28, 73.18, 72.94, 72.62, 71.62, 70.22, 68.66, 68.32, 68.14, 67.72, 62.77, 60.46, 55.45, 29.75, 26.86, 26.80, 21.21, 21.12, 19.45 ppm.

ESI-MS: m/z M_{calcd} for $C_{105}H_{106}O_{19}Si$ = 1698.7098; M_{found} = 1721.6995 $[M+Na]^+$

Polarimeter: $[\alpha]_D^{20}$ = 103.96 (c = 0.1 g/L in $CHCl_3$)

FTIR: 3943.69, 3883.94, 3850.98, 3767.87, 3711.56, 3549.52, 3349.00, 3061.30, 2940.18, 2504.38, 2383.93, 2371.51, 2350.81, 2297.81, 2251.91, 2241.18, 2215.43, 2193.00, 2160.52, 2137.15, 2079.61, 2051.14, 2039.81, 2016.49, 2005.24, 1983.88, 1964.18, 1719.68, 1606.58, 1511.41, 1461.64, 1428.95, 1358.25, 1257.10, 1167.21, 1103.43, 1060.72, 896.19, 855.78, 821.90, 767.42, 733.05, 701.08, 671.32 cm^{-1}.

Trichloracetamido-2-*O*-acetyl-4-*O*-benzyl-6-*O*-*tert*-butyldiphenylsilyl-(-(2,3,6-*O*-tri-2-methyl-naphthyl-4-*O*-*para*-methoxy-benzoyl-D-galactopyranosyl-α1→6)-2,3,4-*O*-tri-benzyl-D-galactopyranosyl-α1→3)-α-D-mannopyranoside (114)

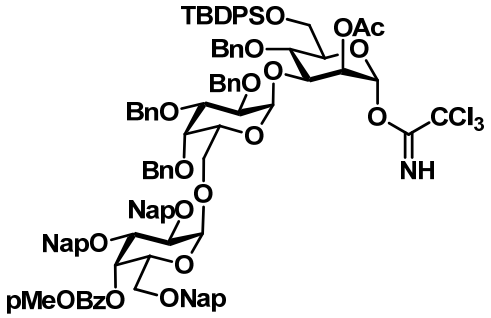

0.076 mmol of lactol **113** (0.130 g) was reacted according to imidate formation (Method 15). Product **114** was obtained in quantitative yield (0.076 mmol, 0.141 g) as colorless oil.

R_f = 0.6 (4:1, Hex:EA)

^{1}H-NMR (400 MHz, acetone-d_6): δ = 7.89 – 7.78 (m, 2H, $H_{Ar.}$), 7.78 – 7.46 (m, 17H, $H_{Ar.}$), 7.43 – 6.98 (m, 34H, $H_{Ar.}$), 6.81 – 6.74 (m, 2H, $H_{Ar.}$), 5.96 – 5.93 (m, 1H, Gal'-4), 5.21 (dd, *J* = 3.3 Hz, 1.9 Hz, 1H, Man-2), 5.19 (d, *J* = 3.5 Hz, 1H, Gal'-1, J_{CH} = 170.18 Hz), 5.13 (d, *J* = 11.5 Hz, 1H, -CH_2-), 5.05 – 5.02 (m, 1H, Man-1, J_{CH} = 175.52 Hz), 4.99 (d, *J* = 3.7 Hz, 1H, Gal-1, J_{CH} = 172.77 Hz), 4.95 (d, *J* = 11.6 Hz, 1H, -CH_2-), 4.87 (d, *J* = 12.1 Hz, 1H, -CH_2-), 4.81 – 4.70 (m, 3 H, -CH_2-), 4.65 – 4.44 (m, 10H, -CH_2-), 4.28 (dt, *J* = 9.7 Hz, 3.7 Hz, 2H), 4.19 – 3.48 (m, 20H), 3.12 (q, *J* = 7.3 Hz, 1H), 1.95 (s, 3H, -CH_3), 0.94 (s, 9H, -C(-CH_3)$_3$) ppm.

1-*O*-Allyl-(-(-(-(4-*O*-*para*-methoxy-benzoyl-2,3,6-*O*-tri-2-methyl-naphthyl-D-galactopyranosyl-α1→6)-2,3,4-*O*-tri-benzyl-D-galactopyranosyl-α1→3)-2-*O*-acetyl-4-*O*-benzly--D-mannopyranosyl-α1→4)-2-azido-2-deoxy-6-*O*-*para*-methoxy-benzyl-3-*O*-2-methyl-naphthyl-D-glucopyranosyl-α1→6)-2,3,4,5-*O*-tetra-2-methyl-naphthyl-*myo*-inositol (117)

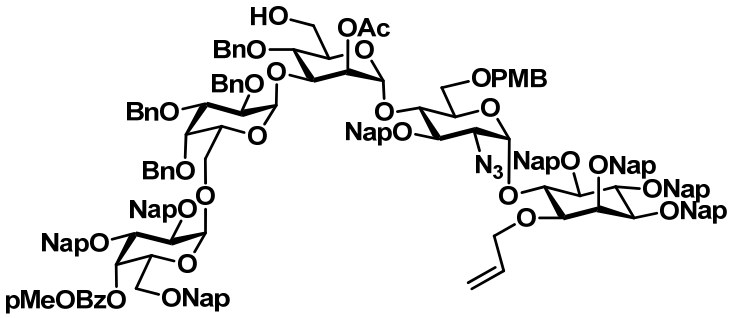

5.150 µmol of pentasaccharide **116** (0.015 g) were reacted according to TBDPS removal (Method 13). Product **117** was isolated and used for the next step.

$\mathbf{R_f}$ = 0.1 (4:1, Hex:EA)

^{1}H-NMR (400 MHz, $CDCl_3$): δ = 7.81 – 6.57 (m, 84H, $H_{Ar.}$), 5.82 (s, 1H, Gal'-4), 5.38 – 2.92 (m, 70H), 1.94 – 1.80 (m, 3H, -CH_3) ppm.

1-(6-Thio-hexyl)-phosphatidyl-(-(-(-(-D-galactopyranosyl-α1→6)-D-galactopyranosyl-α1→3)-D-mannopyranosyl-α1→4)-2-amino-2-deoxy-D-glucopyranosyl-α1→6)-*myo*-inositol (120)

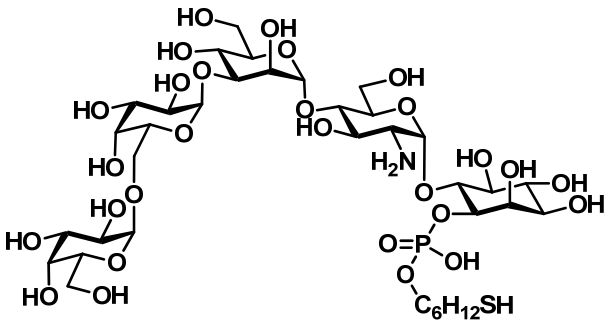

1.797 µmol of phosphate **119** (5.410 mg) was reacted according to Birch reduction (Method 22). Product **120** was obtained in 98% (1.758 µmol, 1.800 mg) as white solid by using sephadex G15 size exclusion chromatography using 5% ethanol in water as eluent.

^{1}H-NMR (400 MHz, D_2O): δ = 5.39 (d, *J* = 1.8 Hz, 1H, GlcN-1), 5.04 (d, *J* = 3.5 Hz, 1H, Gal-1), 4.92 (d, *J* = 1.4 Hz, 1H, Gal'-1), 4.39 (d, *J* = 7.6 Hz, 1H, Man-1), 4.05 – 3.33 (m, 38H), 1.55 – 1.47 (m, 4H, -CH_2-), 1.18 – 1.12 (m, 4H, -CH_2-) ppm.

^{31}P-NMR (162 MHz, D_2O): δ = 25.50 ppm.

ESI-MS: m/z M_{calcd} for $C_{36}H_{60}NO_{28}PS$ = 1023.3230; M_{found} = 1048.5972 $[M-H+D+Na]^+$

1-*O*-Allyl-(-(-(-(4-*O*-*para*-methoxy-benzoyl-2,3,6-*O*-tri-2-methyl-naphthyl-D-galactopyranosyl-α1→6)-2,3,4-*O*-tri-benzyl-D-galactopyranosyl-α1→3)-2-*O*-acetyl-4-*O*-benzyl-6-*O*-*tert*-butyldiphenylsilyl-D-mannopyranosyl-α1→4)-2-azido-3,6-*O*-benzyl-2-deoxy-D-glucopyranosyl-α1→6)-2,3,4,5-*O*-tetra-benzyl-*myo*-inositol (122)

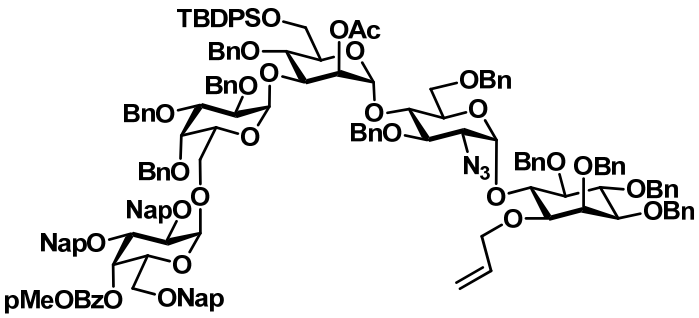

0.079 mmol of imidate **114** (0.145 g) and 0.158 mmol of glycosylacceptor **121** (0.149 g) were dissolved in DCM and reacted according to glycosylation with imidate donor (Method 16)

using TMSOTf at 0°C. Product **122** was obtained in 28% yield (0.022 mmol, 0.058 g) as colorless oil.

R_f = 0.40 (4:1, Hex:EA)

^{1}H-NMR (400 MHz, $CDCl_3$): δ = 7.86 – 6.63 (m, 75H, $H_{Ar.}$), 5.88 – 5.78 (m, 2H, Gal'-4, Allyl-2), 5.58 (d, *J* = 3.8 Hz, 1H, GlcN-1, J_{CH} = 181.61 Hz), 5.31 (d, *J* = 1.8 Hz, 1H, Man-1, J_{CH} = 175.36 Hz), 5.26 (t, *J* = 2.5 Hz, 1H, Man-2), 5.23 – 5.19 (m, 1H, Allyl-3), 5.19 – 5.15 (m, 1H, Allyl-3), 5.09 (dd, *J* = 10.4 Hz, 1.7 Hz, 1H, -CH_2-), 5.00 – 4.88 (m, 4H, Gal'-1, J_{CH} = 170.49 Hz, -CH_2-), 4.86 – 4.78 (m, 7H, -CH_2-, Gal-1, J_{CH} =172.03 Hz), 4.76 – 4.38 (m, 27H, -CH_2-), 4.20 – 3.60 (m, 42H), 3.52 – 2.94 (m, 17H), 1.86 (s, 3H, -CH_3), 1.18 (s, 9H, -C)-$CH_3)_3$) ppm.

^{13}C-NMR (101 MHz, $CDCl_3$): δ = 170.06 (C=O), 165.53 (C=O), 163.31 ($C_{Ar.}$), 163.28 ($C_{Ar.}$), 139.44 ($C_{Ar.}$), 139.17 ($C_{Ar.}$), 138.83 ($C_{Ar.}$), 138.79 ($C_{Ar.}$), 138.57 ($C_{Ar.}$), 138.55 ($C_{Ar.}$), 138.30 ($C_{Ar.}$), 138.28 ($C_{Ar.}$), 138.03 ($C_{Ar.}$), 135.98 ($C_{Ar.}$), 135.79 ($C_{Ar.}$), 135.69 ($C_{Ar.}$), 135.52 ($C_{Ar.}$), 135.25 ($C_{Ar.}$), 134.28 ($C_{Ar.}$), 134.00 (Allyl-2), 133.24 ($C_{Ar.}$), 133.14 ($C_{Ar.}$), 133.11 ($C_{Ar.}$), 132.92 ($C_{Ar.}$), 132.87 ($C_{Ar.}$), 131.79 ($C_{Ar.}$), 129.54 ($C_{Ar.}$), 129.47 ($C_{Ar.}$), 128.41 ($C_{Ar.}$), 128.32 ($C_{Ar.}$), 128.29 ($C_{Ar.}$), 128.23 ($C_{Ar.}$), 128.20 ($C_{Ar.}$), 128.16 ($C_{Ar.}$), 128.12 ($C_{Ar.}$), 128.09 ($C_{Ar.}$), 128.07 ($C_{Ar.}$), 127.98 ($C_{Ar.}$), 127.96 ($C_{Ar.}$), 127.93 ($C_{Ar.}$), 127.90 ($C_{Ar.}$), 127.87 ($C_{Ar.}$), 127.79 ($C_{Ar.}$), 127.75 ($C_{Ar.}$), 127.68 ($C_{Ar.}$), 127.65 ($C_{Ar.}$), 127.61 ($C_{Ar.}$), 127.54 ($C_{Ar.}$), 127.49 ($C_{Ar.}$), 127.43 ($C_{Ar.}$), 127.40 ($C_{Ar.}$), 127.34 ($C_{Ar.}$), 127.31 ($C_{Ar.}$), 127.29 ($C_{Ar.}$), 127.21 ($C_{Ar.}$), 127.18 ($C_{Ar.}$), 127.10 ($C_{Ar.}$), 127.01 ($C_{Ar.}$), 126.99 ($C_{Ar.}$), 126.94 ($C_{Ar.}$), 126.91 ($C_{Ar.}$), 126.65 ($C_{Ar.}$), 126.59 ($C_{Ar.}$), 126.10 ($C_{Ar.}$), 126.07 ($C_{Ar.}$), 125.99 ($C_{Ar.}$), 125.90 ($C_{Ar.}$), 125.85 ($C_{Ar.}$), 125.83 ($C_{Ar.}$), 125.73 ($C_{Ar.}$), 125.62 ($C_{Ar.}$), 122.47 ($C_{Ar.}$), 116.91 (Allyl-3), 113.54 ($C_{Ar.}$), 101.04 (Gal'-1), 99.34 (Gal-1), 98.17 (Man-1), 97.82 (GluN-1), 81.93, 81.70, 80.98, 80.87, 80.37, 79.96, 78.41, 77.37, 77.25, 77.05, 76.73, 76.05, 75.83, 75.70, 75.03, 74.87, 74.65, 74.43, 74.33, 74.23, 74.03, 73.80, 73.57, 73.49, 73.31, 73.04, 72.86, 72.78 (Man-2), 72.66, 72.52, 71.88, 71.37, 70.70, 69.62, 68.06 (Gal'-4), 67.93, 66.37, 63.57, 62.06, 60.45, 55.42 (-CH_3), 29.40 (-C(-$CH_3)_3$), 26.83 (-C(-$CH_3)_3$), 21.10 (-CH_3) ppm.

ESI-MS: m/z M_{calcd} for $C_{162}H_{165}N_3O_{28}Si$ = 2628.1349; M_{found} = 2651.1267 $[M+Na]^+$

Polarimeter: $[\alpha]_D^{20}$ = 24.65 (c = 0.1 g/L in $CHCl_3$)

FTIR: 3822.82, 3680.15, 3628.48, 3522.10, 3455.63, 3358.94, 3026.60, 2928.67, 2535.27, 2334.39, 2284.08, 2251.36, 2239.98, 2193.99, 2171.94, 2160.52, 2136.96, 2106.98, 2070.99, 2052.83, 2036.85, 2021.88, 1996.01, 1970.29, 1948.39, 1931.95, 1736.95, 1606.45, 1511.81, 1497.66, 1455.89, 1429.63, 1359.26, 1257.77, 1167.81, 1102.96, 1056.26, 856.67, 822.31, 792.90, 768.10, 742.28, 719.20, 699.19, 668.98 cm^{-1}.

1-*O*-Allyl-(-(-(-(4-*O*-*para*-methoxy-benzoyl-2,3,6-*O*-tri-2-methyl-naphthyl-D-galactopyranosyl-α1→6)-2,3,4-*O*-tri-benzyl-D-galactopyranosyl-α1→3)-2-*O*-acetyl-4-*O*-benzyl-D-mannopyranosyl-α1→4)-2-azido-3,6-*O*-benzyl-2-deoxy-D-glucopyranosyl-α1→6)-2,3,4,5-*O*-tetra-benzyl-*myo*-inositol (123)

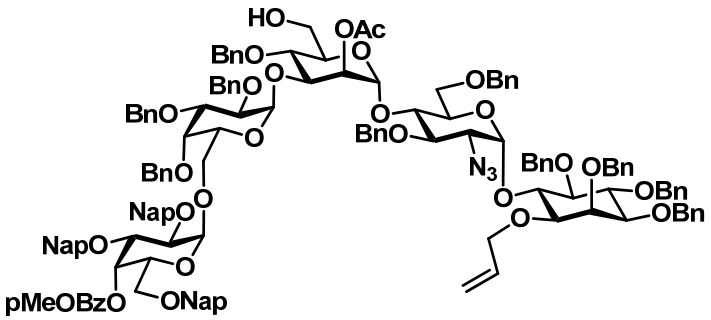

0.019 mmol of pentasaccharide **122** (0.050 g) was reacted according to TBDPS removal (Method 13). Product **123** was obtained in 33% yield (6.270 µmol, 0.015 g) as colorless oil.

$\mathbf{R_f}$ = 0.10 (4:1, Hex:EA)

^{1}H-NMR (400 MHz, $CDCl_3$): δ = 7.80 – 7.75 (m, 2H, $H_{Ar.}$), 7.71 – 6.96 (m, 71H, $H_{Ar.}$), 6.69 – 6.61 (m, 2H, $H_{Ar.}$), 5.91 – 5.76 (m, 2H, Allyl-2, Gal'-4), 5.56 (d, *J* = 3.7 Hz, 1H, GlcN-1), 5.27 – 5.15 (m, 4H, Gal-1, Gal'-1, Man-2, Allyl-3), 5.10 (dd, *J* = 10.4 Hz, 1.6 Hz, 1H, Allyl-3), 4.99 – 4.92 (m, 2H, Man-1, -CH_2-), 4.89 – 4.31 (m, 37H), 4.28 – 3.53 (m, 39H), 3.49 – 2.99 (m, 18H), 1.87 (s, 3H, -CH_3) ppm.

^{13}C-NMR (101 MHz, $CDCl_3$): δ = 169.86 (C=O), 165.48 (C=O), 163.29 ($C_{Ar.}$), 139.06 ($C_{Ar.}$), 138.79 ($C_{Ar.}$), 138.69 ($C_{Ar.}$), 138.66 ($C_{Ar.}$), 138.55 ($C_{Ar.}$), 138.41 ($C_{Ar.}$), 138.28 ($C_{Ar.}$), 138.26 ($C_{Ar.}$), 137.94 ($C_{Ar.}$), 135.77 ($C_{Ar.}$), 135.66 ($C_{Ar.}$), 135.22 ($C_{Ar.}$), 134.28 (Allyl-2), 133.24 ($C_{Ar.}$), 133.12 ($C_{Ar.}$), 133.10 ($C_{Ar.}$), 132.97 ($C_{Ar.}$), 132.92 ($C_{Ar.}$), 132.88 ($C_{Ar.}$), 132.86 ($C_{Ar.}$), 131.78 ($C_{Ar.}$), 129.05 ($C_{Ar.}$), 128.51 ($C_{Ar.}$), 128.42 ($C_{Ar.}$), 128.34 ($C_{Ar.}$), 128.32 ($C_{Ar.}$), 128.24 ($C_{Ar.}$), 128.22 ($C_{Ar.}$), 128.17 ($C_{Ar.}$), 128.15 ($C_{Ar.}$), 128.08 ($C_{Ar.}$), 128.03 ($C_{Ar.}$), 127.99 ($C_{Ar.}$), 127.92 ($C_{Ar.}$), 127.89 ($C_{Ar.}$), 127.86 ($C_{Ar.}$), 127.69 ($C_{Ar.}$), 127.67 ($C_{Ar.}$), 127.65 ($C_{Ar.}$), 127.61 ($C_{Ar.}$), 127.53 ($C_{Ar.}$), 127.50 ($C_{Ar.}$), 127.46 ($C_{Ar.}$), 127.39 ($C_{Ar.}$), 127.34 ($C_{Ar.}$), 127.28 ($C_{Ar.}$), 127.22 ($C_{Ar.}$), 127.02 ($C_{Ar.}$), 126.97 ($C_{Ar.}$), 126.94 ($C_{Ar.}$), 126.61 ($C_{Ar.}$), 126.56 ($C_{Ar.}$), 126.09 ($C_{Ar.}$), 126.03 ($C_{Ar.}$), 125.99 ($C_{Ar.}$), 125.90 ($C_{Ar.}$), 125.86 ($C_{Ar.}$), 125.71 ($C_{Ar.}$), 125.65 ($C_{Ar.}$), 125.31 ($C_{Ar.}$), 122.41 ($C_{Ar.}$), 117.03 (Allyl-3), 113.53 ($C_{Ar.}$), 99.41 (Man-1), 98.24 (brs, Gal-1, Gal'1), 97.81 (GluN-1), 81.94, 81.63, 80.98, 80.91, 80.49, 78.49, 77.35, 77.24, 77.04, 76.72, 75.95, 75.72, 75.12, 74.83, 74.66, 74.55, 74.29, 74.08, 73.82, 73.61, 73.56, 73.46, 72.81, 72.71, 72.16 (Man-2), 71.92, 71.38, 70.75, 69.99, 69.68, 68.32, 68.16, 67.97, 67.72 (Gal'-4), 66.68, 63.76, 55.42 (-CH_3), 21.49 (-CH_3) ppm.

ESI-MS: m/z M_{calcd} for $C_{146}H_{147}N_3O_{28}$ = 2390.0171; M_{found} = 2413.0052 $[M+Na]^+$

Polarimeter: $[\alpha]_D^{20}$ = 58.19 (c = 0.1 g/L in $CHCl_3$)

FTIR: 3033.99, 2927.75, 2107.52, 1718.76, 1606.69, 1511.54, 1498.02, 1455.43, 1359.66, 1257.39, 1167.55, 1097.88, 1055.01, 1028.87, 856.29, 819.77, 737.13, 697.63 cm^{-1}.

1-*O*-Allyl-(-(-(-(4-*O*-*para*-methoxy-benzoyl-2,3,6-*O*-tri-2-methyl-naphthyl-D-galactopyranosyl-α1→6)-2,3,4-*O*-tri-benzyl-D-galactopyranosyl-α1→3)-(-(2,3,4-*O*-tri-benzyl-6-*O*-triisopropylsilyl-D-mannopyranosyl-α1→2)-3,4,6-*O*-tri-benzyl-D-mannopyranosyl-α1→6)-2-*O*-acetyl-4-*O*-benzyl-D-mannopyranosyl-α1→4)-2-azido-3,6-*O*-benzyl-2-deoxy-D-glucopyranosyl-α1→6)-2,3,4,5-*O*-tetra-benzyl-*myo*-inositol (125)

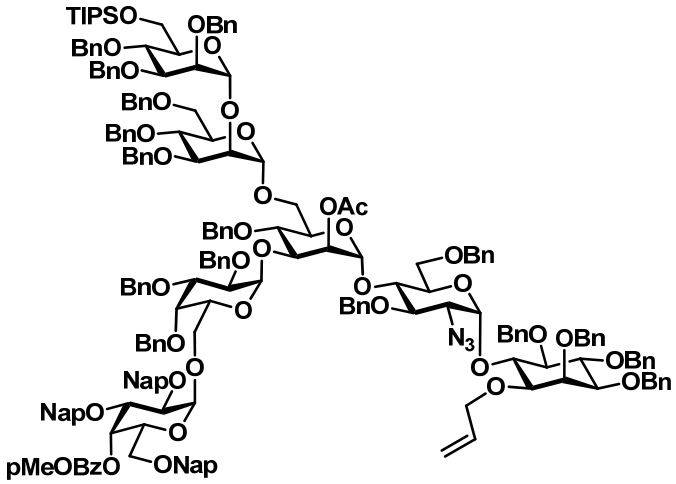

0.013 mmol of imidate **124** (0.015 g) and 6.270 µmol of glycosylacceptor **123** (0.015 g) were dissolved in a 2:1 mixture of thiophene and toluene and reacted according to glycosylation with imidate donor (Method 16) using TBSOTf at room temperature. Product **125** was obtained in 61% yield (3.810 µmol, 0.013 g) as colorless oil.

R_f = 0.50 (6:1, Hex:EA)

^{1}H-NMR (400 MHz, $CDCl_3$): δ = 7.76 (dd, *J* = 9.1 Hz, 2.4 Hz, 2H, $H_{Ar.}$), 7.71 – 6.87 (m, 101H, $H_{Ar.}$), 6.64 (dd, *J* = 9.2 Hz, 2.2 Hz, 2H, $H_{Ar.}$), 5.88 – 5.77 (m, 2H, Allyl-2, Gal'-4), 5.57 (d, *J* = 3.7 Hz, 1H, GlcN-1, J_{CH} = 176.50 Hz), 5.34 – 5.04 (m, 6H, Allyl-3, Gal-1, J_{CH} = 178.31 Hz, Gal'-1, J_{CH} = 176.50 Hz, Man'-1, J_{CH} = 173.49 Hz, Man''-1, J_{CH} = 171.08 Hz), 4.99 – 2.97 (m, 85H, Man-1, J_{CH} = 172.89 Hz), 1.87 (s, 3H, -CH_3), 1.21 – 1.17 (m, 21H, (-CH(-CH_3)$_2$)$_3$) ppm.

1-*O*-H-(-(-(-(4-*O*-*para*-methoxy-benzoyl-2,3,6-*O*-tri-2-methyl-naphthyl-D-galactopyranosyl-α1→6)-2,3,4-*O*-tri-benzyl-D-galactopyranosyl-α1→3)-(-(2,3,4-*O*-tri-benzyl-6-*O*-triisopropylsilyl-D-mannopyranosyl-α1→2)-3,4,6-*O*-tri-benzyl-D-mannopyranosyl-α1→6)-2-*O*-acetyl-4-*O*-benzyl-D-mannopyranosyl-α1→4)-2-azido-3,6-*O*-benzyl-2-deoxy-D-glucopyranosyl-α1→6)-2,3,4,5-*O*-tetra-benzyl-*myo*-inositol (126)

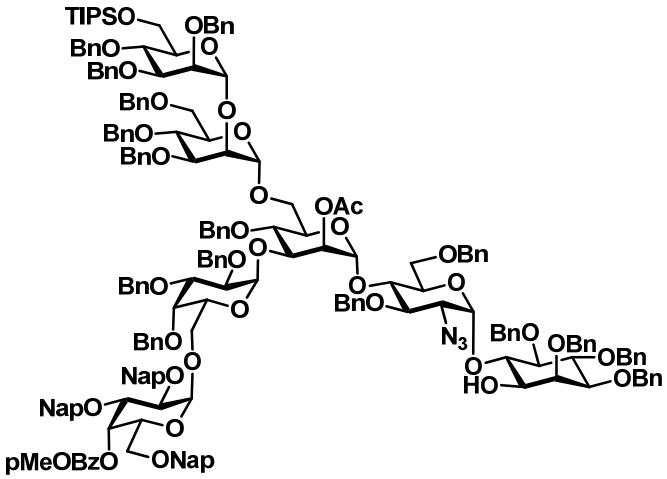

3.810 µmol of heptasaccharide **125** (0.013 g) was reacted according to allyl removal via isomerization and hydrolysis (Method 14). Product **126** was obtained in 82% yield (3.110 µmol, 10.500 mg) as colorless oil.

R_f = 0.20 (4:1, Hex:EA)

^{1}H-NMR (400 MHz, $CDCCl_3$): δ = 8.14 – 6.72 (m, 105H, $H_{Ar.}$), 5.91 (s, 1H, Gal'-4), 5.57 – 3.01 (m, 89H), 1.92 (s, 3H, $-CH_3$), 1.14 – 1.06 (m, 21H, $(-CH(-CH_3)_2)_3$) ppm.

ESI-MS: m/z M_{calcd} for $C_{206}H_{219}N_3O_{38}Si$ = 3370.5066; M_{found} = 3417.5276

Polarimeter: $[\alpha]_D^{20}$ = 58.19 (c = 0.1 g/L in $CHCl_3$)

FTIR: 3033.99, 2927.75, 2107.52, 1718.76, 1606.69, 1511.54, 1498.02, 1455.43, 1359.66, 1257.39, 1167.55, 1097.88, 1055.01, 1028.87, 856.29, 819.77, 737.13, 697.63 cm^{-1}.

1-(6-Thiobenzyl-hexyl)-phosphatidyl-(-(-(-(4-*O*-*para*-methoxy-benzoyl-2,3,6-*O*-tri-2-methyl-naphthyl-D-galactopyranosyl-α1→6)-2,3,4-*O*-tri-benzyl-D-galactopyranosyl-α1→3)-(-(2,3,4-*O*-tri-benzyl-6-*O*-triisopropylsilyl-D-mannopyranosyl-α1→2)-3,4,6-*O*-tri-benzyl-D-mannopyranosyl-α1→6)-2-*O*-acetyl-4-*O*-benzyl-D-mannopyranosyl-α1→4)-2-azido-3,6-*O*-benzyl-2-deoxy-D-glucopyranosyl-α1→6)-2,3,4,5-*O*-tetra-benzyl-*myo*-inositol (127)

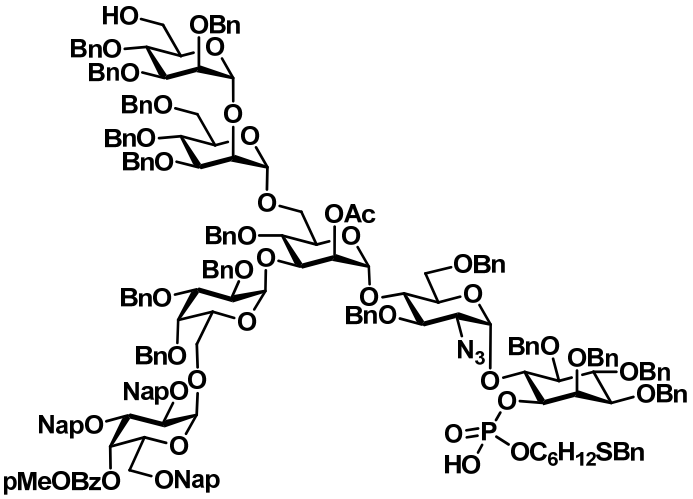

3.110 µmol of alcohol 1**26** (10.500 mg) and 6.230 µmol of H-phosphonate **88** (2.400 mg) were reacted according to phosphate formation (Method 19). Product **127** was obtained in 18% yield (0.571 µmol, 2.000 mg) as colorless oil.

R_f = 0.5 (10% MeOH in DCM)

^{1}H-NMR (400 MHz, $CDCl_3$): δ = 11.42 (s, 1H, P-OH), 8.03 – 6.65 (m, 110H, $H_{Ar.}$), 5.38 – 3.50 (m, 93H), 2.34 – 2.13 (m, 2H, -CH_2-), 2.10 (s, 3H, -CH_3), 1.36 – 1.13 (m, 8H, -CH_2-) ppm.

^{31}P-NMR (162 MHz, $CDCl_3$): δ = -24.60 ppm.

ESI-MS: m/z M_{calcd} for $C_{210}H_{218}N_3O_{41}PS$ = 3500.4524; M_{found} = 1759.2434 $[M+NH_4]^{2+}$

1-(6-Thio-hexyl)-phosphatidyl-(-(-(-(D-galactopyranosyl-α1→6)-D-galactopyranosyl-α1→3)-(-(D-mannopyranosyl-α1→2)-D-mannopyranosyl-α1→6)-D-mannopyranosyl-α1→4)-2-azido-2-deoxy-D-glucopyranosyl-α1→6)-*myo*-inositol (129)

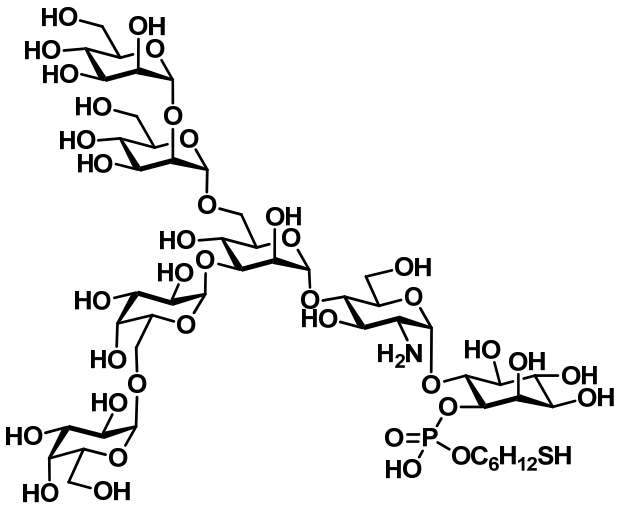

0.571 µmol of phosphate **127** (2.000 mg) was reacted according to Birch reduction (Method 22). Product 1**29** was obtained in 39% (0.223 µmol, 0.300 mg) as white solid by using sephadex G25 size exclusion chromatography using 5% ethanol in water as eluent.

^{1}H-NMR (400 MHz, D_2O): δ = 5.32 – 4.89 (m, 6H), 4.00 – 3.30 (m, 44H), 2.29 (s, 2H, -CH_2-), 1.26 – 0.97 (m, 8H, -CH_2-) ppm.

^{31}P-NMR (162 MHz, D_2O): δ = 0.63 ppm.

ESI-MS: m/z M_{calcd} for $C_{48}H_{86}NO_{38}PS$ = 1347.4286; M_{found} = 1370.4792 $[M+Na]^+$

9.5 SYNTHETIC PART FOR CHAPTER 6

1,2-*O*-Di-myristoyl-3-*O*-phosphonatidyl-sn-glycerol (131)

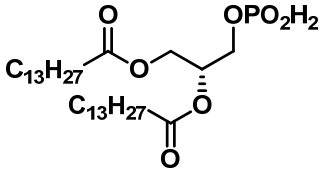

0.975 mmol of glycerol **130** (0.500 g) and 0.975 mmol of pyridinium phosphonate (0.157 g) were reacted according to H-phosphonate formation (Method 18). Product **131** was obtained in quantitative yield brsm (0.409 mmol, 0.236 g) as white solid.

R_f = 0.50 (10% MeOH in DCM)

^{1}H-NMR (400 MHz, $CDCl_3$): δ = 5.15 (s, 1H), 4.29 (s, 1H), 4.08 (s, 1H), 3.94 (s, 2H), 2.22 (s, 5H), 1.51 (s, 6H), 1.18 (s, 61H), 0.80 (d, *J* = 6.4 Hz, 10H) ppm.

^{13}C-NMR (101 MHz, $CDCl_3$): δ = 34.39, 34.20, 32.10, 29.96, 29.93, 29.89, 29.87, 29.82, 29.65, 29.62, 29.57, 29.44, 29.39, 25.07, 25.02, 22.86, 14.27 ppm.

^{31}P-NMR (162 MHz, $CDCl_3$): δ = 4.20 ppm.

Polarimeter: $[\alpha]_D^{20}$ =15.35 (c = 0.1 g/L in $CHCl_3$)

FTIR: 2923.78, 2854.30, 1742.27, 1468.31, 1217.85, 1112.98, 1000.99, 818.07, 723.28 cm^{-1}.

1-*O*-(2,3-*O*-Di-myristoyl-sn-glyceryl)-phosphatidyl-3,4,5-*O*-tri-benzyl-2,6-*O*-di-2-methyl-naphthyl-*myo*-inositol (133)

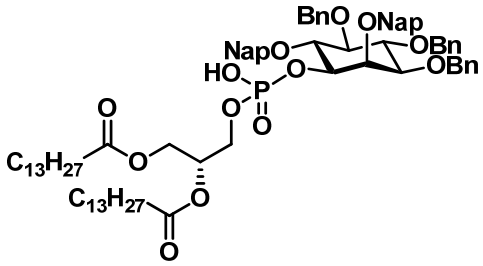

0.041 mmol of *myo*-inositol **132** (0.030 g) and 0.062 mmol of H-phosphonate **131** (0.036 g) were reacted according to phosphate formation (Method 19). Product **133** was obtained in 17% yield (6.890 µmol, 9.000 mg) as colorless oil.

R_f = 0.50 (15% MeOH in DCM)

^{1}H-NMR (400 MHz, $CDCl_3$): δ = 11.81 (s, 1H, P-OH), 7.81 – 7.13 (m, 29H, $H_{Ar.}$), 5.12 – 4.52 (m, 13H), 4.22 – 3.82 (m, 6H), 3.60 – 3.42 (m, 2H), 2.04 - 1.96 (m, 4H, -CH_2-), 1.40 - 1.33 (m, 4H, -CH_2-), 1.25 – 1.01 (m, 40H), 0.81 (t, *J* = 6.8 Hz, 6H) ppm.

^{13}C-NMR (151 MHz, $CDCl_3$): δ = 175.90 (C=O), 175.59 (C=O), 141.54 ($C_{Ar.}$), 141.39 ($C_{Ar.}$), 141.22 ($C_{Ar.}$), 135.93 ($C_{Ar.}$), 135.89 ($C_{Ar.}$), 135.44 ($C_{Ar.}$), 130.88 ($C_{Ar.}$), 130.68 ($C_{Ar.}$), 130.58 ($C_{Ar.}$), 130.41 ($C_{Ar.}$), 130.35 ($C_{Ar.}$), 130.31 ($C_{Ar.}$), 130.23 ($C_{Ar.}$), 130.05 ($C_{Ar.}$), 130.01 ($C_{Ar.}$), 129.98 ($C_{Ar.}$), 128.74 ($C_{Ar.}$), 128.56 ($C_{Ar.}$), 128.48 ($C_{Ar.}$), 128.39 ($C_{Ar.}$), 128.10 ($C_{Ar.}$), 86.02, 84.32, 83.54, 78.49, 78.41, 77.68, 75.10, 73.03, 66.46, 65.25, 48.27, 36.78, 36.60, 34.56, 32.34, 32.32, 32.30, 32.15, 32.01, 31.95, 31.75, 31.73, 27.45, 25.33, 16.75, 11.13 ppm.

^{31}P-NMR (162 MHz, $CDCl_3$): δ = -1.15 ppm.

ESI-MS: m/z M_{calcd} for $C_{80}H_{105}O_{13}P$ = 1304.7293; M_{found} = 1327.7146 $[M+Na]^+$

1-*O*-(2,3-*O*-Di-myristoyl-sn-glyceryl)-phosphatidyl-*myo*-inositol (134)

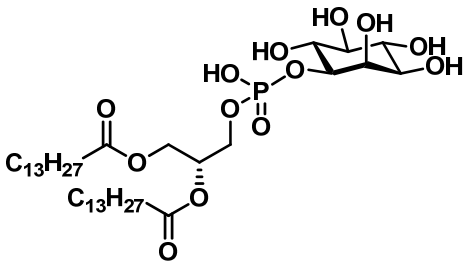

6.890 µmol of phosphate **133** (9.000 mg) was reacted according to hydrogenolysis (Method 21) employing an autoclave. Product **134** was obtained in 40% yield (2.780 µmol, 2.100 mg) as white solid by using sephadex LH20 size exclusion chromatography using a 3:3:1 mixture of chloroform, methanol and water as eluent.

^{1}H-NMR (600 MHz, MeOD-d_4): δ = 4.21 – 3.33 (m, 9H), 3.09 – 3.00 (m, 2H), 2.34 (t, J = 7.9 Hz, 4H, -CH_2-), 1.63 – 1.56 (m, 4H, -CH_2), 1.35 – 1.25 (m, 40H), 0.88 (t, J = 7.0 Hz, 6H) ppm.

^{13}C-NMR (101 MHz, MeOD): δ = 174.54 (C=O), 174.10 (C=O), 72.67, 71.47, 69.72, 65.05, 64.90, 62.63, 33.49, 31.70, 29.38, 29.22, 28.85, 24.60, 22.36, 13.06, 7.80 ppm.

^{31}P-NMR (162 MHz, $CDCl_3$): δ = 4.15 ppm.

ESI-MS: m/z M_{calcd} for $C_{37}H_{71}O_{13}P$ = 754.4632; M_{found} = 753.4550 $[M]^-$

1-*O*-2,3,4,5-*O*-tetra-benzyl-(2,3-*O*-Di-myristoyl-sn-glyceryl)-phosphatidyl-(2-azido-3,4,6-*O*-tri-benzyl-2-deoxy-D-glucopyranosyl-α1→6)-*myo*-inositol (136)

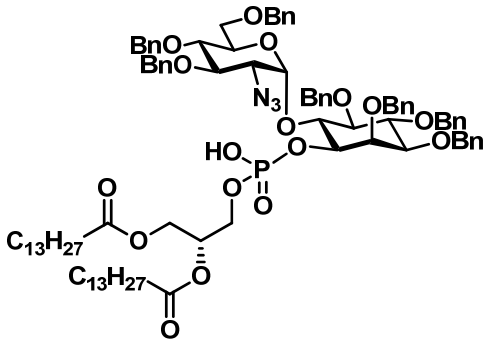

0.030 mmol of pseudodisaccharide **135** (0.030 g) and 0.045 mmol of H-phosphonate **131** (0.026 g) were reacted according to phosphate formation (Method 19). Product **136** was obtained in 74% yield (0.022 mmol, 0.035 g) as colorless oil.

R_f = 0.50 (15% MeOH in DCM)

^{1}H-NMR (400 MHz, $CHCl_3$): δ = 7.40 – 6.85 (m, 35H), 5.36 (s, 1H, Glu-1), 5.02 – 3.73 (m, 35), 3.73 – 2.90 (m, 12H), 2.38 – 1.95 (m, 6H), 1.54 – 1.41 (m, 6H), 1.18 (s, 1H), 0.81 (s, 1H). ppm.

^{13}C-NMR (101 MHz, $CHCl_3$): δ = 138.69 (C_{Ar}), 138.68 (C_{Ar}), 138.59 (C_{Ar}), 138.54 (C_{Ar}), 138.43 (C_{Ar}), 138.33 (C_{Ar}), 138.21 (C_{Ar}), 138.07 (C_{Ar}), 137.97 (C_{Ar}), 137.90 (C_{Ar}), 128.58 (C_{Ar}), 128.54 (C_{Ar}), 128.48 (C_{Ar}), 128.40 (C_{Ar}), 128.38 (C_{Ar}), 128.35 (C_{Ar}), 128.19 (C_{Ar}), 128.05 (C_{Ar}), 127.97 (C_{Ar}), 127.90 (C_{Ar}), 127.84 (C_{Ar}), 127.80 (C_{Ar}), 127.76 (C_{Ar}), 127.73 (C_{Ar}), 127.58 (C_{Ar}), 127.45 (C_{Ar}), 98.51 (Glu-1), 82.11, 81.25, 81.03, 80.87, 80.57, 78.19, 77.48, 77.16, 77.09, 76.84, 75.95, 75.58, 75.38, 74.90, 73.67, 73.48, 73.03, 70.93, 67.50, 64.21, 34.25, 32.09, 29.91, 29.88, 29.85, 29.80, 29.61, 29.55, 29.54, 29.51, 22.85, 14.29 ppm.

ESI-MS: m/z M_{calcd} for $C_{92}H_{122}N_3O_{17}P$ = 1571.8512; M_{found} = 1570.8549 $[M]^-$

Polarimeter: $[\alpha]_D^{20}$ =55.89 (c = 0.1 g/L in $CHCl_3$)

FTIR: 3673.95, 2982.98, 2929.57, 2222.25, 2157.92, 2108.45, 1989.46, 1739.05, 1455.37, 1383.01, 1252.37, 1156.01, 1070.07, 957.74, 868.97, 822.09, 765.74, 742.72, 699.99, 688.04, 671.22, 661.68 cm^{-1}.

1-*O*-(2,3-*O*-Di-myristoyl-sn-glyceryl)-phosphatidyl-(2-azido-2-deoxy-D-glucopyranosyl-α1→6)-*myo*-inositol (137)

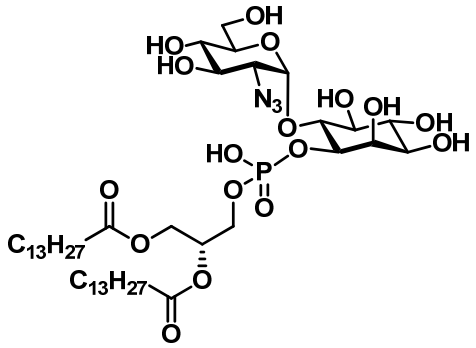

0.022 mmol of phosphate **136** (0.035 g) was reacted according to hydrogenolysis (Method 21) employing an autoclave. Product **137** was obtained in 9% yield (1.965 µmol, 1.800 mg) as white solid by using sephadex LH20 size exclusion chromatography using a 3:3:1 mixture of chloroform, methanol and water as eluent.

^{1}H-NMR (400 MHz, $CDCl_3$): δ = 5.24 – 4.92 (m, 1H), 3.91 – 2.82 (m, 17H), 2.12 – 1.85 (m, 4H), 1.30 (s, 4H), 1.02 – 0.91 (m, 40H), 0.60 (s, 6H) ppm.

^{13}C-NMR (101 MHz, $CDCl_3$): δ = 172.80 (C=O), 172.69 (C=O), 95.07 (GlcN-1), 76.24, 75.63, 73.94, 72.74, 72.18, 70.63, 69.87, 69.42, 64.44, 53.82, 33.70, 31.50, 29.23, 29.04, 28.92, 28.69, 24.53, 24.46, 22.24, 13.46 ppm.

^{31}P-NMR (162 MHz, $CDCl_3$): δ = 4.26, 3.91 ppm.

ESI-MS: m/z M_{calcd} for $C_{43}H_{82}NO_{17}P$ = 915.5320; M_{found} = 914.5486 $[M]^-$

Allyl-4,6-*O*-di-benzyl-(2,3,4,6-*O*-tetra-benzyl-D-galactopyranosyl-α1→3)-α-D-mannopyranoside (139)

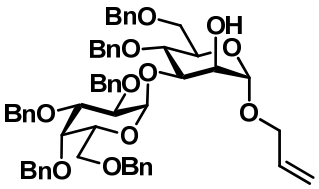

0.104 mmol of disaccharide **138** (0.100 g) was reacted according to potassium carbonate mediated *O*-Acyl removal (Method 4). Product **139** was obtained in 20% yield (0.020 mmol, 0.019 g) as colorless oil.

R_f = 0.40 (4:1, Hex:EA)

^{1}H-NMR (400 MHz, $CDCl_3$): δ = 7.37 – 6.90 (m, 30H, $H_{Ar.}$), 5.87 – 5.77 (m, 1H, Allyl-2), 5.19 (d, *J* = 17.2 Hz, 1H, -CH_2-), 5.11 (d, *J* = 10.1 Hz, 1H, -CH_2-), 4.99 (s, 2H, Man-1), 4.91 – 4.60 (m, 7H), 4.54 – 4.27 (m, 10H), 4.08 – 3.83 (m, 9H), 3.70 – 3.62 (m, 6H), 3.47 (t, *J* = 9.6 Hz, 1H), 3.10 (d, *J* = 9.3 Hz, 1H) ppm.

^{13}C-NMR (101 MHz, $CDCl_3$): δ = 138.84 ($C_{Ar.}$), 138.68 ($C_{Ar.}$), 138.60 ($C_{Ar.}$), 138.40 ($C_{Ar.}$), 137.10 ($C_{Ar.}$), 134.14 (Allyl-2), 128.57 ($C_{Ar.}$), 128.55 ($C_{Ar.}$), 128.53 ($C_{Ar.}$), 128.46 ($C_{Ar.}$), 128.43 ($C_{Ar.}$), 128.39 ($C_{Ar.}$), 128.30 ($C_{Ar.}$), 128.29 ($C_{Ar.}$), 128.14 ($C_{Ar.}$), 128.07 ($C_{Ar.}$), 128.00 ($C_{Ar.}$), 127.93 ($C_{Ar.}$), 127.73 ($C_{Ar.}$), 127.68 ($C_{Ar.}$), 127.57 ($C_{Ar.}$), 127.49 ($C_{Ar.}$), 117.40 (Allyl-3), 99.70, 98.65, 83.45, 78.40, 77.48, 77.16, 77.08, 76.84, 75.37, 75.27, 74.44, 74.03, 73.49, 73.41, 73.20, 71.25, 71.08, 70.60, 69.55, 69.01, 67.93 ppm.

ESI-MS: m/z M_{calcd} for $C_{57}H_{62}O_{11}$ = 922.4292; M_{found} = 945.4150 $[M+Na]^+$

Polarimeter: $[\alpha]_D^{20}$ = 18.30 (c = 0.1 g/L in $CHCl_3$)

FTIR: 3655.06, 2983.10, 2892.94, 2194.01, 2158.09, 2034.04, 1985.22, 1383.70, 1251.47, 1150.32, 1080.06, 957.89, 843.98, 830.71, 775.37, 717.94, 706.84, 688.09, 677.00, 663.79 cm^{-1}.

Propyl-(D-galactopyranosyl-α1→3)-α-D-mannopyranoside (140)

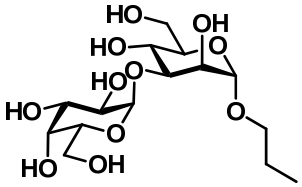

0.020 mmol of alcohol **139** (0.019 g) was reacted according to hydrogenolysis (Method 21). Product **140** was obtained in quantitative yield (0.020 mmol, 7.800 mg) as white solid by using sephadex G15 size exclusion chromatography using 5% ethanol in water as eluent.

^{1}H-NMR (400 MHz, D_2O): δ = 5.23 (d, *J* = 4.1 Hz, 1H, Gal-1), 4.82 (s, 1H, Man-1), 4.11 (s, 1H), 4.04 (s, 1H), 3.96 (s, 1H), 3.92 – 3.59 (m, 9H), 3.51 – 3.45 (m, 1H), 1.59 (q, *J* = 7.8 Hz, 2H), 1.18 – 1.12 (m, 1H), 0.89 (td, *J* = 8.0, 7.1, 2.5 Hz, 3H) ppm.

^{13}C-NMR (101 MHz, D_2O): δ = 100.53 (Gal-1), 99.32 (Man-1), 78.41, 72.59, 71.26, 69.71, 69.38, 69.14, 68.57, 65.95, 61.15, 60.68, 57.28, 21.81, 16.63, 9.75 ppm.

ESI-MS: m/z M_{calcd} for $C_{15}H_{28}O_{11}$ = 384.1632; M_{found} = 407.1536 $[M+Na]^+$

Allyl-4-*O*-benzyl-(-(2,3,4-O-tri-benzyl-D-galactopyranosyl-α1→6)-2,3,4-*O*-tri-benzyl-D-galactopyranosyl-α1→3)-α-D-mannopyranoside (141)

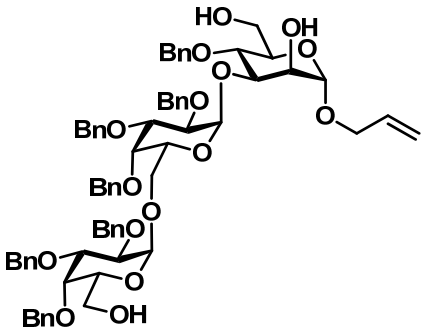

7.180 µmol of trisaccharide **105** (0.011 g) was reacted according to acid mediated mediated *O*-Acyl removal (Method 5). Product **141** was obtained in quantitative yield (7.180 µmol, 8.440 mg) as colorless oil.

R_f = 0.30 (1:1, Hex:EA)

^{1}H-NMR (400 MHz, $CDCl_3$): δ = 7.40 – 7.07 (m, 30H, $H_{Ar.}$), 5.74 (d, *J* = 15.0 Hz, 1H, Allyl-2), 5.15 – 4.96 (m, 4H), 4.94 – 4.34 (m, 17H), 4.18 (s, 1H), 4.04 – 3.27 (m, 15H), 3.02 (d, *J* = 10.2 Hz, 1H) ppm.

Propyl-(-(D-galactopyranosyl-α1→6)-D-galactopyranosyl-α1→3)-α-D-mannopyranoside (142)

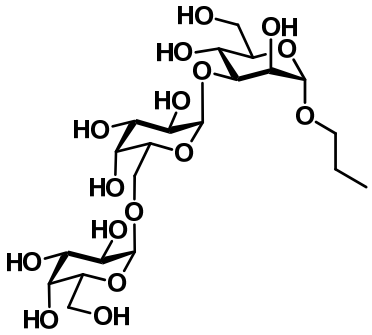

7.490 µmol of triol **141** (8.800 mg) was reacted according to hydrogenolysis (Method 21) employing an autoclave. Product **142** was obtained in 78% yield (5.860 µmol, 3.200 mg) as white solid by using sephadex G15 size exclusion chromatography using 5% ethanol in water as eluent.

^{1}H-NMR (400 MHz, D_2O): δ = 5.14 (s, 1H, Man-1), 4.92 (s, 2H, Gal-1, Gal'-1), 4.32 – 4.21 (m, 2H), 4.02 – 3.34 (m, 31H), 3.17 (s, 2H), 1.25 (s, 5H), 1.15 (s, 3H), 0.90 (s, 4H) ppm.

^{13}C-NMR (101 MHz, D_2O): δ = 102.06 (Gal'-1), 99.77 (Man-1), 99.13 (Gal-1), 80.95, 71.21, 70.11, 69.90, 69.80, 69.66, 69.32, 68.77, 68.60, 68.31, 68.24, 67.91, 67.88, 66.93, 22.52, 10.31, 8.47 ppm.

ESI-MS: m/z M_{calcd} for $C_{21}H_{38}O_{16}$ = 546.2160; M_{found} = 569.2067 $[M+Na]^+$

Propyl-(D-galactopyranosyl-α1→2)-(-(D-galactopyranosyl-α1→2)-D-galactopyranosyl-α1→6)-β-D-galactopyranoside (144)

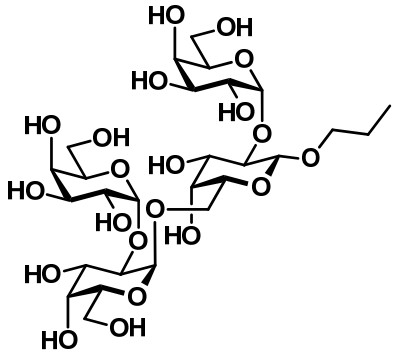

4.250 µmol of tetragalactoside **143** (2.720 mg) was reacted according to sodium methoxide mediated mediated *O*-Acyl removal (Method 3) at 45°C. Product **144** was obtained in 33% yield (1.411 µmol, 1.000 mg) as white solid by using sephadex G15 size exclusion chromatography using 5% ethanol in water as eluent.

^{1}H-NMR (400 MHz, D_2O): δ = 5.26 (d, *J* = 4.0 Hz, 1H, Gal'-1), 5.09 (d, *J* = 2.5 Hz, 1H, Gal^t-1), 4.99 (d, *J* = 3.9 Hz, 1H, Gal^t-1), 4.40 (d, *J* = 7.8 Hz, 1H, Gal-1), 4.11 (t, *J* = 6.4 Hz, 1H), 3.99 (t, *J* = 6.3 Hz, 1H), 3.88 – 3.45 (m, 22H), 1.49 (h, *J* = 7.2 Hz, 2H), 1.02 (t, *J* = 7.1 Hz, 1H), 0.77 (t, *J* = 7.4 Hz, 3H) ppm.

^{13}C-NMR (101 MHz, D_2O): δ = 103.21 (Gal-1), 97.72 (Gal'-1), 95.62 (Gal^t-1), 95.35 (Gal^t-1), 74.78, 72.80, 72.60, 72.58, 72.49, 71.94, 71.42, 70.89, 70.77, 70.63, 70.49, 70.44, 69.15, 69.09, 69.02, 68.97, 68.84, 68.11, 68.06, 67.80, 67.78, 66.19, 60.97, 60.82, 57.31, 22.35, 16.64, 9.81 ppm.

ESI-MS: m/z M_{calcd} for $C_{27}H_{48}O_{21}$ = 708.2688; M_{found} = 731.2437 $[M+Na]^+$

Propyl-(D-galactopyranosyl-β1→3)-(-(D-galactopyranosyl-α1→2)-6-*O*-(2-amino-ethyl-phosphatidyl)-D-mannopyranosyl-α1→2)-α-D-mannoypyranoside (148)

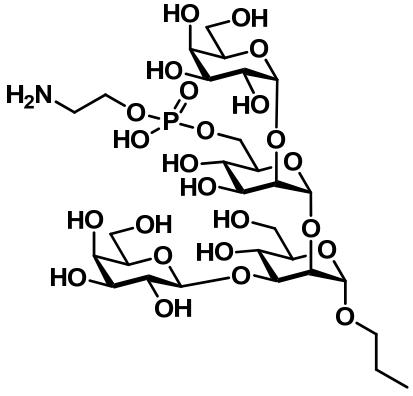

4.890 µmol of phosphate **147** (10.000 mg) was reacted according to hydrogenolysis (Method 21) employing an autoclave. Product **148** was obtained in 62% yield (3.010 µmol, 2.500 mg) as white solid by using sephadex G15 size exclusion chromatography using 5% ethanol in water as eluent.

^{1}H-NMR (400 MHz, D_2O): δ = 5.30 (d, *J* = 1.9 Hz, 1H, Galα-1), 5.01 (d, *J* = 3.8 Hz, 1H, Man-1), 4.95 (d, *J* = 1.6 Hz, 1H, Man‘-1), 4.37 (d, *J* = 7.8 Hz, 1H, Galβ-1), 4.03 – 3.95 (m, 8H), 3.87 – 3.38 (m, 21H), 3.15 (ddd, *J* = 6.2 Hz, 3.6 Hz, 1.0 Hz, 2H), 1.48 (h, *J* = 7.2 Hz, 2H), 1.16 – 1.00 (m, 1H), 0.78 (t, *J* = 7.4 Hz, 3H) ppm.

^{13}C-NMR (101 MHz, D_2O): δ = 101.07 (Man‘-1), 100.54 (Galα-1), 100.47 (Galβ-1), 98.01 (Man-1), 79.66, 79.62, 77.31, 77.29, 77.28, 76.37, 76.33, 75.20, 72.86, 72.56, 72.02, 71.94, 71.38, 71.33, 70.59, 70.53, 69.99, 69.71, 69.64, 69.21, 69.14, 68.73, 68.57, 66.35, 65.27, 65.23, 61.67, 61.62, 61.47, 61.47, 61.44, 60.96, 60.93, 60.73, 39.98, 39.90, 21.93, 9.83 ppm.

^{31}P-NMR (162 MHz, D_2O): δ = 0.22 ppm.

ESI-MS: m/z M_{calcd} for $C_{29}H_{54}NO_{24}P$ = 831.2773; M_{found} = 830.2719 $[M]^-$

Propyl-(D-galactopyranosyl-β1→3)-(D-mannopyranosyl-α1→2)-α-D-mannoypyranoside (150)

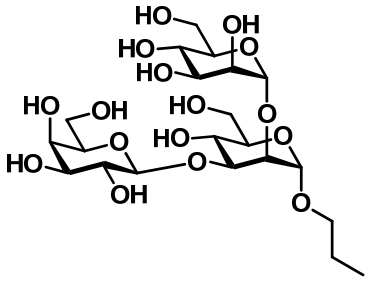

0.016 mmol of trisaccharide **149** (0.020 g) was reacted according to hydrogenolysis (Method 21). Product **150** was obtained in 49% yield (7.690 µmol, 4.200 mg) as white solid.

^{1}H-NMR (400 MHz, D_2O): δ = 5.01 (d, *J* = 1.7 Hz, 1H, Man-1), 4.95 (d, *J* = 1.7 Hz, 1H, Man‘-1), 4.33 (d, *J* = 7.7 Hz, 1H, Gal-1), 4.15 – 4.12 (m, 1H), 3.86 – 3.33 (m, 22H), 1.51 – 1.44 (m, 2H), 0.78 (t, *J* = 7.4 Hz, 3H) ppm.

^{13}C-NMR (101 MHz, D_2O): δ = 101.95 (Gal-1), 100.34 (Man-1), 97.87 (Man‘-1), 78.78, 76.88, 75.12, 73.14, 72.58, 72.52, 72.33, 70.37, 70.34, 70.33, 70.15, 70.12, 69.51, 69.48, 68.54, 66.85, 61.10, 60.78, 60.45, 60.44, 60.37, 38.53, 21.82, 9.78 ppm.

ESI-MS: m/z M_{calcd} for $C_{21}H_{38}O_{16}$ = 546.2160; M_{found} = 569.1926 $[M+Na]^+$

1-H-(-(-(-(D-galactopyranosyl-α1→6)-D-galactopyranosyl-α1→3)-(-(D-mannopyranosyl-α1→2)-D-mannopyranosyl-α1→6)-D-mannopyranosyl-α1→4)-2-azido-2-deoxy-D-glucopyranosyl-α1→6)-*myo*-inositol (152)

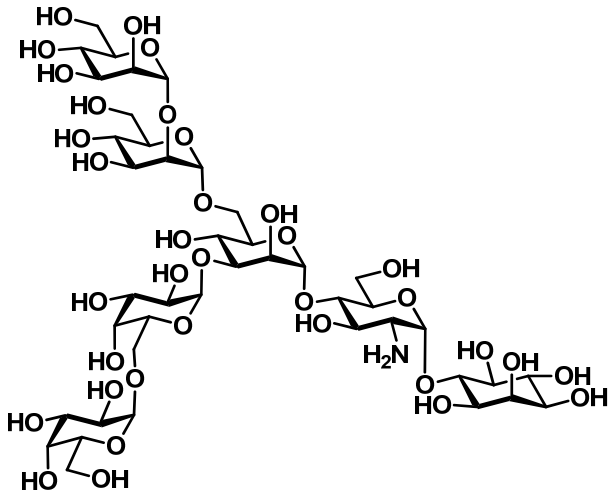

2.372 µmol of diol **151** (7.630 mg) was reacted according to Birch reduction (Method 22). Product **152** was obtained in 44% yield (1.042 µmol, 1.200 mg) as white solid by using sephadex G25 size exclusion chromatography using 5% ethanol in water as eluent.

^{1}H-NMR (400 MHz, D_2O): δ = 5.26 (s, 1H, GlcN-1), 5.10 (d, *J* = 3.7 Hz, 1H, Gal-1), 5.06 (d, *J* = 4.0 Hz, 1H, Gal'-1), 5.04 (d, *J* = 1.6 Hz, 1H, Man-1), 4.92 (d, *J* = 1.8 Hz, 1H, Man'-1), 4.86 (d, *J* = 3.6 Hz, 1H, Man''-1), 4.29 – 4.25 (m, 1H), 4.22 (d, *J* = 2.8 Hz, 1H), 4.01 – 3.44 (m, 37H), 3.41 (dd, *J* = 10.0 Hz, 2.9 Hz, 1H), 3.26 (t, *J* = 9.1 Hz, 1H), 2.68 (dd, *J* = 10.2 Hz, 3.7 Hz, 1H) ppm.

^{13}C-NMR (151 MHz, D_2O): δ = 102.22 (Man'-1), 101.47 (Gal'-1), 100.98 (GlcN-1), 99.81 (Gal-1), 98.67 (Man''-1), 98.05 (Man-1), 80.80, 80.66, 78.61, 78.43, 78.40, 76.34, 74.17, 73.71, 73.14, 72.92, 72.63, 72.41, 72.38, 71.44, 70.93, 70.86, 70.72, 70.24, 70.18, 69.88, 69.74, 69.70, 69.51, 69.31, 69.15, 69.08, 68.66, 68.14, 66.78, 66.74, 61.02 ppm.

ESI-MS: m/z M_{calcd} for $C_{42}H_{73}NO_{35}$ = 1151.3963; M_{found} = 1152.4642 $[M]^+$

9.6 SYNTHETIC PART FORCHAPTER 8

Allyl-2-*O*-acetyl-6-*O*-(2-amino-(carbonyl-benzyloxy)-ethyl-phosphatidyl)-3,4-*O*-di-2-methyl-naphthyl-α-D-mannopyranoside (154)

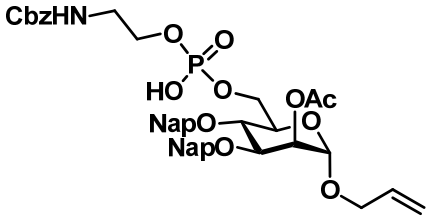

0.092 mmol of mannoside **153** (0.050 g) and 0.138 mmol of H-phosphonate **43** (0.036 g) were reacted according to phosphate formation (Method 19). Product **154** was obtained in 45% yield (0.041 mmol, 0.033 g) as colorless oil.

R_f = 0.10 (5% MeOH in DCM)

^{1}H-NMR (400 MHz, $CDCl_3$): δ = 7.74 – 6.99 (m, 19H), 5.63 (s, 1H, Allyl-2), 5.37 – 5.27 (m, 1H, Man-1), 5.12 – 4.46 (m, 8H), 4.19 – 3.60 (m, 10H), 3.25 (s, 2H), 1.91 (s, 3H, $-CH_3$) ppm.

^{13}C-NMR (101 MHz, $CDCl_3$): δ = 170.36 (C=O), 156.80 (C=O), 136.54 ($C_{Ar.}$), 136.02 ($C_{Ar.}$), 135.37 ($C_{Ar.}$), 133.23 (Allyl-2), 132.96 ($C_{Ar.}$), 132.86 ($C_{Ar.}$), 128.52 ($C_{Ar.}$), 128.41 ($C_{Ar.}$), 128.12 ($C_{Ar.}$), 127.99 ($C_{Ar.}$), 127.93 ($C_{Ar.}$), 127.64 ($C_{Ar.}$), 127.62 ($C_{Ar.}$), 126.91 ($C_{Ar.}$), 126.78 ($C_{Ar.}$), 126.20 ($C_{Ar.}$), 126.07 ($C_{Ar.}$), 126.00 ($C_{Ar.}$), 125.87 ($C_{Ar.}$), 125.77 ($C_{Ar.}$), 117.57 (Allyl-3), 96.89 (Man1-), 77.98, 77.38, 77.26, 77.06, 76.74, 74.99, 74.15, 71.77, 71.18, 68.53, 68.08, 66.59, 64.75, 45.87, 42.36, 41.70, 29.73, 27.24, 22.72, 20.93 ppm.

^{31}P-NMR (162 MHz, $CDCl_3$): δ = -2.68 ppm.

ESI-MS: m/z M_{calcd} for $C_{43}H_{46}NO_{12}P$ = 799.2758; M_{found} = 798.2925 $[M]^-$

Polarimeter: $[\alpha]_D^{20}$ = -27.98 (c = 0.1 g/L in $CHCl_3$)

FTIR: 3373.61, 2932.59, 1745.80, 1720.48, 1603.60, 1511.04, 1456.90, 1370.22, 1234.37, 1066.87, 979.65, 896.66, 857.84, 818.75, 751.65, 698.51, 664.56 cm^{-1}.

Propyl-2-*O*-acetyl-6-*O*-(2-amino-ethyl-phosphatidyl)-α-D-mannopyranoside (155)

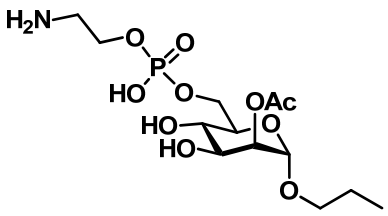

0.039 mmol of phosphate **154** (0.031 g) was reacted according to hydrogenolysis (Method 21). Product **155** was obtained in 8% yield (3.100 µmol, 1.200 mg) as white solid by using sephadex G15 size exclusion chromatography using 5% ethanol in water as eluent.

^{1}H-NMR (400 MHz, D_2O): δ = 4.98 – 4.76 (m, 3H, Man-1), 4.09 – 3.05 (m, 12H), 2.07 (s, 3H, -CH_3), 1.57 – 1.47 (m, 2H), 1.25 – 1.11 (m, 2H), 0.86 – 0.75 (m, 3H) ppm.

^{31}P-NMR (162 MHz, D_2O): δ = 0.38 ppm.

ESI-MS: m/z M_{calcd} for $C_{13}H_{26}NO_{10}P$ = 387.1294; M_{found} = 432.0977 $[M-H+2Na]^+$

Propyl-2-*O*-acetyl-6-*O*-(2-amino-ethyl-phosphatidyl)-3/4-*O*-2-methyl-naphthyl-α-D-mannopyranoside (156)

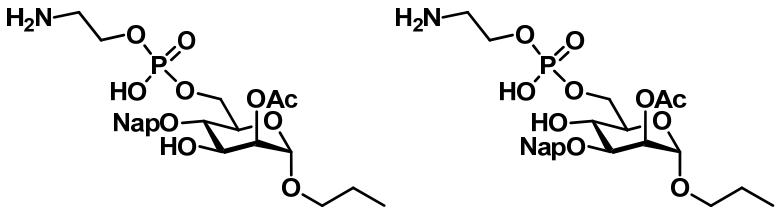

0.039 mmol of phosphate **154** (0.031 g) was reacted according to hydrogenolysis (Method 21). Products **156** were obtained in 10% yield (3.790 µmol, 2.000 mg) as white solid by using sephadex G15 size exclusion chromatography using 5% ethanol in water as eluent.

^{1}H-NMR (400 MHz, D_2O): δ = 7.90 – 7.82 (m, 4H, $H_{Ar.}$), 7.54 – 7.42 (m, 3H, $H_{Ar.}$), 5.05 (s, 1H, Man-1), 4.07 – 3.12 (m, 12H), 1.98 (s, 3H, -CH_3), 1.54 – 1.42 (m, 2H), 0.78 (dt, *J* = 14.8 Hz, 7.4 Hz, 3H) ppm.

^{31}P-NMR (162 MHz, D_2O): δ = 0.35 ppm.

ESI-MS: m/z M_{calcd} for $C_{24}H_{34}NO_{10}P$ = 527.1920; M_{found} = 572.1630 $[M-H+2Na]^+$

Allyl-2-*O*-acetyl-6-*O*-phosphonatidyl-3,4-*O*-di-2-methyl-naphthyl-α-D-mannopyranoside (159)

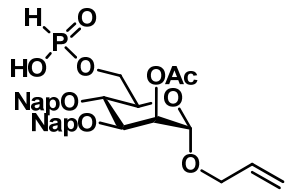

0.184 mmol of mannoside **153** (0.100 g) and 0.221 mmol of phosphonic acid (0.018 g) were reacted according to H-phosphonate formation (Method 18). Product **159** was obtained in 4% yield (8.240 µmol, 5.000 mg) as colorless oil.

R_f = 0.40 (10% MeOH in DCM)

^{1}H-NMR (400 MHz, $CDCl_3$): δ = 7.85 – 7.14 (m, 14H, $H_{Ar.}$), 6.23 – 3.32 (m, 16), 2.13 (s, 3H, -CH_3) ppm.

^{13}C-NMR (101 MHz, $CDCl_3$): δ = 170.35 (C=O), 135.64 ($C_{Ar.}$), 135.22 ($C_{Ar.}$), 133.16 (Allyl-3), 132.92 ($C_{Ar.}$), 128.10 ($C_{Ar.}$), 127.91 ($C_{Ar.}$), 127.74 ($C_{Ar.}$), 127.63 ($C_{Ar.}$), 126.78

($C_{Ar.}$), 126.01 ($C_{Ar.}$), 117.76 (Allyl-3), 96.87 (Man-1), 77.37, 77.26, 77.05, 76.74, 74.97, 74.13, 71.72, 68.35, 68.07, 20.95 ppm.

^{31}P-NMR (162 MHz, $CDCl_3$): δ = 3.88 ppm.

ESI-MS: m/z M_{calcd} for $C_{33}H_{35}O_9P$ = 606.2019; M_{found} = 605.1964 $[M]^-$

Polarimeter: $[\alpha]_D^{20}$ = -134.41 (c = 0.1 g/L in $CHCl_3$)

FTIR: 3509.95, 3056.95, 2922.79, 1748.53, 1510.42, 1371.74, 1234.03, 1080.04, 978.37, 857.10, 819.54, 753.74, 669.21 cm^{-1}.

Allyl-2-*O*-acetyl-3,4-*O*-di-2-methyl-naphthyl-6-*O*-(2-(*N*-(*N*-(*N*-(*tert*-butoxycarbonyl)-*N*,*S*-(methylene)-L-cysteinyl)-*N'*-(*tert*-butoxycarbonyl)-L-lysinyl)-*O*-*tert*-butyl-L-aspartatyl)-aminoethyl-phosphatidyl)-α-D-mannopyranoside (161)

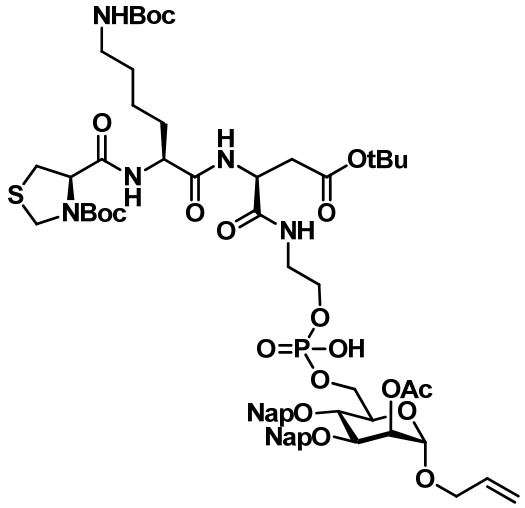

7.400 µmol of tripeptide **160** (5.000 mg) and 0.011 mmol of H-phosphonat **159** (6.730 mg) were reacted according to phosphate formation (Method 19). Product **161** was isolated as colorless oil.

R_f = 0.30 (10% MeOH in DCM)

^{1}H-NMR (400 MHz, $CDCl_3$): δ = 7.84 – 7.00 (m, 14H, $H_{Ar.}$), 6.10 – 2.57 (m, 16H), 1.90 (s, 3H, -CH_3), 1.35 – 0.58 (m) ppm.

^{13}C-NMR (101 MHz, $CDCl_3$): δ = 170.32 (C=0), 135.17 ($C_{Ar.}$), 133.17 (Allyl-2), 132.94 ($C_{Ar.}$), 128.11 ($C_{Ar.}$), 127.90 ($C_{Ar.}$), 127.62 ($C_{Ar.}$), 126.83 ($C_{Ar.}$), 126.02 ($C_{Ar.}$), 125.89 ($C_{Ar.}$), 117.70 (Allyl-3), 96.98 (Man-1), 77.35, 77.24, 77.03, 76.72, 71.73, 68.28, 46.00, 31.95, 29.72, 22.72, 20.98 (-CH_3), 14.16, 8.63 ppm.

^{31}P-NMR (162 MHz, $CDCl_3$): δ = 4.03 ppm.

MALDI-MS: m/z M_{calcd} for $C_{63}H_{86}N_5O_{19}PS$ = 1279.5375; M_{found} = 1279.025 $[M]^-$

Propyl-2-*O*-acetyl-6-*O*-(2-(*N*-(*N*-(*N*-(*tert*-butoxycarbonyl)-*N,S*-(methylene)-L-cysteinyl)-*N'*-(*tert*-butoxycarbonyl)-L-lysinyl)-*O*-*tert*-butyl-L-aspartatyl)-aminoethyl-phosphatidyl)-α-D-mannopyranoside (162)

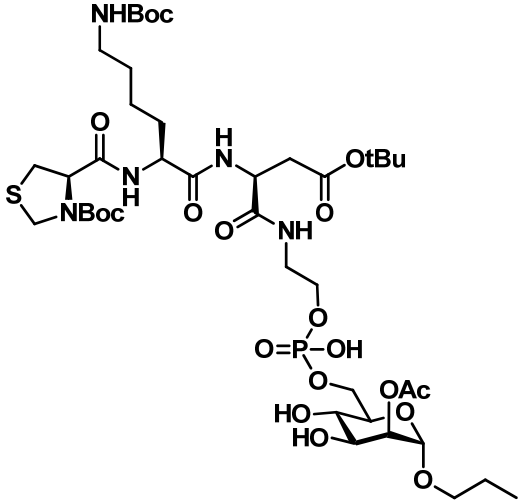

CKD-Man III comjugate **161** was reacted according to hydrogenolysis (Method 21). Product **162** was isolated as colorless oil by using sephadex G15 size exclusion chromatography using 5% ethanol in water as eluent.

^{31}P-NMR (162 MHz, D_2O): δ = 7.03 ppm.

ESI-MS: m/z M_{calcd} for $C_{41}H_{72}N_5O_{19}PS$ = 1001.4280; M_{found} = 1003.2648 $[M]^+$

Propyl-2-*O*-acetyl-6-*O*-(2-(*N*-(*N*-(*N,S*-(methylene)-L-cysteinyl)-L-lysinyl)-L-aspartatyl)-aminoethyl-phosphatidyl)-α-D-mannopyranoside (158)

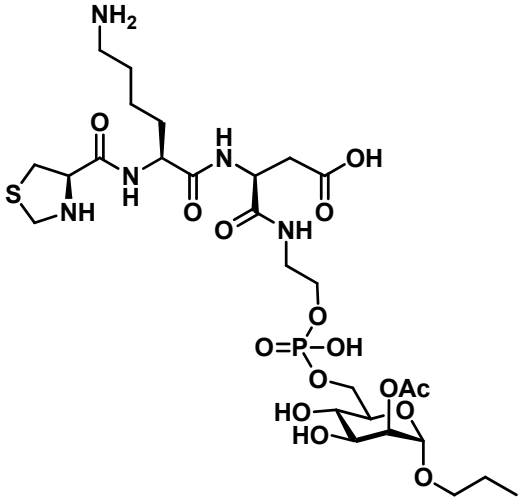

Phosphodiester **162** was reacted according to peptide deprotection (Method 20). Product **158** was isolated in 27% yield (2.011 μmol, 1.500 mg) over three steps as white solid by using sephadex G15 size exclusion chromatography using 5% ethanol in water as eluent.

^{1}H-NMR (400 MHz, D_2O): δ = 7.44 (s, Amide), 5.83 (s, 1H), 4.95 (s, 2H, Man-1), 4.75 (s, 1H), 4.00 – 3.33 (m, 7H), 3.05 (q, *J* = 7.4 Hz, 2H), 2.02 (s, 3H, -CH_3), 1.51 – 1.42 (m, 2H), 1.13 (t, *J* = 7.4 Hz, 3H), 0.77 (t, *J* = 7.3 Hz, 3H) ppm.

^{31}P-NMR (162 MHz, D_2O): δ = 6.94 ppm.

ESI-MS: m/z M_{calcd} for $C_{27}H_{48}N_5O_{15}PS$ = 745.2605; M_{found} = 373.0638 $[M]^{++}$

2-(*N*-(*N*-(*N*-(*tert*-Butoxycarbonyl)-*N,S*-(methylene)-L-cysteinyl)-*N'*-(*tert*-butoxycarbonyl)-L-lysinyl)-*O*-*tert*-butyl-L-aspartatyl)-aminoethyl-phosphonate (163)

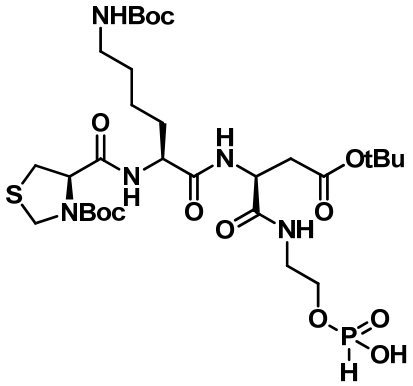

0.041 mmol of tripeptide **160** (0.028 g) and 0.046 mmol of phosphonic acid (5.500 mg) were reacted according to H-phosphonate formation (Method 18). Product **163** was obtained in 29% yield (0.012 mmol, 9.000 mg) as white solid.

R_f = 0.20 (10% MeOH in DCM)

^{31}P-NMR (162 MHz, $CDCl_3$): δ = 9.57 ppm.

ESI-MS: m/z M_{calcd} for $C_{30}H_{54}N_5O_{12}PS$ = 739.3227; M_{found} = 738.3315 $[M]^{-}$

10. REFERENCES

1. (a) Westheide, W., *Spezielle Zoologie. Teil 1: Einzeller und Wirbellose Tiere*. 2006; (b) Grell, K. G., *Protozoologie*. 1968.
2. Paul R Torgerson, P. M., *Bull World Health Organ* **2013,** *91*, 501-508.
3. (a) WHO, World Malaria Report. **2015**; (b) WHO, Chagas disease factsheet. **2013**; (c) WHO, Leishmaniasis factsheet. **2015**.
4. Michael P. Barrett, R. J. B., August Stich, Julio O Lazzari, Alberto Carlos Frasch, Juan Jose Cazzulo, Sanjeev Krishna, *The Lancet* **2003,** *362* (9394), 1469-1480.
5. Pere P Simarro, G. C., Massimo Paone, Jose R Franco, Abdoulaye Diarra, Jose A Ruiz, Eric M Fevre, Fabrice Courtin, Raffaele C Mattioli, Jean G Jannin, *International Journal of Health Geographics* **2010,** *9* (57).
6. (a) Gibson, W. C., The SRA gene: the key to understanding the nature of Trypanosoma brucei rhodesiense. *Parasitology* **2005,** *131* (Pt 2), 143-50; (b) Uzureau, P.; Uzureau, S.; Lecordier, L.; Fontaine, F.; Tebabi, P.; Homble, F.; Grelard, A.; Zhendre, V.; Nolan, D. P.; Lins, L.; Crowet, J. M.; Pays, A.; Felu, C.; Poelvoorde, P.; Vanhollebeke, B.; Moestrup, S. K.; Lyngso, J.; Pedersen, J. S.; Mottram, J. C.; Dufourc, E. J.; Perez-Morga, D.; Pays, E., Mechanism of Trypanosoma brucei gambiense resistance to human serum. *Nature* **2013,** *501* (7467), 430-+; (c) Stephens, N. A.; Kieft, R.; MacLeod, A.; Hajduk, S. L., Trypanosome resistance to human innate immunity: targeting Achilles' heel. *Trends Parasitol.* **2012,** *28* (12), 539-545.
7. (a) Olowe, S. A., Case of Congenital Trypanosomiasis in Lagos. *Trans. R. Soc. Trop. Med. Hyg.* **1975,** *69* (1), 57-59; (b) Rocha, G.; Martins, A.; Gama, G.; Brandao, F.; Atouguia, J., Possible cases of sexual and congenital transmission of sleeping sickness. *Lancet* **2004,** *363* (9404), 247-247.
8. Cherenet, T.; Sani, R. A.; Panandam, J. M.; Nadzr, S.; Speybroeck, N.; Van Den Bossche, P., Seasonal prevalence of bovine trypanosomosis in a tsetse-infested zone and a tsetse-free zone of the Amhara Region, north-west Ethiopia. *Onderstepoort J. Vet. Res.* **2004,** *71* (4), 307-312.
9. wikimedia, f. l.
10. Gerasimos Langousis, K. L. H., *Natrue Reviews Microbiology* **2014,** *12*, 505-518.
11. CDC, **2015**.
12. (a) Sullivan, L.; Fleming, J.; Sastry, L.; Mehlert, A.; Wall, S. J.; Ferguson, M. A. J., Identification of sVSG117 as an Immunodiagnostic Antigen and Evaluation of a Dual-Antigen Lateral Flow Test for the Diagnosis of Human African Trypanosomiasis. *Plos Neglect Trop D* **2014,** *8* (7); (b) Sullivan, L.; Wall, S. J.; Carrington, M.; Ferguson, M. A. J., Proteomic Selection of Immunodiagnostic Antigens for Human African Trypanosomiasis and Generation of a Prototype Lateral Flow Immunodiagnostic Device. *Plos Neglect Trop D* **2013,** *7* (2).
13. Vincent, I. M.; Creek, D.; Watson, D. G.; Kamleh, M. A.; Woods, D. J.; Wong, P. E.; Burchmore, R. J.; Barrett, M. P., A molecular mechanism for eflornithine resistance in African trypanosomes. *Plos Pathog* **2010,** *6* (11), e1001204.
14. Bezie M., G. M., Dagnachew S., Tadesse D., Tadesse G., *Journal of Veterinary Advances* **2014,** *4* (11), 732-745.
15. Davis, C. E., Thrombocytopenia - a Uniform Complication of African Trypanosomiasis. *Acta Trop.* **1982,** *39* (2), 123-133.
16. (a) Nok, A. J.; Nzelibe, H. C.; Yako, S. K., Trypanosoma evansi sialidase: surface localization, properties and hydrolysis of ghost red blood cells and brain cells-implications in trypanosomiasis. *Z Naturforsch C* **2003,** *58* (7-8), 594-601; (b) Buratai,

L. B.; Nok, A. J.; Ibrahim, S.; Umar, I. A.; Esievo, K. A. N., Characterization of sialidase from bloodstream forms of Trypanosoma vivax. *Cell Biochem. Funct.* **2006,** *24* (1), 71-77; (c) Lee, H.; Kelm, S.; Michalski, J. C.; Schauer, R., Influence of Sialic Acids on the Galactose-Recognizing Receptor of Rat Peritoneal-Macrophages. *Biol Chem H-S* **1990,** *371* (4), 307-316.

17. (a) Nikolskaia, O. V.; Kim, Y. V.; Kovbasnjuk, O.; Kim, K. J.; Grab, D. J., Entry of Trypanosoma brucei gambiense into microvascular endothelial cells of the human blood-brain barrier. *Int J Parasitol* **2006,** *36* (5), 513-519; (b) Nikolskaia, O. V.; Lima, A. P. C. D.; Kim, Y. V.; Lonsdale-Eccles, J. D.; Fukuma, T.; Scharfstein, J.; Grab, D. J., Blood-brain barrier traversal by African trypanosomes requires calcium signaling induced by parasite cysteine protease. *J Clin Invest* **2006,** *116* (10), 2739-2747.
18. (a) Troeberg, L.; Pike, R. N.; Morty, R. E.; Berry, M. K.; Coetzer, T. H. T.; LonsdaleEccles, J. D., Proteases from Trypanosoma brucei brucei - Purification, characterisation and interactions with host regulatory molecules. *Eur J Biochem* **1996,** *238* (3), 728-736; (b) Authie, E.; Boulange, A.; Muteti, D.; Lalmanach, G.; Gauthier, F.; Musoke, A. J., Immunisation of cattle with cysteine proteinases of Trypanosoma congolense: targetting the disease rather than the parasite. *Int J Parasitol* **2001,** *31* (13), 1429-1433.
19. Ndung'u, J. M.; Wright, N. G.; Jennings, F. W.; Murray, M., Changes in atrial natriuretic factor and plasma renin activity in dogs infected with Trypanosoma brucei. *Parasitol. Res.* **1992,** *78* (7), 553-6.
20. Anosa, V. O.; Isoun, T. T., Serum proteins, blood and plasma volumes in experimental Trypanosoma vivax infections of sheep and goats. *Trop. Anim. Health Prod.* **1976,** *8* (1), 14-9.
21. Biswas, D.; Choudhury, A.; Misra, K. K., Histopathology of Trypanosoma (Trypanozoon) evansi infection in bandicoot rat. I. visceral organs. *Exp Parasitol* **2001,** *99* (3), 148-59.
22. (a) Tizard, I. R.; Holmes, W. L.; York, D. A.; Mellors, A., The generation and identification of the hemolysin of Trypanosoma congolense. *Experientia* **1977,** *33* (7), 901-2; (b) Tizard, I. R.; Holmes, W. L., The release of soluble vasoactive material from Trypanosoma congolense in intraperitoneal diffusion chambers. *Trans. R. Soc. Trop. Med. Hyg.* **1977,** *71* (1), 52-5.
23. Bachmann, E.; Zbinden, G., Effect of metabolic inhibitors on lauric acid-induced hemolysis. *Agents Actions* **1973,** *3* (1), 45-7.
24. Colley, C. M.; Zwaal, R. F.; Roelofsen, B.; van Deenen, L. L., Lytic and non-lytic degradation of phospholipids in mammalian erythrocytes by pure phospholipases. *Biochim. Biophys. Acta* **1973,** *307* (1), 74-82.
25. Greenwood, B. M., Possible role of a B-cell mitogen in hypergammaglobulinaemia in malaria and trypanosomiasis. *Lancet* **1974,** *1* (7855), 435-6.
26. Vaidya, T.; Bakhiet, M.; Hill, K. L.; Olsson, T.; Kristensson, K.; Donelson, J. E., The gene for a T lymphocyte triggering factor from African trypanosomes. *J Exp Med* **1997,** *186* (3), 433-8.
27. (a) Hudson, K. M.; Byner, C.; Freeman, J.; Terry, R. J., Immunodepression, high IgM levels and evasion of the immune response in murine trypanosomiasis. *Nature* **1976,** *264* (5583), 256-8; (b) Rifkin, M. R.; Landsberger, F. R., Trypanosome variant surface glycoprotein transfer to target membranes: a model for the pathogenesis of trypanosomiasis. *Proc. Natl. Acad. Sci. USA* **1990,** *87* (2), 801-5.
28. (a) Igbokwe, I. O.; Esievo, K. A.; Saror, D. I.; Obagaiye, O. K., Increased susceptibility of erythrocytes to in vitro peroxidation in acute Trypanosoma brucei infection of mice. *Vet. Parasitol.* **1994,** *55* (4), 279-86; (b) Vickerman, K.; Luckins, A. G., Localization of variable antigens in the surface coat of Trypanosoma brucei using

ferritin conjugated antibody. *Nature* **1969,** *224* (5224), 1125-6; (c) Anosa, V. O.; Kaneko, J. J., Pathogenesis of Trypanosoma brucei infection in deer mice (Peromyscus maniculatus): hematologic, erythrocyte biochemical, and iron metabolic aspects. *Am. J. Vet. Res.* **1983,** *44* (4), 639-44.

29. (a) Davies C. E., R. R. S., Weller R. D., Broude A. I., *Clin. Investig.* **1974,** *53*, 1359-1367; (b) Slots, J. M. M.; Vanmiert, A. S. J. P. A. M.; Akkerman, J. W. N.; Degee, A. L. W., Trypanosoma-Brucei and Trypanosoma-Vivax - Antigen-Antibody Complexes as a Cause of Platelet Serotonin Release Invitro and Invivo. *Exp Parasitol* **1977,** *43* (1), 211-219; (c) Mbaya A., K. H., Nwosu C., Book: Anemia. **2012**; (d) Woodruff, A. W., Recent Work on Anemias in Tropics. *Br. Med. Bull.* **1972,** *28* (1), 92-&; (e) Naessens, J.; Kitani, H.; Nakamura, Y.; Yagi, Y.; Sekikawa, K.; Iraqi, F., TNF-alpha mediates the development of anaemia in a murine Trypanosoma brucei rhodesiense infection, but not the anaemia associated with a murine Trypanosoma congolense infection. *Clin. Exp. Immunol.* **2005,** *139* (3), 405-410; (f) Jelkmann, W., Proinflammatory cytokines lowering erythropoietin production. *J. Interferon Cytokine Res.* **1998,** *18* (8), 555-559; (g) Mabbot N., S. J., *Infect. Immunol.* **1995,** *63*, 1563-1566; (h) Millar, A. E.; Sternberg, J.; McSharry, C.; Wei, X. Q.; Liew, F. Y.; Turner, C. M., T-Cell responses during Trypanosoma brucei infections in mice deficient in inducible nitric oxide synthase. *Infect. Immun.* **1999,** *67* (7), 3334-8; (i) Esievo, K. A.; Saror, D. I., Leukocyte response in experimental Trypanosoma vivax infection in cattle. *J Comp Pathol* **1983,** *93* (2), 165-9; (j) Slater, T. F., Free-Radical Mechanisms in Tissue-Injury. *Biochemical Journal* **1984,** *222* (1), 1-15; (k) Umar, I. A.; Ogenyi, E.; Okodaso, D.; Kimeng, E.; Stancheva, G. I.; Omage, J. J.; Isah, S.; Ibrahim, M. A., Amelioration of anaemia and organ damage by combined intraperitoneal administration of vitamins A and C to Trypanosoma brucei brucei-infected rats. *Afr J Biotechnol* **2007,** *6* (18), 2083-2086; (l) Nok, A. J.; Esievo, K. A. N.; Ajibike, M. O.; Achoba, I. I.; Tekdek, K.; Gimba, C. E.; Kagbu, J. A.; Ndams, I. S., Modulation of the Calcium-Pump of the Kidney and Testes of Rats Infected with Trypanosoma-Congolense. *J Comp Pathol* **1992,** *107* (1), 119-123.

30. Vincendeau, P.; Bouteille, B., Immunology and immunopathology of African trypanosomiasis. *An. Acad. Bras. Cienc.* **2006,** *78* (4), 645-65.

31. Reina-San-Martin, B.; Cosson, A.; Minoprio, P., Lymphocyte polyclonal activation: a pitfall for vaccine design against infectious agents. *Parasitol. Today* **2000,** *16* (2), 62-7.

32. Ilemobade, A. A.; Adegboye, D. S.; Onoviran, O.; Chima, J. C., Immunodepressive effects of trypanosomal infection in cattle immunized against contagious bovine pleuropneumonia. *Parasite Immunol* **1982,** *4* (4), 273-82.

33. Gobert, A. P.; Daulouede, S.; Lepoivre, M.; Boucher, J. L.; Bouteille, B.; Buguet, A.; Cespuglio, R.; Veyret, B.; Vincendeau, P., L-Arginine availability modulates local nitric oxide production and parasite killing in experimental trypanosomiasis. *Infect. Immun.* **2000,** *68* (8), 4653-7.

34. Schwede, A.; Jones, N.; Engstler, M.; Carrington, M., The VSG C-terminal domain is inaccessible to antibodies on live trypanosomes. *Mol. Biochem. Parasitol.* **2011,** *175* (2), 201-204.

35. Mansfield, J. M.; Paulnock, D. M., Regulation of innate and acquired immunity in African trypanosomiasis. *Parasite Immunol* **2005,** *27* (10-11), 361-371.

36. (a) Ferrante, A.; Allison, A. C., Alternative pathway activation of complement by African trypanosomes lacking a glycoprotein coat. *Parasite Immunol* **1983,** *5* (5), 491-8; (b) Ziegelbauer, K.; Overath, P., Organization of two invariant surface glycoproteins in the surface coat of Trypanosoma brucei. *Infect. Immun.* **1993,** *61* (11), 4540-5; (c) Chung, W. L.; Carrington, M.; Field, M. C., Cytoplasmic targeting signals

in transmembrane invariant surface glycoproteins of trypanosomes. *J. Biol. Chem.* **2004,** *279* (52), 54887-54895.

37. (a) Engstler, M.; Pfohl, T.; Herminghaus, S.; Boshart, M.; Wiegertjes, G.; Heddergott, N.; Overath, P., Hydrodynamic flow-mediated protein sorting on the cell surface of trypanosomes. *Cell* **2007,** *131* (3), 505-515; (b) Pal, A.; Hall, B. S.; Jeffries, T. R.; Field, M. C., Rab5 and Rab11 mediate transferrin and anti-variant surface glycoprotein antibody recycling in Trypanosoma brucei. *Biochemical Journal* **2003,** *374*, 443-451.
38. Campos, M. A.; Almeida, I. C.; Takeuchi, O.; Akira, S.; Valente, E. P.; Procopio, D. O.; Travassos, L. R.; Smith, J. A.; Golenbock, D. T.; Gazzinelli, R. T., Activation of Toll-like receptor-2 by glycosylphosphatidylinositol anchors from a protozoan parasite. *J. Immunol.* **2001,** *167* (1), 416-23.
39. Tachado, S. D.; Schofield, L., Glycosylphosphatidylinositol Toxin of Trypanosoma-Brucei Regulates Il-1-Alpha and Tnf-Alpha Expression in Macrophages by Protein-Tyrosine Kinase Mediated Signal-Transduction. *Biochem. Bioph. Res. Commun.* **1994,** *205* (2), 984-991.
40. (a) Magez, S.; Stijlemans, B.; Radwanska, M.; Pays, E.; Ferguson, M. A. J.; De Baetselier, P., The glycosyl-inositol-phosphate and dimyristoylglycerol moieties of the glycosylphosphatidylinositol anchor of the trypanosome variant-specific surface glycoprotein are distinct macrophage-activating factors. *J. Immunol.* **1998,** *160* (4), 1949-1956; (b) Tachado, S. D.; Gerold, P.; Schwarz, R.; Novakovic, S.; McConville, M.; Schofield, L., Signal transduction in macrophages by glycosylphosphatidylinositols of Plasmodium, Trypanosoma, and Leishmania: Activation of protein tyrosine kinases and protein kinase C by inositolglycan and diacylglycerol moieties. *Proc. Natl. Acad. Sci. USA* **1997,** *94* (8), 4022-4027.
41. Murray, M.; Morrison, W. I.; Whitelaw, D. D., Host Susceptibility to African Trypanosomiasis - Trypanotolerance. *Adv. Parasitol.* **1982,** *21*, 1-68.
42. (a) Esievo, K. A. N., Trypanosoma-Vivax, Stock-V953 - Inhibitory Effect of Type-a Influenza-Virus Anti-Hav8 Serum on Invitro Neuraminidase (Sialidase) Activity. *J. Parasitol.* **1983,** *69* (3), 491-495; (b) Esievo, K. A. N.; Jaye, A.; Andrews, J. N.; Ukoha, A. I.; Alafiatayo, R. A.; Eduvie, L. O.; Saror, D. I.; Njoku, C. O., Electrophoresis of Bovine Erythrocyte Sialic Acids - Existence of Additional Band in Trypanotolerant Ndama Cattle. *J Comp Pathol* **1990,** *102* (4), 357-361.
43. (a) d'Ieteren, G. D.; Authie, E.; Wissocq, N.; Murray, M., Trypanotolerance, an option for sustainable livestock production in areas at risk from trypanosomosis. *Rev Sci Tech* **1998,** *17* (1), 154-75; (b) Authie, E.; Pobel, T., Serum Hemolytic Complement Activity and C3 Levels in Bovine Trypanosomosis under Natural Conditions of Challenge - Early Indications of Individual Susceptibility to Disease. *Vet. Parasitol.* **1990,** *35* (1-2), 43-59.
44. (a) Cross, G. A. M., Identification, Purification and Properties of Clone-Specific Glycoprotein Antigens Constituting Surface Coat of Trypanosoma-Brucei. *Parasitology* **1975,** *71* (Dec), 393-417; (b) Bridgen, P. J.; Cross, G. A.; Bridgen, J., N-terminal amino acid s equences of variant-specific surface antigens from Trypanosoma brucei. *Nature* **1976,** *263* (5578), 613-4.
45. Ferguson, M. A.; Cross, G. A., Myristylation of the membrane form of a Trypanosoma brucei variant surface glycoprotein. *J Biol Chem* **1984,** *259* (5), 3011-5.
46. Bangs, J. D.; Andrews, N. W.; Hart, G. W.; Englund, P. T., Posttranslational modification and intracellular transport of a trypanosome variant surface glycoprotein. *J Cell Biol* **1986,** *103* (1), 255-63.
47. (a) Seyfang, A.; Mecke, D.; Duszenko, M., Degradation, recycling, and shedding of Trypanosoma brucei variant surface glycoprotein. *J Protozool* **1990,** *37* (6), 546-52; (b) Engstler, M.; Thilo, L.; Weise, F.; Grunfelder, C. G.; Schwarz, H.; Boshart, M.;

Overath, P., Kinetics of endocytosis and recycling of the GPI-anchored variant surface glycoprotein in Trypanosoma brucei. *J Cell Sci* **2004,** *117* (Pt 7), 1105-15.
48. (a) Jackson, D. G.; Owen, M. J.; Voorheis, H. P., A new method for the rapid purification of both the membrane-bound and released forms of the variant surface glycoprotein from Trypanosoma brucei. *The Biochemical journal* **1985,** *230* (1), 195-202; (b) Grunfelder, C. G.; Engstler, M.; Weise, F.; Schwarz, H.; Stierhof, Y. D.; Boshart, M.; Overath, P., Accumulation of a GPI-anchored protein at the cell surface requires sorting at multiple intracellular levels. *Traffic* **2002,** *3* (8), 547-59.
49. (a) Morrison, L. J.; Marcello, L.; McCulloch, R., Antigenic variation in the African trypanosome: molecular mechanisms and phenotypic complexity. *Cell. Microbiol.* **2009,** *11* (12), 1724-34; (b) Blum, M. L.; Down, J. A.; Gurnett, A. M.; Carrington, M.; Turner, M. J.; Wiley, D. C., A structural motif in the variant surface glycoproteins of Trypanosoma brucei. *Nature* **1993,** *362* (6421), 603-9.
50. wonkycompass.wordpress.com.
51. Mehlert, A.; Bond, C. S.; Ferguson, M. A., The glycoforms of a Trypanosoma brucei variant surface glycoprotein and molecular modeling of a glycosylated surface coat. *Glycobiology* **2002,** *12* (10), 607-12.
52. (a) Carrington, M.; Miller, N.; Blum, M.; Roditi, I.; Wiley, D.; Turner, M., Variant specific glycoprotein of Trypanosoma brucei consists of two domains each having an independently conserved pattern of cysteine residues. *J. Mol. Biol.* **1991,** *221* (3), 823-35; (b) Carrington, M.; Boothroyd, J., Implications of conserved structural motifs in disparate trypanosome surface proteins. *Mol. Biochem. Parasitol.* **1996,** *81* (2), 119-26.
53. Parodi, A. J., N-glycosylation in trypanosomatid protozoa. *Glycobiology* **1993,** *3* (3), 193-9.
54. (a) Mehlert, A.; Zitzmann, N.; Richardson, J. M.; Treumann, A.; Ferguson, M. A., The glycosylation of the variant surface glycoproteins and procyclic acidic repetitive proteins of Trypanosoma brucei. *Mol. Biochem. Parasitol.* **1998,** *91* (1), 145-52; (b) Izquierdo, L.; Schulz, B. L.; Rodrigues, J. A.; Guther, M. L.; Procter, J. B.; Barton, G. J.; Aebi, M.; Ferguson, M. A., Distinct donor and acceptor specificities of Trypanosoma brucei oligosaccharyltransferases. *EMBO J.* **2009,** *28* (17), 2650-61; (c) Smith, T. K.; Butikofer, P., Lipid metabolism in Trypanosoma brucei. *Mol. Biochem. Parasitol.* **2010,** *172* (2), 66-79.
55. Warren, G., Transport through the Golgi in Trypanosoma brucei. *Histochem Cell Biol* **2013,** *140* (3), 235-8.
56. Field, M. C.; Sergeenko, T.; Wang, Y. N.; Bohm, S.; Carrington, M., Chaperone requirements for biosynthesis of the trypanosome variant surface glycoprotein. *Plos One* **2010,** *5* (1), e8468.
57. Manna, P. T.; Boehm, C.; Leung, K. F.; Natesan, S. K.; Field, M. C., Life and times: synthesis, trafficking, and evolution of VSG. *Trends Parasitol.* **2014,** *30* (5), 251-8.
58. (a) Wickner, W.; Schekman, R., Protein translocation across biological membranes. *Science* **2005,** *310* (5753), 1452-6; (b) Liu, L.; Liang, X. H.; Uliel, S.; Unger, R.; Ullu, E.; Michaeli, S., RNA interference of signal peptide-binding protein SRP54 elicits deleterious effects and protein sorting defects in trypanosomes. *J Biol Chem* **2002,** *277* (49), 47348-57; (c) Lustig, Y.; Vagima, Y.; Goldshmidt, H.; Erlanger, A.; Ozeri, V.; Vince, J.; McConville, M. J.; Dwyer, D. M.; Landfear, S. M.; Michaeli, S., Down-regulation of the trypanosomatid signal recognition particle affects the biogenesis of polytopic membrane proteins but not of signal peptide-containing proteins. *Eukaryot Cell* **2007,** *6* (10), 1865-75; (d) Goldshmidt, H.; Sheiner, L.; Butikofer, P.; Roditi, I.; Uliel, S.; Gunzel, M.; Engstler, M.; Michaeli, S., Role of protein translocation pathways across the endoplasmic reticulum in Trypanosoma brucei. *J Biol Chem* **2008,**

283 (46), 32085-98; (e) McConnell, J.; Gurnett, A. M.; Cordingley, J. S.; Walker, J. E.; Turner, M. J., Biosynthesis of Trypanosoma brucei variant surface glycoprotein. I. Synthesis, size, and processing of an N-terminal signal peptide. *Mol. Biochem. Parasitol.* **1981,** *4* (3-4), 225-42; (f) Boothroyd, J. C.; Paynter, C. A.; Cross, G. A.; Bernards, A.; Borst, P., Variant surface glycoproteins of Trypanosoma brucei are synthesised with cleavable hydrophobic sequences at the carboxy and amino termini. *Nucleic Acids Res* **1981,** *9* (18), 4735-43.

59. (a) Barlowe, C. K.; Miller, E. A., Secretory protein biogenesis and traffic in the early secretory pathway. *Genetics* **2013,** *193* (2), 383-410; (b) Wang, J.; Bohme, U.; Cross, G. A., Structural features affecting variant surface glycoprotein expression in Trypanosoma brucei. *Mol. Biochem. Parasitol.* **2003,** *128* (2), 135-45.
60. Udenfriend, S.; Kodukula, K., How glycosylphosphatidylinositol-anchored membrane proteins are made. *Annu. Rev. Biochem.* **1995,** *64*, 563-91.
61. (a) Nagamune, K.; Ohishi, K.; Ashida, H.; Hong, Y.; Hino, J.; Kangawa, K.; Inoue, N.; Maeda, Y.; Kinoshita, T., GPI transamidase of Trypanosoma brucei has two previously uncharacterized (trypanosomatid transamidase 1 and 2) and three common subunits. *Proc. Natl. Acad. Sci. USA* **2003,** *100* (19), 10682-7; (b) Mayor, S.; Menon, A. K.; Cross, G. A., Galactose-containing glycosylphosphatidylinositols in Trypanosoma brucei. *J Biol Chem* **1992,** *267* (2), 754-61; (c) Ferguson, M. A. J., The structure, biosynthesis and functions of glycosylphosphatidylinositol anchors, and the contributions of trypanosome research. *J Cell Sci* **1999,** *112* (17), 2799-2809; (d) Bohme, U.; Cross, G. A., Mutational analysis of the variant surface glycoprotein GPI-anchor signal sequence in Trypanosoma brucei. *J Cell Sci* **2002,** *115* (Pt 4), 805-16; (e) Triggs, V. P.; Bangs, J. D., Glycosylphosphatidylinositol-dependent protein trafficking in bloodstream stage Trypanosoma brucei. *Eukaryot Cell* **2003,** *2* (1), 76-83.
62. Manna, P. T.; Boehm, C.; Leung, K. F.; Natesan, S. K.; Field, M. C., Life and times: synthesis, trafficking, and evolution of VSG. *Trends Parasitol* **2014,** *30* (5), 251-8.
63. Sevova, E. S.; Bangs, J. D., Streamlined architecture and glycosylphosphatidylinositol-dependent trafficking in the early secretory pathway of African trypanosomes. *Mol Biol Cell* **2009,** *20* (22), 4739-50.
64. (a) Bangs, J. D.; Doering, T. L.; Englund, P. T.; Hart, G. W., Biosynthesis of a variant surface glycoprotein of Trypanosoma brucei. Processing of the glycolipid membrane anchor and N-linked oligosaccharides. *J Biol Chem* **1988,** *263* (33), 17697-705; (b) Mcconville, M. J.; Ferguson, M. A. J., The Structure, Biosynthesis and Function of Glycosylated Phosphatidylinositols in the Parasitic Protozoa and Higher Eukaryotes. *Biochemical Journal* **1993,** *294*, 305-324.
65. Manthri, S.; Guther, M. L.; Izquierdo, L.; Acosta-Serrano, A.; Ferguson, M. A., Deletion of the TbALG3 gene demonstrates site-specific N-glycosylation and N-glycan processing in Trypanosoma brucei. *Glycobiology* **2008,** *18* (5), 367-83.
66. Anitei, M.; Hoflack, B., Exit from the trans-Golgi network: from molecules to mechanisms. *Curr. Opin. Cell Biol.* **2011,** *23* (4), 443-51.
67. (a) Field, M. C.; Carrington, M., The trypanosome flagellar pocket. *Nat Rev Microbiol* **2009,** *7* (11), 775-86; (b) Morgan, G. W.; Hall, B. S.; Denny, P. W.; Field, M. C.; Carrington, M., The endocytic apparatus of the kinetoplastida. Part II: machinery and components of the system. *Trends Parasitol.* **2002,** *18* (12), 540-6; (c) Natesan, S. K.; Peacock, L.; Matthews, K.; Gibson, W.; Field, M. C., Activation of endocytosis as an adaptation to the mammalian host by trypanosomes. *Eukaryot Cell* **2007,** *6* (11), 2029-37.
68. Manna, P. T.; Kelly, S.; Field, M. C., Adaptin evolution in kinetoplastids and emergence of the variant surface glycoprotein coat in African trypanosomatids. *Mol. Phylogen. Evol.* **2013,** *67* (1), 123-8.

69. Grunfelder, C. G.; Engstler, M.; Weise, F.; Schwarz, H.; Stierhof, Y. D.; Morgan, G. W.; Field, M. C.; Overath, P., Endocytosis of a glycosylphosphatidylinositol-anchored protein via clathrin-coated vesicles, sorting by default in endosomes, and exocytosis via RAB11-positive carriers. *Mol Biol Cell* **2003,** *14* (5), 2029-40.
70. (a) Ziegelbauer, K.; Multhaup, G.; Overath, P., Molecular characterization of two invariant surface glycoproteins specific for the bloodstream stage of Trypanosoma brucei. *J Biol Chem* **1992,** *267* (15), 10797-803; (b) Chung, W. L.; Leung, K. F.; Carrington, M.; Field, M. C., Ubiquitylation is required for degradation of transmembrane surface proteins in trypanosomes. *Traffic* **2008,** *9* (10), 1681-97; (c) Leung, K. F.; Riley, F. S.; Carrington, M.; Field, M. C., Ubiquitylation and developmental regulation of invariant surface protein expression in trypanosomes. *Eukaryot Cell* **2011,** *10* (7), 916-31; (d) Leung, K. F.; Dacks, J. B.; Field, M. C., Evolution of the multivesicular body ESCRT machinery; retention across the eukaryotic lineage. *Traffic* **2008,** *9* (10), 1698-716; (e) Silverman, J. S.; Muratore, K. A.; Bangs, J. D., Characterization of the late endosomal ESCRT machinery in Trypanosoma brucei. *Traffic* **2013,** *14* (10), 1078-90.
71. Berriman, M.; Ghedin, E.; Hertz-Fowler, C.; Blandin, G.; Renauld, H.; Bartholomeu, D. C.; Lennard, N. J.; Caler, E.; Hamlin, N. E.; Haas, B.; Bohme, U.; Hannick, L.; Aslett, M. A.; Shallom, J.; Marcello, L.; Hou, L.; Wickstead, B.; Alsmark, U. C.; Arrowsmith, C.; Atkin, R. J.; Barron, A. J.; Bringaud, F.; Brooks, K.; Carrington, M.; Cherevach, I.; Chillingworth, T. J.; Churcher, C.; Clark, L. N.; Corton, C. H.; Cronin, A.; Davies, R. M.; Doggett, J.; Djikeng, A.; Feldblyum, T.; Field, M. C.; Fraser, A.; Goodhead, I.; Hance, Z.; Harper, D.; Harris, B. R.; Hauser, H.; Hostetler, J.; Ivens, A.; Jagels, K.; Johnson, D.; Johnson, J.; Jones, K.; Kerhornou, A. X.; Koo, H.; Larke, N.; Landfear, S.; Larkin, C.; Leech, V.; Line, A.; Lord, A.; Macleod, A.; Mooney, P. J.; Moule, S.; Martin, D. M.; Morgan, G. W.; Mungall, K.; Norbertczak, H.; Ormond, D.; Pai, G.; Peacock, C. S.; Peterson, J.; Quail, M. A.; Rabbinowitsch, E.; Rajandream, M. A.; Reitter, C.; Salzberg, S. L.; Sanders, M.; Schobel, S.; Sharp, S.; Simmonds, M.; Simpson, A. J.; Tallon, L.; Turner, C. M.; Tait, A.; Tivey, A. R.; Van Aken, S.; Walker, D.; Wanless, D.; Wang, S.; White, B.; White, O.; Whitehead, S.; Woodward, J.; Wortman, J.; Adams, M. D.; Embley, T. M.; Gull, K.; Ullu, E.; Barry, J. D.; Fairlamb, A. H.; Opperdoes, F.; Barrell, B. G.; Donelson, J. E.; Hall, N.; Fraser, C. M.; Melville, S. E.; El-Sayed, N. M., The genome of the African trypanosome Trypanosoma brucei. *Science* **2005,** *309* (5733), 416-22.
72. Robinson, N. P.; Burman, N.; Melville, S. E.; Barry, J. D., Predominance of duplicative VSG gene conversion in antigenic variation in African trypanosomes. *Mol. Cell. Biol.* **1999,** *19* (9), 5839-46.
73. (a) Futse, J. E.; Brayton, K. A.; Dark, M. J.; Knowles, D. P., Jr.; Palmer, G. H., Superinfection as a driver of genomic diversification in antigenically variant pathogens. *Proc. Natl. Acad. Sci. USA* **2008,** *105* (6), 2123-7; (b) Coutte, L.; Botkin, D. J.; Gao, L.; Norris, S. J., Detailed analysis of sequence changes occurring during vlsE antigenic variation in the mouse model of Borrelia burgdorferi infection. *Plos Pathog* **2009,** *5* (2), e1000293; (c) Criss, A. K.; Kline, K. A.; Seifert, H. S., The frequency and rate of pilin antigenic variation in Neisseria gonorrhoeae. *Mol Microbiol* **2005,** *58* (2), 510-9; (d) Giacani, L.; Molini, B. J.; Kim, E. Y.; Godornes, B. C.; Leader, B. T.; Tantalo, L. C.; Centurion-Lara, A.; Lukehart, S. A., Antigenic variation in Treponema pallidum: TprK sequence diversity accumulates in response to immune pressure during experimental syphilis. *J. Immunol.* **2010,** *184* (7), 3822-9; (e) Iverson-Cabral, S. L.; Astete, S. G.; Cohen, C. R.; Totten, P. A., mgpB and mgpC sequence diversity in Mycoplasma genitalium is generated by segmental reciprocal recombination with repetitive chromosomal sequences. *Mol Microbiol* **2007,** *66* (1),

55-73; (f) Al-Khedery, B.; Allred, D. R., Antigenic variation in Babesia bovis occurs through segmental gene conversion of the ves multigene family, within a bidirectional locus of active transcription. *Mol Microbiol* **2006,** *59* (2), 402-14.
74. Zhuang, Y.; Futse, J. E.; Brown, W. C.; Brayton, K. A.; Palmer, G. H., Maintenance of antibody to pathogen epitopes generated by segmental gene conversion is highly dynamic during long-term persistent infection. *Infect. Immun.* **2007,** *75* (11), 5185-90.
75. (a) Michels, P. A.; Liu, A. Y.; Bernards, A.; Sloof, P.; Van der Bijl, M. M.; Schinkel, A. H.; Menke, H. H.; Borst, P.; Veeneman, G. H.; Tromp, M. C.; Van Boom, J. H., Activation of the genes for variant surface glycoproteins 117 and 118 in Trypanosoma brucei. *J. Mol. Biol.* **1983,** *166* (4), 537-56; (b) Aline, R. F., Jr.; Myler, P. J.; Gobright, E.; Stuart, K. D., Early expression of a Trypanosoma brucei VSG gene duplicated from an incomplete basic copy. *The Journal of eukaryotic microbiology* **1994,** *41* (1), 71-8.
76. (a) Roth, C.; Bringaud, F.; Layden, R. E.; Baltz, T.; Eisen, H., Active late-appearing variable surface antigen genes in Trypanosoma equiperdum are constructed entirely from pseudogenes. *Proc. Natl. Acad. Sci. USA* **1989,** *86* (23), 9375-9; (b) Thon, G.; Baltz, T.; Giroud, C.; Eisen, H., Trypanosome variable surface glycoproteins: composite genes and order of expression. *Genes Dev.* **1990,** *4* (8), 1374-83; (c) Kamper, S. M.; Barbet, A. F., Surface epitope variation via mosaic gene formation is potential key to long-term survival of Trypanosoma brucei. *Mol. Biochem. Parasitol.* **1992,** *53* (1-2), 33-44.
77. (a) Hall, J. P.; Wang, H.; Barry, J. D., Mosaic VSGs and the scale of Trypanosoma brucei antigenic variation. *Plos Pathog* **2013,** *9* (7), e1003502; (b) Mugnier, M. R.; Cross, G. A.; Papavasiliou, F. N., The in vivo dynamics of antigenic variation in Trypanosoma brucei. *Science* **2015,** *347* (6229), 1470-3.
78. Kinoshita, T.; Fujita, M.; Maeda, Y., Biosynthesis, remodelling and functions of mammalian GPI-anchored proteins: recent progress. *J. Biochem.* **2008,** *144* (3), 287-94.
79. (a) Schofield, L.; Hewitt, M. C.; Evans, K.; Siomos, M. A.; Seeberger, P. H., Synthetic GPI as a candidate anti-toxic vaccine in a model of malaria. *Nature* **2002,** *418* (6899), 785-9; (b) Arrighi, R. B.; Faye, I., Plasmodium falciparum GPI toxin: a common foe for man and mosquito. *Acta Trop.* **2010,** *114* (3), 162-5.
80. Gotze, S.; Azzouz, N.; Tsai, Y. H.; Gross, U.; Reinhardt, A.; Anish, C.; Seeberger, P. H.; Varon Silva, D., Diagnosis of toxoplasmosis using a synthetic glycosylphosphatidylinositol glycan. *Angew. Chem.* **2014,** *53* (50), 13701-5.
81. (a) Ferguson, M. A. J.; Homans, S. W.; Dwek, R. A.; Rademacher, T. W., Glycosyl-Phosphatidylinositol Moiety That Anchors Trypanosoma-Brucei Variant Surface Glycoprotein to the Membrane. *Science* **1988,** *239* (4841), 753-759; (b) Ferguson, M. A. J.; Mehlert, A.; Richardson, J. M., Structure of the glycosylphosphatidylinositol membrane anchor glycan of a class-2 variant surface glycoprotein from Trypanosoma brucei. *J. Mol. Biol.* **1998,** *277* (2), 379-392; (c) Soares, R. P.; Torrecilhas, A. C.; Assis, R. R.; Rocha, M. N.; Moura e Castro, F. A.; Freitas, G. F.; Murta, S. M.; Santos, S. L.; Marques, A. F.; Almeida, I. C.; Romanha, A. J., Intraspecies variation in Trypanosoma cruzi GPI-mucins: biological activities and differential expression of alpha-galactosyl residues. *Am J Trop Med Hyg* **2012,** *87* (1), 87-96.
82. Bertozzi, C. R.; Paulick, M. G., The glycosylphosphatidylinositol anchor: A complex membrane-anchoring structure for proteins. *Biochemistry-Us* **2008,** *47* (27), 6991-7000.
83. (a) Tartakoff, A. M.; Singh, N., How to Make a Glycoinositol Phospholipid Anchor. *Trends Biochem. Sci.* **1992,** *17* (11), 470-473; (b) Englund, P. T., The structure and biosynthesis of glycosyl phosphatidylinositol protein anchors. *Annu. Rev. Biochem.*

1993, *62*, 121-38; (c) Kinoshita, T.; Inoue, N., Dissecting and manipulating the pathway for glycosylphosphatidylinositol-anchor biosynthesis. *Curr. Opin. Chem. Biol.* **2000,** *4* (6), 632-638.
84. Sangiorgio, V.; Pitto, M.; Palestini, P.; Masserini, M., GPI-anchored proteins and lipid rafts. *Ital J Biochem* **2004,** *53* (2), 98-111.
85. unpublished results.
86. (a) Wilson, J. M.; Fasel, N.; Kraehenbuhl, J. P., Polarity of Endogenous and Exogenous Glycosyl-Phosphatidylinositol-Anchored Membrane-Proteins in Madin-Darby Canine Kidney-Cells. *J Cell Sci* **1990,** *96*, 143-149; (b) Brown, D. A.; Crise, B.; Rose, J. K., Mechanism of Membrane Anchoring Affects Polarized Expression of 2 Proteins in Mdck Cells. *Science* **1989,** *245* (4925), 1499-1501.
87. (a) Lisanti, M. P.; Sargiacomo, M.; Graeve, L.; Saltiel, A. R.; Rodriguezboulan, E., Polarized Apical Distribution of Glycosyl-Phosphatidylinositol-Anchored Proteins in a Renal Epithelial-Cell Line. *Proc. Natl. Acad. Sci. USA* **1988,** *85* (24), 9557-9561; (b) Lisanti, M. P.; Caras, I. W.; Davitz, M. A.; Rodriguezboulan, E., A Glycophospholipid Membrane Anchor Acts as an Apical Targeting Signal in Polarized Epithelial-Cells. *J Cell Biol* **1989,** *109* (5), 2145-2156.
88. Dotti, C. G.; Parton, R. G.; Simons, K., Polarized Sorting of Glypiated Proteins in Hippocampal-Neurons. *Nature* **1991,** *349* (6305), 158-160.
89. (a) Kurzchalia, T. V.; Parton, R. G., Membrane microdomains and caveolae. *Curr. Opin. Cell Biol.* **1999,** *11* (4), 424-431; (b) Brown, D. A.; London, E., Functions of lipid rafts in biological membranes. *Annu Rev Cell Dev Bi* **1998,** *14*, 111-136.
90. (a) Mayor, S.; Rothberg, K. G.; Maxfield, F. R., Sequestration of Gpi-Anchored Proteins in Caveolae Triggered by Cross-Linking. *Science* **1994,** *264* (5167), 1948-1951; (b) Schnitzer, J. E.; Mcintosh, D. P.; Dvorak, A. M.; Liu, J.; Oh, P., Separation of Caveolae from Associated Microdomains of Gpi-Anchored Proteins. *Science* **1995,** *269* (5229), 1435-1439; (c) Mayor, S.; Varma, R., GPI-anchored proteins are organized in submicron domains at the cell surface. *Nature* **1998,** *394* (6695), 798-801; (d) Kurzchalia, T. V.; Friedrichson, T., Microdomains of GPI-anchored proteins in living cells revealed by crosslinking. *Nature* **1998,** *394* (6695), 802-805.
91. Schofield, L.; McConville, M. J.; Hansen, D.; Campbell, A. S.; Fraser-Reid, B.; Grusby, M. J.; Tachado, S. D., CD1d-restricted immunoglobulin G formation to GPI-anchored antigens mediated by NKT cells. *Science* **1999,** *283* (5399), 225-229.
92. (a) Bendelac, A., Cd1 - Presenting Unusual Antigens to Unusual T-Lymphocytes. *Science* **1995,** *269* (5221), 185-186; (b) Campbell, A. S.; Fraserreid, B., First Synthesis of a Fully Phosphorylated Gpi Membrane Anchor - Rat-Brain Thy-1. *J. Am. Chem. Soc.* **1995,** *117* (41), 10387-10388; (c) Stijlemans, B.; Baral, T. N.; Guilliams, M.; Brys, L.; Korf, J.; Drennan, M.; Van Den Abbeele, J.; De Baetselier, P.; Magez, S., A glycosylphosphatidylinositol-based treatment alleviates trypanosomiasis-associated immunopathology. *J. Immunol.* **2007,** *179* (6), 4003-14.
93. (a) Tachado, S. D.; Schofield, L., Glycosylphosphatidylinositol toxin of Trypanosoma brucei regulates IL-1 alpha and TNF-alpha expression in macrophages by protein tyrosine kinase mediated signal transduction. *Biochem. Bioph. Res. Commun.* **1994,** *205* (2), 984-91; (b) Schofield, L.; Novakovic, S.; Gerold, P.; Schwarz, R. T.; McConville, M. J.; Tachado, S. D., Glycosylphosphatidylinositol toxin of Plasmodium up-regulates intercellular adhesion molecule-1, vascular cell adhesion molecule-1, and E-selectin expression in vascular endothelial cells and increases leukocyte and parasite cytoadherence via tyrosine kinase-dependent signal transduction. *J. Immunol.* **1996,** *156* (5), 1886-1896; (c) Tachado, S. D.; Gerold, P.; McConville, M. J.; Baldwin, T.; Quilici, D.; Schwarz, R. T.; Schofield, L., Glycosylphosphatidylinositol toxin of Plasmodium induces nitric oxide synthase expression in macrophages and vascular

endothelial cells by a protein tyrosine kinase-dependent and protein kinase C-dependent signaling pathway. *J. Immunol.* **1996,** *156* (5), 1897-1907.
94. Schofield, L.; Hackett, F., Signal transduction in host cells by a glycosylphosphatidylinositol toxin of malaria parasites. *J. Exp. Med.* **1993,** *177* (1), 145-53.
95. Debierre-Grockiego, F.; Azzouz, N.; Schmidt, J.; Dubremetz, J. F.; Geyer, H.; Geyer, R.; Weingart, R.; Schmidt, R. R.; Schwarz, R. T., Roles of glycosylphosphatidylinositols of Toxoplasma gondii - Induction of tumor necrosis factor-alpha production in macrophages. *J. Biol. Chem.* **2003,** *278* (35), 32987-32993.
96. Zamze, S. E.; Ferguson, M. A.; Collins, R.; Dwek, R. A.; Rademacher, T. W., Characterization of the cross-reacting determinant (CRD) of the glycosyl-phosphatidylinositol membrane anchor of Trypanosoma brucei variant surface glycoprotein. *European journal of biochemistry / FEBS* **1988,** *176* (3), 527-34.
97. W.R. FISH, D. J. G. a. J. D. L.-E., The Cross-Reacting Determinant of the Variable Surface Glycoprotein of Metacyclic Trypanosoma congolense.
98. Inoue, Y.; Nagasawa, K., Selective N-desulfation of heparin with dimethyl sulfoxide containing water or methanol. *Carbohydr Res* **1976,** *46* (1), 87-95.
99. Guimond, S. E.; Puvirajesinghe, T. M.; Skidmore, M. A.; Kalus, I.; Dierks, T.; Yates, E. A.; Turnbull, J. E., Rapid purification and high sensitivity analysis of heparan sulfate from cells and tissues: toward glycomics profiling. *J Biol Chem* **2009,** *284* (38), 25714-22.
100. (a) Powell, A. K.; Yates, E. A.; Fernig, D. G.; Turnbull, J. E., Interactions of heparin/heparan sulfate with proteins: appraisal of structural factors and experimental approaches. *Glycobiology* **2004,** *14* (4), 17R-30R; (b) Powell, A. K.; Ahmed, Y. A.; Yates, E. A.; Turnbull, J. E., Generating heparan sulfate saccharide libraries for glycomics applications. *Nat Protoc* **2010,** *5* (5), 821-33; (c) Grootenhuis, P. D.; Westerduin, P.; Meuleman, D.; Petitou, M.; van Boeckel, C. A., Rational design of synthetic heparin analogues with tailor-made coagulation factor inhibitory activity. *Nat Struct Biol* **1995,** *2* (9), 736-9.
101. (a) Ratner, D. M., *Biol. Tech. Int* **2005,** (17), 8–11; (b) Bryan, M. C.; Plettenburg, O.; Sears, P.; Rabuka, D.; Wacowich-Sgarbi, S.; Wong, C. H., Saccharide display on microtiter plates. *Chem Biol* **2002,** *9* (6), 713-20; (c) Fazio, F.; Bryan, M. C.; Blixt, O.; Paulson, J. C.; Wong, C. H., Synthesis of sugar arrays in microtiter plate. *J Am Chem Soc* **2002,** *124* (48), 14397-402; (d) Park, S.; Shin, I., Fabrication of carbohydrate chips for studying protein-carbohydrate interactions. *Angew Chem Int Ed Engl* **2002,** *41* (17), 3180-2.
102. (a) Fukui, S.; Feizi, T.; Galustian, C.; Lawson, A. M.; Chai, W., Oligosaccharide microarrays for high-throughput detection and specificity assignments of carbohydrate-protein interactions. *Nat Biotechnol* **2002,** *20* (10), 1011-7; (b) Wang, D.; Liu, S.; Trummer, B. J.; Deng, C.; Wang, A., Carbohydrate microarrays for the recognition of cross-reactive molecular markers of microbes and host cells. *Nat Biotechnol* **2002,** *20* (3), 275-81; (c) Houseman, B. T.; Mrksich, M., Carbohydrate arrays for the evaluation of protein binding and enzymatic modification. *Chem Biol* **2002,** *9* (4), 443-54; (d) Ma, X.; Mohammad, S. F.; Kim, S. W., Heparin removal from blood using poly(L-lysine) immobilized hollow fiber. *Biotechnol Bioeng* **1992,** *40* (4), 530-6.
103. (a) Zhi, Z. L.; Laurent, N.; Powell, A. K.; Karamanska, R.; Fais, M.; Voglmeir, J.; Wright, A.; Blackburn, J. M.; Crocker, P. R.; Russell, D. A.; Flitsch, S.; Field, R. A.; Turnbull, J. E., A versatile gold surface approach for fabrication and interrogation of glycoarrays. *ChemBioChem* **2008,** *9* (10), 1568-75; (b) Sanchez-Ruiz, A.; Serna, S.; Ruiz, N.; Martin-Lomas, M.; Reichardt, N. C., MALDI-TOF mass spectrometric

analysis of enzyme activity and lectin trapping on an array of N-glycans. *Angew Chem Int Ed Engl* **2011,** *50* (8), 1801-4.

104. (a) Houseman, B. T. G., E.S.; Mrksich, M., *Langmuir* **2003,** (19), 1522–1531; (b) Park, S.; Lee, M. R.; Pyo, S. J.; Shin, I., Carbohydrate chips for studying high-throughput carbohydrate-protein interactions. *J Am Chem Soc* **2004,** *126* (15), 4812-9.
105. (a) Zhi, Z. L.; Powell, A. K.; Turnbull, J. E., Fabrication of carbohydrate microarrays on gold surfaces: direct attachment of nonderivatized oligosaccharides to hydrazide-modified self-assembled monolayers. *Anal Chem* **2006,** *78* (14), 4786-93; (b) Barie, N.; Rapp, M.; Sigrist, H.; Ache, H. J., Covalent photolinker-mediated immobilization of an intermediate dextran layer to polymer-coated surfaces for biosensing applications. *Biosens Bioelectron* **1998,** *13* (7-8), 855-60; (c) Platz, M.; Admasu, A. S.; Kwiatkowski, S.; Crocker, P. J.; Imai, N.; Watt, D. S., Photolysis of 3-aryl-3-(trifluoromethyl)diazirines: a caveat regarding their use in photoaffinity probes. *Bioconjug Chem* **1991,** *2* (5), 337-41; (d) Angeloni, S.; Ridet, J. L.; Kusy, N.; Gao, H.; Crevoisier, F.; Guinchard, S.; Kochhar, S.; Sigrist, H.; Sprenger, N., Glycoprofiling with micro-arrays of glycoconjugates and lectins. *Glycobiology* **2005,** *15* (1), 31-41; (e) Yates, E. A. J., M.O.; Clarke, C.E.; Powell, A.K.; Johnson, S.R.; Porch, A.; Edwards, P.P.; Turnbull, J.E., *J. Mater. Chem.* **2003,** (13), 2061–2063; (f) Puvirajesinghe, T. M.; Ahmed, Y. A.; Powell, A. K.; Fernig, D. G.; Guimond, S. E.; Turnbull, J. E., Array-based functional screening of heparin glycans. *Chem Biol* **2012,** *19* (5), 553-8.
106. (a) Vora, G. J.; Meador, C. E.; Anderson, G. P.; Taitt, C. R., Comparison of detection and signal amplification methods for DNA microarrays. *Mol Cell Probes* **2008,** *22* (5-6), 294-300; (b) Fero, M.; Pogliano, K., Automated quantitative live cell fluorescence microscopy. *Cold Spring Harb Perspect Biol* **2010,** *2* (8), a000455; (c) Zheng, G.; Horstmeyer, R.; Yang, C., Wide-field, high-resolution Fourier ptychographic microscopy. *Nat Photonics* **2013,** *7* (9), 739-745.
107. (a) Kamena, F.; Tamborrini, M.; Liu, X.; Kwon, Y. U.; Thompson, F.; Pluschke, G.; Seeberger, P. H., Synthetic GPI array to study antitoxic malaria response. *Nat. Chem. Biol.* **2008,** *4* (4), 238-240; (b) Brattig, N. W.; Kowalsky, K.; Liu, X. Y.; Burchard, G. D.; Kamena, F.; Seeberger, P. H., Plasmodium falciparum glycosylphosphatidylinositol toxin interacts with the membrane of non-parasitized red blood cells: a putative mechanism contributing to malaria anemia. *Microb. Infect.* **2008,** *10* (8), 885-891.
108. Kwon, Y. U.; Soucy, R. L.; Snyder, D. A.; Seeberger, P. H., Assembly of a series of malarial glycosylphosphatidylinositol anchor oligosaccharides. *Chem. Eur. J.* **2005,** *11* (8), 2493-2504.
109. Ratner, D. M.; Adams, E. W.; Su, J.; O'Keefe, B. R.; Mrksich, M.; Seeberger, P. H., Probing protein-carbohydrate interactions with microarrays of synthetic oligosaccharides. *ChemBioChem* **2004,** *5* (3), 379-382.
110. (a) Maeda, Y.; Kinoshita, T., Structural remodeling, trafficking and functions of glycosylphosphatidylinositol-anchored proteins. *Prog. Lipid Res.* **2011,** *50* (4), 411-24; (b) Fujita, M.; Kinoshita, T., Structural remodeling of GPI anchors during biosynthesis and after attachment to proteins. *FEBS Lett* **2010,** *584* (9), 1670-7.
111. (a) Almeida, A. M.; Murakami, Y.; Layton, D. M.; Hillmen, P.; Sellick, G. S.; Maeda, Y.; Richards, S.; Patterson, S.; Kotsianidis, I.; Mollica, L.; Crawford, D. H.; Baker, A.; Ferguson, M.; Roberts, I.; Houlston, R.; Kinoshita, T.; Karadimitris, A., Hypomorphic promoter mutation in PIGM causes inherited glycosylphosphatidylinositol deficiency. *Nat Med* **2006,** *12* (7), 846-851; (b) Krawitz, P. M.; Schweiger, M. R.; Rodelsperger, C.; Marcelis, C.; Kolsch, U.; Meisel, C.; Stephani, F.; Kinoshita, T.; Murakami, Y.; Bauer, S.; Isau, M.; Fischer, A.; Dahl, A.; Kerick, M.; Hecht, J.; Kohler, S.; Jager, M.;

Grunhagen, J.; de Condor, B. J.; Doelken, S.; Brunner, H. G.; Meinecke, P.; Passarge, E.; Thompson, M. D.; Cole, D. E.; Horn, D.; Roscioli, T.; Mundlos, S.; Robinson, P. N., Identity-by-descent filtering of exome sequence data identifies PIGV mutations in hyperphosphatasia mental retardation syndrome. *Nat Genet* **2010,** *42* (10), 827-829.

112. Debierre-Grockiego, F.; Schwarz, R. T., Immunological reactions in response to apicomplexan glycosylphosphatidylinositols. *Glycobiology* **2010,** *20* (7), 801-11.
113. (a) Takeda, J., Inoue, N., and Kinoshita, T. , Glycosylphosphatidylinositol (GPI)-anchor Biosynthesis. *Comprehensive Natural Products Chemistry* **1999**; (b) Watanabe, R.; Inoue, N.; Westfall, B.; Taron, C. H.; Orlean, P.; Takeda, J.; Kinoshita, T., The first step of glycosylphosphatidylinositol biosynthesis is mediated by a complex of PIG-A, PIG-H, PIG-C and GPI1. *EMBO J.* **1998,** *17* (4), 877-85.
114. Nakamura, N.; Inoue, N.; Watanabe, R.; Takahashi, M.; Takeda, J.; Stevens, V. L.; Kinoshita, T., Expression cloning of PIG-L, a candidate N-acetylglucosaminyl-phosphatidylinositol deacetylase. *J Biol Chem* **1997,** *272* (25), 15834-40.
115. (a) Mayor, S.; Menon, A. K.; Cross, G. A., Glycolipid precursors for the membrane anchor of Trypanosoma brucei variant surface glycoproteins. II. Lipid structures of phosphatidylinositol-specific phospholipase C sensitive and resistant glycolipids. *J Biol Chem* **1990,** *265* (11), 6174-81; (b) Mayor, S.; Menon, A. K.; Cross, G. A.; Ferguson, M. A.; Dwek, R. A.; Rademacher, T. W., Glycolipid precursors for the membrane anchor of Trypanosoma brucei variant surface glycoproteins. I. Can structure of the phosphatidylinositol-specific phospholipase C sensitive and resistant glycolipids. *J Biol Chem* **1990,** *265* (11), 6164-73; (c) Urakaze, M.; Kamitani, T.; DeGasperi, R.; Sugiyama, E.; Chang, H. M.; Warren, C. D.; Yeh, E. T., Identification of a missing link in glycosylphosphatidylinositol anchor biosynthesis in mammalian cells. *J Biol Chem* **1992,** *267* (10), 6459-62.
116. Costello, L. C.; Orlean, P., Inositol acylation of a potential glycosyl phosphoinositol anchor precursor from yeast requires acyl coenzyme A. *J Biol Chem* **1992,** *267* (12), 8599-603.
117. Houjou, T.; Hayakawa, J.; Watanabe, R.; Tashima, Y.; Maeda, Y.; Kinoshita, T.; Taguchi, R., Changes in molecular species profiles of glycosylphosphatidylinositol anchor precursors in early stages of biosynthesis. *J Lipid Res* **2007,** *48* (7), 1599-1606.
118. Menon, A. K.; Schwarz, R. T.; Mayor, S.; Cross, G. A., Cell-free synthesis of glycosyl-phosphatidylinositol precursors for the glycolipid membrane anchor of Trypanosoma brucei variant surface glycoproteins. Structural characterization of putative biosynthetic intermediates. *J Biol Chem* **1990,** *265* (16), 9033-42.
119. Ferguson, M. A.; Williams, A. F., Cell-surface anchoring of proteins via glycosyl-phosphatidylinositol structures. *Annu. Rev. Biochem.* **1988,** *57*, 285-320.
120. (a) Tanaka, S.; Maeda, Y.; Tashima, Y.; Kinoshita, T., Inositol deacylation of glycosylphosphatidylinositol-anchored proteins is mediated by mammalian PGAP1 and yeast Bst1p. *J. Biol. Chem.* **2004,** *279* (14), 14256-14263; (b) Fujita, M.; Maeda, Y.; Ra, M.; Yamaguchi, Y.; Taguchi, R.; Kinoshita, T., GPI Glycan Remodeling by PGAP5 Regulates Transport of GPI-Anchored Proteins from the ER to the Golgi. *Cell* **2009,** *139* (2), 352-365.
121. Ferguson, M. A.; Brimacombe, J. S.; Brown, J. R.; Crossman, A.; Dix, A.; Field, R. A.; Guther, M. L.; Milne, K. G.; Sharma, D. K.; Smith, T. K., The GPI biosynthetic pathway as a therapeutic target for African sleeping sickness. *Biochim Biophys Acta* **1999,** *1455* (2-3), 327-40.
122. Menon, A. K.; Mayor, S.; Ferguson, M. A.; Duszenko, M.; Cross, G. A., Candidate glycophospholipid precursor for the glycosylphosphatidylinositol membrane anchor of Trypanosoma brucei variant surface glycoproteins. *J Biol Chem* **1988,** *263* (4), 1970-7.

123. Smith, T. K.; Kimmel, J.; Azzouz, N.; Shams-Eldin, H.; Schwarz, R. T., The role of inositol acylation and inositol deacylation in the Toxoplasma gondii glycosylphosphatidylinositol biosynthetic pathway. *J Biol Chem* **2007,** *282* (44), 32032-42.
124. Shams-Eldin, H.; de Macedo, C. S.; Niehus, S.; Dorn, C.; Kimmel, J.; Azzouz, N.; Schwarz, R. T., Plasmodium falciparum dolichol phosphate mannose synthase represents a novel clade. *Biochem. Bioph. Res. Commun.* **2008,** *370* (3), 388-93.
125. Whitfield, D. M.; Nukada, T.; Berces, A.; Zgierski, M. Z., Exploring the mechanism of neighboring group assisted glycosylation reactions. *J. Am. Chem. Soc.* **1998,** *120* (51), 13291-13295.
126. Koizumi, A.; Yamano, K.; Schweizer, F.; Takeda, T.; Kiuchi, F.; Hada, N., Synthesis of the carbohydrate moiety from the parasite Echinococcus multilocularis and their antigenicity against human sera. *Eur J Med Chem* **2011,** *46* (5), 1768-1778.
127. (a) Jervis, P. J.; Veerapen, N.; Bricard, G.; Cox, L. R.; Porcelli, S. A.; Besra, G. S., Synthesis and biological activity of alpha-glucosyl C24:0 and C20:2 ceramides. *Bioorg Med Chem Lett* **2010,** *20* (12), 3475-3478; (b) Bols, M., Synthesis of Kojitriose using silicon-tethered glycosidation. *Acta Chem Scand* **1996,** *50* (10), 931-937.
128. Murakata, C.; Ogawa, T., Synthetic Studies on Cell-Surface Glycans .85. Stereoselective Total Synthesis of the Glycosyl Phosphatidylinositol (Gpi) Anchor of Trypanosoma-Brucei. *Carbohyd. Res.* **1992,** *235*, 95-114.
129. (a) Szabo, Z. B.; Mihaly, H.; Fekete, A.; Gyula, B.; Borbas, A.; Andras, L.; Sandor, A., Synthesis of three regioisomers of the pentasaccharide part of the Skp1 glycoprotein of Dictyostelium discoideum. *Tetrahedron-Asymmetr* **2009,** *20* (6-8), 808-820; (b) Norberg, T.; Walding, M.; Westman, E., Synthesis of the Methyl, 1-Octyl, and Para-Trifluoroacetamidophenylethyl Alpha-Glycosides of 3,6-Di-O-(Alpha-D-Galactopyranosyl)-D-Glucopyranose and an Acyclic Analog Thereof. *J Carbohyd Chem* **1988,** *7* (2), 283-292.
130. Hahm, H. S.; Hurevich, M.; Seeberger, P. H., Automated assembly of oligosaccharides containing multiple cis-glycosidic linkages. *Nature communications* **2016,** *7*, 12482.
131. (a) Murakata, C.; Ogawa, T., Synthetic Studies on Cell-Surface Glycans .78. A Total Synthesis of Gpi Anchor of Trypanosoma Brucei. *Tetrahedron Lett.* **1991,** *32* (5), 671-674; (b) Murakata, C.; Ogawa, T., Synthetic Studies on Cell-Surface Glycans .75. Synthetic Study on Glycophosphatidyl Inositol (Gpi) Anchor of Trypanosoma-Brucei - Glycoheptaosyl Core. *Tetrahedron Lett.* **1990,** *31* (17), 2439-2442.
132. Guo, Z., Synthetic Studies of Glycosylphosphatidylinositol (GPI) Anchors and GPI-Anchored Peptides, Glycopeptides, and Proteins. *Curr Org Synth* **2013,** *10* (3), 366-383.
133. (a) Ley, S. V.; Baeschlin, D. K.; Chaperon, A. R.; Charbonneau, V.; Green, L. G.; Lucking, U.; Walther, E., Rapid assembly of oligosaccharides: Total synthesis of a glycosylphosphatidylinositol anchor of Trypanosoma brucei. *Angew. Chem. Int. Ed.* **1998,** *37* (24), 3423-3428; (b) Ley, S. V.; Baeschlin, D. K.; Chaperon, A. R.; Green, L. G.; Hahn, M. G.; Ince, S. J., 1,2-diacetals in synthesis: Total synthesis of a glycosylphosphatidylinositol anchor of Trypanosoma brucei. *Chem-Eur J* **2000,** *6* (1), 172-186.
134. (a) Tsai, Y.-H.; Götze, S.; Azzouz, N.; Hahm, H. S.; Seeberger, P. H.; Varon Silva, D., A General Method for Synthesis of GPI Anchors Illustrated by the Total Synthesis of the Low-Molecular-Weight Antigen from Toxoplasma gondii. *Angew. Chem. Int. Ed.* **2011,** *50* (42), 9961-9964; (b) Tsai, Y.-H.; Götze S.; Vilotijevic I.; Grube M.; Varon Silva, D.; Seeberger, P. H., *Chem. Sci.* **2012**, DOI:10.1039/c2sc21515b.
135. Tsai, Y. H.; Gotze, S.; Azzouz, N.; Hahm, H. S.; Seeberger, P. H.; Varon Silva, D., A general method for synthesis of GPI anchors illustrated by the total synthesis of the

low-molecular-weight antigen from Toxoplasma gondii. *Angew. Chem.* **2011,** *50* (42), 9961-4.

136. (a) Yashunsky, D. V.; Borodkin, V. S.; Ferguson, M. A. J.; Nikolaev, A. V., The chemical synthesis of bioactive glycosylphosphatidylinositols from Trypanosoma cruzi containing an unsaturated fatty acid in the lipid. *Angew. Chem. Int. Ed.* **2006,** *45* (3), 468-474; (b) Guo, Z. W.; Swarts, B. M., Synthesis of a Glycosylphosphatidylinositol Anchor Bearing Unsaturated Lipid Chains. *J. Am. Chem. Soc.* **2010,** *132* (19), 6648-6650; (c) Yashunsky, D. V.; Borodkin, V. S.; Ferguson, M. A.; Nikolaev, A. V., The chemical synthesis of bioactive glycosylphosphatidylinositols from Trypanosoma cruzi containing an unsaturated fatty acid in the lipid. *Angew Chem Int Ed Engl* **2006,** *45* (3), 468-74.
137. Lee, B. Y.; Seeberger, P. H.; Varon Silva, D., Synthesis of glycosylphosphatidylinositol (GPI)-anchor glycolipids bearing unsaturated lipids. *Chem Commun (Camb)* **2016,** *52* (8), 1586-9.
138. Pan, K. M.; Baldwin, M.; Nguyen, J.; Gasset, M.; Serban, A.; Groth, D.; Mehlhorn, I.; Huang, Z.; Fletterick, R. J.; Cohen, F. E.; et al., Conversion of alpha-helices into beta-sheets features in the formation of the scrapie prion proteins. *Proc. Natl. Acad. Sci. USA* **1993,** *90* (23), 10962-6.
139. Becker, C. F.; Liu, X.; Olschewski, D.; Castelli, R.; Seidel, R.; Seeberger, P. H., Semisynthesis of a glycosylphosphatidylinositol-anchored prion protein. *Angew. Chem. Int. Ed.* **2008,** *47* (43), 8215-9.
140. D. Ganten, K. R., W. Birchmeier, J. T. Epplen, K. Genser, M. Gossen, B. Kersten, H. Lehrach, H. Oschkinat, P. Ruiz, P. Schmieder, E. Wanker, C. Nolte Encyclopedic Reference of Genomics and Proteomics in Molecular Medicin. **2006**.
141. Dawson, P. E.; Muir, T. W.; Clark-Lewis, I.; Kent, S. B., Synthesis of proteins by native chemical ligation. *Science* **1994,** *266* (5186), 776-9.
142. (a) Kirchhoff, C.; Schroter, S.; Derr, P.; Conrad, H. S.; Nimtz, M.; Hale, G., Male-specific modification of human CD52. *J. Biol. Chem.* **1999,** *274* (42), 29862-29873; (b) Treumann, A.; Lifely, M. R.; Schneider, P.; Ferguson, M. A. J., Primary Structure of Cd52. *J. Biol. Chem.* **1995,** *270* (11), 6088-6099.
143. (a) Hale, G.; Xia, M. Q.; Tighe, H. P.; Dyer, M. J.; Waldmann, H., The CAMPATH-1 antigen (CDw52). *Tissue Antigens* **1990,** *35* (3), 118-27; (b) Tsuji, Y., *Immunology of Human Reproduction* **1995**; (c) Eccleston, E. D.; White, T. W.; Howard, J. B.; Hamilton, D. W., Characterization of a cell surface glycoprotein associated with maturation of rat spermatozoa. *Mol. Reprod. Dev* **1994,** *37* (1), 110-9.
144. Shao, N.; Xue, B.; Guo, Z. W., Chemical synthesis of a skeleton structure of sperm CD52 - A GPI-anchored glycopeptide. *Angew. Chem. Int. Ed.* **2004,** *43* (12), 1569-1573.
145. Kennedy, P. G. E., Clinical features, diagnosis, and treatment of human African trypanosomiasis (sleeping sickness). *Lancet Neurol* **2013,** *12* (2), 186-194.
146. Wu, X. M.; Shen, Z. H.; Zeng, X. Q.; Lang, S. H.; Palmer, M.; Guo, Z. W., Synthesis and biological evaluation of sperm CD52 GPI anchor and related derivatives as binding receptors of pore-forming CAMP factor. *Carbohyd. Res.* **2008,** *343* (10-11), 1718-1729.
147. Gotze, S.; Reinhardt, A.; Geissner, A.; Azzouz, N.; Tsai, Y. H.; Kurucz, R.; Varon Silva, D.; Seeberger, P. H., Investigation of the protective properties of glycosylphosphatidylinositol-based vaccine candidates in a Toxoplasma gondii mouse challenge model. *Glycobiology* **2015**.
148. Ferguson, M. A.; Low, M. G.; Cross, G. A., Glycosyl-sn-1,2-dimyristylphosphatidylinositol is covalently linked to Trypanosoma brucei variant surface glycoprotein. *J Biol Chem* **1985,** *260* (27), 14547-55.

149. (a) Magez, S.; Stijlemans, B.; Baral, T.; De Baetselier, P., VSG-GPI anchors of African trypanosomes: their role in macrophage activation and induction of infection-associated immunopathology. *Microb. Infect.* **2002,** *4* (9), 999-1006; (b) Magez, S.; Schwegmann, A.; Atkinson, R.; Claes, F.; Drennan, M.; De Baetselier, P.; Brombacher, F., The role of B-cells and IgM antibodies in parasitemia, anemia, and VSG switching in Trypanosoma brucei-infected mice. *Plos Pathog* **2008,** *4* (8); (c) Radwanska, M.; Guirnalda, P.; De Trez, C.; Ryffel, B.; Black, S.; Magez, S., Trypanosomiasis-induced B cell apoptosis results in loss of protective anti-parasite antibody responses and abolishment of vaccine-induced memory responses. *Plos Pathog* **2008,** *4* (5).
150. Henry M. Leicester, H. S. K., Theory of Aetherification. *Philosophical Magazine* **1850,** *37*, 350-356.
151. Silverstein, R. M. W., F.X., Spectrometric Identification of orhanic Compounds. *Wiley-India-Edition* **2002**.
152. Birch, A. J., Reduction by dissolving metals. Part I. *J. Chem. Soc.* **1944**, 430-436.
153. Alais, J.; Maranduba, A.; Veyrieres, A., Regioselective Mono-O-Alkylation of Disaccharide Glycosides through Their Dibutylstannylene Complexes. *Tetrahedron Lett.* **1983,** *24* (23), 2383-2386.
154. Huang, W.; Gao, Q.; Boons, G. J., Assembly of a Complex Branched Oligosaccharide by Combining Fluorous-Supported Synthesis and Stereoselective Glycosylations using Anomeric Sulfonium Ions. *Chemistry* **2015,** *21* (37), 12920-6.
155. La Greca, F.; Magez, S., Vaccination against trypanosomiasis Can it be done or is the trypanosome truly the ultimate immune destroyer and escape artist? *Hum Vaccines* **2011,** *7* (11), 1225-1233.
156. Volbeda, A. G.; Kistemaker, H. A.; Overkleeft, H. S.; van der Marel, G. A.; Filippov, D. V.; Codee, J. D. C., Chemoselective Cleavage of p-Methoxybenzyl and 2-Naphthylmethyl Ethers Using a Catalytic Amount of HCl in Hexafluoro-2-propanol. *J Org Chem* **2015,** *80* (17), 8796-8806.
157. Rajib Panchadhayee, A. K. M., *ChemInform* **2010,** *29* (47), 76-83.
158. Amblard, M.; Fehrentz, J. A.; Martinez, J.; Subra, G., Methods and protocols of modern solid phase Peptide synthesis. *Mol Biotechnol* **2006,** *33* (3), 239-54.

11. ACKNOWLEDGMENTS

I am deeply thankful to Dr. Daniel Varón Silva for his support, guidance, patronage and understanding.

I am thankful to Prof. Dr. Christoph A. Schalley for agreeing to review this thesis.

I thank Prof. Dr. Peter H. Seeberger for the opportunity to work, learn and thrive in the Biomolecular Systems Department.

I thank the Beilstein-Institut zur Förderung der Chemischen Wissenschaften, the Max Planck Society and the RIKEN-Max Planck Joint Center for Systems Chemical Biology for financial support.

I thank current and former members of group and department for successful collaborations in many projects and the stimulating atmosphere of working with so many talented scientists. Without particular order I want to highlight Renée Roller, Dr. Reka Kurucz, Safak Bayram, Ankita Malik, Dr. Maria Antonietta Carillo, Johanna Knaak, Eike Wamhoff, Uwe Möginger, Hannes Hinneburg, Kathirvel Alagesan and Prof. Dr. Ivan Vilotijević.

I am particularly thankful to Monika Garg, Dr. Bo-Young Lee, Dana Michel, Andreas Geissner and Dr. Benoit Stijlemans. Without their tremendous support *T. brucei* would have kept some more galactose modified secrets, deeply buried beneath a dense coat.

I thank Eva Settels, Dorothee Böhme, Katrin Sellrie, Olaf Niemeyer and Felix Hentschel for the lunch group, support and help whenever needed.

I thank Dr. Antje Reinecke and Dr. Tom Robinson for countless insightful interdisciplinary meetings.

I want to express my deepest gratitude to my family and friends. Without their endless support this PhD thesis would have not been possible.

Dana, thank you! For everything and more.

12. APPENDIX

Box-plot: Normalized intensity of fluorescence indicating recognition by IgM against five groups of a mice *T. brucei* infection model. Plot for each *T. brucei* VSG-GPI structure synthesized in chapter 4.

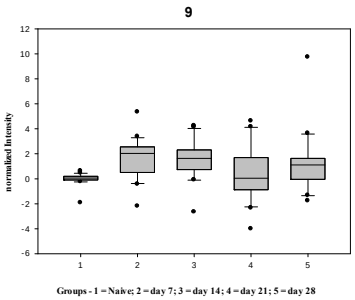

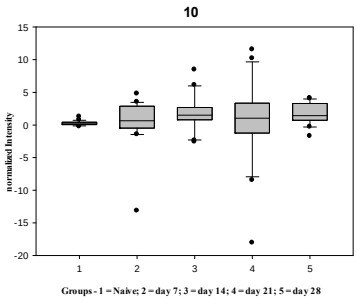

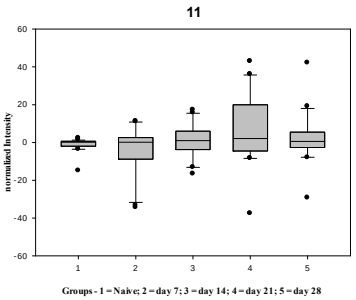

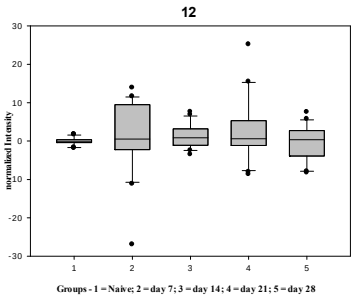

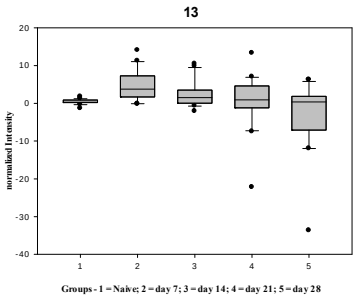

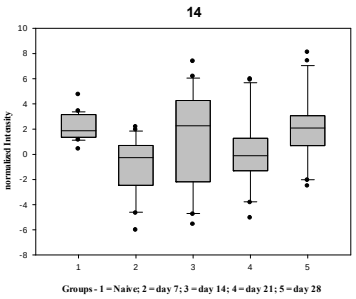

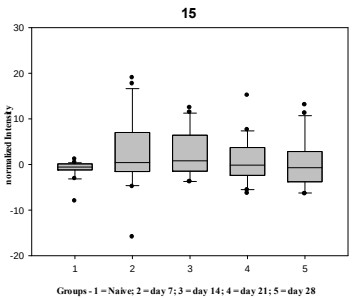

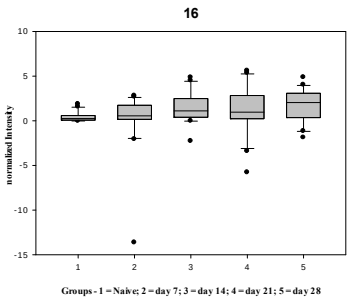

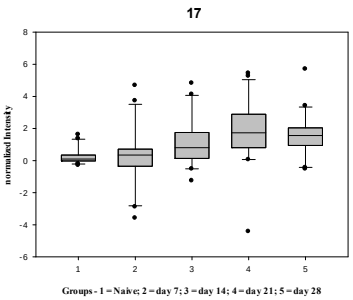

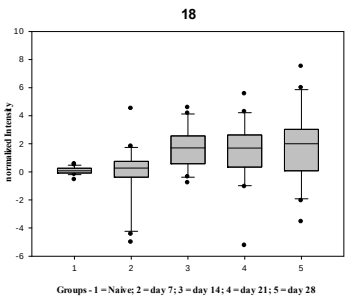

Box-plot: Normalized intensity of fluorescence indicating recognition by IgG against five groups of a mice *T. brucei* infection model. Plot for each *T. brucei* VSG-GPI structure synthesized in chapter 4.

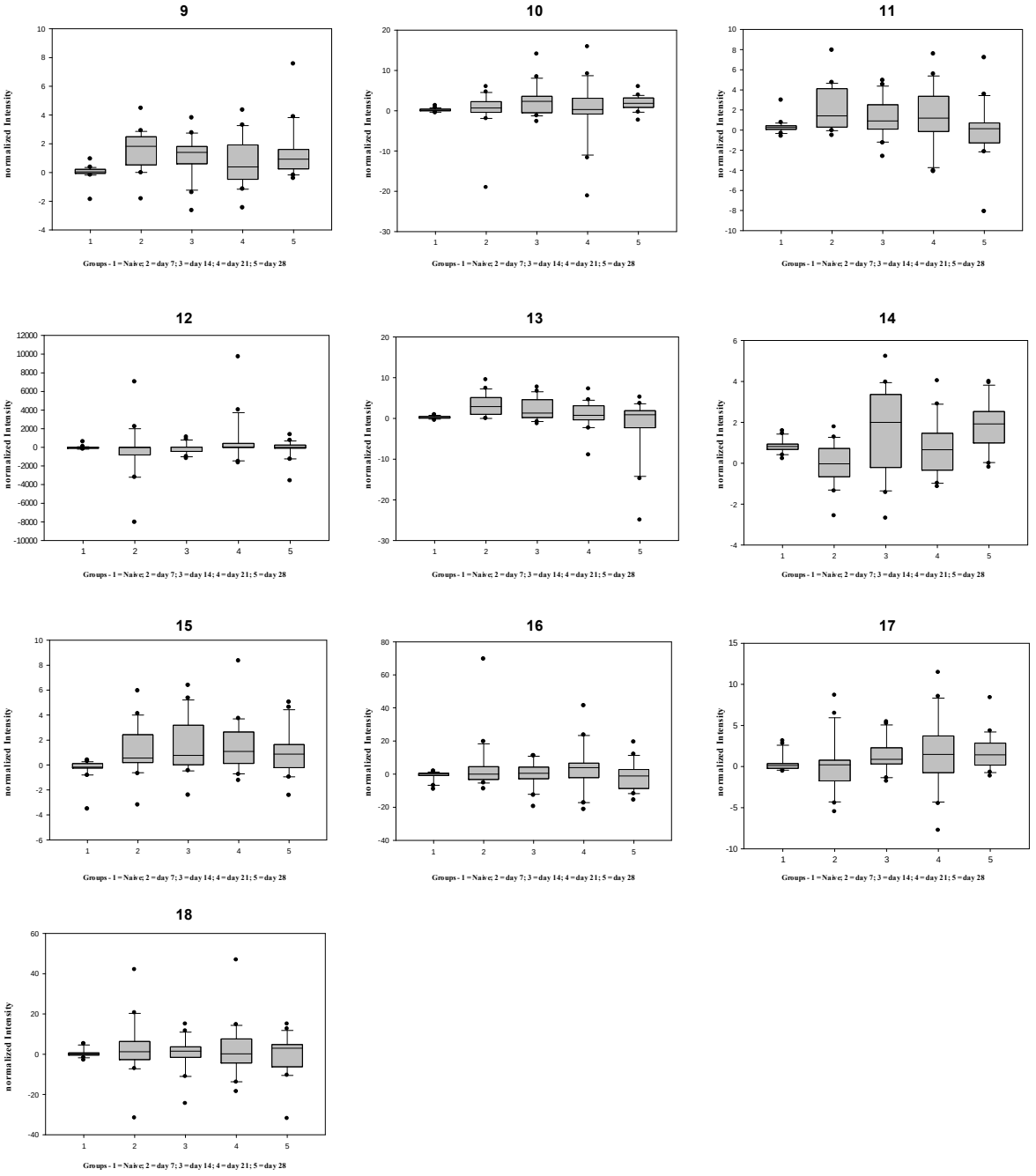

Box-plot: Normalized intensity of fluorescence indicating recognition by IgM against three groups in a *T. brucei gambiense* infection in human. Plot for each *T. brucei* VSG-GPI structure synthesized in chapter 4.

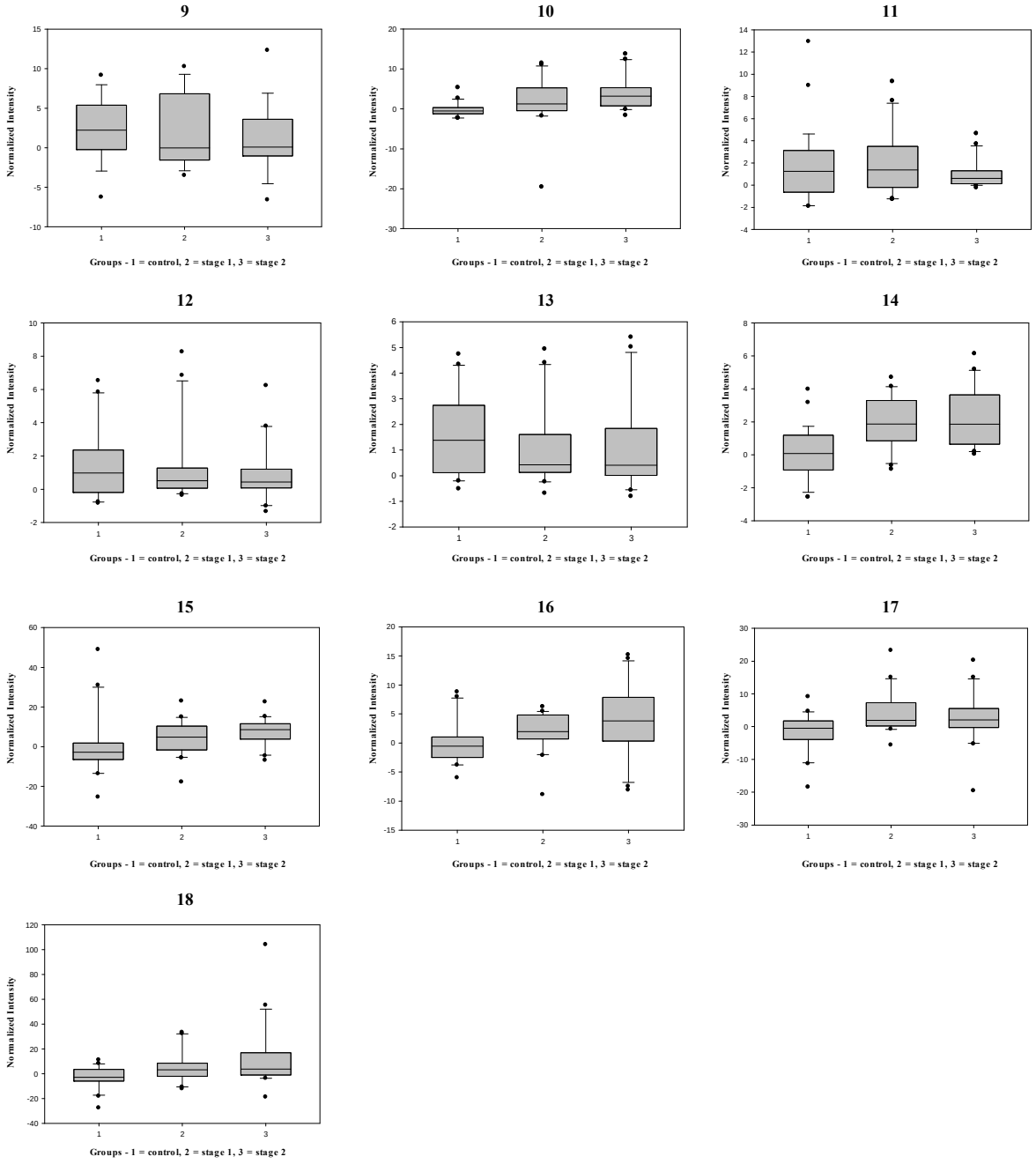

Box-plot: Normalized intensity of fluorescence indicating recognition by IgM against three groups in a *T. brucei rhodesiense* infection in human. Plot for each *T. brucei* VSG-GPI structure synthesized in chapter 4.

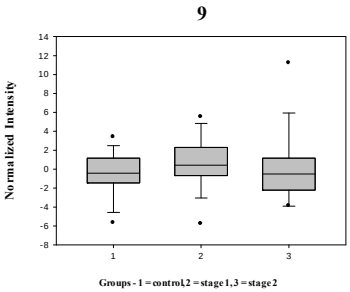

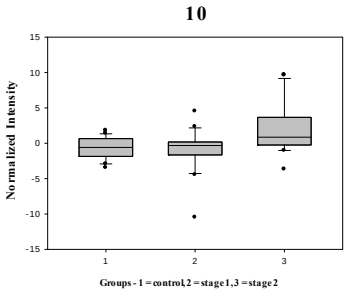

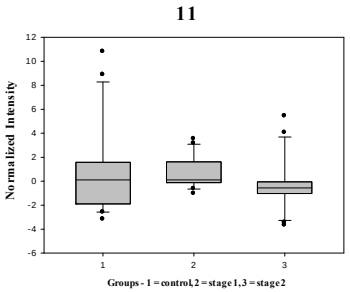

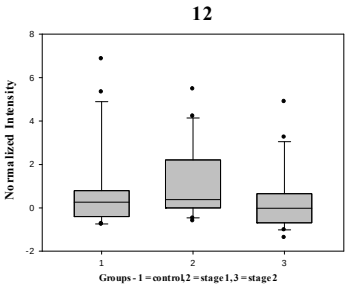

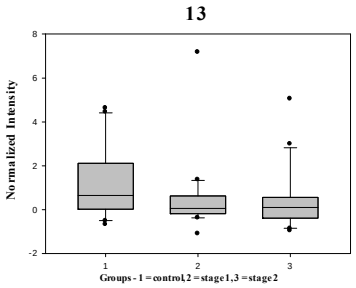

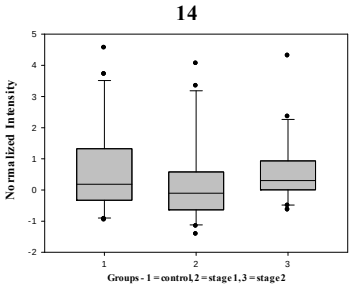

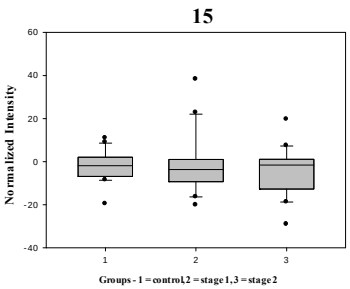

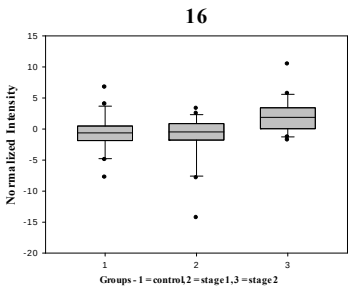

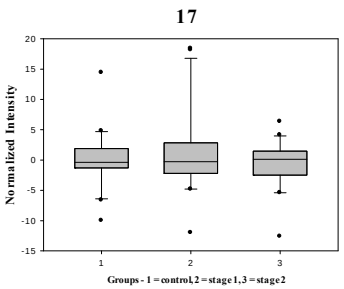

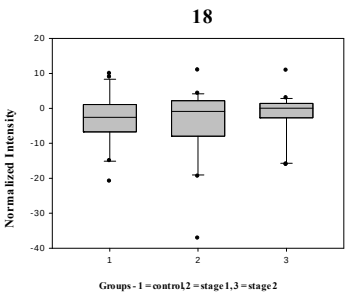

Box-plot: Normalized intensity of fluorescence indicating recognition by IgG against three groups in a *T. brucei gambiense* infection in human. Plot for each *T. brucei* VSG-GPI structure synthesized in chapter 4.

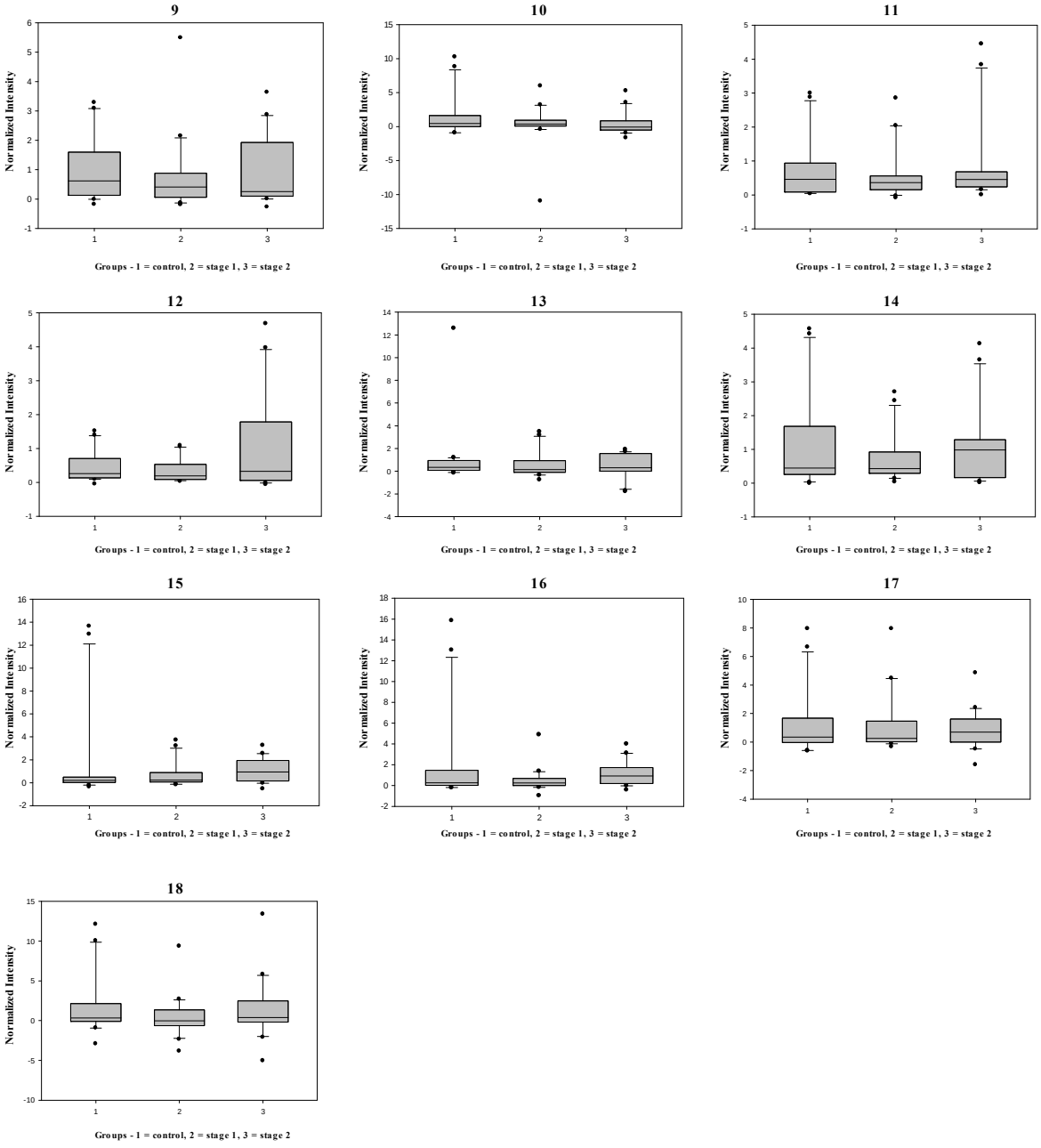

Box-plot: Normalized intensity of fluorescence indicating recognition by IgG against three groups in a *T. brucei rhodesiense* infection in human. Plot for each *T. brucei* VSG-GPI structure synthesized in chapter 4.

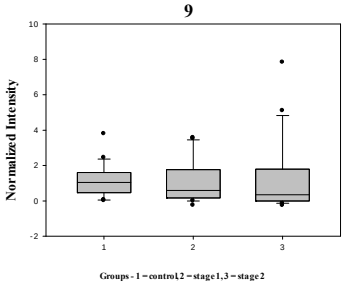

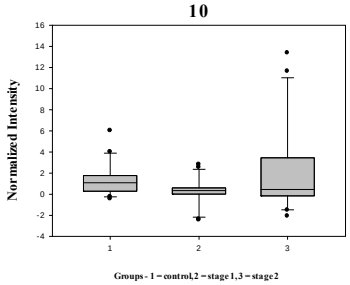

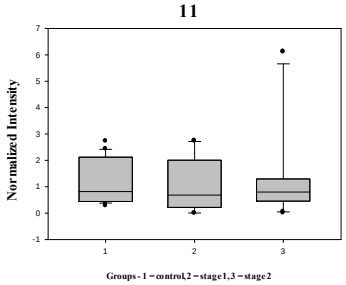

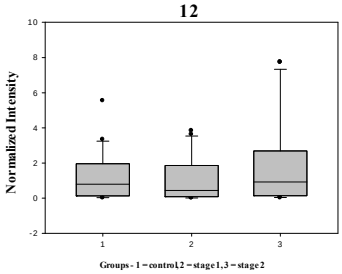

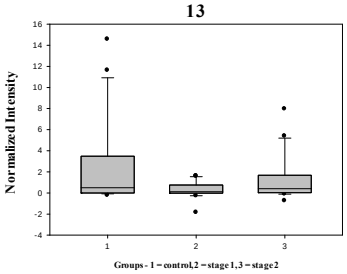

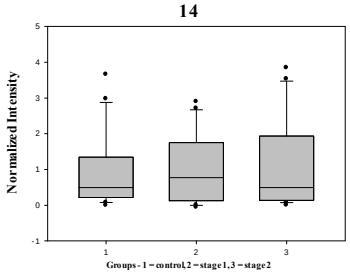

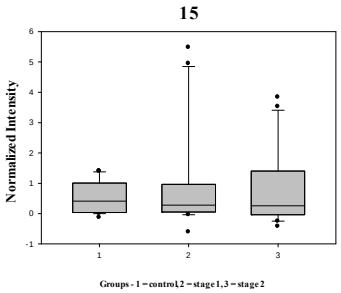

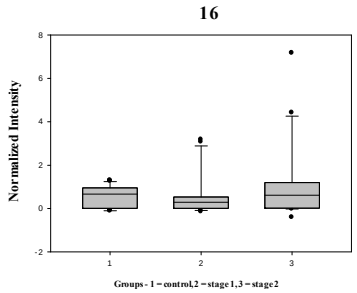

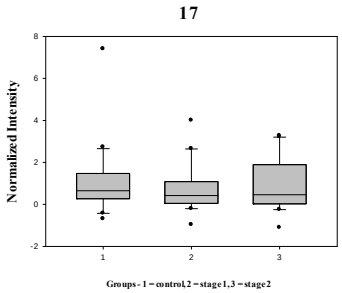

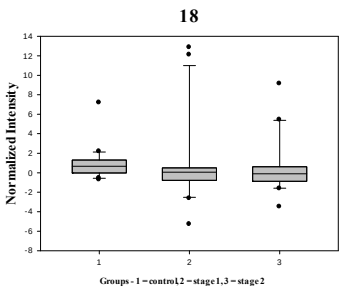

Box-plot: Normalized intensity of fluorescence indicating recognition by IgM against five groups in a *T. gondii* infection in human. Plot for each *T. brucei* VSG-GPI structure synthesized in chapter 4.

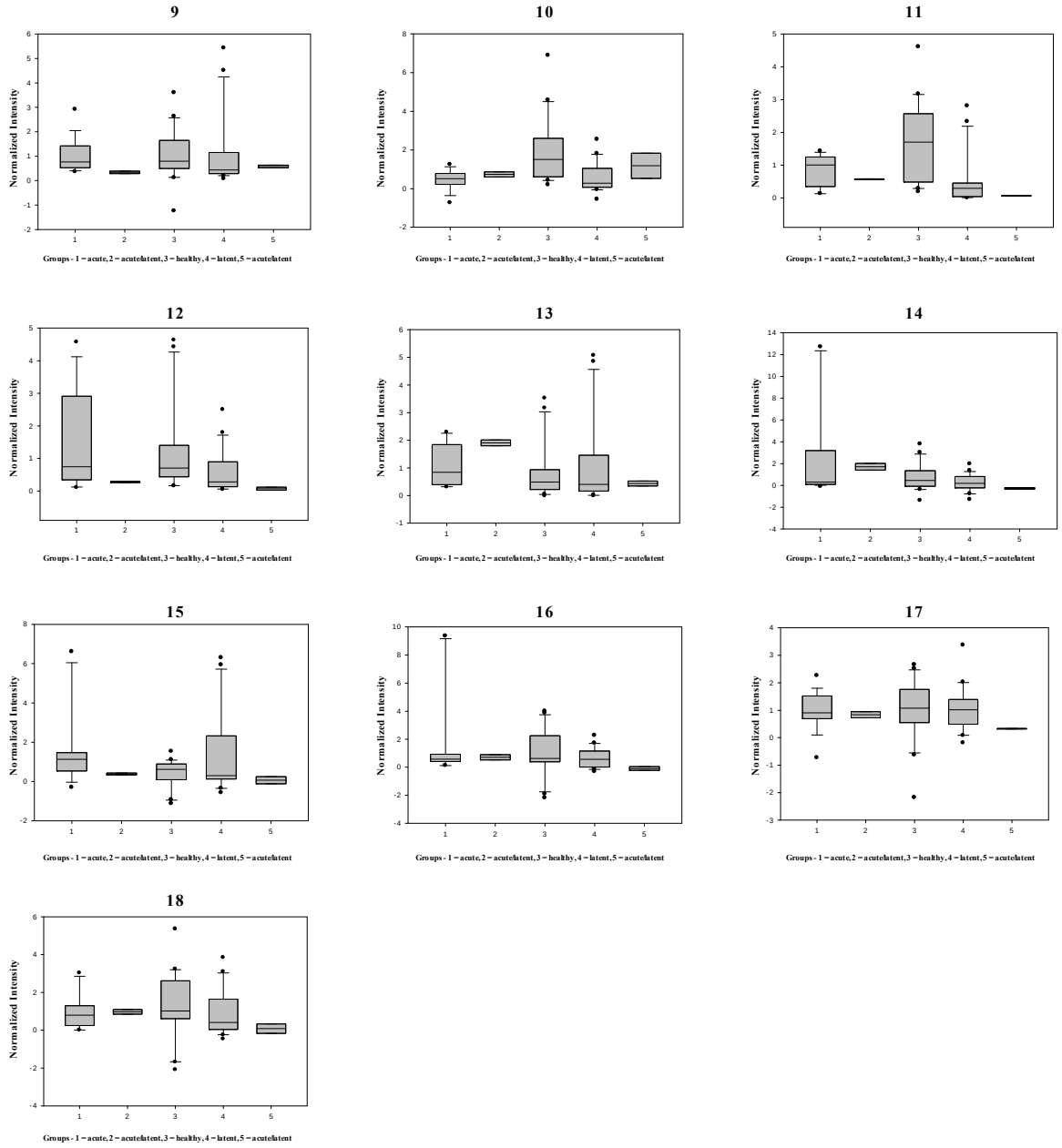

Box-plot: Normalized intensity of fluorescence indicating recognition by IgM against five groups in a *T. gondii* infection in human. Plot for each *T. brucei* VSG-GPI structure synthesized in chapter 4.